NASA CONTRACTOR REPORT

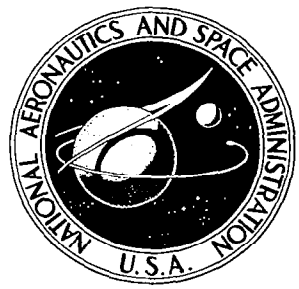

NASA CR-949

DYNAMIC STABILITY OF SPACE VEHICLES

Volume XV - Shell Dynamics With Special Applications to Control Problems

by L. E. Penzes

Prepared by
GENERAL DYNAMICS CORPORATION
San Diego, Calif.
for George C. Marshall Space Flight Center

NATIONAL AERONAUTICS AND SPACE ADMINISTRATION • WASHINGTON, D. C. • MAY 1968

DYNAMIC STABILITY OF SPACE VEHICLES

Volume XV – Shell Dynamics With Special Applications to Control Problems

By L. E. Penzes

Issued by Originator as Report No. GDC-BTD67-120

Prepared under Contract No. NAS 8-11486 by
GENERAL DYNAMICS CORPORATION
San Diego, Calif.

for George C. Marshall Space Flight Center

NATIONAL AERONAUTICS AND SPACE ADMINISTRATION

For sale by the Clearinghouse for Federal Scientific and Technical Information
Springfield, Virginia 22151 – CFSTI price $3.00

FOREWORD

This report is one of a series in the field of structural dynamics prepared under contract NAS 8-11486. The series of reports is intended to illustrate methods used to determine parameters required for the design and analysis of flight control systems of space vehicles. Below is a complete list of the reports of the series.

Volume I	Lateral Vibration Modes
Volume II	Determination of Longitudinal Vibration Modes
Volume III	Torsional Vibration Modes
Volume IV	Full Scale Testing for Flight Control Parameters
Volume V	Impedence Testing for Flight Control Parameters
Volume VI	Full Scale Dynamic Testing for Mode Determination
Volume VII	The Dynamics of Liquids in Fixed and Moving Containers
Volume VIII	Atmospheric Disturbances that Affect Flight Control Analysis
Volume IX	The Effect of Liftoff Dynamics on Launch Vehicle Stability and Control
Volume X	Exit Stability
Volume XI	Entry Disturbance and Control
Volume XII	Re-entry Vehicle Landing Ability and Control
Volume XIII	Aerodynamic Model Tests for Control Parameters Determination
Volume XIV	Testing for Booster Propellant Sloshing Parameters
Volume XV	Shell Dynamics with Special Applications to Control Problems

The work was conducted under the direction of Clyde D. Baker and George F. McDonough, Aero Astro Dynamics Laboratory, George C. Marshall Space Flight Center. The General Dynamics Convair Program was conducted under the direction of David R. Lukens.

TABLE OF CONTENTS

TABLE OF CONTENTS, Contd

TABLE OF CONTENTS, Contd

TABLE OF CONTENTS, Contd

LIST OF ILLUSTRATIONS

LIST OF ILLUSTRATIONS, Contd

LIST OF ILLUSTRATIONS, Contd

LIST OF ILLUSTRATIONS, Contd

LIST OF TABLES

NOMENCLATURE

A. NOMENCLATURE FOR "MATHEMATICAL REVIEW OF DIFFERENTIAL GEOMETRY"

A	area of surface
$\bar{b}$	binormal
$E = \bar{r}_u \bar{r}_u$ $F = \bar{r}_u \bar{r}_v$ and $G = \bar{r}_v \bar{r}_v$	
$\bar{i}, \bar{j}, \bar{k}$	unit vectors fixed to the coordinate system
$\bar{k}$	vector of curvature
$\bar{N}$	unit normal vector to the surface
$\bar{r}$	radius vector (general)
$\bar{r}_1, \bar{r}_2$	radius vector to a given point in space
R_1, R_2	radii of principal curvatures
s	arc length
$\bar{t}$	unit tangent vector
t, u, v	arbitrary parameters
$\bar{T}$	tangent vector
u	arbitrary parameter
$\varkappa$	curvature of a curve
$\varkappa_1$ and $\varkappa_2$	principal curvature of the normal curvature vector
τ	torsion
$\dot{} =$	$\frac{d}{du}$
$' =$	$\frac{d}{ds}()$ or $' = \frac{d}{dx}()$

B. NOMENCLATURE FOR "THIN ELASTIC SHELLS"

a	radius of cylinder or sphere
C_{ij}	orthotropic elastic constants associated with stretching (Hoppmann II)

C_{66}	orthotropic elastic constant associated with shearing (Hoppmann II)
$D = \frac{E h^3}{12 (1 - \nu^2)}$	
$D_x, D_\nu, D_\varphi, D_{x\varphi}$	orthotropic coefficients associated with stretching of the middle surface (Flügge)
e	eccentricity of oblate spheriod
E	total energy or modulus of elasticity
E_1, E_2	modulus of elasticity in a specified direction
h	thickness of the shell
h_b	orthotropic shell thickness, associated with bending and twisting (Hoppmann II)
h_m	mean thickness of the shells (equivalent shell thickness, associated with the dynamics of the shell) (Hoppmann II)
h_s	orthotropic shell thickness, associated with stretching and shearing (Hoppman II)
I	the expression of variational integral or moment of inertia of homogenous element or modulus of inertia of beam
I*	moment of inertia of honeycomb element
$K_x, K_\nu, K_\varphi, K_{x\varphi}$	orthotropic coefficients associated with bending and twisting (Flügge)
ℓ	length of cylinder
m or n	the numbers of circumferential waves
M_x, M_φ	bending moments
$M_{x\varphi}$, $M_{\varphi x}$	twisting moments
$N_x, N_y, N_{xy}, N_\varphi, N_\theta, N_{\varphi\theta}$	membrane forces per unit length of the normal section
p	pressure or external normal load on the shell
p_n	angular frequency (rad/sec)
p_n'	angular frequencies of unbounded set
p_n''	angular frequencies of bounded set
$P_n^m(x)$	Legendre's function for order of m and degree of n

q_i	generalized coordinates
Q_i	external forces
Q_x, Q_φ	shear forces
r_1, r_2	principal radii of shell of revolution
r_x, r_y, r_φ, r_θ	principal radii of curvature
s	strain energy of the shell
S_{ij}	orthotropic elastic constants associated with bending (Hoppmann II)
S_{66}	orthotropic elastic constant associated with twisting (Hoppmann II)
t	time (sec) or temperature
T_n	harmonic time function
u, v, w	displacements of the shell
u_n, v_n, w_n	longitudinal, tangential, and normal mode shapes for cylindrical and conical shells
x, y, z	coordinates of the Cartesian coordinate system
X, Y, Z	external surface loads on the shell
v_n, w_n	tangential and normal mode shapes for spherical and oblate spheriodal shell
y	deflection
γ'	strain associated with twisting (Hoppmann II)
γ''	strain associated with shearing (Hoppmann II)
ϵ_i'	strain associated with bending (Hoppmann II)
ϵ_i''	strain associated with stretching (Hoppmann II)
ϵ_x, ϵ_y, ϵ_φ, ϵ_θ γ_{xy}, $\gamma_{\varphi\theta}$, $\gamma_{\varphi x}$	strains of the shell
$\varkappa_x$, $\varkappa_y$, $\varkappa_{x\varphi}$	curvatures of cylindrical shell
λ_i	characteristic values of eigen functions
ν	Poisson's ratio
ρ	mass density of the shell $\left(\frac{\text{lb} \times \text{sec}^2}{\text{in.}^4}\right)$

σ_j'	stress associated with bending (Hoppmann II)
σ_j''	stress associated with stretching (Hoppmann II)
$\sigma_x, \sigma_y, \sigma_\varphi, \sigma_\theta$ $\tau_{xy}, \tau_{\varphi\theta}$	stresses
τ'	shear stress associated with twisting (Hoppmann II)
τ''	shear stress associated with shearing (Hoppmann II)
φ	angle between the normal surface vector and the coordinate z-axis; or just an angle
ω	angular frequency (rad/sec)

1/INTRODUCTION

A great variety of thin-walled shells are used in the structures of missile and space launch hardware. Development of mathematical models of cylindrical launch vehicles, consequently, requires dynamic analysis of many structures which fall within the realm of shell theory. A detailed knowledge of the dynamics of a launch vehicle structure is required for analysis of vehicle stability and control, since the dynamics of the structure affects the motion of the primary control elements and introduces extraneous signals into the feedback (motion) sensors on the vehicle. Proper evaluation of launch vehicle dynamics thus requires a knowledge of shell dynamics theory.

Primary attention in this monograph is focused on calculation of dynamic model parameters which affect stability and control. Emphasis is placed on modes for which the system frequency falls within the bandwidth of the control system, i.e., below 20 Hz for a large space booster.

The vibrations of thin elastic shells have attracted interest amoung researchers in the fields of mechanics and acoustics for almost a century. The foundations of thin elastic shell theory were formulated by Lord Rayleigh[1] and H. Lamb[2], and by the classical work of A. E. Love[3]. The works of S. Timoshenko, while quite brief in the aspects of shell theory[4], are understandable and up to date. However, neither of his works discusses any problems in shell dynamics. The work of W. Flügge[6] also contains an excellent collection of shell problems in the aspect of statics. The theoretical foundations of shell theories can best be obtained in the work of Goldenveizer[7]. His tensorial formulation of the shell equations represents the general case; however, the applications of shell equations include only static problems.

The basis of modern dynamics of thin-walled shells can be found primarily in papers published during the last 30 years. The purpose of this monograph is to explain the essential foundations of thin-walled elastic shells and the basis of theoretical derivations. The monograph attempts to fill the gap which presently exists between the contents of dynamics textbooks and recently published literature in the field of shell dynamics and explain the differences in their treatment of the subject. Examples and problems are included to demonstrate the use of the theories. Static problems are discussed in some cases to compare them with the equivalent dynamic problems. In addition, the relationship of shell vibration theory to practical application in the field of missiles and launch vehicles is described.

2/STATE OF THE ART

Owing to the intrinsic complications of the problem of shell dynamics, the analytical as well as the experimental results accumulated in technical literature are far from adequate to present a clear picture of the dynamics problem for even a relatively simple shell configuration. The main difficulty lies not in the formulation of a set of equations describing the vibrations of the shell but, rather, in the simplification and solution of these equations. Because the basic assumptions of the equations of thin elastic shells always introduces some restriction, all the solutions of thin-shell problems contain some restriction. This is a result of the derivations and basic assumptions. In other words, the solutions of shell problems are never as complete as the solutions of theoretical elasticity problems. Normally, several simplifying assumptions can be introduced to simplify very complex shell equations and derive a solution which approximates physical reality and can be handled mathematically.

One of the difficulties encountered in the study of shell theories is the great variety of assumptions and simplifications applied by different authors. This variation appears most often in the strain-displacement relationships. A careful study of the individual problems, however, will easily convince the reader that in most cases the differences are either not important or do not greatly affect the results in the particular problem under study. It is necessary to understand the theoretical aspects of the problems so that one will understand why the assumptions and simplifications applied to one problem cannot be applied to a different problem. The boundary conditions and the strain-displacement relations are one example.

As stated previously, this monograph reviews the differences in treatment of the dynamics problem between several textbooks applicable to the field and attempts to close the gap between the textbook theories and those contained in recent literature. The second part of the monograph reviews some of the important and typical papers published in the field of shell vibration.

2.1 MATHEMATICAL REVIEW OF DIFFERENTIAL GEOMETRY

Since mathematical representations of shell surfaces are made according to the theory of differential geometry, an understanding of some of the basic theories in this branch of mathematics is necessary.

The discussion of differential geometry can be separated into two parts: 1) the theory of space curves, and 2) the theory of surfaces. Note: In the present level of discussion, the subject of tensor analysis will be excluded.

2.1.1 THEORY OF SPACE CURVES. The mathematical theory of surfaces cannot be understood without some explanation of space curves. We can define the curves in space as paths of a point in motion. In three-dimensional space a curve can be represented by the vector equation (see Figure 2)

$$\bar{r} = \bar{r}(u) = x(u)\bar{i} + y(u)\bar{j} + z(u)\bar{k} \tag{1}$$

where $\bar{r}$ is the radius vector to the curve and u is an arbitrary parameter.

Equation 1 can be expressed in another form,

$$x_i = x_i(u) \tag{2}$$

where

$i = 1, 2, 3$ and x_i expresses the components of the radius vector for $\bar{r}$.

2.1.1.1 Tangent to a Space Curve. Figure 1 illustrates the tangent vector to a space curve of point P.

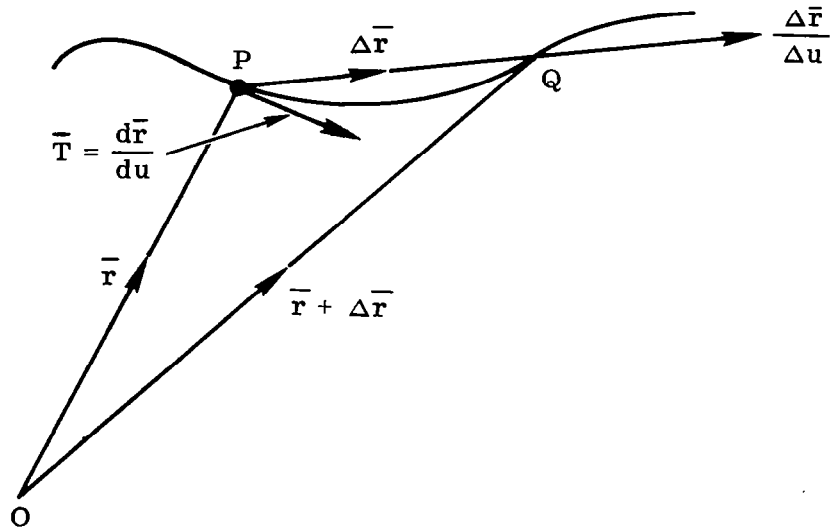

Figure 1. Tangent Vector to Space Curve

We may define the fact that the tangent is the limiting position of a line through P and a point Q in the given interval of u, where $Q \rightarrow P$, by saying that the tangent passes through two consecutive points on the curve. The equation of tangent $\bar{T}$ can be expressed therefore

$$\bar{T} = \frac{d\bar{r}}{du} = \dot{x}\bar{i} + \dot{y}\bar{j} + \dot{z}\bar{k} \tag{3}$$

where

$$\dot{} = \frac{d}{du}$$

2.1.1.2 Arc Length. The arc length of a segment of the curve between points A (u_o) and P (u) can be expressed by the following integral (see Figure 2).

$$s(u) = \int_{u_o}^{u} ds = \int_{u_o}^{u} (\dot{\bar{r}}\,\dot{\bar{r}})^{1/2}\, du \tag{4}$$

where

$$\frac{d\bar{r}}{du} = \dot{\bar{r}}$$

$$d\bar{r} = \dot{\bar{r}}\, du \tag{5}$$

and

$$d\bar{r}^2 = ds^2 = \dot{\bar{r}}\,\dot{\bar{r}}\, du^2$$

Equation 5 can be expressed in the form

$$ds = (\dot{\bar{r}}\,\dot{\bar{r}})^{1/2}\, du \tag{6}$$

2.1.1.3 Unit Tangent Vector. In the case of the parameters, u is equal to the arc length of s, or u = s. The tangent vector of the space curve becomes a unit vector.

$$\left|\frac{d\bar{r}}{ds}\right| = 1 \tag{7}$$

if

$$\bar{r} = \bar{r}(s)$$

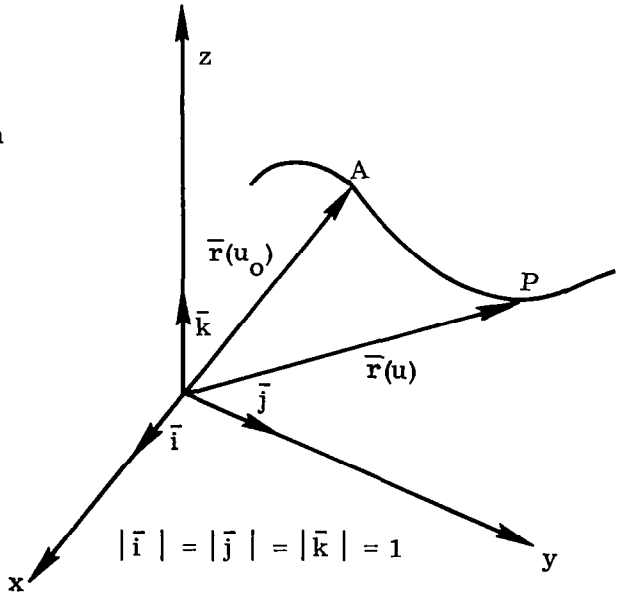

Figure 2. Arc Length of a Space Curve

Proof of the theory is given below. If

$$u = s$$

then

$$\bar{r} = \bar{r}(s)$$

One can express Equation 6 in the form

$$ds^2 = \dot{\bar{r}}\,\dot{\bar{r}}\,du^2 = \dot{\bar{r}}\,\dot{\bar{r}}\,ds^2$$

Therefore,

$$\dot{\bar{r}}\,\dot{\bar{r}} = 1 \tag{8}$$

The vector $\dot{\bar{r}} = \frac{d\bar{r}}{ds}$ is therefore a unit vector.

Let u be an independent variable, a general parameter, then

$$\bar{T} = \frac{d\bar{r}}{du} = \frac{d\bar{r}}{ds} \cdot \frac{ds}{du} = \bar{t}\left(\frac{ds}{du}\right) = \bar{t}\varphi(u) \tag{9}$$

where:

$$\bar{t} = \frac{d\bar{r}}{ds} \tag{10}$$

$\bar{t}$ is the unit tangent vector and $\varphi(u) = \frac{ds}{du}$ is a scalar function.

2.1.1.4 Osculating Plane. The tangent was defined previously as the line passing through two consecutive points of the curve. The osculating plane can be defined as the plane through three consecutive points, which means the limiting position of a plane passing through three nearby points of the curve, when two of these points approach the third (Figure 3).

The equation of the osculating plane can be expressed (see Figure 4) as

$$(\bar{r} - \bar{r}_1)(\dot{\bar{r}}_1 \times \ddot{\bar{r}}_1) = 0 \tag{11}$$

or

$$(\bar{r} - \bar{r}_1) = \lambda\dot{\bar{r}}_1 + \mu\ddot{\bar{r}}_1 \tag{12}$$

where λ and μ are arbitrary constants.

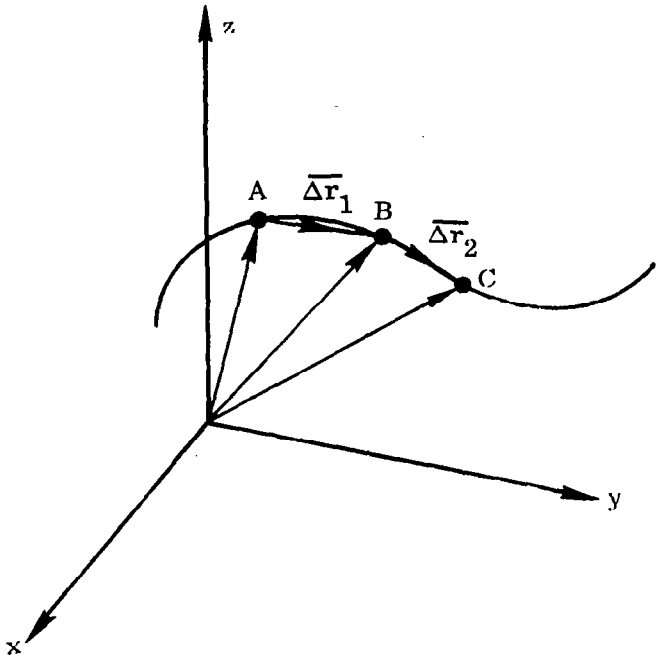

Figure 3. Osculating Plane

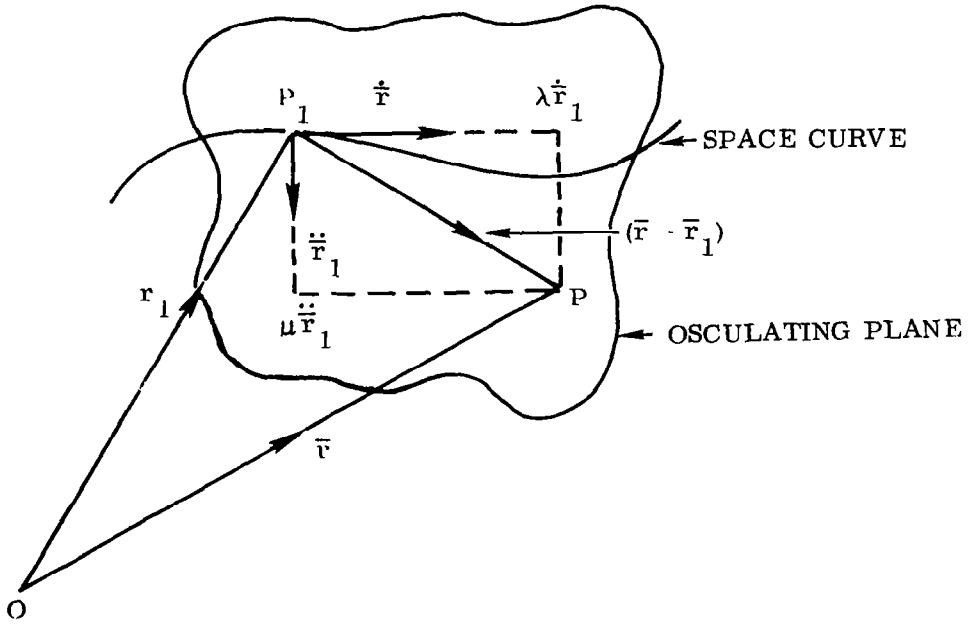

Figure 4. Osculating Plane Equation

2.1.1.5 Curvature and Principal Normal. The line in the osculating plane at point P perpendicular to the tangent line is called the principal normal (see Figure 5, points P_1, P_2 and P_3). A unit vector, $\bar{n}$, is placed in its direction, the sense of which may be arbitrarily selected, provided it is continuous along the curve. If it is assumed that the arc length is the parameter, $\bar{r} = \bar{r}(s)$, one can write

$$\bar{t} \cdot \bar{t} = 1 \tag{13}$$

where

$$\bar{t} = \frac{d\bar{r}}{ds} = \bar{r}'$$

Differentiating Equation 13 with respect to s,

$$\bar{t} \cdot \bar{t}' = 0 \tag{14}$$

Therefore

$$\bar{t} \perp \bar{t}'$$

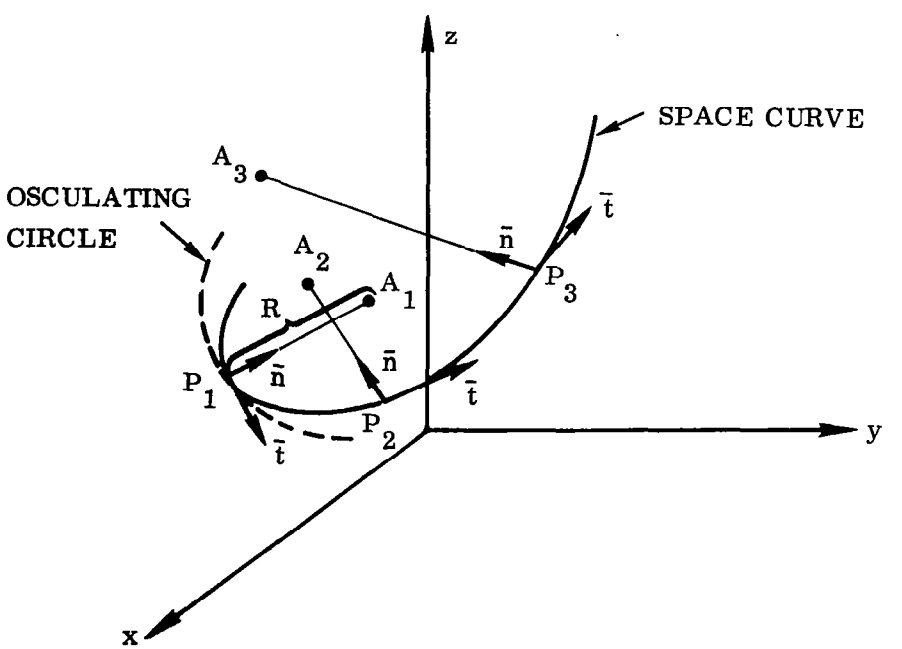

Figure 5. Principal Normal

Equation 14 shows that the vector $\bar{t}' = \frac{d\bar{t}}{ds}$ is perpendicular to $\bar{t}$, since

$$\bar{t} = \dot{\bar{r}} u'$$

and

$$\bar{t}' = \ddot{\bar{r}} (u')^2 + \dot{\bar{r}} u'' \tag{15}$$

where the symbols are defined as

$$' = \frac{d}{ds}$$

and

$$\cdot = \frac{d}{du}$$

The comparison of Equations 15 and 12 shows that $\bar{t}'$ lies in the plane of $\dot{\bar{r}}$ and $\ddot{\bar{r}}$ and, hence, in the osculating plane.

The vector $\frac{d\bar{t}}{ds} = \bar{k}$, which expresses the rate of change of the tangent, is called the curvature vector. The curvature vector can be expressed in terms of the normal unit vector.

$$\bar{k} = \frac{d\bar{t}}{ds} = \varkappa \bar{n} \tag{16}$$

where

$$|\bar{n}| = 1$$

The factor $\varkappa$ is called curvature. The radius R of the osculating circle can be defined as $R = \varkappa^{-1}$. The absolute value of R is the radius of curvature, which is the radius of the circle passing through three consecutive points of the curve, the osculating circle.

2.1.1.6 Torsion. The torsion of a curve can be expressed by the rate of change of the osculating plane. For this purpose the vector binormal, $\bar{b}$, was introduced according to the expression

$$\bar{b} = (\bar{t} \times \bar{n}) \tag{17}$$

Equation 17 shows that the binormal, $\bar{b}$, is perpendicular to the osculating plane. It also follows that

$$\bar{b} \cdot \bar{t} = 0 \tag{18}$$

Differentiating Equation 18 with respect to s,

$$\bar{b}' \cdot \bar{t} + \bar{b} \cdot \bar{t}' = 0 \tag{19}$$

or

$$\bar{b}'\bar{t} = -\bar{b}(\varkappa\bar{n}) = 0$$

Therefore

$$\bar{b}' \perp \bar{t}$$

and

$$\bar{b}' \perp \bar{b}$$

since

$$\bar{b} \cdot \bar{b} = 1$$

Since the unit vectors $\bar{t}$, $\bar{n}$, and $\bar{b}$ are mutually perpendicular to each other, it follows that the rate of change of the binormal, $\bar{b}'$, has to be parallel with vector $\bar{n}$. The last statement, in mathematical terms, is

$$\bar{b}' = \frac{d\bar{b}}{ds} = -\tau\,\bar{n} \tag{20}$$

where the proportionality factor, τ, is called the torsion of the curve.

The torsion, τ, can be expressed in the following form

$$\tau = -\bar{n}(\bar{t}\times\bar{n})' = -\bar{n}(\bar{t}\times\bar{n}') = -\frac{\bar{r}''}{\varkappa}\left[\bar{r}'\times\left(\frac{\bar{r}''}{\varkappa}\right)'\right] \tag{21}$$

Equation 21 can be expressed in the final form.

$$\tau = \frac{(\bar{r}'\bar{r}''\bar{r}''')}{\bar{r}'\cdot\bar{r}'} \tag{22}$$

where

$$' = \frac{d}{ds}$$

2.1.1.7 Formulas of Frenet (Moving Trihedron Along a Curve). The formulas of moving trihedron will be completed by the equation of rate change of the normal vector, $\bar{n}'$.

Since

$$\bar{n} \cdot \bar{n} = 1,$$

$$\bar{n} \cdot \bar{n}' = 0 \tag{23}$$

The derivative of the normal vector, $\bar{n}'$, can be expressed linearly in terms of $\bar{t}$ and $\bar{b}$.

$$\bar{n}' = \frac{d\bar{n}}{ds} = \alpha\bar{t} + \beta\bar{b} \tag{24}$$

where α and β are, so far, undetermined constants. The multiplication of Equation 24 by vectors $\bar{t}$ and $\bar{b}$ leads to the determination of the unknown coefficients, α and β.

$$\left.\begin{aligned} \alpha_1 &= \bar{t}\cdot\bar{n}' = -\bar{n}\cdot\bar{t}' = -\bar{n}\cdot\varkappa\bar{n} = -\varkappa \\ \alpha_2 &= \bar{b}\cdot\bar{n}' = -\bar{n}\cdot\bar{b}' = \bar{n}\cdot\tau\bar{n} = \tau \end{aligned}\right\} \tag{25}$$

Equation 24 becomes, in the final form,

$$\bar{n}' = \frac{d\bar{n}}{ds} = -\varkappa\bar{t} + \tau\bar{b} \tag{26}$$

The formulas of Frenet can be summarized for space curves.

$$\left.\begin{aligned} \frac{d\bar{t}}{ds} &= \varkappa\bar{n} \\ \frac{d\bar{n}}{ds} &= -\varkappa\bar{t} + \tau\bar{b} \\ \frac{d\bar{b}}{ds} &= -\tau\bar{n} \end{aligned}\right\} \tag{27}$$

Three planes can be associated by the moving trihedron according to Figure 6.

2.1.2 THEORY OF SURFACES. A surface can be expressed as the function of two independent variables by the following equation.

$$\bar{r} = \bar{r}(u, v) \tag{28}$$

where the independent variables are u and v. Let the sphere serve as an example (see Figure 7).

The equations of a spherical surface are:

$$x = a\cos\varphi\cos\theta$$

$$y = a\cos\varphi\sin\theta$$

$$z = a\sin\varphi$$

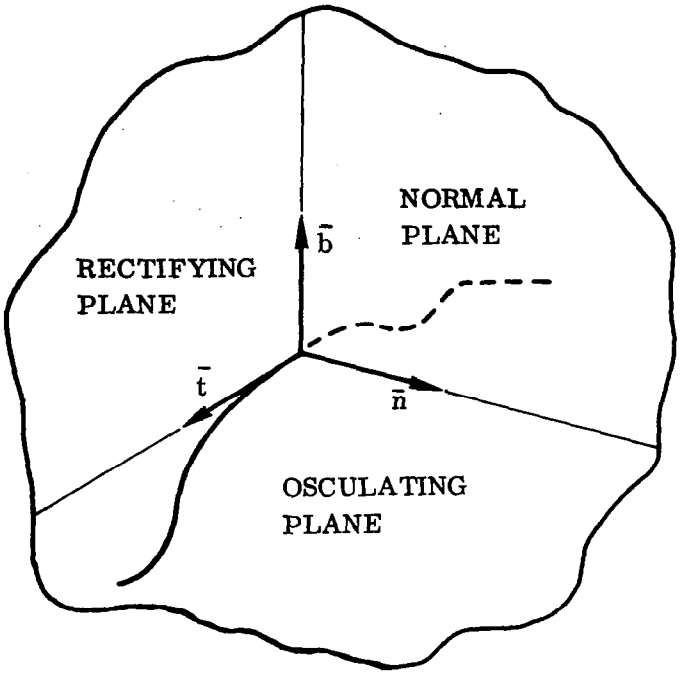

Figure 6. Moving Trihedron

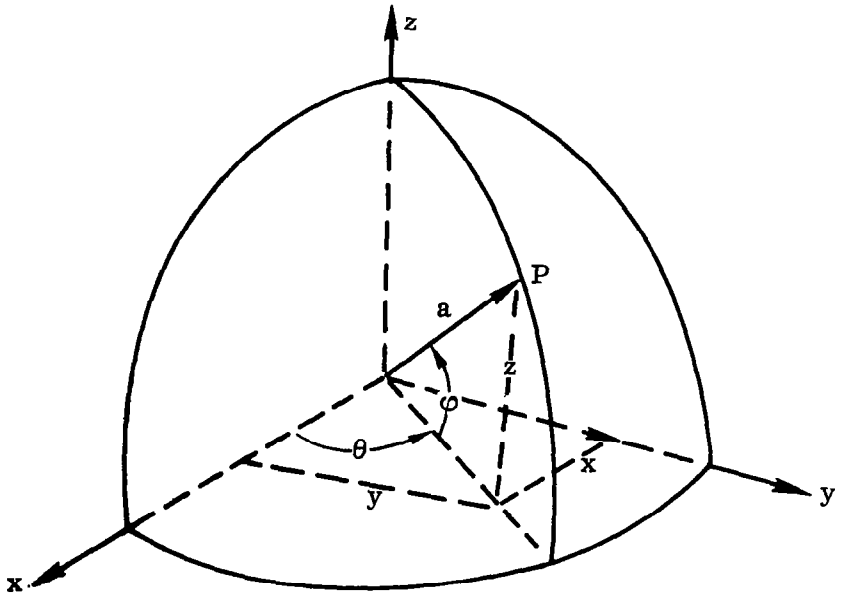

Figure 7. Spherical Surface

The net of parametric curves was constructed on the surface, keeping first one of the independent variables constant and then the other one. Figure 8 illustrates the concept.

At point P the vector $\bar{r}_u$ is tangent to the curve v = constant, and $\bar{r}_v$ is tangent to the curve u = constant.

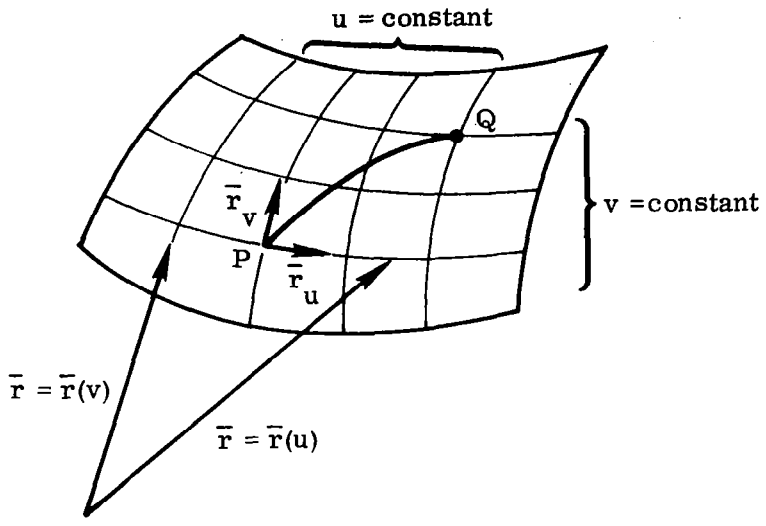

Figure 8. Net of Parabolic Curves on the Surface

2.1.2.1 First Fundamental Form of Surface. The relation $\varphi(u, v) = 0$ between the curvilinear coordinates determines a curve on the surface. Such a curve can also be given in parametric form.

$$u = u(t) \qquad \text{and} \qquad v = v(t) \tag{29}$$

The vector $\frac{d\bar{r}}{dt} = \dot{\bar{r}}$ at a point P of the surface, given by

$$\frac{d\bar{r}}{dt} = \frac{\partial \bar{r}}{\partial u} \cdot \frac{du}{dt} + \frac{\partial \bar{r}}{\partial v} \frac{dv}{dt} \tag{30}$$

is tangent to the curve and therefore to the surface. Equation 30 can also be expressed in a form independent of the choice of parameter.

$$d\bar{r} = \bar{r}_u du + \bar{r}_v dv \tag{31}$$

The distance of two points P and Q on a curve is found by integrating (see Figure 8)

$$ds^2 = d\bar{r} \cdot d\bar{r} = \bar{r}_u \cdot \bar{r}_u du^2 + 2\,\bar{r}_u \bar{r}_u\, du\, dv + \bar{r}_v \cdot \bar{r}_v dv^2 \tag{32}$$

where $d\bar{r}$ was expressed according to Equation 31.

The following notations are introduced.

$$E = \bar{r}_u \cdot \bar{r}_u \qquad F = \bar{r}_u \cdot \bar{r}_v \qquad \text{and} \qquad G = \bar{r}_v \cdot \bar{r}_v \tag{33}$$

The elements of the curve are expressed by the symbols of Equation 33.

$$ds^2 = E\,du^2 + 2\,F\,du\,dv + G\,dv^2 \tag{34}$$

The expression 34 for ds^2 is called the first fundamental form of the surface.

The distance between P and Q on the curve u = u(t) and v = v(t) can now be expressed as follows.

$$S = \int_{t_o}^{t} \left[E\left(\frac{du}{dt}\right)^2 + 2\,F\,\frac{du}{dt}\frac{dv}{dt} + G\left(\frac{dv}{dt}\right)^2 \right]^{1/2} dt \tag{35}$$

2.1.2.2 Surface Element. Figure 9 shows the element of a surface area.

The element of a surface area may be expressed as

$$dA = |\bar{r}_u du \times \bar{r}_v dv| \tag{36}$$

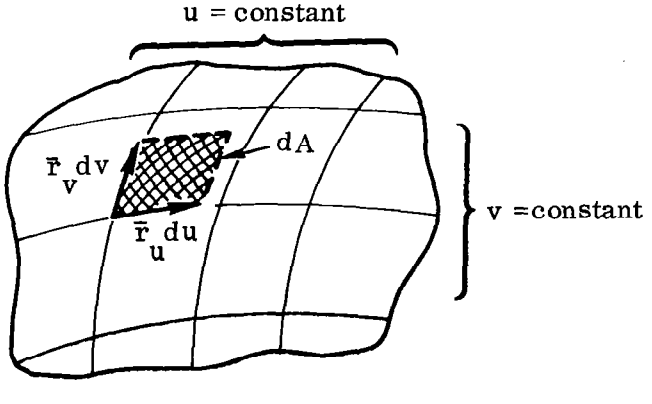

Figure 9. Surface Area Element

Equation 36 can be expressed as follows.

$$dA^2 = (\bar{r}_u \times \bar{r}_v)(\bar{r}_u \times \bar{r}_v) du^2 dv^2 \tag{37}$$

because

$$(\bar{r}_u \times \bar{r}_v)(\bar{r}_u \times \bar{r}_v) = (\bar{r}_u \bar{r}_u)(\bar{r}_v \bar{r}_v) - (\bar{r}_u \bar{r}_v)^2 = E\,G - F^2 \tag{38}$$

The substitution of Equation 38 into Equation 37 yields finally

$$dA = (E\,G - F^2)^{1/2}\,du\,dv \tag{39}$$

The integration of Equation 39 leads to the area of a region on a surface.

$$A = \iint (E\,G - F^2)^{1/2}\,du\,dv \tag{40}$$

2.1.2.3 Normal Vector to the Surface. The surface normal is the line at a point P perpendicular to the tangent plane.

The unit normal based on Figure 10 can be defined as

$$\bar{N} = \frac{(\bar{r}_u \times \bar{r}_v)}{|\bar{r}_u \times \bar{r}_v|}$$

$$= \frac{(\bar{r}_u \times \bar{r}_v)}{(E\,G - F^2)^{1/2}} \tag{41}$$

since

$$|\bar{r}_u \times \bar{r}_v| = (E\,G - F^2)^{1/2} \tag{42}$$

The explanation of Equation 42 can be found in Equation 38.

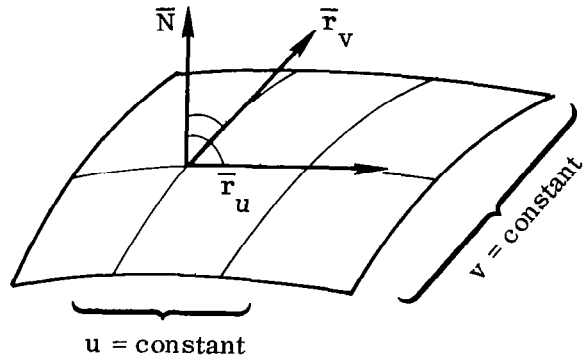

Figure 10. Normal Vector to Surface

2.1.2.4 Second Fundamental Form, Euler's Theory. The second fundamental of a surface expresses the normal curvature of an arbitrary curve on the surface. When $\bar{t}$ is the unit tangent vector of point P on the surface, the curvature vector, $\bar{k}$, can be expressed as

$$\bar{k} = \frac{d\bar{t}}{ds} = \bar{k}_n + \bar{k}_g \tag{43}$$

where the curvature vector, $\bar{k}$, was decomposed into a component, $\bar{k}_n$, normal and a component, $\bar{k}_g$, tangential to the surface (see Figure 11).

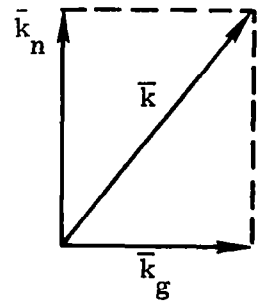

Figure 11. Components of Curvature Vector

The vector $\bar{k}_n$ is called the normal curvature vector and can be expressed in terms of the unit surface normal vector, $\bar{N}$.

$$\bar{k}_n = \varkappa_n \bar{N} \tag{44}$$

where $\varkappa_n$ is the normal curvature.

The scalar $\varkappa_n$ depends for its sign on the sense of $\bar{N}$. The vector $\bar{k}_g$ is called the tangential curvature vector or geodesic curvature vector. The present theory is intended to explore the calculation of vector $\bar{k}_n$ only. Since the surface normal vector, $\bar{N}$, is perpendicular to any of the tangent vectors, $\bar{t}$, one can write

$$\bar{N} \cdot \bar{t} = 0 \tag{45}$$

Differentiating Equation 45 with respect to s,

$$\frac{d\bar{N}}{ds} \cdot \bar{t} + \bar{N} \frac{d\bar{t}}{ds} = 0 \tag{46}$$

Equation 46 can be expressed in the following form.

$$\frac{d\bar{t}}{ds} \cdot \bar{N} = -\bar{t} \frac{d\bar{N}}{ds} = -\frac{d\bar{r}}{ds} \cdot \frac{d\bar{N}}{ds} = -\frac{d\bar{r}}{d\bar{r}} \cdot \frac{d\bar{N}}{d\bar{r}} \tag{47}$$

The multiplication of Equation 43 by vector $\bar{N}$ leads to

$$\frac{d\bar{t}}{ds} \cdot \bar{N} = \bar{k}_n \cdot \bar{N} = \varkappa_n \tag{48}$$

since

$$\bar{k}_g \cdot \bar{N} = 0$$

and

$$\bar{k}_n = \varkappa_n \bar{N}$$

(For further explanations, see Equation 44.)

The comparison of Equations 47 and 48 yields finally

$$\varkappa_n = -\frac{d\bar{r} \cdot d\bar{N}}{d\bar{r} \cdot d\bar{r}} \tag{49}$$

The following derivations are intended to study the right side of Equation 49. The term $d\bar{r}$ was expressed by Equation 31 as:

$$d\bar{r} = \bar{r}_u\,du + \bar{r}_v\,dv$$

Similarly

$$d\bar{N} = \bar{N}_u\,du + \bar{N}_v\,dv \tag{50}$$

The substitution of Equations 31 and 50 into Equation 49 leads to

$$\kappa_n = -\frac{(\bar{r}_u\bar{N}_u)\,du^2 + (\bar{r}_u\bar{N}_v + \bar{r}_v\bar{N}_u)\,du\,dv + (\bar{r}_v\bar{N}_v)\,dv^2}{(\bar{r}_u \cdot \bar{r}_u)\,du^2 + 2\,(\bar{r}_u \cdot \bar{r}_v)\,du\,dv + (\bar{r}_v \cdot \bar{r}_v)\,dv^2} \tag{51}$$

It can be seen from Equation 41 that vector $\bar{N}$ is perpendicular to vector $\bar{r}_u$; consequently

$$\bar{r}_u \cdot \bar{N} = 0 \tag{52}$$

Differentiating Equation 52 with respect to u, one has

$$-(\bar{r}_u\bar{N}_u) = \bar{r}_{uu} \cdot \bar{N} = \bar{r}_{uu} \cdot \frac{(\bar{r}_u \times \bar{r}_v)}{|\bar{r}_u \times \bar{r}_v|} = \frac{(\bar{r}_{uu}\bar{r}_u\bar{r}_v)}{(E\,G - F^2)^{1/2}} \tag{53}$$

Introducing the symbol e for Equation 53, one has

$$e = \frac{(\bar{r}_{uu}\bar{r}_u\bar{r}_v)}{(E\,G - F^2)^{1/2}} \tag{54}$$

Similarly

$$\bar{r}_v \cdot \bar{N} = 0$$

Therefore

$$-(\bar{r}_v\bar{N}_v) = \bar{r}_{vv} \cdot \bar{N} = \frac{(\bar{r}_{vv}\bar{r}_u\bar{r}_v)}{(E\,G - F^2)^{1/2}} \tag{55}$$

Again, introducing the symbol g for Equation 55,

$$g = \frac{(\bar{r}_{vv}\bar{r}_u\bar{r}_v)}{(E\,G - F^2)^{1/2}} \tag{56}$$

Similarly

$$2f = -(\bar{r}_u \bar{N}_v + \bar{r}_v \bar{N}_u) = 2\bar{r}_{uv}\bar{N} = 2\frac{(\bar{r}_{uv}\bar{r}_u\bar{r}_v)}{(EG - F^2)^{1/2}} \tag{57}$$

or

$$f = \frac{(\bar{r}_{uv}\bar{r}_u\bar{r}_v)}{(EG - F^2)^{1/2}} \tag{58}$$

The substitution of Equations 32 and 33 (and furthermore 54, 56 and 58) into Equation 51 leads to the final equation of normal curvature of a surface.

$$\varkappa_n = \frac{e\,du^2 + 2f\,du\,dv + g\,dv^2}{E\,du^2 + 2F\,du\,dv + G\,dv^2} \tag{59}$$

If the curvilinear coordinate system of the surface is orthogonal, then vector $\bar{r}_u$ is orthogonal to $\bar{r}_v$ or $\bar{r}_u \cdot \bar{r}_v = 0$; consequently $F = f = 0$. The formula of normal curvature was reduced in this case to

$$\varkappa_n = \frac{e\,du^2 + g\,dv^2}{E\,du^2 + G\,dv^2} = e\left(\frac{du}{ds}\right)^2 + g\left(\frac{dv}{ds}\right)^2 \tag{60}$$

The denominator of Equation 60 was expressed according to Equation 34. This formula can be cast into a simple form. Substituting first $dv = 0$ and then $du = 0$ into Equation 60,

$$\left.\begin{aligned} dv = 0 \qquad & \varkappa_n = \varkappa_1 = \frac{e}{E} \\ du = 0 \qquad & \varkappa_n = \varkappa_2 = \frac{g}{G} \end{aligned}\right\} \tag{61}$$

$\varkappa_1$ and $\varkappa_2$ are the so-called principal curvatures of the normal curvature vector. Without the mathematical proof, the definition of principal curvatures is desirable for some explanations. The principal curvatures $\varkappa_1$ and $\varkappa_2$ are the extreme values of the normal curvature as functions of the varying tangent directions to the surface given by du/dv. It can also be proved that these curvature directions are orthogonal.

Euler's Theorem. The normal curvature, $\varkappa_n$, can be expressed in an arbitrary direction in terms of principal curvatures $\varkappa_1$ and $\varkappa_2$ in the following. With the aid of the terms E, F, G one can express the angle α of two tangent directions to the surface given by du/dv and $\delta u/\delta v$. Then

$$\left.\begin{aligned} d\bar{r} &= \bar{r}_u\,du + \bar{r}_v\,dv \\ \delta\bar{r} &= \bar{r}_u\,\delta u + \bar{r}_v\,\delta v \end{aligned}\right\} \tag{62}$$

and

$$\cos\alpha = \frac{d\bar{r}\cdot\delta\bar{r}}{|d\bar{r}|\cdot|\delta\bar{r}|} = \frac{E\,du\,\delta u + G\,dv\,\delta v}{ds\,(E\,\delta u^2 + G\,\delta v^2)^{1/2}} \tag{63}$$

Assuming $\delta v = 0$, Equation 63 may be written

$$\cos\alpha = E^{1/2}\left(\frac{du}{ds}\right) \tag{64}$$

Similarly

$$\delta u = 0$$

Equation 63 can then be reduced to

$$\cos\left(\frac{\pi}{2} - \alpha\right) = \sin\alpha = G^{1/2}\left(\frac{dv}{ds}\right) \tag{65}$$

The substitution of expressions 62, 64 and 65 into Equation 60 leads to the final formula.

$$\varkappa_n = \varkappa_1 \cos^2\alpha + \varkappa_2 \sin^2\alpha \tag{66}$$

2.1.3 EXAMPLES. The equation of an oblate spheroidal can be defined by the following equations (see Figure 12).

$$\left.\begin{aligned} x &= a\cos\beta\cos\theta \\ y &= a\cos\beta\sin\theta \\ z &= a\,(1-\epsilon^2)^{1/2}\sin\beta \end{aligned}\right\} \tag{67}$$

where the eccentricity is

$$\epsilon = \left(1 - \frac{b^2}{a^2}\right)^{1/2} \tag{68}$$

2.1.3.1 Calculation of the Surface Area of the Oblate Spheroid. The vectorial equation of surface is in the present case

$$\bar{r} = x\bar{i} + y\bar{j} + z\bar{k} = a\left[\cos\beta\cos\theta\,\bar{i} + \cos\beta\sin\theta\,\bar{j} + (1-\epsilon^2)^{1/2}\sin\beta\,\bar{k}\right] \tag{69}$$

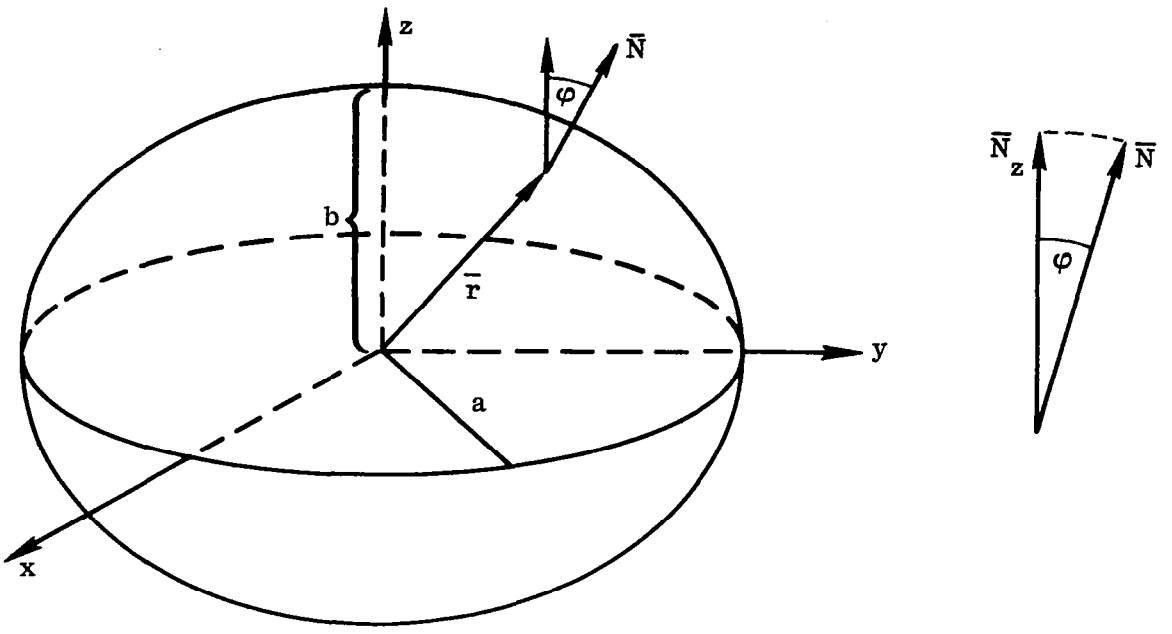

Figure 12. Angle of Normal Unit Vector

The values of expressions E, F, and G have to be calculated according to Equation 33 since

$$\bar{r}_\beta = a\left[-\sin\beta\cos\theta\,\bar{i} - \sin\beta\sin\theta\,\bar{j} + (1-\epsilon^2)^{1/2}\cos\beta\,\bar{k}\right]$$

$$\bar{r}_\theta = a\left[-\cos\beta\sin\theta\,\bar{i} + \cos\beta\cos\theta\,\bar{j}\right]$$

$$E = \bar{r}_\beta \cdot \bar{r}_\beta = a^2(1-\epsilon^2\cos^2\beta)$$

$$F = \bar{r}_\beta \cdot \bar{r}_\theta = 0$$

$$G = \bar{r}_\theta \cdot \bar{r}_\theta = a^2\cos^2\beta$$

Therefore

$$(E\,G - F^2)^{1/2} = a^2\cos\beta(1-\epsilon^2\cos^2\beta)^{1/2} \tag{70}$$

The surface area of the oblate spheroid is, according to Equation 40 and the utilization of Equation 70,

$$A = \int_0^{2\pi} \int_{-\pi/2}^{\pi/2} (E\,G - F^2)^{1/2}\, d\theta\, d\beta$$

$$= \int_0^{2\pi} \int_{-\pi/2}^{\pi/2} a^2 \cos\beta\, (1 - \epsilon^2 \cos^2\beta)^{1/2}\, d\theta\, d\theta \tag{71}$$

The computation of integral 71 leads finally to

$$A = 2\pi a^2 + \frac{\pi b^2}{\epsilon} \ell n \frac{(1+\epsilon)}{(1-\epsilon)} \tag{72}$$

where the value of eccentricity is given by Equation 68.

2.1.3.2 Normal Unit Vector. Equations 41 and 42 represent the general formulas for the present problem since

$$(\bar{r}_\theta \times \bar{r}_\beta) = \begin{vmatrix} \bar{i} & \bar{j} & \bar{k} \\ -a\cos\beta\sin\theta & a\cos\beta\cos\theta & 0 \\ -a\sin\beta\cos\theta & -a\sin\beta\sin\theta & a(1-\epsilon^2)^{1/2}\cos\beta \end{vmatrix}$$

Therefore

$$\bar{N} = (1 - \epsilon^2\cos^2\beta)^{-1/2}\Big[(1-\epsilon^2)^{1/2}\cos\beta\cos\theta\,\bar{i} + (1-\epsilon^2)^{1/2}\cos\beta\sin\theta\,\bar{j} + \sin\beta\,\bar{k}\Big] \tag{73}$$

2.1.3.3 Calculation of the Angle of Normal Unit Vector and the Z Axis. (See Figure 12.) The cosine of the angle can be calculated based on Figure 12 and Equation 73, as follows.

$$\cos\varphi = \frac{|\bar{N}_Z|}{|\bar{N}|} = \frac{\sin\beta}{(1 - \epsilon^2\cos^2\beta)^{1/2}} \tag{74}$$

since

$$|\bar{N}| = 1$$

$$\bar{N}_Z = \frac{\sin\beta}{(1 - \epsilon^2\cos^2\beta)^{1/2}}\,\bar{k}$$

2.1.3.4 Calculation of the Expressions of e, f, g. Since

$$(\bar{r}_{\beta\beta}\bar{r}_{\beta}\bar{r}_{\theta}) = \begin{vmatrix} -a\cos\beta\cos\theta & -a\cos\beta\sin\theta & -a(1-\epsilon^2)^{1/2}\sin\beta \\ -a\sin\beta\cos\theta & -a\sin\beta\sin\theta & a(1-\epsilon^2)^{1/2}\cos\beta \\ -a\cos\beta\sin\theta & a\cos\beta\cos\theta & 0 \end{vmatrix}$$

to carry out the computation, one has

$$(\bar{r}_{\beta\beta}\bar{r}_{\beta}\bar{r}_{\theta}) = a^3\cos\beta(1-\epsilon^2)^{1/2}$$

Equation 54 represents the formula

$$e = \frac{(\bar{r}_{\beta\beta}\bar{r}_{\beta}\bar{r}_{\theta})}{(EG-F^2)^{1/2}} = \frac{a(1-\epsilon^2)^{1/2}}{(1-G^2\cos^2\beta)^{1/2}} \tag{75}$$

Similarly

$$(\bar{r}_{\beta\theta}\bar{r}_{\beta}\bar{r}_{\theta}) = 0$$

One has, according to Equation 58,

$$f = \frac{(\bar{r}_{uv}\bar{r}_{u}\bar{r}_{v})}{(EG-F^2)^{1/2}} = 0 \tag{76}$$

Again, one has, from Equation 56

$$g = \frac{(\bar{r}_{\theta\theta}\bar{r}_{\beta}\bar{r}_{\theta})}{(EG-F^2)^{1/2}} = \frac{a(1-\epsilon^2)^{1/2}\cos\beta}{(1-\epsilon^2\cos^2\beta)^{1/2}} \tag{77}$$

2.1.3.5 Calculation of the Principal Curvatures and the Principal Radii of the Surface. Equation 61 presents the required formula.

$$\left.\begin{aligned} \varkappa_1 &= \frac{e}{E} = \frac{(1-\epsilon^2)^{1/2}}{a(1-\epsilon^2\cos^2\beta)^{3/2}} \\ \varkappa_2 &= \frac{g}{G} = \frac{(1-\epsilon^2)^{1/2}}{a(1-\epsilon^2\cos^2\beta)^{1/2}} \end{aligned}\right\} \tag{78}$$

where the expressions E, G, e, and g were calculated previously.

The two principal radii of the surface are

$$R_1 = \frac{1}{\varkappa_1} = \frac{a(1 - \epsilon^2 \cos^2 \beta)^{3/2}}{(1 - \epsilon^2)^{1/2}} \tag{79}$$

$$R_2 = \frac{1}{\varkappa_2} = \frac{a(1 - \epsilon^2 \cos^2 \beta)^{1/2}}{(1 - \epsilon^2)^{1/2}} \tag{80}$$

2.1.4 BIBLIOGRAPHY

1. Dirk J. Struik: Lectures on Classical Differential Geometry, Addison-Wesley Pub. Co., Second printing, 1957

2. Harry Lass: Vector and Tensor Analysis, McGraw-Hill Book Co., 1950

3. L. P. Eisenhart: An Introduction to Differential Geometry with use of the Tensor Calculus, Princeton University Press, Princeton, 1940

2.2 THEORY OF THIN ELASTIC SHELLS

2.2.1 THEORY OF MEMBRANE SHELLS. The membrane theory is an approximate method of analysis of thin elastic shells based upon the assumption that the transverse shear forces (bending and twisting moments) can be neglected as small quantities compared with the membrane forces acting on the shell. The theory can be a useful tool in cases when these theoretical assumptions approach physical reality.

The real advantage of membrane theory is the mathematical simplification; however, the simplification has only limited physical applications, as will be shown by the discussion of the boundary conditions. The present theory assumed the validity of Hooke's law (linear stress-strain relations) and that the shell thickness is relatively quite small compared with the general geometry of the shell.

To analyze the internal forces of the shell, an infinitely small element is cut out from the shell by two pairs of adjacent planes which are normal to the middle surface of the shell and which contain its principal curvatures (Figure 13).

The coordinate axes x and y are tangent at O to the lines of principal curvature and the axis z is normal to the middle surface. The principal radii of curvature which lie in the xz and yz planes are denoted by r_x and r_y.

The stresses acting on the plane faces of the element are resolved in the directions of the coordinate axes, and the stress components are denoted by the symbols σ_x, σ_y and τ_{xy}. The resultant membrane forces per unit length of the normal sections are shown in Figure 14.

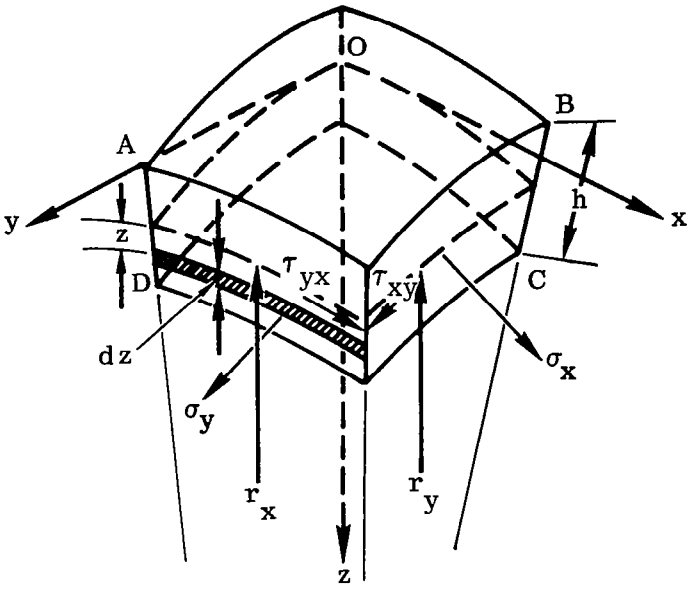

Figure 13. Shell Element

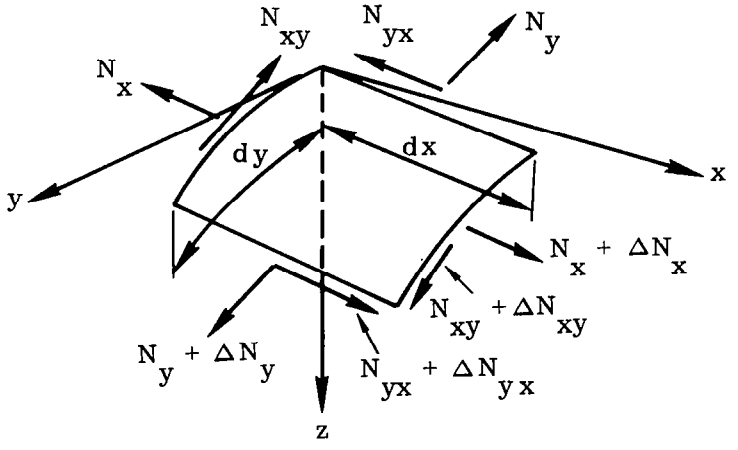

Figure 14. Resultant Membrane Forces

The forces per unit length of the normal sections can be expressed in the following form.

$$N_x = \int_{-h/2}^{h/2} \sigma_x \frac{(r_y - z)}{r_y} dz = \int_{-h/2}^{h/2} \sigma_x \left(1 - \frac{z}{r_y}\right) dz \tag{81}$$

$$N_y = \int_{-h/2}^{h/2} \sigma_y \frac{(r_x - z)}{r_x} dz = \int_{-h/2}^{h/2} \sigma_y \left(1 - \frac{z}{r_x}\right) dz \tag{82}$$

Similarly, one has

$$N_{xy} = \int_{-h/2}^{h/2} \tau_{xy} \left(1 - \frac{z}{r_y}\right) dz \tag{83}$$

and

$$N_{yx} = \int_{-h/2}^{h/2} \tau_{yx} \left(1 - \frac{z}{r_x}\right) dz \tag{84}$$

The small quantities z/r_x and z/r_y appear in Equations 81 through 84 because the lateral sides of the element shown in Figure 13 have a trapezoidal form due to the curvature of the shell.

Since the membrane theory assumed that the thickness h is very small in comparison with the radii r_x, r_y the terms z/r_x and z/r_y are omitted in Equations 81 through 84.

$$N_x = \sigma_x h, \quad N_y = \sigma_y h \quad \text{and} \quad N_{xy} = N_{yx} = \tau_{xy} h \tag{85}$$

since

$$\tau_{xy} = \tau_{yx} \tag{86}$$

Equation 85 represents one of the fundamental assumptions of membrane theory:

> "The forces N_x, N_y and N_{xy} obtained in this manner are sometimes called membrane forces, and the theory of shells based on the omission of bending stresses is called membrane theory." (See Reference 4, Page 433.)

The strains can be expressed based on the theoretical elasticity.

$$\left.\begin{aligned} \epsilon_x &= \frac{1}{E}[\sigma_x - \nu(\sigma_y + \sigma_z)] \\ \text{and} \\ \epsilon_y &= \frac{1}{E}[\sigma_y - \nu(\sigma_x + \sigma_z)] \end{aligned}\right\} \qquad (87)$$

where

E = modulus of elasticity

ν = Poisson's ratio

The stress σ_z may be assumed to be much smaller than stresses σ_x and σ_y in Equation 87, and its influence in Hooke's law may be neglected ($\sigma_z = 0$).

Equation 87 in this case may be written

$$\left.\begin{aligned} \epsilon_x &= \frac{1}{E}(\sigma_x - \nu\sigma_y) \\ \epsilon_y &= \frac{1}{E}(\sigma_y - \nu\sigma_x) \end{aligned}\right\} \qquad (88)$$

The solution of Equation 88 in terms of stresses leads to

$$\left.\begin{aligned} \sigma_x &= \frac{E}{(1 - \nu^2)}(\epsilon_x + \nu\epsilon_y) \\ \sigma_y &= \frac{E}{(1 - \nu^2)}(\epsilon_y + \nu\epsilon_x) \end{aligned}\right\} \qquad (89)$$

Equation 89 shows that the membrane stresses are reduced to a plane stress problem.

The equilibrium equations of some of the most important shell configurations will be discussed in the following subsections.

2.2.1.1 Membrane Theory of Cylindrical Shells. The differential equations of equilibrium will be derived for a cylindrical shell element. Figure 15a illustrates the general arrangement and Figure 15b shows the shell element and the membrane forces acting on the sides of the element. In addition, a load will be distributed over the surface of the element, the components of the intensity of this load being denoted by X, Y and Z.

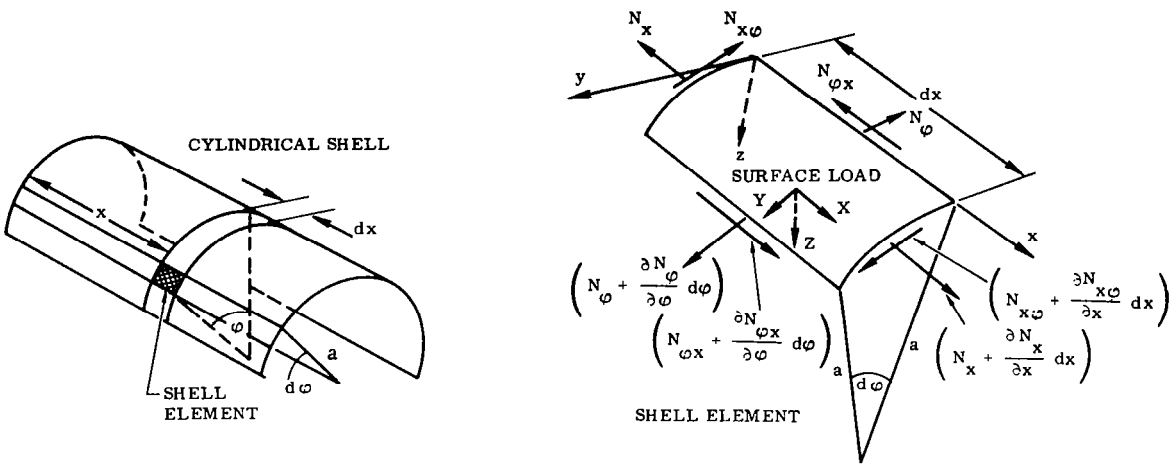

Figure 15. Membrane Forces Acting on Sides of Shell Element

Considering the equilibrium of the element and summing up the forces in the x-direction, one has

$$\frac{\partial N_x}{\partial x} a\, d\varphi\, dx + \frac{\partial N_{\varphi x}}{\partial \varphi} d\varphi\, dx + X a\, d\varphi\, dx = 0 \tag{90}$$

Similarly, the forces in the direction of the tangent to the normal cross section (in other words in the y-direction) expressed as the equation of equilibrium, are

$$\frac{\partial N_{x\varphi}}{\partial x} a\, d\varphi\, dx + \frac{\partial N_\varphi}{\partial \varphi} d\varphi\, dx + Y a\, d\varphi\, dx = 0 \tag{91}$$

The forces acting in the direction of the normal to the shell (in other words in the z-direction), are

$$N_\varphi d\varphi\, dx + Z a\, d\varphi\, dx = 0 \tag{92}$$

The differential equations of equilibrium can be written, after simplification, as follows.

$$\frac{\partial N_x}{\partial x} + \frac{1}{a}\frac{\partial N_{x\varphi}}{\partial \varphi} = -X \tag{93}$$

$$\frac{\partial N_{x\varphi}}{\partial x} + \frac{1}{a}\frac{\partial N_{\varphi}}{\partial \varphi} = -Y \tag{94}$$

$$N_{\varphi} = -Z\,a \tag{95}$$

2.2.1.2 Shells of Revolution with Axially Symmetric Loads. A surface of revolution is generated by the rotation of a plane curve about an axis in its plane. Figure 16 shows an element of a shell cut out by two adjacent meridians and two parallel circles. The position of a point on the shell is measured in the meridional direction by the angle θ, and in the so-called parallel direction by the angle φ. The angle φ is the angle between the normal surface vector and the coordinate z-axis. The meridional plane and the plane perpendicular to the meridian are the planes of principal curvature at any point on a surface of revolution, and the corresponding radii of curvature are designated by r_1 and r_2. The radius of the parallel circle is denoted by r_o and it can be expressed, based on Figure 16, as

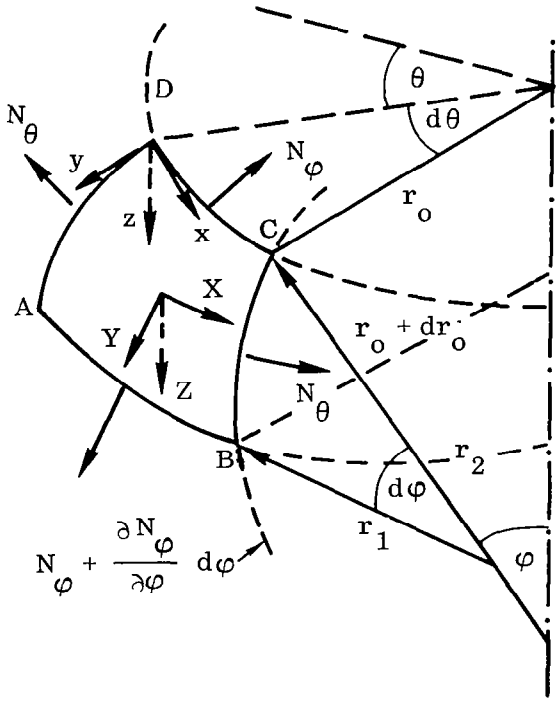

Figure 16. Element of Surface of Revolution

$$r_o = r_2 \sin\varphi \tag{96}$$

From the assumed symmetry of loading and deformation, it can be concluded that all the forces and deformations are independent of angle θ, and that there will be no shearing forces acting on the side of the element. The membrane forces per unit length are designated by N_φ and N_θ. The components of the external force per unit area of shell surface are designated by X, Y and Z; however, the assumption of symmetry requires that load X = 0. Again, the differential equations of equilibrium of the shell element will be derived.

The membrane force on the parallel curve $\widehat{DC}$ is

$$N_\varphi r_o d\theta \tag{97}$$

The force on curve $\widehat{AB}$ is (see Figure 16)

$$\left(N_\varphi + \frac{\partial N_\varphi}{\partial \varphi} d\varphi\right)(r_o + dr_o)\, d\theta = \left(N_\varphi + \frac{\partial N_\varphi}{\partial \varphi} d\varphi\right)\left(r_o + \frac{\partial r_o}{\partial \varphi} d\varphi\right) d\theta \tag{98}$$

The membrane force on meridional curve $\widehat{BC}$ is

$$N_\theta r_1 d\varphi \tag{99}$$

Figure 17 shows the components of membrane forces N_θ in a meridional plane.

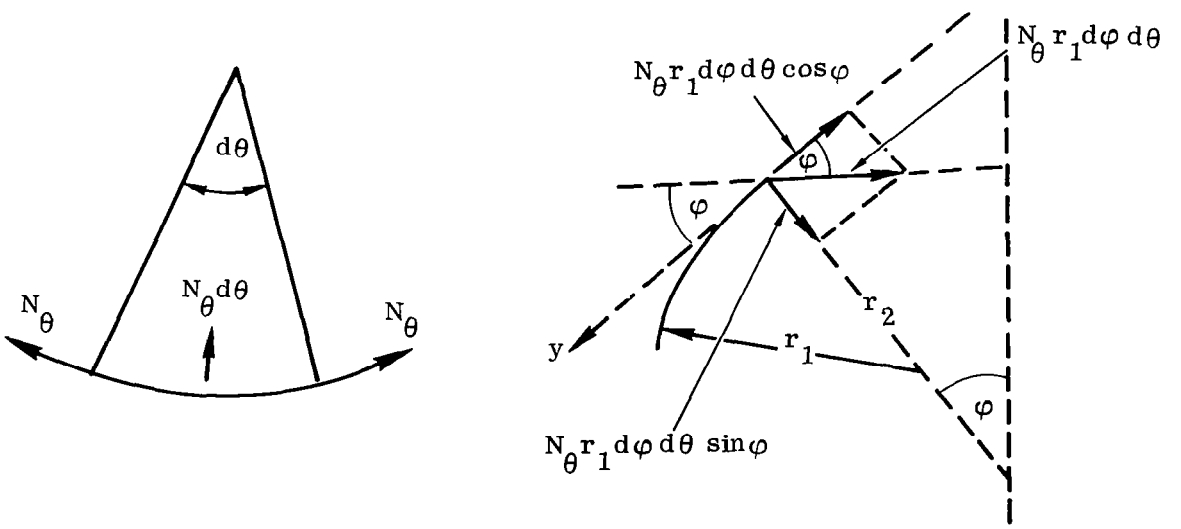

Figure 17. Membrane Force Components on a Surface of Revolution

It can be seen from Figure 17 that force N_θ has a component in the direction of the tangent meridians (y-direction).

$$-N_\theta r_1 d\varphi d\theta \cos\varphi \tag{100}$$

The component of external force in the same direction is

$$Y r_1 r_o d\varphi\, d\theta \tag{101}$$

Summing up forces in the direction tangent to the meridian (in direction y), according to Equations 98, 97, 100, and 101, the equation of equilibrium is

$$\left(N_\varphi + \frac{\partial N_\varphi}{\partial \varphi} d\varphi\right)\left(r_o + \frac{\partial r_o}{\partial \varphi} d\varphi\right) d\theta - N_\varphi r_o d\theta - N_\theta r_1 d\varphi\, d\theta \cos\varphi$$

$$+ Y r_o d\theta\, r_1 d\varphi = 0 \tag{102}$$

Neglecting a small quantity of second order, Equation 102 becomes

$$\frac{\partial N_\varphi}{\partial \varphi} r_o d\varphi\, d\theta + N_\varphi \frac{\partial r_o}{\partial \varphi} d\varphi\, d\theta - N_\theta r_1 \cos\varphi\, d\varphi\, d\theta + Y r_o r_1 d\varphi\, d\theta = 0 \tag{103}$$

since

$$\frac{\partial N_\varphi}{\partial \varphi} r_o d\varphi\, d\theta + N_\varphi \frac{\partial r_o}{\partial \varphi} d\varphi\, d\theta = \frac{\partial}{\partial \varphi}(N_\varphi r_o)\, d\varphi\, d\theta \tag{104}$$

Substitution of Equation 104 into Equation 103 and division of Equation 103 by $d\varphi\, d\theta$ yields the equation of equilibrium of forces in a direction tangent to the meridian.

$$\frac{\partial}{\partial \varphi}(r_o N_\varphi) - N_\theta r_1 \cos\varphi = -Y r_o r_1 \tag{105}$$

The second equation of equilibrium is obtained by summing the projections of the forces in the direction normal to the shell surface (in the z-direction). Figure 18 shows the forces acting on the upper and lower sides of the element. The resultant force, based on Figure 18, is

$$N_\varphi r_o d\theta\, d\varphi \tag{106}$$

The component of the lateral force, N_θ, acting in the z-direction is, according to Figure 17,

$$N_\theta r_1 d\varphi\, d\theta \sin\varphi \tag{107}$$

The external load acting on the shell element also has a component in this direction.

$$Z r_1 r_o d\theta\, d\varphi \tag{108}$$

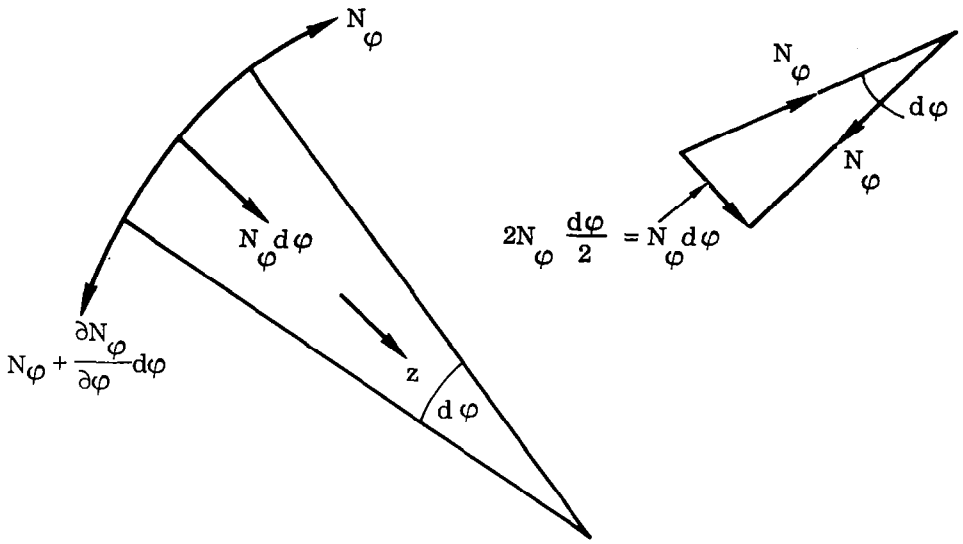

Figure 18. Forces Acting on Elements

Summing up the forces from Equations 106, 107 and 108, the following equation can be obtained.

$$N_\varphi \, d\varphi \, r_o \, d\theta + N_\theta \, r_1 \, d\varphi \, d\theta \sin \varphi + Z \, r_o \, d\theta \, r_1 \, d\varphi = 0 \tag{109}$$

The substitution of Equation 96 into Equation 106 and division of Equation 106 by $d\theta \, d\varphi$ yields the equilibrium equation in the z-direction.

$$\frac{N_\varphi}{r_1} + \frac{N_\theta}{r_2} = -Z \tag{110}$$

The two equilibrium equations are the functions of the independent variable φ. These equations can also be expressed as the independent variable of the meridian length s, or as the independent variable of the z-coordinate. Figure 19 shows the meridional curve of the shell. The line element ds of the meridian can be written

$$ds = r_1 \, d\varphi \tag{111}$$

The line element dz of the z-coordinate is expressed as

$$dz = ds \sin \varphi \tag{112}$$

Equations 111 and 112 lead also to the following relation.

$$dz = r_1 \sin \varphi \, d\varphi \tag{113}$$

Equation 111 can be expressed as

$$\frac{\partial}{\partial \varphi} = r_1 \frac{\partial}{\partial s} \tag{114}$$

The substitution of Equation 114 into Equations 105 and 110 and the replacement of the subindex φ by s gives another type of equation of equilibrium for shells of revolution.

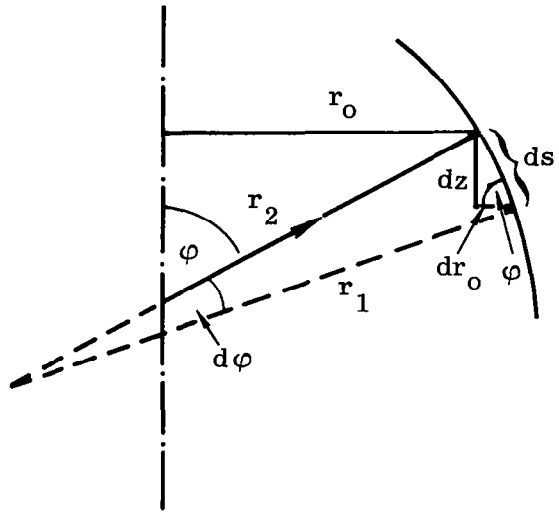

Figure 19. Meridional Curve

$$\frac{\partial}{\partial s}(r_o N_s) - N_\theta \cos \varphi = -Y r_o \tag{115}$$

$$\frac{N_s}{r_1} + \frac{N_\theta}{r_2} = -Z \tag{116}$$

Equation 113 may be expressed as

$$\frac{\partial}{\partial \varphi} = r_1 \sin \varphi \frac{\partial}{\partial z} \tag{117}$$

Substituting differential operator 117 into Equations 105 and 110 and replacing subindex φ by z, one has

$$\frac{\partial}{\partial z}(r_o N_z) - N_\theta \cos \varphi = -Y r_2 \tag{118}$$

$$\frac{N_z}{r_1} + \frac{N_\theta}{r_2} = -Z \tag{119}$$

2.2.1.3 Equilibrium Equation of a Symmetrically Loaded Conical Shell. Figure 20 shows the coordinate system which is suitable for a conical shell.

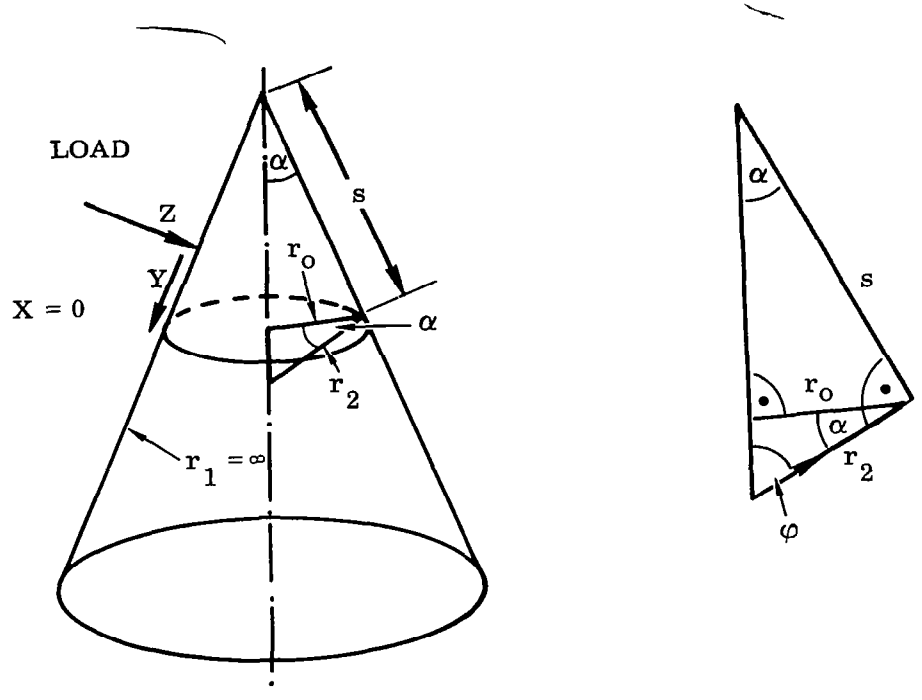

Figure 20. Conical Shell Coordinate System

It can be concluded from Figure 20 that

$$\left.\begin{aligned} \varphi &= \frac{\pi}{2} - \alpha \\ r_o &= s \sin \alpha \\ r_2 &= s \tan \alpha \\ r_1 &= \infty \end{aligned}\right\} \qquad (120)$$

It is assumed that the conical shell is loaded symmetrically by the external forces; therefore, Equations 115 and 116 are applicable in the present case. Substituting Equation 120 into Equations 115 and 116 yields

$$\frac{\partial}{\partial s}(s \sin \alpha \, N_s) - N_\theta \cos\left(\frac{\pi}{2} - \alpha\right) = - Y s \sin \alpha \qquad (121)$$

$$\frac{N_s}{\infty} + \frac{N_\theta}{s \tan \alpha} = - Z \tag{122}$$

The equilibrium equations of the conical shell, in the final form, are

$$\frac{\partial}{\partial s}(s N_s) - N_\theta = - s Y \tag{123}$$

$$N_\theta = - Z s \tan \alpha \tag{124}$$

2.2.1.4 Equilibrium Equation of a Symmetrically Loaded Cylindrical Shell. The general case of external loading was derived by Equations 93, 94 and 95. In the case of a symmetrical load, the following assumptions can be made.

$$N_{x\varphi} = N_{\varphi x} = Y = 0 \tag{125}$$

Equations 93 through 95 can be reduced by the previous assumptions to

$$\frac{\partial N_x}{\partial x} = - X \tag{126}$$

$$N_\varphi = - Z a \tag{127}$$

where force N_φ is independent of angle φ.

These equations can also be derived from Equations 118 and 119 with the following assumptions.

$$\left.\begin{aligned} \varphi &= \frac{\pi}{2} \\ r_o &= r_2 = a \\ r_1 &= \infty \end{aligned}\right\} \tag{128}$$

Equations 118 and 119 become

$$\frac{\partial}{\partial z}(N_z) = - Y \tag{129}$$

and

$$N_\theta = - Z a \tag{130}$$

Equations 126 and 127 differ only in symbology when compared with Equations 129 and 130.

2.2.1.5 Strain-Displacement Equations of Membrane Shells. In the following discussions the secondary strains were neglected. (For further explanation, see Figure 13 and Equations 81 through 84.)

Strain-Displacement Relations of a Cylinder. Figure 21 illustrates the general arrangement, the directions of the coordinate system, and two arbitrary points, A and B, on the surface of the shell. The displacements of the shell are in the longitudinal direction, u; circumferential direction, v; and normal direction, w (+w toward the center of the cylinder).

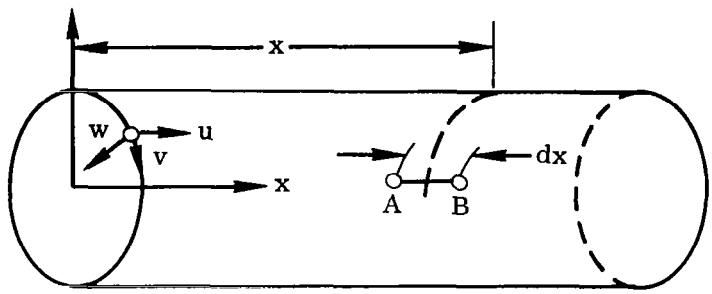

Figure 21. General Arrangement

Figure 22 shows the deformations of points A and B in the longitudinal direction. Unprimed letters represent the undeformed state, and the primed letters express the deformed state.

The strain is in the longitudinal direction.

$$\epsilon_x = \frac{\overline{BB'} - \overline{AA'}}{\widehat{AB}}$$

$$= \frac{\left(u + \frac{\partial u}{\partial x} dx\right) - u}{dx}$$

$$= \frac{\partial u}{\partial x} \qquad (131)$$

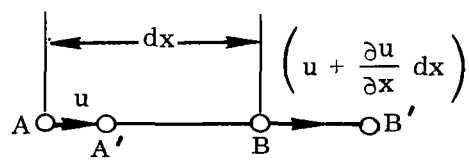

Figure 22. Points A and B Deformation

Figure 23 demonstrates the shell deformations in the circumferential direction.

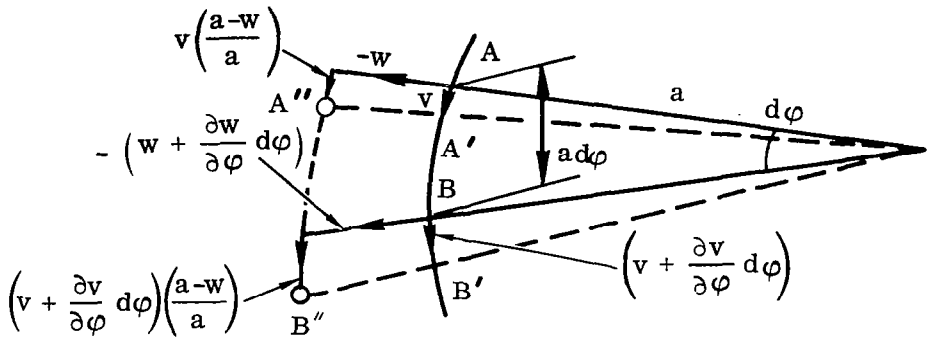

Figure 23. Circumferential Deformations of Cylindrical Shell

The undeformed points, A and B, have deformations not only in the circumferential direction, A′ and B′, but the cylinder and consequently points A′ and B′ also move in the radial direction. The final positions of the points A and B are A″ and B″, since

$$\widehat{A'B'} = \widehat{AB} + \widehat{BB'} - \widehat{AA'} = a\,d\varphi + \left(v + \frac{\partial v}{\partial \varphi} d\varphi\right) - v$$

or

$$\widehat{A'B'} = a\,d\varphi + \frac{\partial v}{\partial \varphi} d\varphi \tag{132}$$

Similarly, one has

$$\widehat{A''B''} = \widehat{A'B'}\left(\frac{a-w}{a}\right) = \left(a\,d\varphi + \frac{\partial v}{\partial \varphi} d\varphi\right)\left(1 - \frac{w}{a}\right) \tag{133}$$

The circumferential strain can be expressed on the basis of the previous derivations.

$$\epsilon_\varphi = \frac{\widehat{A''B''} - \widehat{AB}}{\widehat{AB}} = \frac{\left(a\,d\varphi + \frac{\partial v}{\partial \varphi} d\varphi\right)\left(1 - \frac{w}{a}\right) - a\,d\varphi}{a\,d\varphi}$$

Finally, one has

$$\epsilon_\varphi = \frac{1}{a}\frac{\partial v}{\partial \varphi} - \frac{w}{a} \tag{134}$$

The shear-strain is the sum of the rotations of the two line elements dx and $a\,d\varphi$ (see Figure 24).

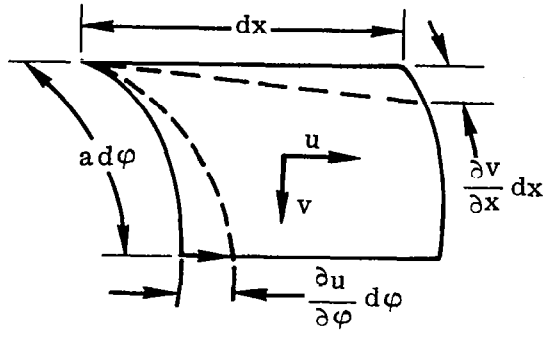

Figure 24. Shear Strain

$$\gamma_{x,\varphi} = \frac{\frac{\partial v}{\partial x}\,dx}{dx} + \frac{\frac{\partial u}{\partial \varphi}\,d\varphi}{a\,d\varphi} = \frac{\partial v}{\partial x} + \frac{1}{a}\frac{\partial u}{\partial \varphi} \tag{135}$$

The derived strain-displacement relations are in correspondence with the load functions assumed in Section 2.2.1.1.

Strain-Displacement Relations of Shells of Revolution. The external load is assumed to be distributed symmetrically on the shell; therefore, the deformations also have symmetry

$$\gamma_{\varphi,\theta} = 0 \tag{136}$$

Figure 25 shows again two points, A and B, on the shell in the meridional plane of the surface. The unprimed letters again correspond to the undeformed state, and the primed letters designate the deformed state. The displacement of the shell in the tangential direction is v, and the displacement in the normal direction of the surface is w. The deformation of the shell can again be resolved in the tangential and normal directions.

The points A and B moved due to the tangential deformation to the positions of A′ and B′.

$$\widehat{A'B'} = \widehat{AB} + \widehat{BB'} - \widehat{AA'} = r_1\,d\varphi + \left(v + \frac{\partial v}{\partial \varphi}\,d\varphi\right) - v$$

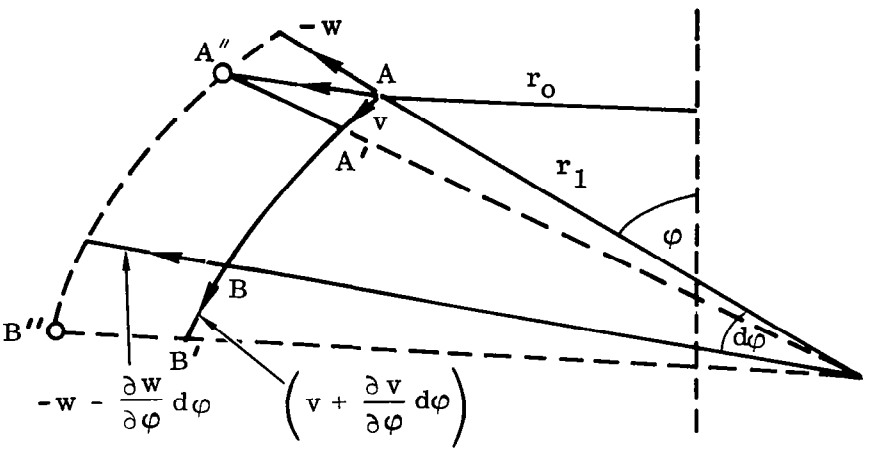

Figure 25. Strain-Displacement Relations of Surface of Revolution

Therefore

$$\widehat{A'B'} = r_1 d\varphi + \frac{\partial v}{\partial \varphi} d\varphi \tag{137}$$

Due to the normal deformation of the shell, the point A′ and B′ moved to the final positions A″ and B″. The following relations can be written, based on Figure 25.

$$\widehat{A''B''} = \widehat{A'B'}\left(\frac{r_1 - w}{r_1}\right) = \left(r_1 d\varphi + \frac{\partial v}{\partial \varphi} d\varphi\right)\left(1 - \frac{w}{r_1}\right) \tag{138}$$

The tangential strain can be expressed

$$\epsilon_\varphi = \frac{\widehat{A''B''} - \widehat{AB}}{\widehat{AB}} = \frac{\left(r_1 d\varphi + \frac{\partial v}{\partial \varphi} d\varphi\right)\left(1 - \frac{w}{r_1}\right) - r_1 d\varphi}{r_1 d\varphi} \tag{139}$$

Ignoring the second-order quantity, $\frac{\partial v}{\partial \varphi} d\varphi \frac{w}{r_1}$, the tangential strain is expressed.

$$\epsilon_\varphi = \frac{1}{r_1}\left(\frac{\partial v}{\partial \varphi} - w\right) \tag{140}$$

The circumferential deformation of the shell can be seen in Figure 26. The deformation and the corresponding strain are now in the parallel plane of the shell.

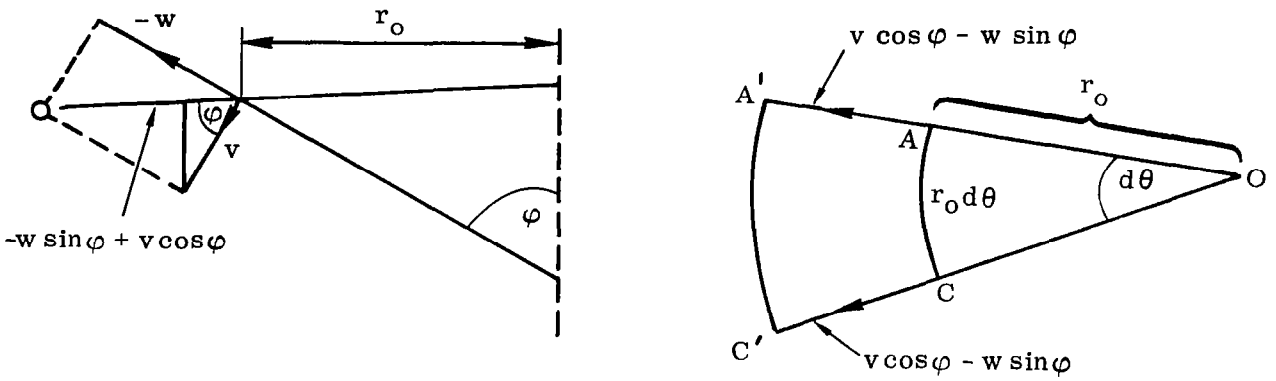

Figure 26. Circumferential Deformation of Surface of Revolution

The undeformed state is expressed by points A and C and the deformed state by A′ and C′.

The circumferential strain is

$$\epsilon_\theta = \frac{\widehat{A'C'} - \widehat{AC}}{\widehat{AC}} = \frac{(\widehat{OA} + \widehat{AA'})d\theta - \widehat{OA}\,d\theta}{\widehat{OA}\,d\theta}$$

because

$$\epsilon_\theta = \frac{(r_o + v\cos\varphi - w\sin\varphi)d\theta - r_o d\theta}{r_o d\theta} \tag{141}$$

By substitution of Equation 96 into Equation 141, the circumferential strain, is in the final form,

$$\epsilon_\theta = \frac{1}{r_2}(v\cot\varphi - w) \tag{142}$$

Strain-Displacement Relations of Conical Shells. It is assumed that the external load is symmetric; therefore, the deformations of the conical shell are also symmetric. The strains can be derived in this case as the degenerate case of the shells of revolution. Differential operator 114 was substituted into Equation 140.

$$\epsilon_{\varphi} = \frac{1}{r_1}\left[r_1 \frac{\partial v}{\partial s} - w\right] = \frac{\partial v}{\partial s} - \frac{w}{r_1} \tag{143}$$

The conical shell can be specified by the following data.

Substituting Equation 120 into Equations 143 and 142, one has

$$\epsilon_{\varphi} = \frac{\partial v}{\partial s} - \frac{w}{\infty} = \frac{\partial v}{\partial s} \tag{144}$$

$$\epsilon_{\theta} = \frac{1}{s \tan \alpha}(v \tan \alpha - w) = \frac{v}{s} - \frac{w}{s} \cot \alpha \tag{145}$$

In the case of a small cone angle, α, the following assumption may be made.

$$w \cot \alpha \gg v \tag{146}$$

Equation 145 was reduced in this case.

$$\epsilon_{\theta} = -\frac{w \cot \alpha}{s} \tag{147}$$

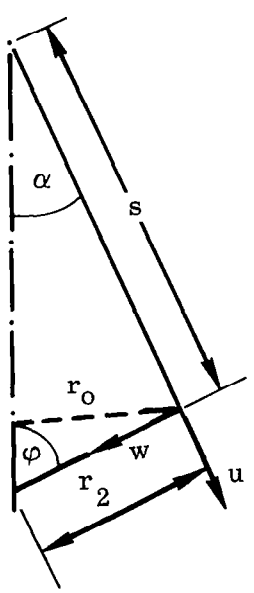

Figure 27. Conical Shell Notation

Figure 27 shows the customary notation of the conical shell; therefore, the longitudinal strain is expressed by Equation 144.

$$\epsilon_s = \frac{\partial u}{\partial s} \tag{148}$$

The circumferential strain is unchanged.

$$\epsilon_{\theta} = -\frac{w \cot \alpha}{s} \tag{149}$$

2.2.1.6 Static Problems. The following static problems serve a comparison purpose with the equivalent dynamic problems. It can be seen in the following discussion that the order of differential equations is not the same in the case of statics as it is in dynamics. As a consequence, the order of

displacement functions and the arbitrary constants are not necessarily the same in the two different cases.

Stresses and Displacements of a Sphere by a Uniform Load. Figure 28 shows a half sphere loaded by a uniform pressure, p.

a. Calculation of the Stresses of the Shell. The load function is

$$Y = 0 \quad \text{and} \quad Z = p \tag{150}$$

One has, from the geometry of the sphere,

$$r_1 = r_2 = a$$

and (151)

$$r_o = a \sin \varphi$$

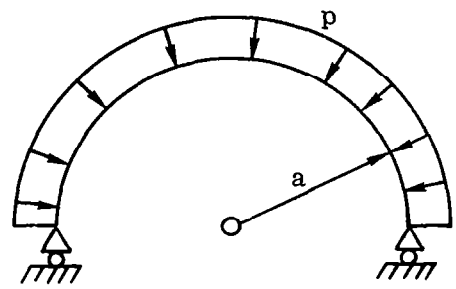

Figure 28. Loaded Half Sphere

Equations 105 and 110 become, in the case of the spherical shell,

$$\frac{\partial}{\partial \varphi}(a \sin \varphi \, N_\varphi) - N_\theta \, a \cos \varphi = 0 \tag{152}$$

$$\frac{N_\varphi}{a} + \frac{N_\theta}{a} = -p \tag{153}$$

The substitution of Equation 153 into Equation 152 yields

$$\frac{d}{d\varphi}(\sin \varphi \, N_\varphi) + N_\varphi \cos \varphi = -p \, a \cos \varphi \tag{154}$$

Let the new independent variable

$$x = \cos \varphi \qquad \text{and} \qquad \frac{d}{d\varphi} = -(1 - x^2)^{1/2} \frac{d}{dx} \tag{155}$$

Equation 154 becomes, by substitution of Expression 155,

$$-(1 - x^2)^{1/2} \frac{d}{dx}\left[(1 - x^2)^{1/2} N_\varphi\right] + x N_\varphi = -p a x$$

or

$$-\frac{d}{dx}\left[(1 - x^2) N_\varphi\right] = -p a x \tag{156}$$

The result after integration of Equation 156 is

$$N_\varphi = \frac{p a x^2}{2(1 - x^2)} + \frac{C}{(1 - x^2)} \tag{157}$$

where C is an arbitrary constant.

The constant, C, can be evaluated from the condition of the support. Based on Figure 29, the following equation can be written

$$p a^2 \pi = - 2 \pi a N_\varphi \Big|_{x=0} \tag{158}$$

The solution of Equation 158 is

$$C = - \frac{p a}{2} \tag{159}$$

Equation 157 is, by the use of Expression 159

$$N_\varphi = - \frac{p a}{2} \tag{160}$$

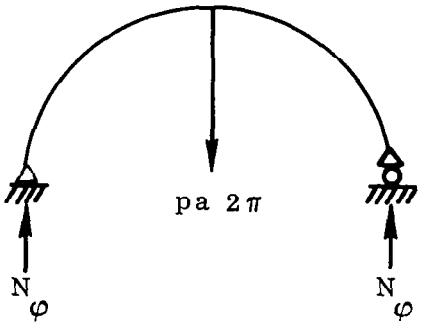

Figure 29. Forces on a Half Spherical Shell

The following relation can be obtained from Equation 153.

$$N_\theta = - p a - N_\varphi = - p a + \frac{p a}{2} = - \frac{p a}{2} \tag{161}$$

The stresses of the shell can be written

$$\sigma_\varphi = \sigma_\theta = \frac{N_\varphi}{h} = - \frac{p a}{2 h} \tag{162}$$

where h is the thickness of the shell.

b. Calculation of the Displacements of the Shell. Based on Equation 162, the following equations can be written

$$N_\varphi = N_\theta$$

Therefore

$$\epsilon_\varphi = \epsilon_\theta \tag{163}$$

Equation 163 can be expressed by the displacements (see Equations 140 and 142)

$$\frac{\partial v}{\partial \varphi} - w = v \cot \varphi - w$$

or

$$\int \frac{dv}{v} = \int \cot \varphi \, d\varphi \tag{164}$$

After integration, one has

$$v = C(1 - x^2)^{1/2} \tag{165}$$

The arbitrary constant C can again be evaluated from the boundary condition at the support, which is

$$v(0) = 0$$

Therefore

$$C = 0 \tag{166}$$

The tangential displacement is

$$v \equiv 0 \tag{167}$$

Similarly

$$N_\varphi = \frac{E\,h}{(1 - \nu^2)} (\epsilon_\varphi + \nu \epsilon_\theta) = \frac{E\,h}{(1 - \nu)} \epsilon_\theta \tag{168}$$

Substituting the values of Expressions 160 and 167, the following equation can be obtained.

$$-\frac{p\,a}{2} = -\frac{E\,h\,w}{a\,(1 - \nu)} \tag{169}$$

Expressing w from the last equation, one has

$$w = \frac{p\,a^2(1 - \nu)}{2\,E\,h} \tag{170}$$

Figure 30 shows the deformation of the shell.

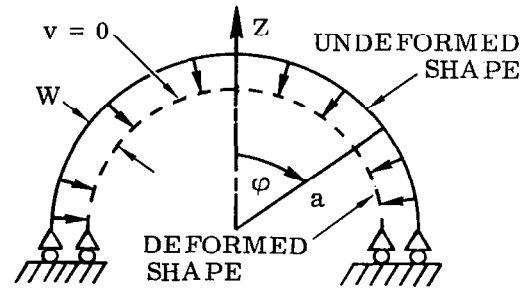

Figure 30. Shell Deformation

Membrane Cylinder Loaded with a Uniform Force Parallel with the Axis. A membrane cylinder is loaded with a uniform force parallel with the axis as shown in Figure 31.

a. Calculation of the Membrane Forces. The force per unit length on the periphery of the cylinder is

$$P_o = \frac{F}{2\pi a} \tag{171}$$

Because of symmetry, one has

$$N_{x\varphi} = \frac{\partial N_\varphi}{\partial \varphi} = 0 \tag{172}$$

The load functions are the following

$$X = Y = Z = 0 \tag{173}$$

Equations 93, 94, and 95 can be expressed as

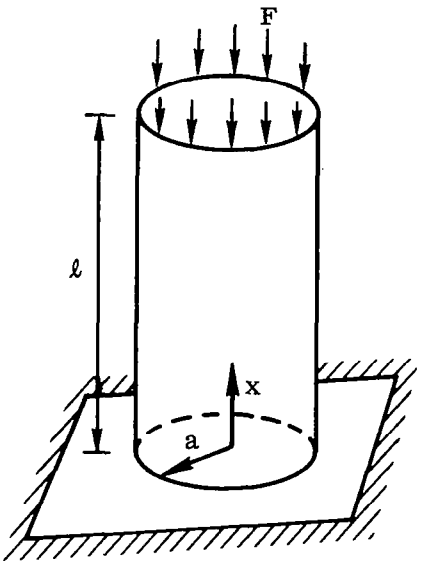

Figure 31. Axially Loaded Membrane Cylinder

$$\frac{\partial N_x}{\partial x} = 0 \tag{174}$$

$$N_\varphi = 0 \tag{175}$$

The integration of Equation 174 leads to

$$N_x = \text{Constant} = C \tag{176}$$

The boundary conditions are, in this case

$$N_x = N_x\Big|_{x=0} = N_x\Big|_{x=\ell} = -P_o \tag{177}$$

Therefore

$$C = -P_o$$

b. Calculation of the Displacements. Equation 175 can be obtained as

$$N_\varphi = \frac{E\,h}{(1-\nu^2)}(\epsilon_\varphi + \nu\epsilon_x) = 0$$

Therefore

$$\epsilon_{\varphi} = -\nu\epsilon_{x} \tag{178}$$

The membrane force, N_x, can be expressed, based on Equations 178 and 131 as

$$N_x = \frac{E\,h}{(1-\nu^2)}(\epsilon_x + \nu\epsilon_{\varphi}) = E\,h\,\epsilon_x = -P_o$$

since

$$\epsilon_x = \frac{\partial u}{\partial x} = -\frac{P_o}{E\,h} \tag{179}$$

Integrating Equation 179, one has

$$u(x) = -\frac{P_o\,x}{E\,h} \tag{180}$$

The circumferential strain was expressed, according to Equation 134

$$\epsilon_{\varphi} = \frac{1}{a}\left(\frac{\partial v}{\partial \varphi} - w\right) = -\frac{w}{a} \tag{181}$$

Because of symmetry

$$\frac{\partial v}{\partial \varphi} = 0$$

The use of Relations 178 and 179 leads to

$$\epsilon_{\varphi} = -\frac{w}{a} = -\nu\epsilon_x = \frac{\nu P_o}{E\,h} \tag{182}$$

The radial displacement, w, can be expressed from Equation 182 as

$$w = -\frac{\nu a P_o}{E\,h} \tag{183}$$

Figure 32 shows the deformation of the shell. It is obvious that the boundary conditions in this case are a function of the loading condition.

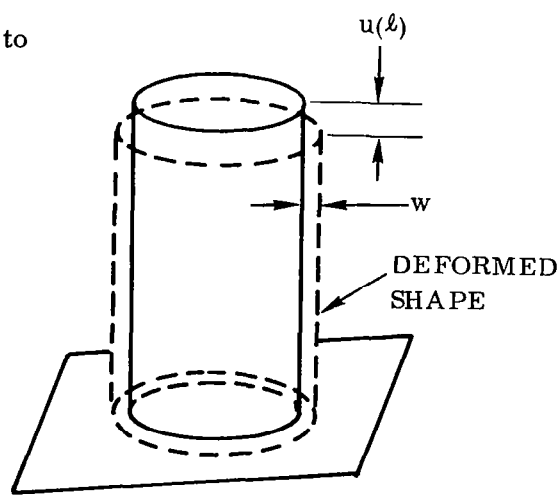

Figure 32. Cylindrical Shell Deformation

Stresses and Deformations of a Pressurized Cylindrical Membrane Shell. Figure 33 shows the cylindrical membrane shell which is pressurized and covered by a rigid plate. Since the technique of solution is the same as in the previous problem, the calculation and explanation will, in this case, be rather brief.

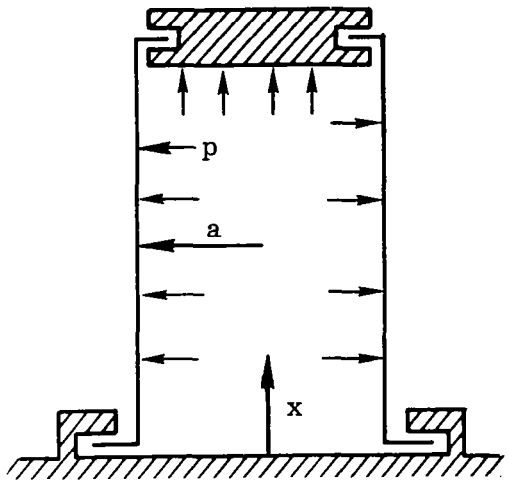

Figure 33. Pressurized Cylindrical Shell

a. Membrane Forces. Because of symmetry

$$N_{x\varphi} = N_{\varphi x} = 0 \tag{184}$$

The loading functions are

$$X = Y = 0 \qquad Z = -p \tag{185}$$

The differential equations are

$$\frac{\partial N_x}{\partial x} = 0 \tag{186}$$

$$\frac{\partial N_\varphi}{\partial \varphi} = 0 \tag{187}$$

$$N_\varphi = p\,a \tag{188}$$

Integrating Equations 186 and 187, one has

$$\left.\begin{aligned} N_x &= \text{Constant} = C_1 \\ N_\varphi &= \text{Constant} = p\,a \end{aligned}\right\} \tag{189}$$

The force is in the axial direction

$$F = p\,a^2\,\pi$$

The axial force, P_o, on the shell is

$$P_o = \frac{F}{2\,a\,\pi} = \frac{p\,a^2\,\pi}{2\,a\,\pi} = \frac{p\,a}{2} = C_1$$

Therefore

$$\boxed{\begin{aligned} N_x &= \frac{p\,a}{2} \\ N_\varphi &= p\,a \end{aligned}} \tag{190}$$

b. Displacements. The membrane force and displacement relations, from the previous calculations, are

$$\left.\begin{aligned} \frac{pa}{2} &= \frac{Eh}{(1-\nu^2)}\left(\frac{\partial u}{\partial x} - \frac{\nu}{a}w\right) \\ pa &= \frac{Eh}{(1-\nu^2)}\left(-\frac{w}{a} + \nu\frac{\partial u}{\partial x}\right) \end{aligned}\right\} \quad (191)$$

The solution of Equation 191 leads to the desired displacement functions.

$$u(x) = \frac{pax}{Eh}\left(\frac{1}{2} - \nu\right) \quad (192)$$

$$w = -\frac{pa^2}{Eh}\left(1 - \frac{\nu}{2}\right) \quad (193)$$

Figure 34 illustrates the deformations.

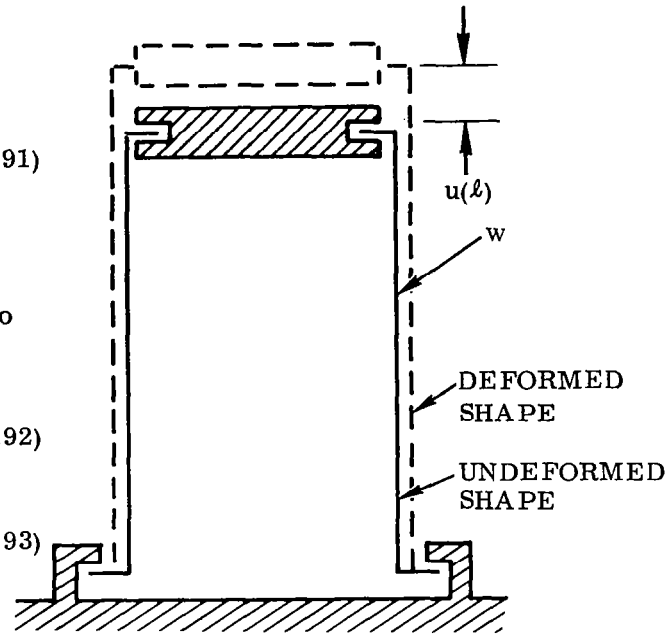

Figure 34. Pressurized Cylindrical Shell Deformations

Practical Applications of Paragraph 2.2.1.6 in the Theory of Missiles. The importance of longitudinal oscillation is well known in the control theory of missiles. The derivation of the spring-mass longitudinal model is based on the problems discussed in Paragraph 2.2.1.6.

3/DYNAMICS OF MEMBRANE SHELLS

3.1 FREE VIBRATION OF A THIN SPHERICAL SHELL

It is assumed that the shell is vibrating axisymmetrically. The equilibrium equations of a shell element can be used (see previous derivations).

$$\frac{\partial}{\partial \varphi}(r_o N_\varphi) - N_\theta r_1 \cos\varphi = -Y r_o r_1 \qquad (105)$$

$$\frac{N_\varphi}{r_1} + \frac{N_\theta}{r_2} = -Z \qquad (110)$$

Again,

$$r_1 = r_2 = a$$

and

$$r_o = a \sin\varphi$$

(See Figure 35.)

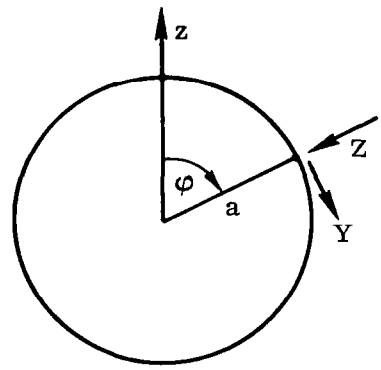

Figure 35. Coordinate System of Thin Spherical Shell

The external forces can be written in terms of the inertial forces of the shell.

$$\left.\begin{aligned} Y &= -\rho h \frac{\partial^2 v}{\partial t^2} \\ Z &= -\rho h \frac{\partial^2 w}{\partial t^2} \end{aligned}\right\} \qquad (194)$$

where

v = tangential displacement of the shell

w = normal displacement of the shell

ρ = mass density of the shell

h = thickness of the shell

The forces on the shell are, according to Equations 140 and 142

$$N_\varphi = \frac{E\,h}{(1-\nu^2)}(\epsilon_\varphi + \nu\,\epsilon_\theta) = \frac{E\,h}{(1-\nu^2)a}\left[\frac{\partial v}{\partial \varphi} + \nu\, v \cot\varphi - (1+\nu)\,w\right] \tag{195}$$

$$N_\theta = \frac{E\,h}{(1-\nu^2)}(\epsilon_\theta + \nu\,\epsilon_\varphi) = \frac{E\,h}{(1-\nu^2)a}\left[\nu\frac{\partial v}{\partial \varphi} + v\cot\varphi - (1+\nu)\,w\right] \tag{196}$$

where

E = modulus of elasticity

ν = Poisson's ratio

Equations 105 and 110 can, in the case of a spherical shell, be expressed

$$\sin\varphi\,\frac{\partial N_\varphi}{\partial \varphi} + (N_\varphi - N_\theta)\cos\varphi = -Y\,a\sin\varphi \tag{197}$$

$$N_\varphi + N_\theta = -a\,Z \tag{198}$$

The substitutions of Equations 194, 195 and 196 into Equations 197 and 198 lead to

$$\frac{\partial^2 v}{\partial \varphi^2} + \cot\varphi\,\frac{\partial v}{\partial \varphi} - (1+\nu)\frac{\partial w}{\partial \varphi} - (\nu + \cot^2\varphi)\,v = A\,\frac{\partial^2 v}{\partial t^2} \tag{199}$$

$$\frac{\partial v}{\partial \varphi} + v\cot\varphi - 2w = B\,\frac{\partial^2 w}{\partial t^2} \tag{200}$$

where

$$A = \frac{\rho\,a^2(1-\nu^2)}{E} \qquad \text{and} \qquad B = \frac{\rho\,a^2(1-\nu)}{E} \tag{201}$$

The partial differential equations (199 and 200) are the mathematical representation of a thin vibrating spherical shell. The unknown frequencies and mode shapes of the vibrating spherical shell may be obtained by the solutions of these equations. The first attempt is to reduce these equations to ordinary differential equations. Let us assume separation of variables and let

$$\left.\begin{aligned} v_n(\varphi, t) &= v_n(\varphi)\cdot T_n/t) \\ w_n(\varphi, t) &= w_n(\varphi)\cdot T_n/t) \end{aligned}\right\} \tag{202}$$

where

T_n = harmonic time function

v_n = tangential mode shapes

w_n = normal mode shapes

Assuming harmonic motion, one has

$$\frac{d^2 T_n}{dt^2} + p_n^2 T_n = 0 \tag{203}$$

where

p_n = angular frequency (rad/sec)

The substitution of Equations 202 and 203 into Equations 199 and 200 leads to

$$\frac{d^2 v_n}{d\varphi^2} + \cot\varphi \frac{dv_n}{d\varphi} - (1 + \nu) \frac{dw_n}{d\varphi} - (\nu + \cot^2\varphi) \nu_n = -A p_n^2 v_n \tag{204}$$

$$\frac{dv_n}{d\varphi} + v_n \cot\varphi - 2w_n = -B p_n^2 w_n \tag{205}$$

w_n can be expressed from Equation 205 as

$$w_n = \frac{\frac{dv_n}{d\varphi} + v_n \cot\varphi}{(2 - B p_n^2)} \tag{206}$$

For mathematical convenience, the independent variable, φ, was replaced by $x = \cos\varphi$. Therefore

$$\left.\begin{aligned} x &= \cos\varphi \\ \frac{d}{d\varphi} &= -\sqrt{1 - x^2}\,\frac{d}{dx} \\ \frac{d^2}{d\varphi^2} &= (1 - x^2)\frac{d^2}{dx^2} - x\frac{d}{dx} \end{aligned}\right\} \tag{207}$$

The use of differential operators 207 in Equations 204 and 206 yields

$$(1 - x^2)\frac{d^2v_n}{dx^2} - 2x\frac{dv_n}{dx} + (1 + \nu)\sqrt{1 - x^2}\,\frac{dw_n}{dx}$$

$$- \left[\frac{\nu}{(1 - x^2)} + \frac{(1 - \nu)x^2}{(1 - x^2)} - A p_n^2\right] v_n = 0 \tag{208}$$

$$w_n = \frac{-\sqrt{1 - x^2}\,\dfrac{dv_n}{dx} + \dfrac{x}{\sqrt{1 - x^2}}\,v_n}{(2 - B p_n^2)} \tag{209}$$

By substituting Equation 209 into Equation 208, the problem of the vibrating spherical shell was reduced to a single differential equation.

$$(1 - x^2)\frac{d^2v_n}{dx^2} - 2x\frac{dv_n}{dx} + \left[\frac{(2 - B p_n^2)(A p_n^2 + 1 - \nu)}{(1 - \nu - B p_n^2)} - \frac{1}{1 - x^2}\right] v_n = 0 \tag{210}$$

Equation 210 represents the vibration of a thin spherical shell. Let

$$\lambda_n = \frac{(2 - B p_n^2)(A p_n^2 + 1 - \nu)}{(1 - \nu - B p_n^2)} \tag{211}$$

where λ_n represents the frequency equation. Introducing λ_n in Equation 210 yields

$$(1 - x^2)\frac{d^2v_n}{dx^2} - 2x\frac{dv_n}{dx} + \left(\lambda_n - \frac{1}{1 - x^2}\right) v_n = 0 \tag{212}$$

The solution of Equation 212 proceeds as follows. This second-order differential equation is an ordinary differential equation with variable coefficients. It is a Legendre type of differential equation and can be satisfied by the Legendre functions. The Legendre type of differential equation is, in general

$$(1 - x^2)\frac{d^2y_n}{dx^2} - 2x\frac{dy_n}{dx} + \left[n(n + 1) - \frac{m^2}{(1 - x^2)}\right] y_n = 0 \tag{213}$$

The general solution of this equation is the Legendre function.

$$y_n(x) = P_n^m(x) \tag{214}$$

where n and m are some rational numbers. (They do not have to be integers.) In this general case the Legendre functions can be represented by an infinite series. (For further information, see References 8, 9 and 10.)

3.2 SOLUTION OF EQUATION 212, THE MATHEMATICAL FORMULATION OF A VIBRATING MEMBRANE SPHERE

To avoid any misunderstanding, differential Equation 212 represents the motion of a small shell element. This equation is the same regardless of what kind of boundary conditions one may try to apply. As will be shown in the following discussion, the applicable boundary conditions are also limited because of the use of membrane theory. The frequency equation expressed by Equation 211 has to be solved simultaneously with Equation 212. In other words, the frequency equation is a function of boundary conditions or the definition of bounded solutions of the displacements. Comparison of Equation 212 with Equation 213 leads to the solution of the tangential displacements, v_n, and the angular frequencies, p_n, in the following form.

$$v_n(x) = P_n^1(x) \tag{215}$$

$$\lambda_n = \frac{(2 - Bp_n^2)(Ap_n^2 + 1 - \nu)}{(1 - \nu - Bp_n^2)} = n(n+1) \tag{216}$$

where n can still be any rational number. We proceed further to determine the proper values of n in the following discussion.

3.3 COMPLETE SPHERE

For a complete sphere there is no real physical boundary condition applicable. The only mathematical boundary condition one can apply is that the displacement functions have to be single-valued and bounded all over the surface of the shell.

If n is not an integer, but a positive real number, then $P_n^1(x)$ is unbounded at $x = -1$; therefore

$$P_n^1(-1) = \pm\infty$$

Since the solution has to be bounded everywhere, one has to restrict the values of n to integer values.

In the case of $n = 1, 2, 3 \ldots$ $P_n^1(-1)$ is bounded; therefore, $P_n^1(x)$ is the solution of differential equation 212 and the frequency equation 211.

The frequency equation is

$$\frac{(2 - Bp_n^2)(Ap_n^2 + 1 - \nu)}{(1 - \nu - Bp_n^2)} = n(n + 1) \tag{217}$$

where $n = 1, 2, 3, 4$

Equation 217 can be solved in the form

$$AB p_n^4 + \left\{[1 - \nu - n(n + 1)]B - 2A\right\} p_n^2 + (1 - \nu)[n(n + 1) - 2] = 0 \tag{218}$$

The solution of Equation 218 leads to two sets of frequencies for each value of n. One of the sets is bounded and the frequency is p_n''; the other frequency set is unbounded and the frequency is p_n' (see Figure 36).

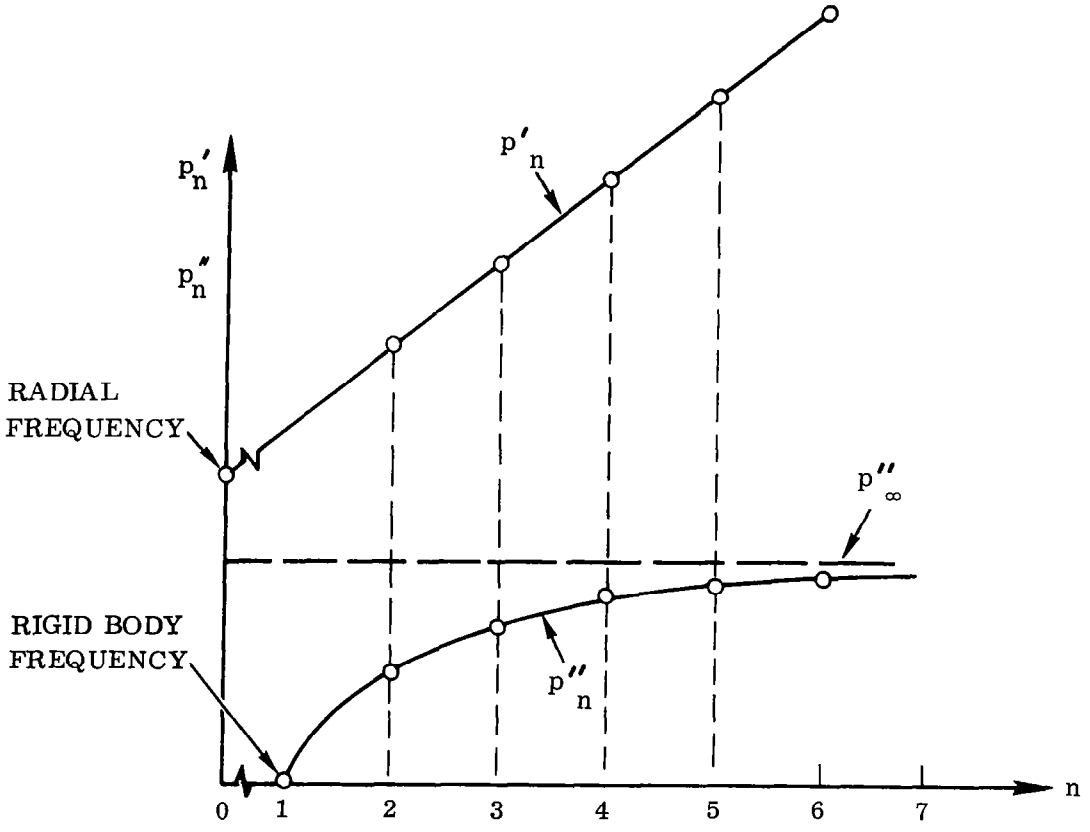

Figure 36. Frequency Curves for the Bounded and Unbounded Set

The bounded frequency set approaches an upper limit and it can be shown as

$$\lim_{n \to \infty} p_n'' = \sqrt{\frac{(1 - \nu)}{B}} \tag{219}$$

3.3.1 TANGENTIAL MODE SHAPE. As was proved previously, the tangential mode shape, $v_n(x)$, can be expressed as

$$v_n(x) = P_n^1(x) \tag{220}$$

where

$$n = 1, 2, 3 \ldots$$

The structure of $P_n^1(x)$ is

$$P_n^1(x) = \sqrt{1 - x^2}\ \{\text{polynomial}\} \tag{221}$$

3.3.2 NORMAL MODE SHAPE w_n. The substitution of Equation 220 into Equation 209 leads to

$$w_n(x) = \frac{-\sqrt{1 - x^2}\ \frac{dP_n^1}{dx} + \frac{x}{\sqrt{1 - x^2}} P_n^1}{(2 - B p_n^2)} \tag{222}$$

From the theory of Legendre functions, one has

$$P_n^1(x) = \sqrt{1 - x^2}\ \frac{d}{dx} P_n(x) \tag{223}$$

Substituting Equation 223 into Equation 222, the following equation can be obtained.

$$w_n(x) = \frac{-(1 - x^2)\frac{d^2 P_n(x)}{dx^2} + 2x\frac{dP_n(x)}{dx}}{(2 - B p_n^2)} \tag{224}$$

Again, from the theory of Legendre functions, one has

$$(1 - x^2)\frac{d^2 P_n(x)}{dx^2} - 2x\frac{dP_n(x)}{dx} + n(n + 1) P_n(x) = 0 \tag{225}$$

This is the equation of zero-order Legendre functions (m = 0, see Equation 213). One has, from Equation 225

$$-(1 - x^2)\frac{d^2 P_n(x)}{dx^2} + 2x\frac{d P_n(x)}{dx} = n(n + 1) P_n(x) \tag{226}$$

The substitution of Equation 226 into Equation 224 leads finally to

$$w_n(x) = \frac{n(n + 1) P_n(x)}{(2 - B p_n^2)} \tag{227}$$

where

$$n = 1, 2, 3 \ldots$$

3.3.3 ORTHOGONALITY CONDITIONS OF SHELL MODES IN THE CASE OF COMPLETE SPHERICAL SHELL. The conditions of orthogonality can be expressed in this special case.

$$\int_{-1}^{1} v_i v_j = 0 \quad \text{if} \quad i \neq j \tag{228}$$

where

$$i, j = 1, 2, 3 \ldots$$

Similarly

$$\int_{-1}^{1} w_i w_j = 0 \quad \text{if} \quad i \neq j \tag{229}$$

where

$$i, j = 1, 2, 3, 4 \ldots$$

The condition of orthogonality always has to be proved, using shell theory; however, this statement is also true for other types of continuous mechanics.

3.4 LEGENDRE'S DIFFERENTIAL EQUATION AND THE PROPERTIES OF LEGENDRE'S FUNCTIONS

As stated previously, the Legendre type of differential equation is in general

$$(1 - x^2)\frac{d^2y_n}{dx^2} - 2x\frac{dy_n}{dx} + \left[n(n+1) - \frac{m^2}{1-x^2}\right]y_n = 0 \quad \text{(see 213)}$$

The general solution of this equation is the Legendre functions

$$y_n(x) = P_n^m(x) \quad \text{(see 214)}$$

where n and m are some rational numbers. In the case of integer values of m, the Legendre functions can be expressed as

$$P_n^m(x) = (1 - x^2)^{m/2}\frac{d^m}{dx^m}P_n(x) \tag{230}$$

where $P_n(x)$ is the order of zero and degree of n (m = 0).

From the theory of hypergeometric functions, one has

$$F(\alpha, \beta, \gamma, z) = 1 + \frac{\alpha\beta}{1.\gamma}z + \frac{\alpha(\alpha+1)\beta(\beta+1)}{1.2.\gamma(\gamma+1)}z^2$$

$$+ \frac{\alpha(\alpha+1)(\alpha+2)\beta(\beta+1)(\beta+2)}{1.2.3\gamma(\gamma+1)(\gamma+2)}z^3 + \ldots \tag{231}$$

$P_n(x)$ can be expressed by the hypergeometric function as

$$P_n(x) = F\left(-n, n+1, 1, \frac{1-x}{2}\right) \tag{232}$$

Equation 232 can be written, based on Equation 231, as

$$P_n(x) = \left[1 - \frac{n(n+1)}{1.2}(1-x) - \frac{n(1-n)(n+1)(n+2)}{1.2.1.2.2^2}(1-x)^2\right.$$

$$\left. - \frac{n(1-n)(2-n)(n+1)(n+2)(n+3)}{1.2.3.1.2.3.2^3}(1-x)^3 - \ldots.\right] \tag{233}$$

The series is convergent, if $|1 - x| < 2$. If n are integer values, the infinite series becomes a polynomial. For example

$$n = 1 \qquad P_1(x) = \left[1 - \frac{1(2)}{1(2)}(1 - x)\right] = x$$

$$n = 2 \qquad P_2(x) = \left[1 - \frac{2(3)}{1(2)}(1 - x) - \frac{2(-1)(3)(4)}{2^4}(1 - x)^2\right]$$

$$P_2(x) = \frac{1}{2}(3x^2 - 1)$$

Similarly

$$P_3(x) = \frac{x}{2}(5x^2 - 3)$$

3.4.1 ORTHOGONALITY CONDITIONS OF LEGENDRE FUNCTIONS. It is assumed that i and j are some rational numbers and m are integers. The differential equations in this case are

$$\frac{d}{dx}\left[(1 - x^2)\frac{d}{dx}P_i^m(x)\right] + \left[i(i + 1) - \frac{m^2}{1 - x^2}\right]P_i^m(x) = 0 \tag{234}$$

$$\frac{d}{dx}\left[(1 - x^2)\frac{d}{dx}P_j^m(x)\right] + \left[j(j + 1) - \frac{m^2}{1 - x^2}\right]P_j^m(x) = 0 \tag{235}$$

Multiplying Equation 234 by $P_j^m(x)$ and Equation 235 by $P_i^m(x)$, integrating these products between limits -1 to +1, and subtracting these values yields

$$\int_{-1}^{1}\left\{P_j^m\frac{d}{dx}\left[(1 - x^2)\frac{d}{dx}P_i^m\right] - P_i^m\frac{d}{dx}\left[(1 - x^2)\frac{d}{dx}P_j^m\right]\right\}dx$$

$$+ (i - j)(i + j + 1)\int_{-1}^{1}P_i^m P_j^m dx = 0 \tag{236}$$

Since

$$\int_{-1}^{1}P_j^m\frac{d}{dx}\left[(1 - x^2)\frac{d}{dx}P_i^m\right]dx = (1 - x^2)P_j^m\frac{d}{dx}P_i^m\Bigg|_{-1}^{1}$$

$$-\int_{-1}^{1}(1 - x^2)\frac{d}{dx}P_j^m\frac{d}{dx}P_i^m dx \tag{237}$$

Substituting Equation 237 into Equation 236, yields

$$(i - j)(i + j + 1) \int_{-1}^{1} P_i^m(x)\, P_j^m(x)\, dx =$$

$$(1 - x^2)\left[P_i^m(x) \frac{d}{dx} P_j^m(x) - P_j^m(x) \frac{d}{dx} P_i^m(x) \right]_{-1}^{1} = 0 \qquad (238)$$

if $i \neq j$ and m is an integer.

The orthogonality condition of Legendre's function can be written in general

$$\int_{-1}^{1} P_i^m(x)\, P_j^m(x)\, dx = 0 \qquad (239)$$

if

$$i \neq j$$

where

m = integer values

i, j = arbitrary rational numbers

In the present case, one has

$$m = 1 \rightarrow \int_{-1}^{1} P_i^1(x)\, P_j^1(x)\, dx = 0 \qquad (240)$$

if $i \neq j$.

$$m = 0 \rightarrow \int_{-1}^{1} P_i(x)\, P_j(x)\, dx = 0 \qquad (241)$$

if $i \neq j$.

3.4.2 TABLE OF LEGENDRE FUNCTIONS. The Legendre functions and polynomials were calculated based on Equations 233 and 230. The results of the calculations can be seen in Table 1.

If the values of n are not integer values, the Legendre functions can also be calculated from Equation 233; however, the Legendre functions will be an infinite series.

Table 1. Legendre Functions

n	$P_n(x)$	$P_n^1(x)$
0	1	0
1	x	$\sqrt{1 - x^2}$
2	$\frac{1}{2}(3x^2 - 1)$	$3x\sqrt{1 - x^2}$
3	$\frac{1}{2}(5x^3 - 3x)$	$\frac{3}{2}(5x^2 - 1)\sqrt{1 - x^2}$
4	$\frac{1}{8}(35x^4 - 30x^2 + 3)$	$\frac{5}{2}(7x^3 - 3x)\sqrt{1 - x^2}$
5	$\frac{1}{8}(63x^5 - 70x^3 + 15x)$	$\frac{1}{8}(315x^4 - 210x^2 + 15)\sqrt{1 - x^2}$

3.5 DIFFERENT BOUNDARY CONDITIONS OF THE VIBRATING SPHERICAL MEMBRANE SHELLS

3.5.1 COMPLETE SPHERE. The mode shapes can be constructed, based on Table 1, by Equations 220 and 227. The frequency equation is given by Equation 218.

3.5.2 HALF SPHERICAL SHELL. The membrane theory can satisfy only three types of boundary conditions for a half spherical shell. Figure 37a shows the boundary condition, when the shell is fixed in the radial direction, $w_n|_{x=0} = 0$. Figure 37b illustrates another boundary condition, when the shell is fixed in the tangential direction, $v_n|_{x=0} = 0$. Figure 37c shows the third type of boundary condition, when the stress, $\sigma_\varphi|_{x=0} = 0$.

a. Solution of $w_n|_{x=0} = 0$. Since

$$w_n = \frac{n(n+1)P_n(x)}{(2 - Bp_n^2)} \qquad (227)$$

as was proved previously.

$$w_n(x) \rightarrow P_n(x)|_{x=0} = 0 \qquad (242)$$

where n = 1, 3, 5 ... odd numbers. (See Table 1.)

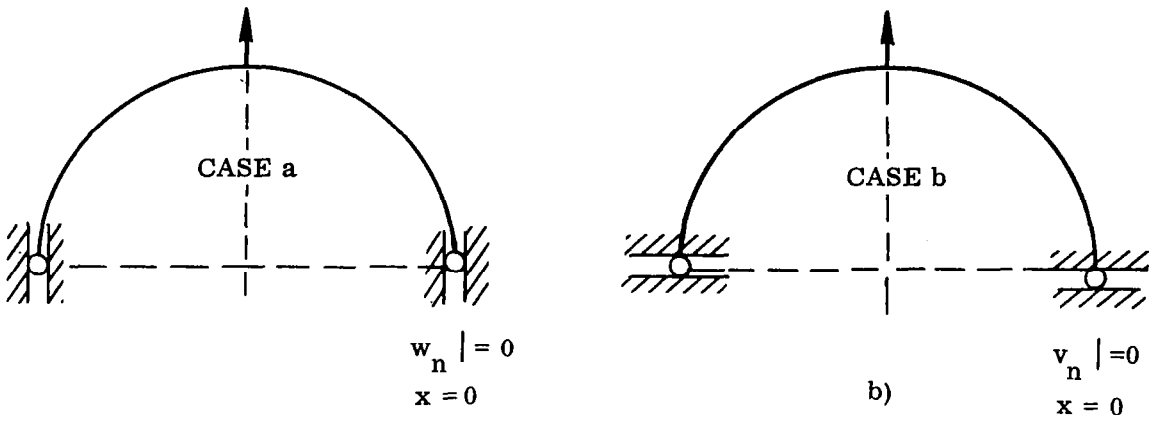

a. $w_n| = 0$ b. $v_n| = 0$

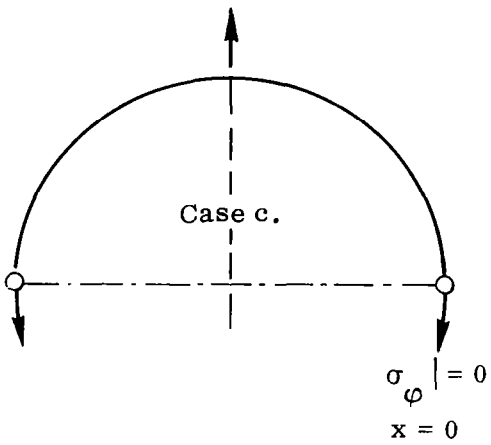

c. $\sigma_\varphi| = 0$

Figure 37. Boundary Conditions for a Membrane Sphere

b. Solution of $v_n|_{x=0} = 0$. Since

$$v_n(x) = P_n^1(x) \qquad (220)$$

as was proved previously.

$$v_n(x)\big|_{x=0} = P_n^1(x)\big|_{x=0} = 0$$

where n = 0, 2, 4 ... even numbers.

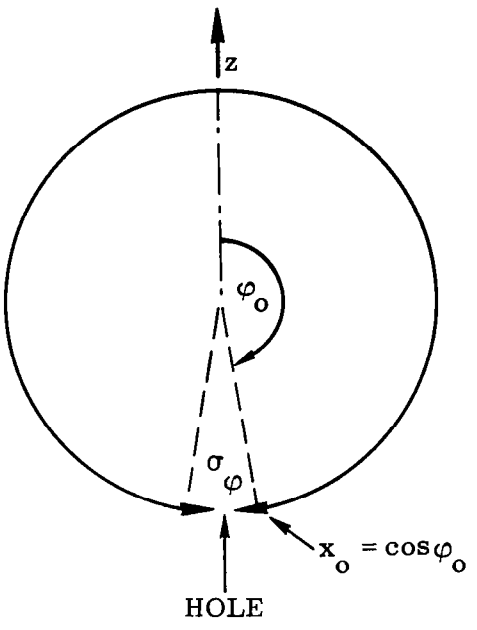

Figure 38. Spherical Shell with Hole

The frequencies can be calculated from Equation 218 and n = 1, 3, 5 .. for case a; n = 0, 2, 4 for case 6.

3.5.2.1 Physical Explanation of Boundary Conditions Cases a and b. In case a, the shell vibrates with odd-numbered normal modes ($w_{1,3,5...}$); in case b, the shell vibrates with even-numbered normal modes ($w_{0,2,4...}$).

3.5.2.2 Case c, $\sigma_\varphi|_{x=x_o} = 0$. This case can be generalized mathematically for an arbitrary value of $x = x_o$, and the influence of a small hole on a spherical surface can be discussed. Figure 38 illustrates the general case.

The boundary condition is

$$\sigma_\varphi|_{x=x_o} = 0 \tag{243}$$

From Equation 195 one has

$$\sigma_\varphi = \frac{N_\varphi}{h} = \frac{E}{a(1-\nu^2)}\left[\frac{\partial v}{\partial \varphi} + \nu v \cot\varphi - (1+\nu)w\right] \tag{244}$$

Since

$$x = \cos\varphi$$

Equation 244 can be expressed as

$$\sigma_\varphi = \frac{E}{a(1-\nu^2)}\sum_n\left[-\sqrt{1-x^2}\,\frac{dv_n}{dx} + \nu\frac{x}{\sqrt{1-x^2}}\,v_n - (1+\nu)w_n\right] \tag{245}$$

The substitution of Equations 245 and 209 into Equation 243 leads to

$$-\sqrt{1-x^2}\,\frac{dv_n}{dx} + \nu\frac{x}{\sqrt{1-x^2}}\,v_n - (1+\nu)\left\{\frac{-\sqrt{1-x^2}\,\frac{dv_n}{dx} + \frac{x}{\sqrt{1-x^2}}\,v_n}{(2 - Bp_n^2)}\right\}\Bigg|_{x=x_o} = 0 \tag{246}$$

Since

$$v_n = P_n^1(x)$$

where n is unknown. Equation 246 is by substitution of the Legendre functions P_n^1 thus

$$-\sqrt{1-x^2}\frac{d}{dx}P_n^1(x)+\nu\frac{x}{\sqrt{1-x^2}}P_n^1(x)-(1+\nu)\left\{\frac{-\sqrt{1-x^2}\frac{d}{dx}P_n^1(x)+\frac{x}{\sqrt{1-x^2}}P_n^1(x)}{(2-Bp_n^2)}\right\}\Bigg|_{x=x_o}=0 \quad (247)$$

The frequency equation is unchanged.

$$\frac{(2-Bp_n^2)(Ap_n^2+1-\nu)}{(1-\nu-Bp_n^2)} = n(n+1) \qquad (217)$$

The simultaneous solution of Equations 247 and 217 leads to the unknown frequencies, p_n^2, and the indices, n. The mode shapes are represented by the Legendre functions and are an infinite series, since the values of n are not integers.

A special case of this problem is the half sphere, where

$$x = x_o = \cos\frac{\pi}{2} = 0$$

References 11 and 12 may be counted as classics in shell dynamics. Reference 13 has been published recently and it also contains test results.

3.6 A REVIEW OF BAKER'S PAPER: "AXISYMMETRIC MODES OF VIBRATION OF THIN SPHERICAL SHELL" (Reference 13)

3.6.1 SUMMARY. The paper presents a study of the theory of free, axisymmetric vibrations of a thin elastic spherical shell and demonstrates by experiment that the normal modes of vibration predicted by theory do exist. The author used membrane theory and predicted the existence of two infinite sets of modes, one of which is bounded in frequency and the other unbounded. The first four modes in each set are identified by experiments on a small steel shell.

3.6.2 EXPLANATION OF THE THEORY. The equilibrium equations of the paper (1 and 2) can be compared to Equations 197 and 198 of this monograph. The differential equations (5 and 6) of the paper are identical with Equations 199 and 200 of this monograph. Equation 17 of the paper, the tangential mode shape, can be obtained with Equation 215 of the monograph. Equation 19 in the paper defines the normal mode

shape, which is related to Equation 227 of the monograph. These equations differ by a constant, which is due to the different formulations of the displacement functions. The paper defined the displacement functions as the solution of an initial value problem. However, the monograph investigated the problem of free vibration, and the initial value problem was left open. The frequency equations (28 and 29) of the paper are identical to Equation 218 of the monograph.

Figure 39 shows the frequency curves as published by the author. The unbounded angular frequencies are designated by the letters a_n and the bounded set by letters b_n. Figure 40 shows the different mode shapes and Tables 2 and 3 the calculated and measured frequencies published by the author.

Table 2. Comparison of Measured and Predicted Vibration Frequencies for "a" Modes

Mode	Predicted Frequency (Hz)	Measured Frequency (Hz)
a_0	3720	3500
a_1	4570	4500
a_2	6250	6200
a_3	8350	8500

Table 3. Comparison of Measured and Predicted Vibration Frequencies for "b" Modes

Mode	Predicted Frequency (Hz)	Measured Frequency (Hz)
b_2	1560	1540
b_3	1860	1880
b_4	1975	1950
b_5	2000	2000

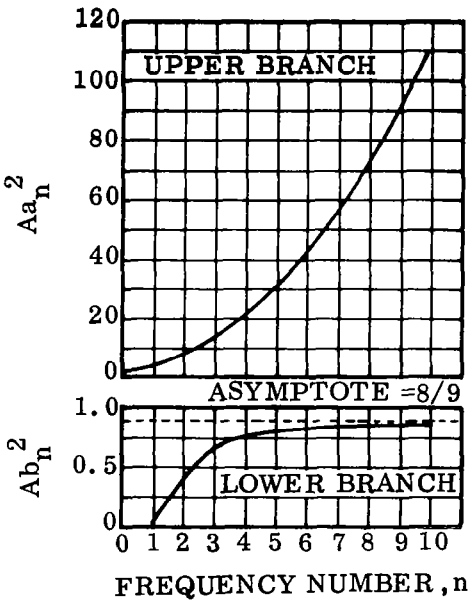

Constants: $\nu = 1/3$

$$A = \frac{\rho(1-\nu^2)a^2}{E}$$

Figure 39. Frequency Curves for Spherical Shell

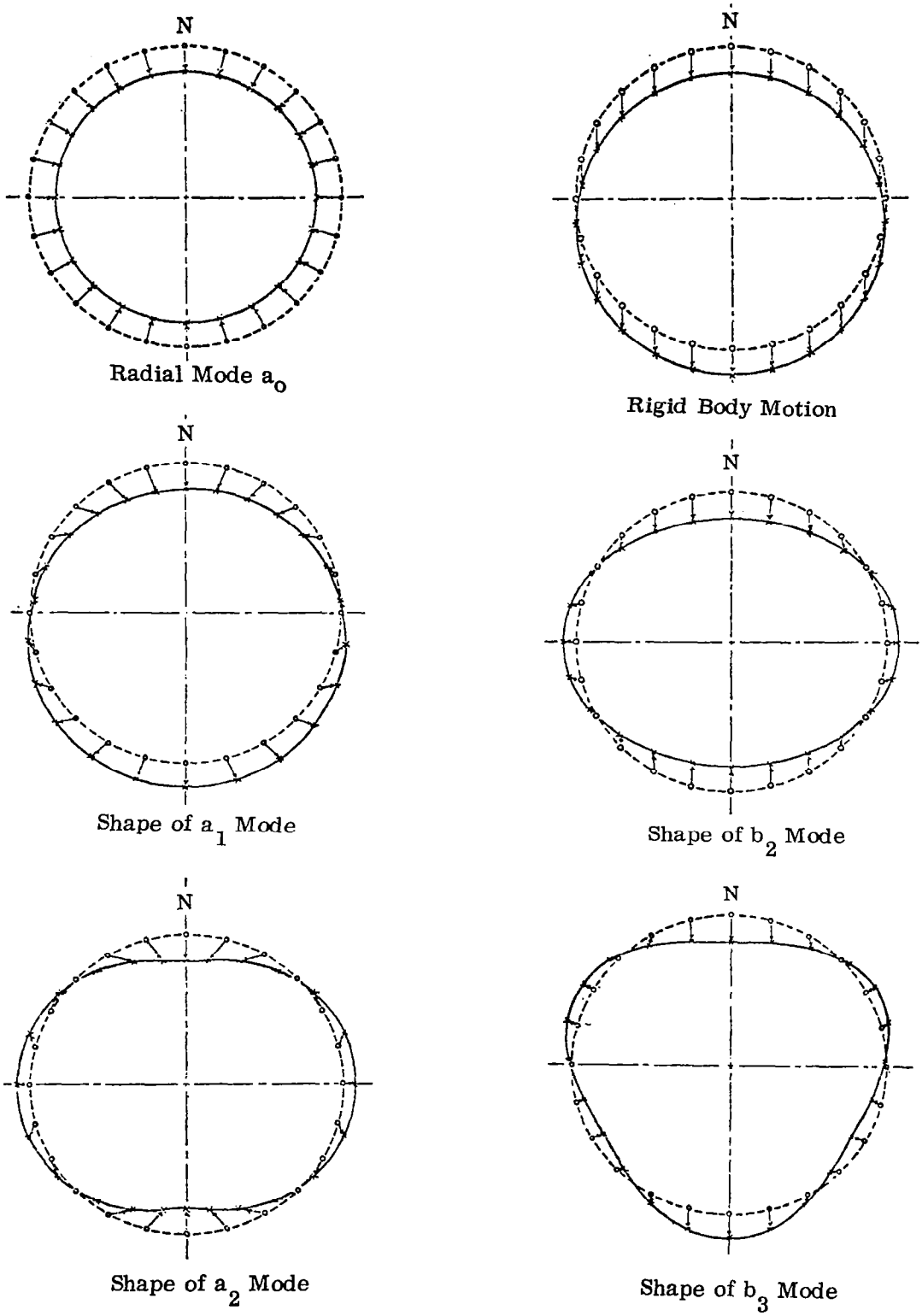

Figure 40. Mode Shapes of Spherical Shell

3.6.3 CONCLUSIONS. The paper shows the experimental evidence of the existence of two types of frequencies and mode shapes for a vibrating, thin-walled spherical shell. However, the recent theoretical investigations, using membrane-bending theory for a spherical shell, have shown the unbounded character of the so-called bounded frequencies defined by the membrane theory.

3.7 FREE AXISYMMETRIC VIBRATION OF MEMBRANE CYLINDERS

The problem of symmetric free vibration of membrane cylinders is under study. In this case, the following assumptions can be made

$$v = N_{x\varphi} = N_{\varphi x} = Y = 0 \tag{248}$$

In addition, the inertial forces are the load functions

$$X = -\rho h \frac{\partial^2 u}{\partial t^2} \qquad \text{and} \qquad Z = -\rho h \frac{\partial^2 w}{\partial t^2} \tag{249}$$

The substitution of Equations 248 and 249 into Equations 93, 94 and 95 leads to the differential equations of motion.

$$\frac{\partial N_x}{\partial x} = \rho h \frac{\partial^2 u}{\partial t^2} \tag{250}$$

$$N_\varphi = \rho h a \frac{\partial^2 w}{\partial t^2} \tag{251}$$

The strain-displacement functions are based on Equations 131 and 134.

$$\epsilon_x = \frac{\partial u}{\partial x} \qquad \epsilon_\varphi = -\frac{w}{a} \qquad \text{and} \qquad v = 0 \tag{252}$$

The substitution of Equation 252 into Equations 250 and 251 yields

$$\frac{\partial^2 u}{\partial x^2} - \frac{\nu}{a}\frac{\partial w}{\partial x} = \frac{\rho(1-\nu^2)}{E}\frac{\partial^2 u}{\partial t^2} \tag{253}$$

$$\nu \frac{\partial u}{\partial x} - \frac{w}{a} = \rho \frac{(1-\nu^2)}{E} a \frac{\partial^2 w}{\partial t^2} \tag{254}$$

Assuming separation of variables, the following expression can be obtained.

$$\left.\begin{aligned} u_n(x,t) &= u_n(x)\, T_n(t) \\ w_n(x,t) &= w_n(x)\, T_n(t) \end{aligned}\right\} \tag{255}$$

The assumption of harmonic motion may be formulated

$$\frac{d^2 T_n}{dt^2} + p_n^2 T_n = 0 \tag{256}$$

Let

$$\frac{d}{dx}(\ ) = {}' \qquad \text{and} \qquad A = \frac{\rho(1-\nu^2)}{E} \tag{257}$$

Partial differential Equations (253 and 254) can be reduced to two ordinary differential equations, if Equations 255, 256 and 257 are substituted into them.

$$u_n'' - \frac{\nu}{a} w_n' = -A p_n^2 u_n \tag{258}$$

$$\nu u_n' - \frac{w_n}{a} = -A a p_n^2 w_n \tag{259}$$

One of the variables can be eliminated from the last equations. The following equation may be obtained.

$$u_n'' + \frac{A p_n^2 (1 - A a^2 p_n^2)}{\left[1 - \nu^2 - A a^2 p_n^2\right]} u_n = 0 \tag{260}$$

The frequency equation may be expressed as follows.

$$\lambda_n^2 = \frac{A p_n^2 (1 - A a^2 p_n^2)}{\left[1 - \nu^2 - A a^2 p_n^2\right]} \tag{261}$$

where

$$\lambda_n^2 \geq 0$$

Equation 258 is, in the final form

$$u_n'' + \lambda_n^2 u_n = 0 \tag{262}$$

The solution of this equation is written

$$u_n(x) = A_n \cos \lambda_n x + B_m \sin \lambda_m x \tag{263}$$

The problem of free vibration may be solved by establishment of some applicable boundary conditions. It can be seen from previous equations that the membrane theory again gives a limited number of possibilities for the boundary conditions.

3.8 EXPLANATION OF BOUNDARY CONDITIONS IN THE CASE OF MEMBRANE THEORY

Let the theory of beams serve as an example. Assume that the beam is loaded uniformly by load p (as shown in Figure 41). The deflection curve can then be investigated.

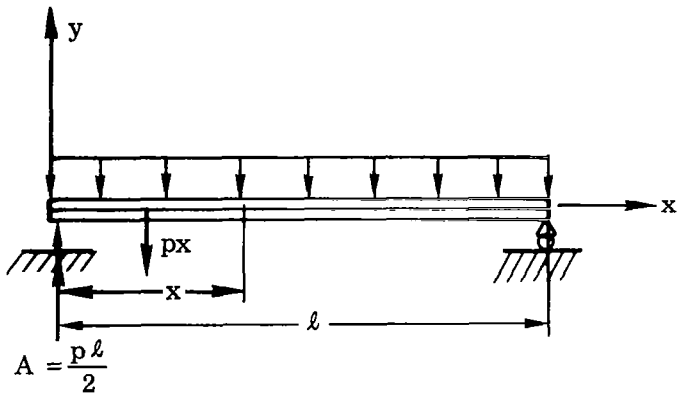

Figure 41. Uniformly Loaded Beam

The differential equation of deflection is

$$IE \frac{d^2y}{dx^2} = -M = -\frac{px^2}{2} + \frac{p\ell x}{2}$$

Solution of this equation is

$$y = -\frac{p}{12IE}\left(\frac{x^4}{2} - \ell x^3\right) + \frac{C_1 x}{IE} + \frac{C_2}{IE}$$

The two constants can be evaluated from the boundary conditions that $y(0) = 0$ and $y(\ell) = 0$. Since the differential equation is second order, the solution has two arbitrary constants. In shell analysis the use of membrane theory leads to first-order differential equations for the forces and displacements, when static problems are discussed, and therefore has only one arbitrary constant. With only one arbitrary constant, membrane theory cannot satisfy all arbitrary boundary conditions and is therefore limited in its application, for example: a half sphere loaded uniformly (see Figure 42).

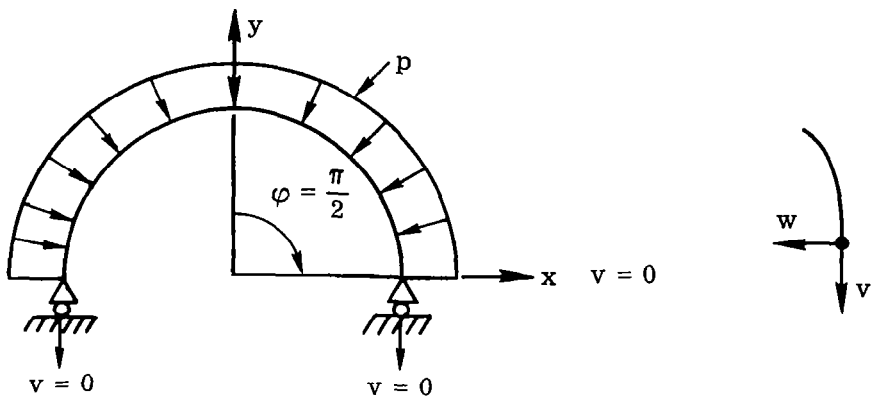

Figure 42. Uniformly Loaded Half Sphere

It can be seen from the previous equations that the only boundary condition that can be applied for the half sphere with the uniform load is $v = 0$ and $w = \frac{p a^2 (1 - \nu)}{2 E h} = \text{constant}$. When other types of boundary conditions are to be applied, the combined membrane-bending shell theory has to be used. To avoid any misunderstanding, the beam theory served only as an illustration for the present shell problem, since everybody is familiar with that. However, it can be stated that there is no real comparison between beam theory and membrane-shell theory, since entirely different approximations are used (membrane-shells → membrane stresses, beam theory → bending stresses). In the case of dynamic problems, the membrane theory leads to second-order differential equations, and, as a consequence, the applicable boundary conditions were increased.

3.9 PRACTICAL APPLICATIONS OF MEMBRANE SHELL DYNAMICS IN THE THEORY OF MISSILES

Spherical, thin-walled bottles and spherical tanks have many practical applications in aerospace vehicles. The problems related to these hardware applications are mainly dynamics. Thus, any theoretical analysis has to be based on the concept of shell dynamics; therefore, the previous basic explanations have fundamental importance.

4/GENERAL THEORY OF CYLINDRICAL SHELLS

The general theory of thin elastic shells takes into account both membrane and bending effects. This theory can handle most of the desired boundary conditions; however, the equations become quite lengthy. Because of its relative simplicity, the cylindrical shell will serve as an example of this theory. Similar equations — but considerably longer and more complicated ones — can be developed for any other shell geometry. The symmetrically loaded cylindrical shell will be discussed first, with some examples. The thermal and dynamic effects are usually coupled during missile flights; therefore, the importance of thermal stresses in shells is discussed. Thermal stresses will also be discussed in this chapter, as a practical application of theory for cylindrical shells. Finally, the sign convention difference between Timoshenko and Flügge will also be investigated (References 4 and 6), since overlooking this concept can be quite a disturbing factor.

4.1 CYLINDRICAL SHELL LOADED SYMMETRICALLY IN THE CIRCUMFERENTIAL DIRECTION

The cylinder is assumed to be loaded symmetrically in the circumferential direction. This assumption is also valid for an element of the cylinder. Figure 43 shows the shell element with the corresponding membrane forces, N_x and N_φ, and the corresponding bending moments, M_x and M_φ.

The following relations can be written, as the result of symmetry

$$N_{x\varphi} = N_{\varphi x} = M_{x\varphi} = M_{\varphi x} = 0$$

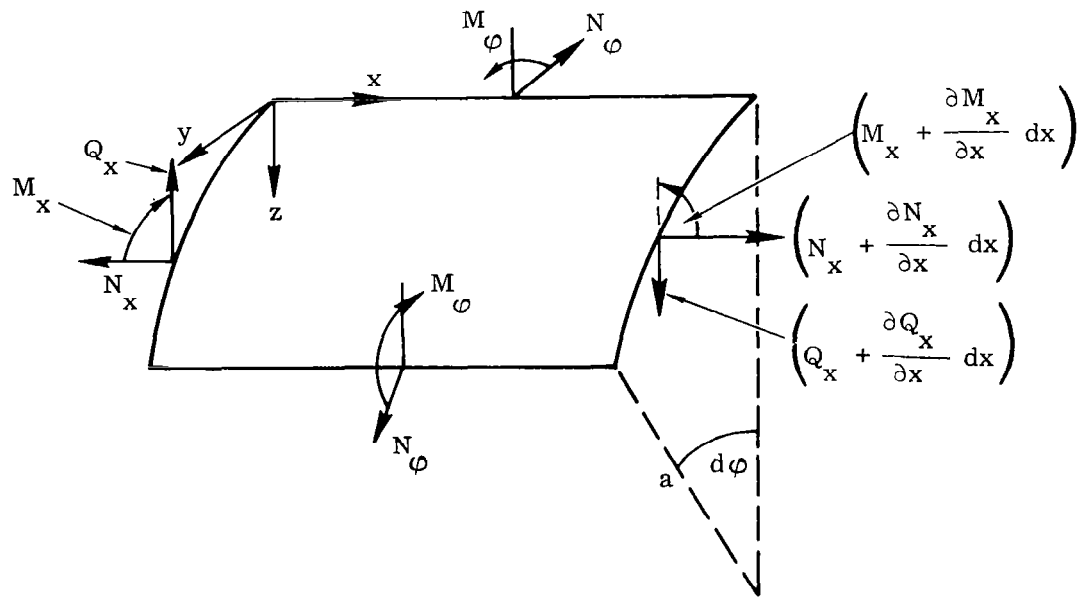

Figure 43. Shell Element

In this case, two force equilibrium equations and one moment equation can be written. The forces in the x-direction are unchanged. (For further information, see Equations 90 and 126.)

The forces in the z-direction are

$$N_\varphi \, d\varphi \, dx + Z \, a \, d\varphi \, dx + \frac{\partial Q_x}{\partial x} a \, d\varphi \, dx = 0 \tag{264}$$

The moment of the forces around the y-axis is

$$\frac{\partial M_x}{\partial x} a \, dx \, d\varphi - Q_x a \, dx \, d\varphi = 0 \tag{265}$$

Dividing these equations by $a \, d\varphi \, dx$, one has

$$\frac{\partial N_x}{\partial x} = -X \tag{266}$$

$$\frac{1}{a} N_\varphi + \frac{\partial Q_x}{\partial x} = -Z \tag{267}$$

$$\frac{\partial M_x}{\partial x} - Q_x = 0 \tag{268}$$

Equation 268 can be written

$$Q_x = \frac{\partial M_x}{\partial x} \tag{269}$$

The substitution of Equation 269 into Equation 267 leads to two equations of forces, which are now modified by the bending theory.

$$\frac{\partial N_x}{\partial x} = -X \tag{270}$$

$$\frac{1}{a} N_\varphi + \frac{\partial^2 M_x}{\partial x^2} = -Z \tag{271}$$

4.2 EQUATION OF BENDING MOMENT IN TERMS OF DISPLACEMENT

The effects of bending moments on a cylindrical shell will be investigated. It will be assumed that the external forces consist only of a pressure normal to the surface and that the longitudinal force, N_x, is also equal to zero. If the force N_x is different from zero, the deformation and stress corresponding to such forces can be easily calculated and superimposed on stresses and deformations produced by the lateral load. The

following relations may therefore be written

$$N_x = X = v = 0 \tag{272}$$

The stress relation given by Equation 89 is still valid

$$\left.\begin{aligned} \sigma_x &= \frac{E}{(1-\nu^2)}(\epsilon_x + \nu\,\epsilon_\varphi) \\ \sigma_\varphi &= \frac{E}{(1-\nu^2)}(\epsilon_\varphi + \nu\,\epsilon_x) \end{aligned}\right\} \tag{89}$$

since

$$\sigma_z = 0$$

The strain can be expressed as a function of curvature change. Because of symmetry, there is no change in curvature in the circumferential direction. The pure bending of beams leads to the following relations.

$$\left.\begin{aligned} \epsilon_x &= -z\varkappa_x = -z\frac{\partial^2 w}{\partial x^2} \\ \epsilon_\varphi &= -z\varkappa_\varphi = -z\cdot 0 = 0 \end{aligned}\right\} \tag{273}$$

where

$\varkappa_x$ = change of curvature in direction x

$\varkappa_\varphi$ = change of curvature in direction y

The substitution of Equation 273 into Equation 89, leads to

$$\left.\begin{aligned} \sigma_x &= -\frac{E}{(1-\nu^2)}\,z\,\frac{\partial^2 w}{\partial x^2} \\ \sigma_\varphi &= -\frac{E}{(1-\nu^2)}\,\nu\,z\,\frac{\partial^2 w}{\partial x^2} \end{aligned}\right\} \tag{274}$$

The equation of bending moment may be derived from Figure 44.

$$M_x\,a\,d\varphi = \left(\int_{-h/2}^{h/2} \sigma_x\,z\,dz\right) a\,d\varphi \tag{275}$$

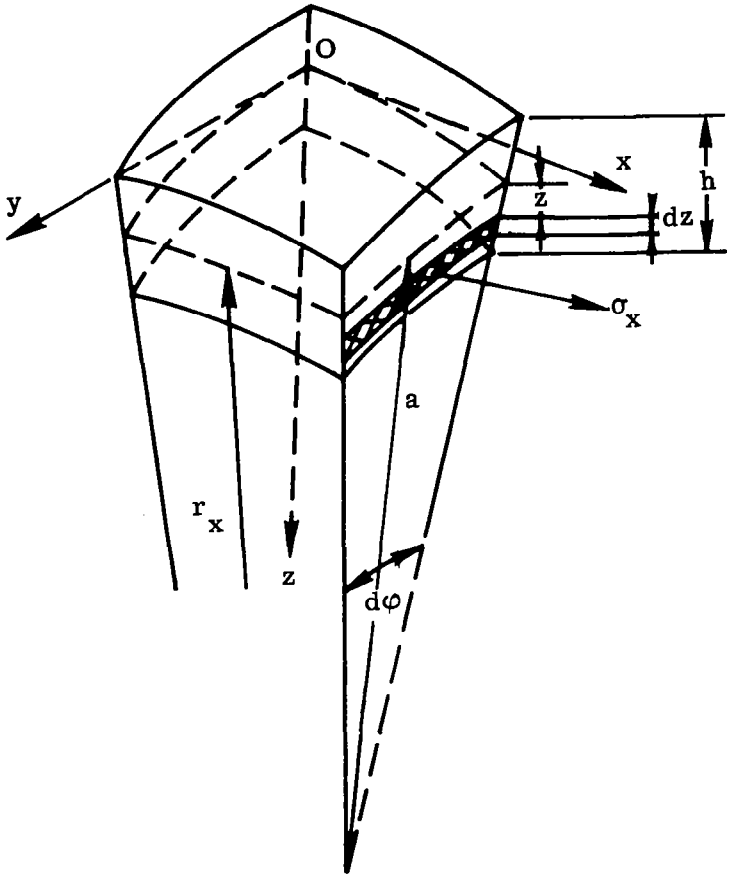

Figure 44. Shell Element with the Radius of Curvature

Equation 275 is expressed by Equation 274; the cancellation of expression "a dφ" leads to

$$M_x = -\int_{-h/2}^{h/2} \frac{E}{(1-\nu^2)} z^2 \frac{\partial^2 w}{\partial x^2} dz = -\frac{E h^3}{12(1-\nu^2)} \frac{\partial^2 w}{\partial x^2} \tag{276}$$

Since

$$D = \frac{E h^3}{12(1-\nu^2)} \tag{277}$$

the bending moments are, in the final form

$$\left.\begin{aligned} M_x &= -D \frac{\partial^2 w}{\partial x^2} \\ M_\varphi &= -\nu D \frac{\partial^2 w}{\partial x^2} \end{aligned}\right\} \tag{278}$$

The longitudinal strain, ϵ_x, may be expressed, from Equation 272 as

$$\epsilon_x = -\nu\epsilon_\varphi \tag{279}$$

The substitution of Equation 279 into Equation 89 and the use of expression 134 leads to

$$N_\varphi = \frac{Eh}{(1-\nu^2)}(\epsilon_\varphi - \nu^2\epsilon_\varphi) = Eh\epsilon_\varphi = -\frac{Ehw}{a} \tag{280}$$

The substitution of Equations 278 and 280 into Equation 271 yields the following expression.

$$\frac{Eh}{a^2}w + D\frac{\partial^4 w}{\partial x^4} = Z \tag{281}$$

$$\frac{\partial^4 w}{\partial x^4} + 4\beta^4 w = \frac{Z}{D} \tag{282}$$

where

$$\beta^4 = \frac{Eh}{4a^2D} = \frac{3(1-\nu^2)}{a^2h^2} \tag{283}$$

The general solution of Equation 283 can be expressed as

$$w(x) = e^{\beta x}(C_1\cos\beta x + C_2\sin\beta x) + e^{-\beta x}(C_3\cos\beta x + C_4\sin\beta x) + f(x) \tag{284}$$

4.3 EXAMPLES

4.3.1 SHEAR FORCE AND BENDING MOMENT.

Figure 45 shows a cylindrical shell loaded uniformly by a shear force, Q_o, and a bending moment, M_o, at one end. The cylinder is considered to be very long.

If the cylinder is long the following assumptions can be made.

$$C_1 = C_2 = 0 \tag{285}$$

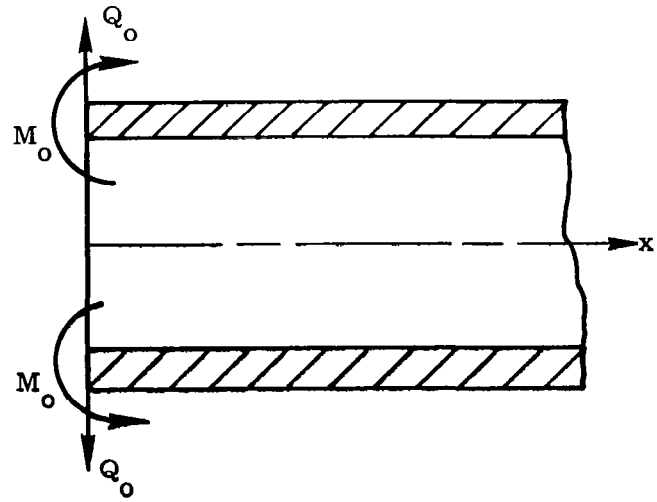

Figure 45. Loaded Cylindrical Shell with Moments and Shear Forces

In this case there is no pressure, Z, distributed over the surface of the shell, and f(x) = 0 in the general solution. Equation 284 can be expressed in this case as

$$w(x) = e^{-\beta x}(C_3 \cos \beta x + C_4 \sin \beta x) \tag{286}$$

The two arbitrary constants can be obtained from the boundary conditions at the loaded end and may be expressed as

$$Q_x = \frac{\partial M_x}{\partial x} = -D \frac{\partial^3 w}{\partial x^3}\bigg|_{x=0} = Q_o \tag{287}$$

$$M_x = -D \frac{\partial^2 w}{\partial x^2}\bigg|_{x=0} = M_o \tag{288}$$

The solutions of the last equations are the following.

$$C_3 = -\frac{1}{2\beta^3 D}(Q_o + \beta M_o) \qquad C_4 = \frac{M_o}{2\beta^2 D} \tag{289}$$

The substitution of Equation 289 into Equation 286 leads to

$$w(x) = \frac{e^{-\beta x}}{2\beta^3 D}[\beta M_o(\sin \beta x - \cos \beta x) - Q_o \cos \beta x] \tag{290}$$

The maximum deflection is at the loaded end.

$$w_{max} = w(x)\Big|_{x=0} = -\frac{(\beta M_o + Q_o)}{2\beta^3 D} \tag{291}$$

4.3.2 CONCENTRATED FORCE LOADING. An infinitely long cylindrical shell is loaded by a uniformly concentrated force system, as illustrated in Figure 46. The problem is to calculate the deflection of the shell. If the cylindrical shell is long enough and the load is far from the ends, the results of the previous example can be used. The boundary conditions may be set based on the condition of symmetry.

$$Q_o = -\frac{P}{2} \qquad \text{and} \qquad \frac{dw}{dx}\bigg|_{x=0} = 0 \tag{292}$$

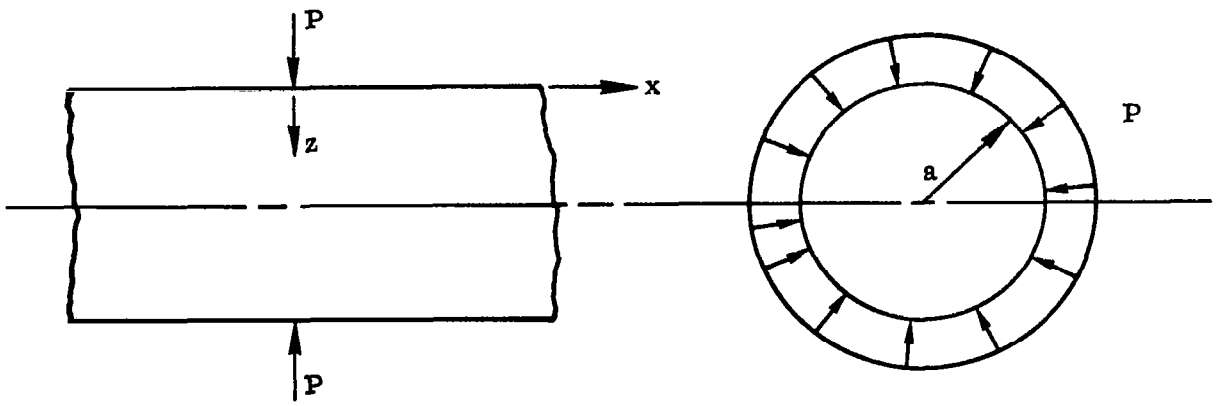

Figure 46. Shell Loaded With Concentrated Force

The substitution of Equation 286 into the boundary condition 292 leads to

$$\left.\frac{dw}{dx}\right|_{x=0} = (C_4 - C_3) = 0$$

Therefore

$$C_3 = C_4 \tag{293}$$

If Equations 289 and 292 are substituted into Equation 293, one obtains

$$\frac{1}{2\beta^3 D}\left(\frac{P}{2} - \beta M_o\right) = \frac{M_o}{2\beta^2 D} \tag{294}$$

The unknown bending moment, M_o, expressed from the last equation is

$$M_o = \frac{P}{4\beta} \tag{295}$$

The displacement function w(x) can be expressed as

$$w(x) = \frac{e^{-\beta x} P}{8\beta^3 D}(\sin \beta x + \cos \beta x) \tag{296}$$

Figure 47 illustrates the results of the theory.

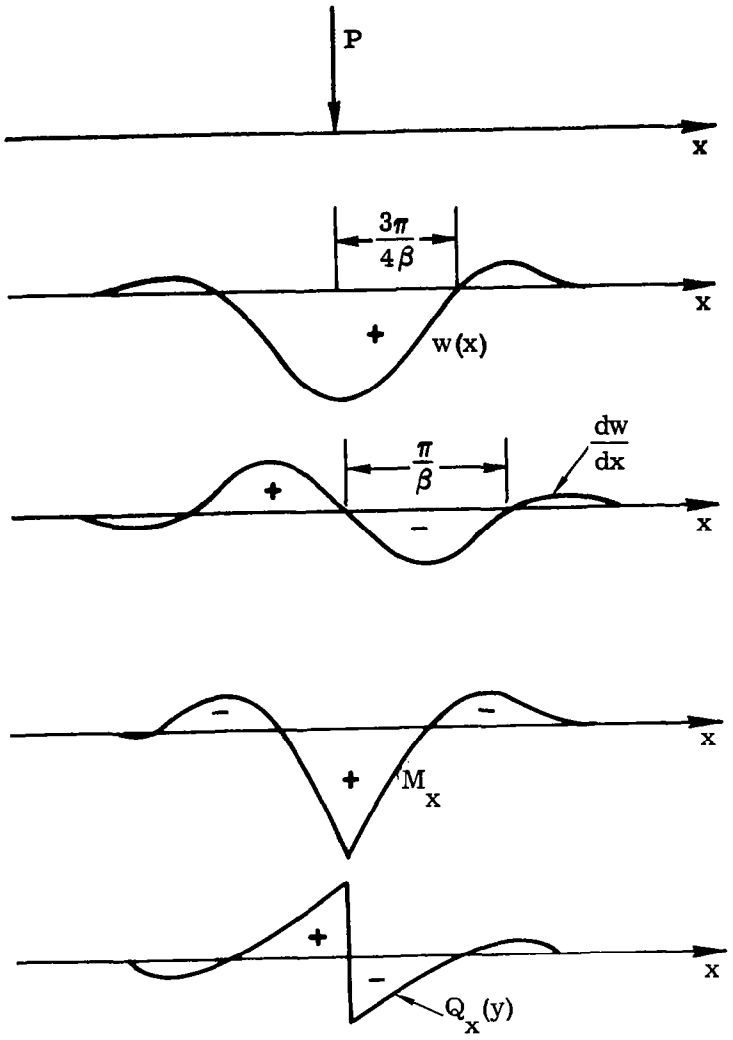

Figure 47. Deflection, Slope, Bending Moment, and Shear Forces

4.3.3 PRESSURIZED SHELL. Figure 48 shows a cylindrical shell clamped at the edges and pressurized with a uniform internal pressure. It is again assumed that the shell is long enough that the previously developed equations can be used.

The unknown bending moment and shear force at the clamped edge can now be calculated. The membrane stresses were expressed according to Equation 190

$$\sigma_{\varphi} = \frac{N_{\varphi}}{h} = \frac{p\,a}{h} = 2\sigma_x \tag{297}$$

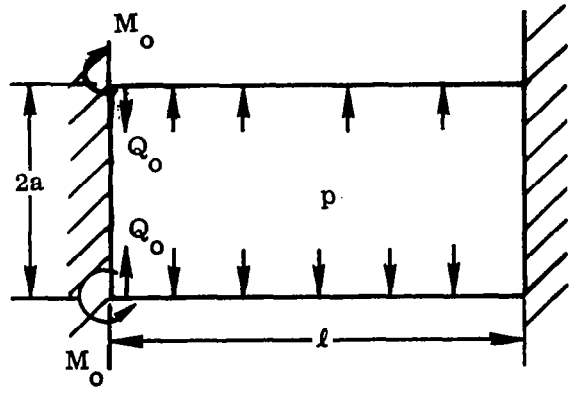

Figure 48. Pressurized Cylindrical Shell

The radial deflection can be obtained from membrane equations (280 and 190), with the following assumptions: $N_x = 0$, $X = 0$ and $Z = -p$. The simple derivation yields

$$-w = \frac{N_\varphi a}{E h} = \frac{p a^2}{E h} \tag{298}$$

The boundary conditions at the edge can be expressed by Equations 291, 298, and 290.

$$-\frac{1}{2\beta^3 D}(\beta M_o + Q_o) = \frac{p a^2}{E h} \tag{299}$$

$$\left.\frac{dw}{dx}\right|_{x=0} = \frac{1}{2\beta^2 D}(2\beta M_o + Q_o) = 0 \tag{300}$$

The solutions of the last two equations are

$$M_o = \frac{p}{2\beta^2} \qquad Q_o = -\frac{p}{\beta} \tag{301}$$

4.4 THERMAL STRESSES

The importance of edge effect due to thermal expansion will be discussed as an application of the theory developed in Section 4.2. As an expansion of the present theory, the approximate theory of laminated material (honeycomb) is also discussed.

4.4.1 BASIC PLATE EQUATION. The thermal expansion of a square plate is investigated first. Figure 49 shows the general arrangement. The temperature difference between the walls is $\Delta t = t$.

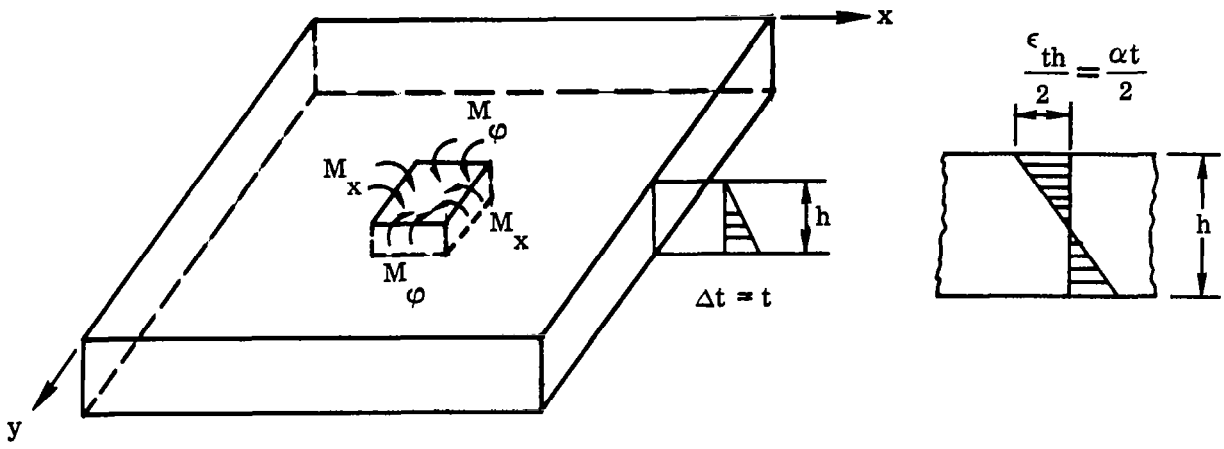

Figure 49. General Arrangement of Plate

A linear temperature change through the plate is assumed. The bending moment can be expressed in the x-direction

$$M_x = D(\varkappa_x + \nu\varkappa_y) = D\left(\frac{1}{r_x} + \frac{\nu}{r_y}\right) \tag{302}$$

It also may be assumed for a square plate

$$\frac{1}{r} = \frac{1}{r_x} = \frac{1}{r_y} = \frac{M_x}{D(1+\nu)} \tag{303}$$

The stress-strain law for a beam element may be applied, in this case, as an approximation ($M_y = 0$)

$$\sigma_x = \frac{E\epsilon_x}{(1-\nu^2)} = -\frac{Ez}{(1-\nu^2)}\frac{d^2w}{dx^2} \tag{304}$$

The bending moment for an element may be expressed by Equation 304

$$M_x = \int_{-h/2}^{h/2} \sigma_x z\,dz = -\frac{E}{(1-\nu^2)}\frac{d^2w}{dx^2}\int_{-h/2}^{h/2} z^2\,dz = -\frac{E}{(1-\nu^2)}\frac{d^2w}{dx^2} I \tag{305}$$

where

$$I = \int_{-h/2}^{h/2} z^2 \, dz \tag{306}$$

Figure 50 shows the cross-section of a homogenous plate element, and Figure 51 illustrates a honeycomb element.

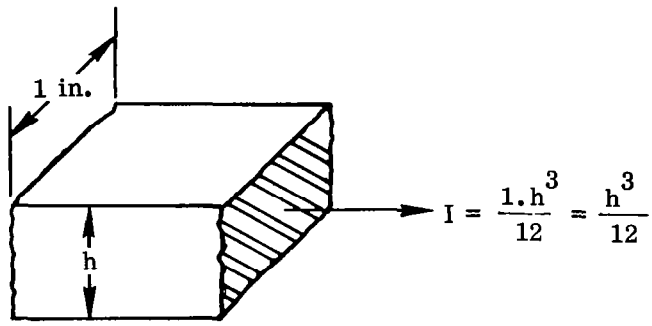

Figure 50. Cross-section of Plate Element

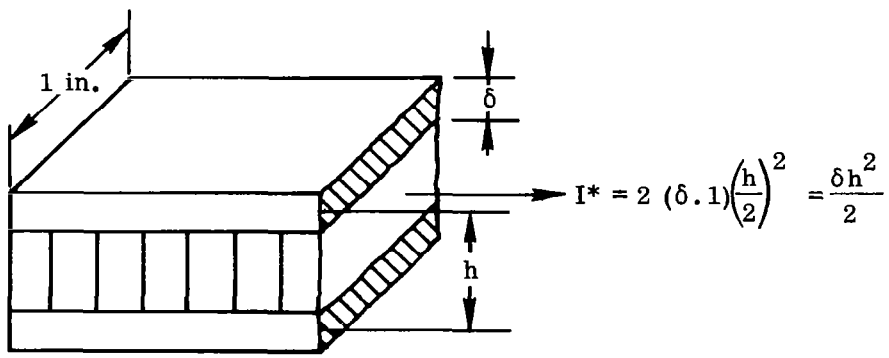

Figure 51. Cross-Section of Honeycomb Element

The modulus of cross-section is

$$K_x = \frac{I}{h/2} = \frac{h^2}{6} \tag{309}$$

The modulus of cross-section is, for a honeycomb plate

$$K_x^* = \frac{I^*}{h/2} = \delta h \tag{310}$$

The strain from thermal expansion, as can seen in Figure 49, can be expressed as

$$\epsilon_{thermal} = \frac{\alpha t}{2} = \frac{\sigma_{th}}{E} = \frac{M_x}{EK_x} \tag{311}$$

where α is the thermal expansion coefficient.

Introducing the beam approximation, the following relations can be obtained

$$\frac{1}{r_x} \approx \frac{M_x}{IE} = \frac{M_x}{E(K_x h/2)} \tag{312}$$

Substituting the expression of M_x/K_x from Equation 312 into Equation 311 one has

$$\frac{1}{r_x} = \frac{1}{r} = \frac{\alpha t}{h} \tag{313}$$

Since the bending moments are acting in an orthogonal direction for a plate or a shell, Equation 313 may be expressed by the use of Equation 303 in the following form

$$\frac{\alpha t}{h} = \frac{M_x}{D(1 + \nu)} \tag{314}$$

From Equation 314, the expression of bending moment, M_x, is

$$M_x = \frac{\alpha t D (1 + \nu)}{h} \tag{315}$$

The thermal stress has been obtained from Equation 315 as

$$\sigma_x = \frac{M_x}{K_x} = \frac{\alpha t D (1 + \nu)}{h K_x} \tag{316}$$

The expression D is designated the homogenous plate and D* the honeycomb element. For D and D* the following expressions can be written

$$D = \frac{E}{(1 - \nu^2)} I = \frac{E h^3}{12 (1 - \nu^2)} \tag{317}$$

$$D^* = \frac{E}{(1 - \nu^2)} I^* = \frac{E h^2 \delta}{2(1 - \nu^2)} \tag{318}$$

The thermal stress for a homogenous plate can be written, based on Equations 316, 317 and 309 as

$$\sigma_x = \frac{\alpha t E}{2 (1 - \nu)} \tag{319}$$

The thermal stress for a honeycomb plate can be obtained from Equations 316, 318, and 310.

$$\sigma_x = \frac{\alpha t D^* (1 + \nu)}{h K_x^*} = \frac{\alpha t E}{2 (1 - \nu)} \tag{320}$$

Conclusion. The thermal stresses are the same for a honeycomb and a homogenous plate, assuming the same material constants and thicknesses.

Equations 319 and 320 can be used as an approximation for a cylindrical shell when the thermal stress is induced by a linear temperature difference through the wall. This expression for the thermal stress does not take into account the edge effect, which can be significant (see Figure 52).

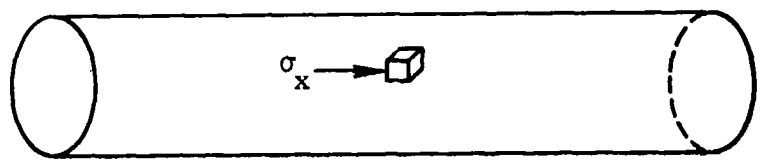

Figure 52. Long Cylinder

4.4.2 THE EFFECT OF BOUNDARY CONDITIONS. Figure 53 shows a clamped boundary condition. The radial deformation of the cylinder is due to thermal effects.

$$d = a\epsilon_{ther} = a\alpha t \tag{321}$$

where

a = radius of the cylinder

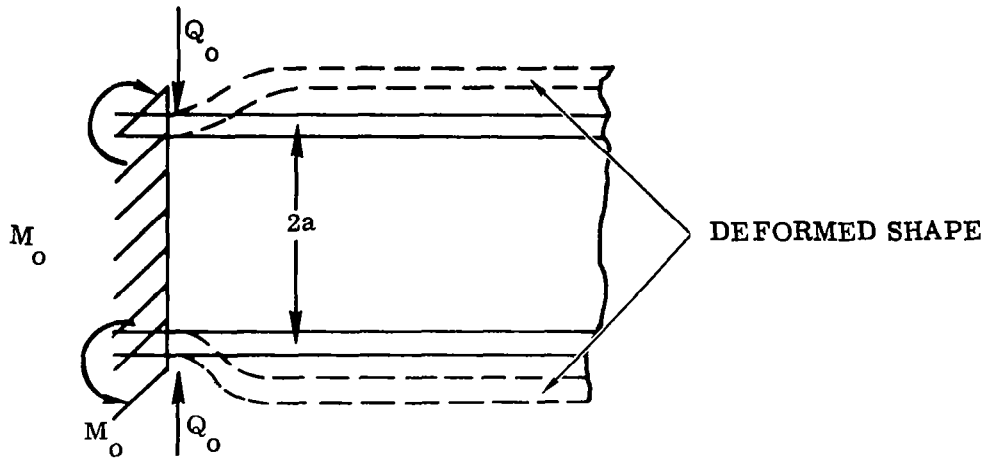

Figure 53. Clamped Boundary Condition of Cylindrical Shell

The unknown bending moment, M_o, and shear force, Q_o, can be calculated from Equations 299 and 300.

$$-\frac{1}{2\beta^3 D}(\beta M_o + Q_o) = a\alpha t \tag{322}$$

$$(2\beta M_o + Q_o) = 0 \tag{323}$$

The solutions of these equations are

$$M_o = 2\beta^2 D a\alpha t \tag{324}$$

$$Q_o = -4\beta^3 D a\alpha t \tag{325}$$

The boundary conditions can be written

$$M_x\big|_{x=0} = M_o \qquad M_\varphi\big|_{x=0} = \nu M_x\big|_{x=0} = \nu M_o \tag{326}$$

$$N_\varphi\big|_{x=0} = -\frac{E h}{a} d \tag{327}$$

4.4.3 HONEYCOMB STRUCTURE. The present theory can be applied easily to a honeycomb structure. The following equations can be obtained

$$N_{\varphi} = -\frac{2E\delta}{a} w \tag{328}$$

$$M_x = -\frac{E I^*}{(1-\nu^2)} \frac{d^2w}{dx^2} = -D^* \frac{d^2w}{dx^2} \tag{329}$$

where

$$D^* = \frac{E\delta h^2}{2(1-\nu^2)} \tag{318}$$

The substitution of Equations 328 and 329 into Equation 271 leads to

$$\frac{d^4w}{dx^4} + \frac{2E\delta}{a^2 D^*} w = \frac{Z}{D^*} \tag{330}$$

or

$$\frac{d^4w}{dx^4} + 4\beta^4 w = \frac{Z}{D^*} \tag{331}$$

where

$$\beta^4 = \frac{E\delta}{2a^2 D^*} = \frac{(1-\nu^2)}{a^2 h^2} \tag{332}$$

The shear force, Q_o, can be obtained by substituting Equations 318 and 332 into Equation 325.

$$Q_o = -4\beta^3 D^* a \alpha t = -\frac{2\delta E \alpha t}{(1-\nu^2)^{1/4}} \left(\frac{h}{a}\right)^{1/2} \tag{333}$$

An approximate formula for the shear stress in the core may be written

$$\tau = \frac{Q_o}{h} = \frac{2\delta E \alpha t}{(ah)^{1/2} (1-\nu^2)^{1/4}} \tag{334}$$

4.4.3.1 Stresses in the Circumferential Direction. Application of Equation 321 to Equation 298 leads to

$$N_\varphi = -\frac{2E\delta}{a} a\alpha t = -2E\delta\alpha t \tag{335}$$

When Equations 318 and 332 are substituted into Equation 324 one has

$$M_o = 2\beta^2 D^* a\alpha t = \frac{E\delta h\alpha t}{(1-\nu^2)^{1/2}} \tag{336}$$

The bending moment, M_φ, can be calculated from Equation 326

$$M_\varphi\big|_{x=0} = \nu M_x\big|_{x=0} = \nu M_o = \frac{\nu E\delta h\alpha t}{\sqrt{1-\nu^2}} \tag{337}$$

The stress, σ_φ, has three components in the circumferential direction

$$\sigma_{\varphi_1} \approx \mp\frac{E\alpha t}{2(1-\nu)} \approx \sigma_x \tag{338}$$

$$\sigma_{\varphi_2} = \frac{\nu M_o}{\delta h} = \mp\frac{\nu E\alpha t}{\sqrt{1-\nu^2}} \tag{339}$$

$$\sigma_{\varphi_3} = \frac{N_\varphi}{2\delta} = -E\alpha t \tag{340}$$

Figure 54 shows the stresses separately.

The maximum stress, σ_φ, is in the circumferential direction

$$\sigma_\varphi\big|_{max} = \sigma_{\varphi_1} + \sigma_{\varphi_2} + \sigma_{\varphi_3} = -\frac{E\alpha t}{2(1-\nu)}\left[1 + 2\nu\sqrt{\frac{1-\nu}{1+\nu}} + 2(1-\nu)\right] \tag{341}$$

Assuming Poisson's ratio, $\nu = 0.17$

$$\sigma_\varphi\big|_{max} = -\frac{E\alpha t}{2(1-\nu)}[1 + 0.286 + 1.66] \approx -3\left[\frac{E\alpha t}{2(1-\nu)}\right] \tag{342}$$

The last equation shows that the clamped edge can triple the thermal stress. Similar problems can be found in Reference 4, pages 497-501.

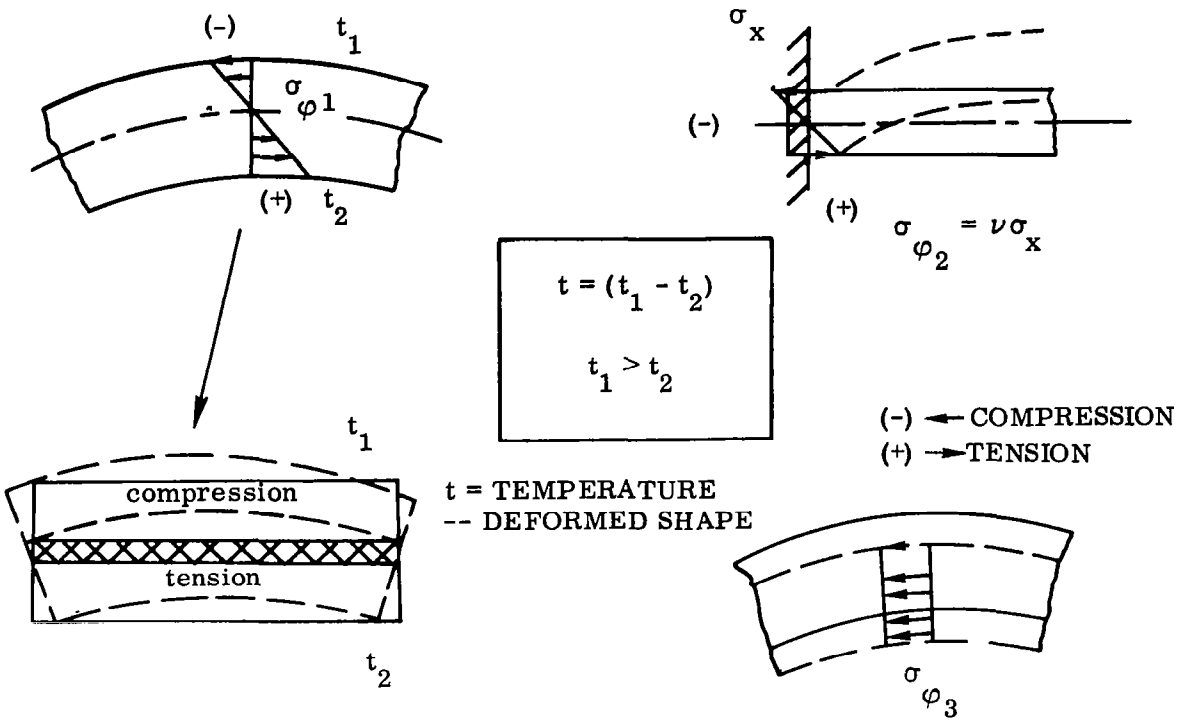

Figure 54. Illustration of Thermal Stresses

One has to be aware that the previously developed formulas of thermal stresses are approximately valid, as long as the theoretical assumptions approximate the physical reality.

4.4.4 EXAMPLE, THERMAL STRESS CALCULATION. A long, clamped honeycomb cylindrical shell has the following physical properties:

a. Modulus of elasticity, $E = 3.2 \times 10^6$ lb/in.^{2}

b. Radius of cylinder, $a = 21.5$ in.

c. Poisson's ratio, $\gamma = 0.17$

d. Shell thickness, $h = 1.75$ in.

e. Skin thickness, $\delta = 0.045$ in.

f. Thermal expansion coefficient, $\alpha = 4.93 \times 10^{-6}$ in./in.° F

g. Temperature difference, $t = \Delta t = 300°$ F

The thermal stresses can be calculated as follows. First, calculate the maximum shear stress in the core. Second, calculate the maximum circumferential stress at the clamped edge. The shear stress in the core can be computed by Equation 334.

$$\tau_{core} = \frac{(0.09)(3.2 \times 10^6)(4.93 \times 10^{-6})(300)}{(21.5 \times 1.75)^{1/2}(1 - 0.17^2)^{1/4}} = 70 \text{ lb/in.}^2$$

If a = 14.8 in., $\tau_{core} = 84$ lb/in.^{2} .

The maximum circumferential stress was computed from Equations 338 and 341.

$$\sigma_{\varphi_1} = \frac{(3.2 \times 10^6)(4.93 \times 10^{-6})(300)}{2(1 - 0.17)} = 2850 \text{ lb/in.}^2$$

$$\sigma_{\varphi, max} = 2.946 \times 2850 = 8400 \text{ lb/in.}^2$$

4.5 COMBINED BENDING - MEMBRANE THEORY OF CYLINDRICAL SHELLS

The theory discussed up to now was restricted to the case of a uniform force distribution in the circumferential direction. The present theory will discuss the problem in general. Figure 55 shows the forces, and Figure 56 illustrates the bending and twisting moments on the same shell element.

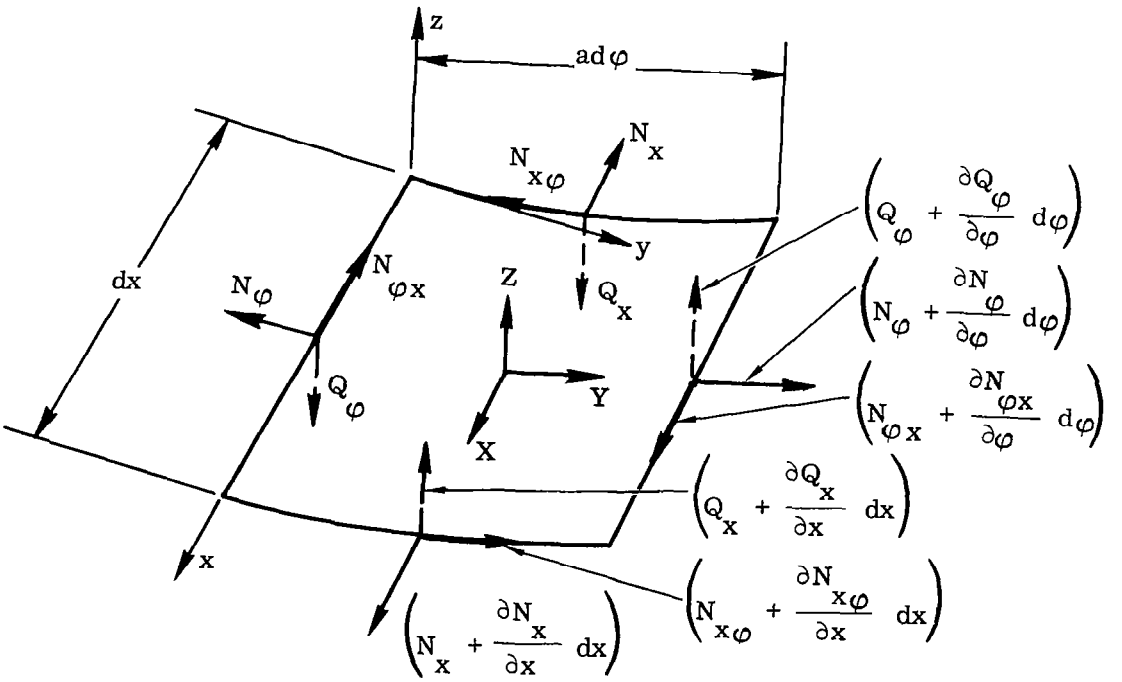

Figure 55. Cylindrical Shell Element Under General Loading

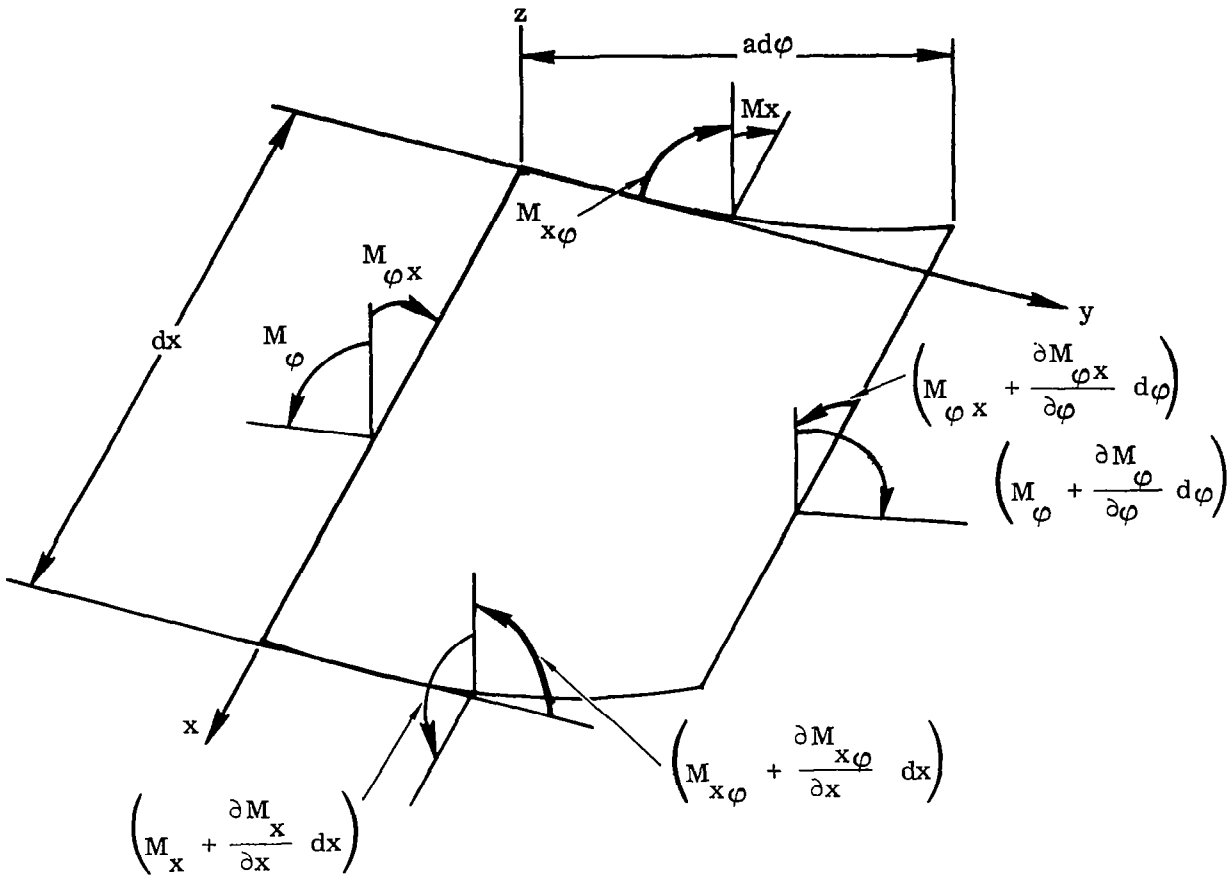

Figure 56. Bending and Twisting Moments

The equation of forces in direction x is identical with Equation 93; therefore, the final result of the calculation is

$$\frac{\partial N_x}{\partial x} + \frac{1}{a}\frac{\partial N_{\varphi x}}{\partial \varphi} = -X \tag{343}$$

The forces in the direction y were written based on Figures 55 and 57a

$$\left(N_{\varphi} + \frac{\partial N_{\varphi}}{\partial \varphi} d\varphi\right)dx - N_{\varphi} dx + \left(N_{x\varphi} + \frac{\partial N_{x\varphi}}{\partial x} dx\right) a\, d\varphi - N_{x\varphi}\, a\, d\varphi$$

$$- Q_{\varphi} dx \frac{d\varphi}{2} - \left(Q_{\varphi} + \frac{\partial Q_{\varphi}}{\partial \varphi} d\varphi\right) dx \frac{d\varphi}{2} + Y a\, d\varphi\, dx = 0 \tag{344}$$

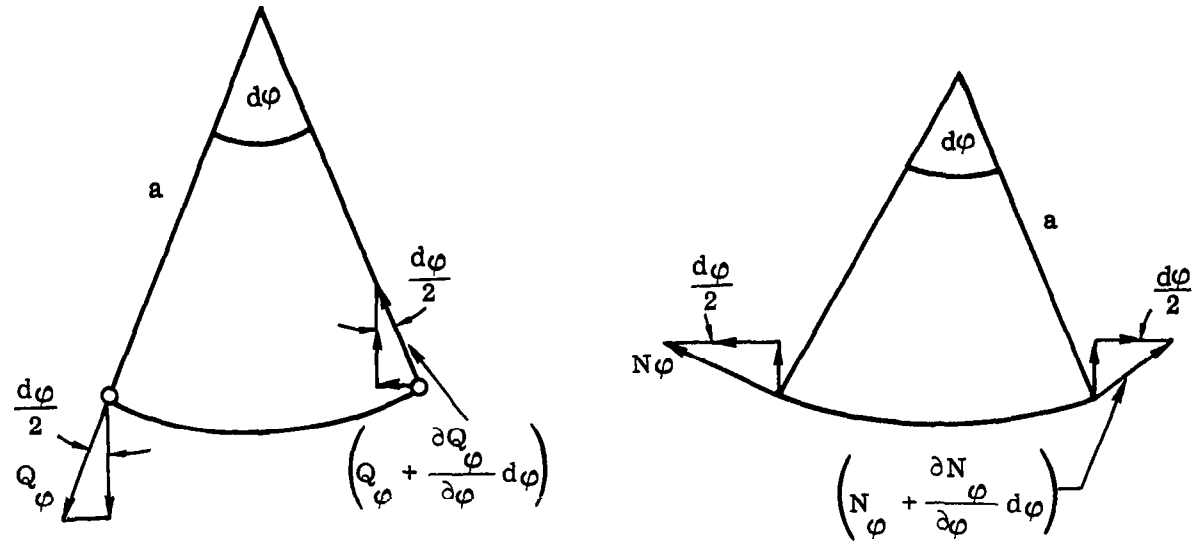

a. b.

Figure 57. Directional Forces

Neglecting a second-order shear term, in the final form, Equation 344 is

$$\frac{1}{a}\frac{\partial N_\varphi}{\partial \varphi} + \frac{\partial N_{x\varphi}}{\partial x} - \frac{Q_\varphi}{a} = -Y \tag{345}$$

The forces in the direction z can be obtained, based on Figures 55 and 57b

$$\left(Q_x + \frac{\partial Q_x}{\partial x}dx\right)a\,d\varphi - Q_x\,a\,d\varphi + \left(Q_\varphi + \frac{\partial Q_\varphi}{\partial \varphi}d\varphi\right)dx - Q_\varphi dx$$

$$+ N_\varphi\,d\varphi\,dx + Z\,a\,d\varphi\,dx = 0 \tag{346}$$

Since several terms were cancelled out in Equation 346, the calculation yields finally

$$\frac{\partial Q_x}{\partial x} + \frac{1}{a}\frac{\partial Q_\varphi}{\partial \varphi} + \frac{N_\varphi}{a} = -Z \tag{347}$$

The moments around the x-axis may be obtained, based on Figures 55 and 56

$$\left(M_\varphi + \frac{\partial M_\varphi}{\partial \varphi}d\varphi\right)dx - M_\varphi dx - \left(M_{x\varphi} + \frac{\partial M_{x\varphi}}{\partial x}dx\right)a\,d\varphi$$

$$+ M_{x\varphi}\,a\,d\varphi - Q_\varphi dx\,a\,d\varphi = 0 \tag{348}$$

Equation 348 is, in its final form

$$\frac{1}{a}\frac{\partial M_{\varphi}}{\partial \varphi} - \frac{\partial M_{x\varphi}}{\partial x} - Q_{\varphi} = 0 \tag{349}$$

The moments around the y-axis can be written based on Figures 55 and 56

$$\left(M_x + \frac{\partial M_x}{\partial x}dx\right)a\,d\varphi - M_x\,a\,d\varphi + \left(M_{\varphi x} + \frac{\partial M_{\varphi x}}{\partial \varphi}d\varphi\right)dx$$

$$- M_{\varphi x}\,dx - Q_x\,a\,d\varphi\,dx = 0 \tag{350}$$

Cancelling out several terms, Equation 350 is, in its final form

$$\frac{\partial M_x}{\partial x} + \frac{1}{a}\frac{M_{\varphi x}}{\partial \varphi} - Q_x = 0 \tag{351}$$

A sixth equation representing the moments around a radius of the cylinder may be obtained

$$N_{x\varphi}\,a\,d\varphi\,dx - N_{\varphi x}\,dx\,a\,d\varphi + M_{\varphi x}\,dx\,d\varphi = 0 \tag{352}$$

Equation 352 is, in its final form

$$N_{x\varphi} - N_{\varphi x} + \frac{M_{\varphi x}}{a} = 0 \tag{353}$$

Some authors have neglected the last term in this equation, as a second-order quantity; therefore, Equation 353 may be modified as

$$N_{x\varphi} = N_{\varphi x} \tag{354}$$

(For a further explanation of Equation 352, see Figures 55 and 56.)

The substitution of the shear force Q_{φ} in the terms of moments (from Equation 349) into Equation 345 leads to

$$\frac{1}{a}\frac{\partial N_{\varphi}}{\partial \varphi} + \frac{\partial N_{x\varphi}}{\partial x} - \frac{1}{a^2}\frac{\partial M_{\varphi}}{\partial \varphi} + \frac{1}{a}\frac{\partial M_{x\varphi}}{\partial x} = -Y \tag{355}$$

The shear forces Q_x and Q_{φ} can be eliminated from Equation 347 by the use of Equations 349 and 351. One then has

$$\frac{\partial^2 M_x}{\partial x^2} + \frac{1}{a}\frac{\partial^2 M_{\varphi x}}{\partial x \partial \varphi} + \frac{1}{a^2}\frac{\partial^2 M_\varphi}{\partial \varphi^2} - \frac{1}{a}\frac{\partial^2 M_{x\varphi}}{\partial x \partial \varphi} + \frac{N_\varphi}{a} = -Z \tag{356}$$

Summary. The three equilibrium equations of the shell element were expressed in terms of moments and membrane forces.

$$\frac{\partial N_x}{\partial x} + \frac{1}{a}\frac{\partial N_{\varphi x}}{\partial \varphi} = -X \tag{357}$$

$$\frac{1}{a}\frac{\partial N_\varphi}{\partial \varphi} + \frac{\partial N_{x\varphi}}{\partial x} - \frac{1}{a^2}\frac{\partial M_\varphi}{\partial \varphi} + \frac{1}{a}\frac{\partial M_{x\varphi}}{\partial x} = -Y \tag{358}$$

$$\frac{\partial^2 M_x}{\partial x^2} + \frac{1}{a}\frac{\partial^2 M_{\varphi x}}{\partial x \partial \varphi} + \frac{1}{a^2}\frac{\partial^2 M_\varphi}{\partial \varphi^2} - \frac{1}{a}\frac{\partial^2 M_{x\varphi}}{\partial x \partial \varphi} + \frac{N_\varphi}{a} = -Z \tag{359}$$

The two auxiliary equations for shear forces and the one for the membrane shear force can be expressed from Equations 349, 351, 353 and 354

$$Q_\varphi = \frac{1}{a}\frac{\partial M_\varphi}{\partial \varphi} - \frac{\partial M_{x\varphi}}{\partial x} \tag{360}$$

$$Q_x = \frac{\partial M_x}{\partial x} + \frac{1}{a}\frac{\partial M_{\varphi x}}{\partial \varphi} \tag{361}$$

$$N_{x\varphi} = N_{\varphi x} + \frac{M_{\varphi x}}{a} \qquad \text{or} \qquad N_{x\varphi} = N_{\varphi x} \tag{362}$$

4.5.1 SIGN CONVENTION DIFFERENCE BETWEEN TIMOSHENKO AND FLÜGGE. Figure 58 shows the sign convention for moments of Timoshenko and Figure 59 for Flügge.

The sign convention of the shear forces, Q_φ and Q_x, are also opposite; however, the opposite direction of axis z cancels out the effect. Figure 60 illustrates the differences.

Comparison of the two authors' works can easily lead to confusion since their equations are different in signs. The following transformations can be introduced to compare the same equations

$$\left.\begin{aligned} Z_T &= -Z_F \\ W_T &= -W_F \\ M_{x\varphi}\big|_T &= -M_{x\varphi}\big|_F \end{aligned}\right\} \tag{363}$$

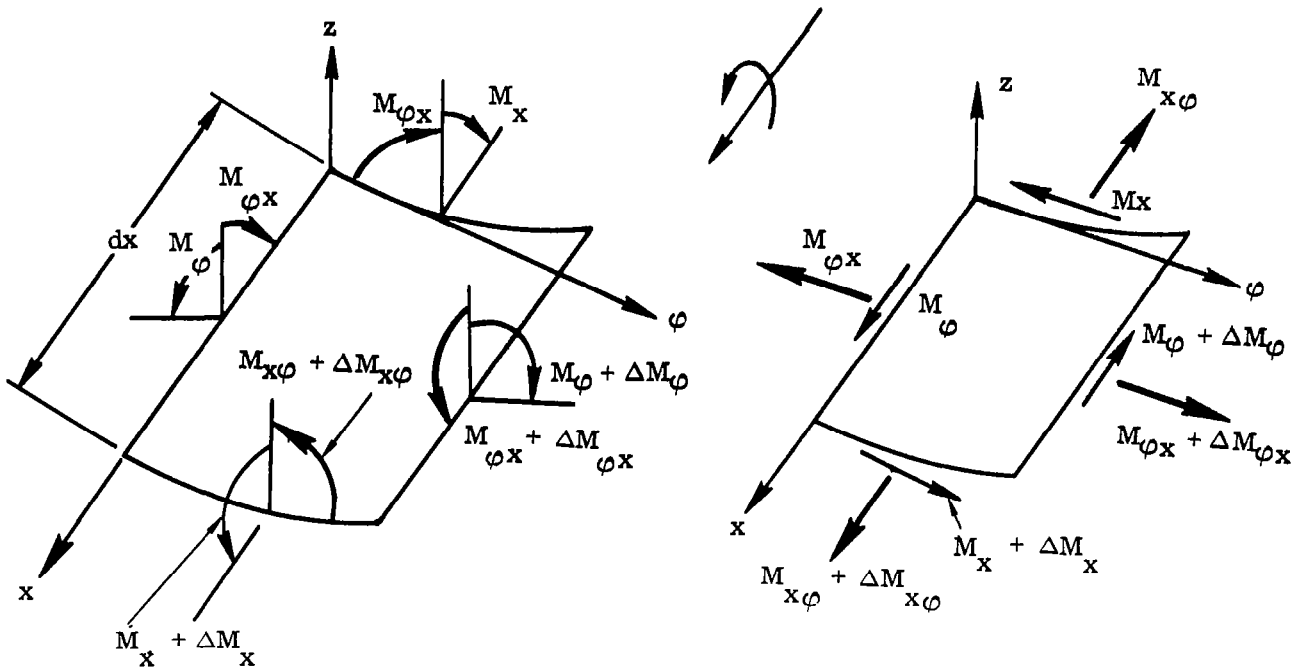

TIMOSHENKO

Figure 58. Sign Convention (Timoshenko)

4.5.2 STRAIN-DISPLACEMENT RELATIONS. The membrane theory considered only the stretching and compressing effect of the middle surface of the shell element. This theory ignored the stress variation through the thickness of the shell. The membrane-bending theory will correct this error. The deformation of the shell is illustrated by Figures 61 and 62.

The cylindrical shell is defined by radius a and thickness h. Figures 61 and 62 show only half of the shell thickness. An arbitrary point A is located in the middle surface and an arbitrary point A is located a distance z from the middle surface. The membrane theory considers only the deformation of point A on the middle surface. The combined theory will be defined by the deformation of point A, which includes the membrane deformation and an additional rotation. The following assumptions were made:

a. All points lying on a normal to the middle surface before deformation are in the same position after deformation.

b. The distance A_0A is unchanged after deformation, which means the stress σ_z in the z-direction may be considered negligible compared with the stresses σ_x and σ_φ.

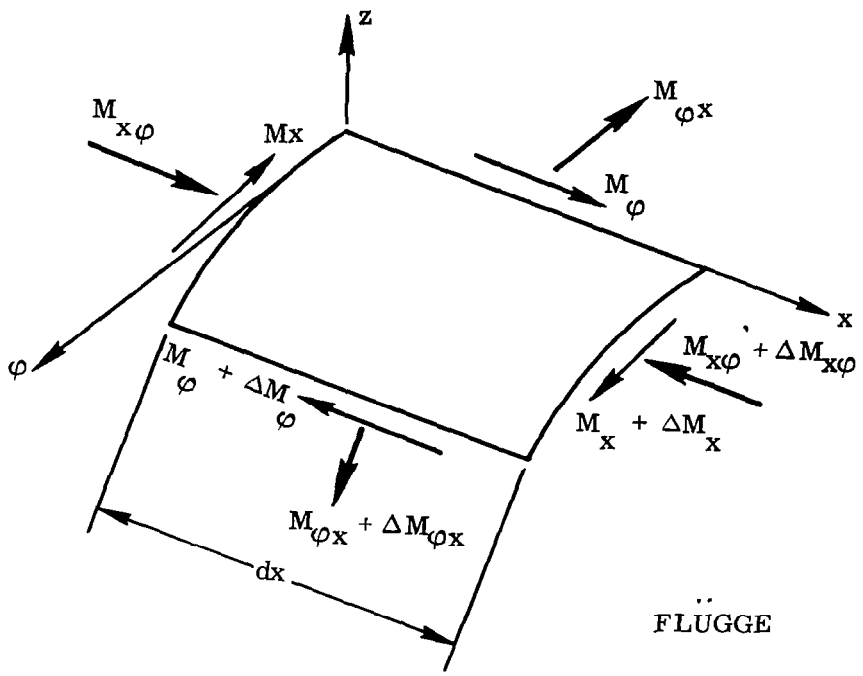

Figure 59. Sign Convention (Flügge)

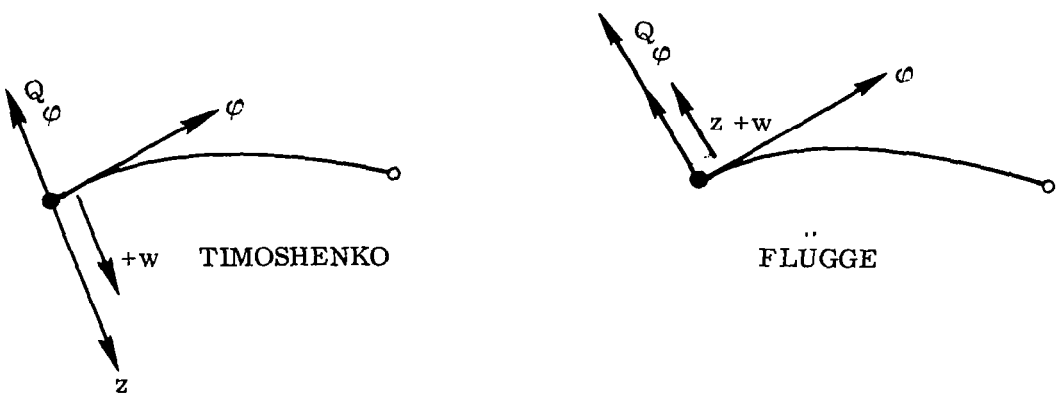

Figure 60. Shear Force and Displacement Conventions

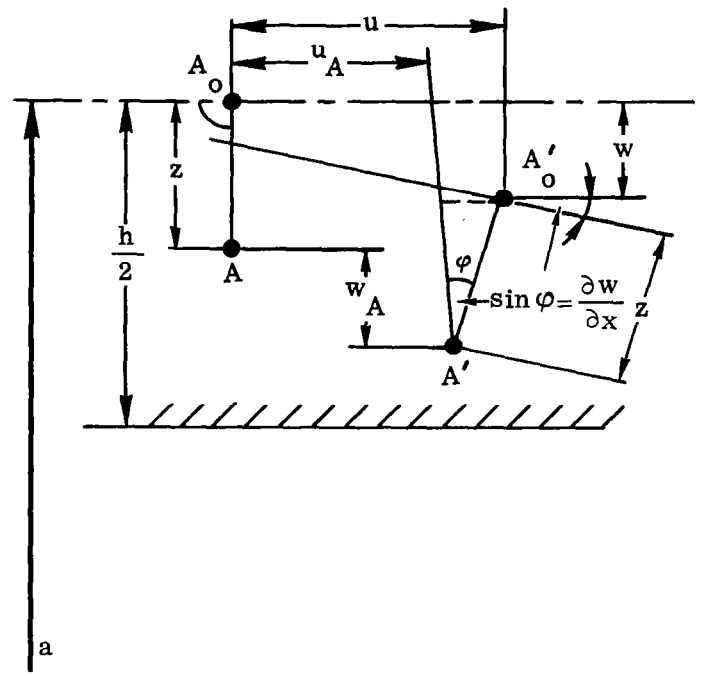

Figure 61. Shell Deformation in Radial Direction

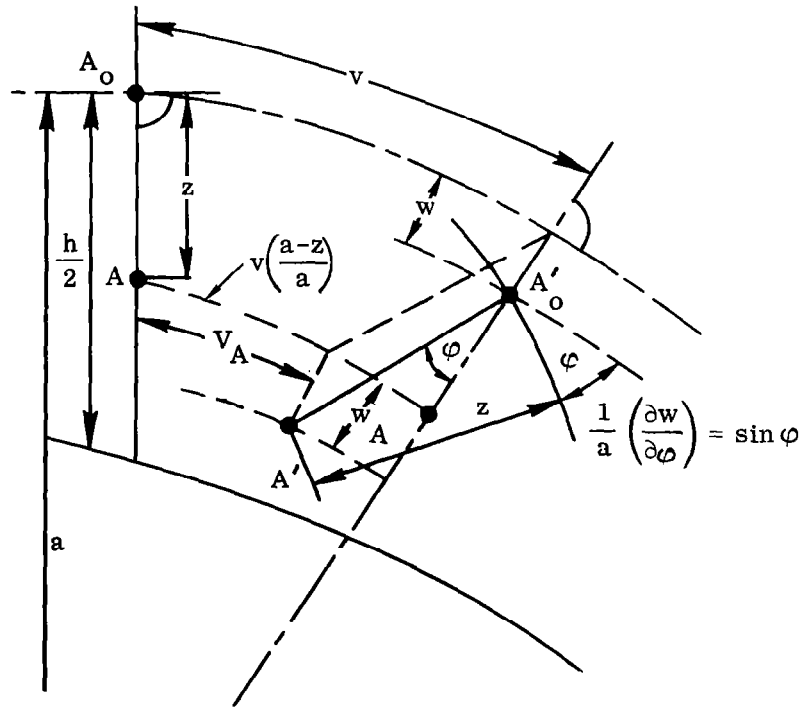

Figure 62. Shell Deformation in Circumferential Direction

Let the undeformed state be designated by the unprimed letters and the deformed state by primed ones. Figure 61 illustrates a section of the cylinder along a generator. The displacement, u_A, of point A is therefore equal to the displacement, u, of point A_o minus the distance A is shifted back by the rotation of $\overline{A_oA}$

$$u_A = \overline{A_oA_o}' - z \sin \varphi = u - z \frac{\partial w}{\partial x} \tag{364}$$

The circumferential displacement, v_A, can be derived from the transverse section of the shell, as illustrated by Figure 62. The point A_o is displaced by v along the middle surface, and since the normal $\overline{A_oA}$ stays normal to this surface, the point A is displaced by $v\left(\frac{a-z}{a}\right)$. The rotation of the normal is $\frac{1}{a}\frac{\partial w}{\partial \varphi}$, and it produces an additional displacement, $-\frac{z}{a}\frac{\partial w}{\partial \varphi}$. The displacement of point A in the circumferential direction is

$$v_A = v\left(\frac{a-z}{a}\right) - z \sin \varphi = v\left(\frac{a-z}{a}\right) - \frac{z}{a}\frac{\partial w}{\partial \varphi} \tag{365}$$

The distance $\overline{A\,A_o}$ is unchanged during deformation because of assumption b. and because the slope of the deformation is small compared with unity. Furthermore, the displacements are also small compared with the radii of curvature of the middle surface. For these reasons, the following equation can be written

$$w = w_A \tag{366}$$

Since the motion of point A considered the elongation and rotation simultaneously, the equations derived for membrane theory may be used with the replacement of a with (a - z).

The longitudinal strain can be derived by the substitution of Equation 364 into Equation 131.

$$\epsilon_x = \frac{\partial u_A}{\partial x} = \frac{\partial u}{\partial x} - z \frac{\partial^2 w}{\partial x^2} \tag{367}$$

The circumferential strain was calculated similarly; the substitution of Equations 365 and 366 into Equation 134 leads to

$$\epsilon_\varphi = \frac{1}{a-z}\left(\frac{\partial v_A}{\partial \varphi} - w_A\right) = \frac{1}{a}\frac{\partial v}{\partial \varphi} - \frac{w}{(a-z)} - \frac{z}{a(a-z)}\frac{\partial^2 w}{\partial \varphi^2} \tag{368}$$

Similarly, the shear-strain may be derived from Equations 135, 364 and 365

$$\gamma_{x\varphi} = \frac{1}{(a - z)} \frac{\partial u_A}{\partial \varphi} + \frac{\partial v_A}{\partial x} = \frac{1}{(a - z)} \frac{\partial u}{\partial \varphi} + \frac{(a - z)}{a} \frac{\partial v}{\partial x} - \left(\frac{z}{a} + \frac{z}{a - z}\right) \frac{\partial^2 w}{\partial x \partial \varphi} \quad (369)$$

4.5.3 FORCES AND MOMENTS IN TERMS OF DISPLACEMENTS. The forces and moments may be derived based on Figure 63. It is necessary to consider, first, an element in the cross-section (such an element has been shaded in Figure 63).

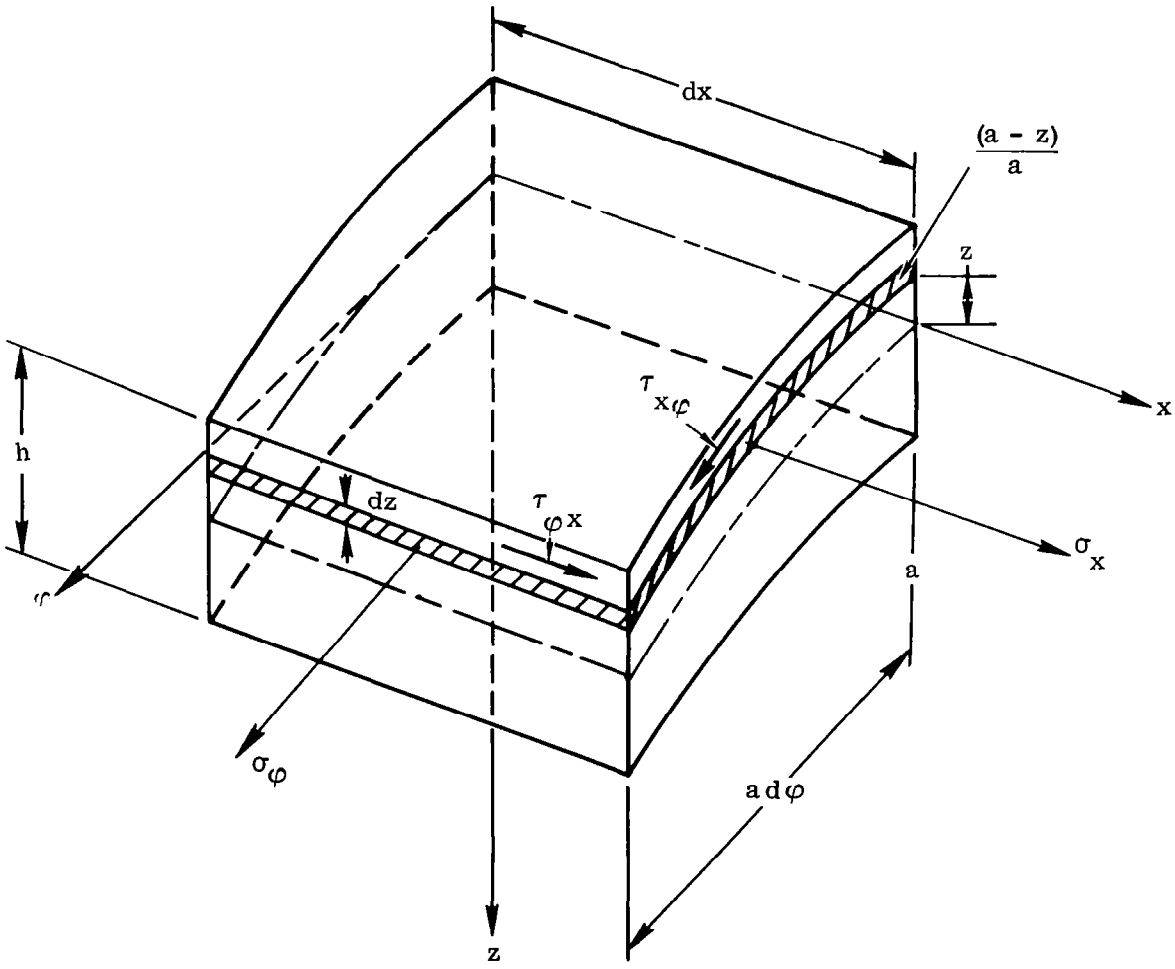

Figure 63. Cross Section of Shell Element with Stresses

Because of the curvature of the shell, its width is not simply $a\,d\varphi$, but $a\,d\varphi\,\frac{(a-z)}{a}$. The force in the direction x may now be written

$$N_x(a\,d\varphi) = \int_{-h/2}^{h/2} \sigma_x(a\,d\varphi)\,\frac{(a-z)}{a}\,dz \tag{370}$$

Since the factor $(a\,d\varphi)$ on both sides is dropped, a relation is derived between the force N_x and stress σ_x. Equation 370 can be expressed

$$N_x = \int_{-h/2}^{h/2} \sigma_x\left(\frac{a-z}{a}\right)dz \tag{371}$$

The rest of the forces were obtained from similar derivations

$$N_\varphi = \int_{-h/2}^{h/2} \sigma_\varphi dz\,, \quad N_{x\varphi} = \int_{-h/2}^{h/2} \tau_{x\varphi}\left(\frac{a-z}{a}\right)dz, \quad N_{\varphi x} = \int_{-h/2}^{h/2} \tau_{\varphi x}dz \tag{372}$$

The change of curvature has again been considered in the calculation of moments. The width of the shaded element is $a\,d\varphi\,\frac{(a-z)}{a}$ and this was applied to obtain the bending moment, M_x

$$M_x(a\,d\varphi) = \int_{-h/2}^{h/2} \sigma_x(a\,d\varphi)\,\frac{(a-z)}{a}\,z\,dz \tag{373}$$

The cancellation of the common factor $a\,d\varphi$ leads to the expression of bending moment, M_x

$$M_x = \int_{-h/2}^{h/2} \sigma_x\,\frac{(a-z)}{a}\,z\,dz \tag{374}$$

The bending moment, M_φ, and furthermore, the twisting moments, $M_{x\varphi}$ and $M_{\varphi x}$, can be calculated similarly

$$M_\varphi = \int_{-h/2}^{h/2} \sigma_\varphi z\,dz; \quad M_{x\varphi} = -\int_{-h/2}^{h/2} \tau_{x\varphi}\,\frac{(a-z)}{a}z\,dz, \quad M_{\varphi x} = \int_{-h/2}^{h/2} \tau_{\varphi x}z\,dz \tag{375}$$

There is no change of curvature of the strip element; consequently, the term representing this effect is unity. The stress-strain relations can still be obtained from the equations of membrane theory, since the stress, σ_z, is assumed to be small compared with the others. These equations can be written as

$$\left.\begin{aligned} \sigma_x &= \frac{E}{(1-\nu^2)}(\epsilon_x + \nu\epsilon_\varphi) \\ \sigma_\varphi &= \frac{E}{(1-\nu^2)}(\epsilon_\varphi + \nu\epsilon_x) \\ \tau_{x\varphi} &= G\,\gamma_{x\varphi} \end{aligned}\right\} \qquad (376)$$

The substitution of Equations 367 and 368 into Equation 376 and again into Equation 371 leads to expressions for forces. The stress σ_x is

$$\sigma_x = \frac{E}{(1-\nu^2)}\left\{\left(\frac{\partial u}{\partial x} - z\frac{\partial^2 w}{\partial x^2}\right) + \nu\left[\frac{1}{a}\frac{\partial v}{\partial \varphi} - \frac{z}{a(a-z)}\frac{\partial^2 w}{\partial \varphi^2} - \frac{w}{(a-z)}\right]\right\} \qquad (377)$$

The force N_x is, from the previous considerations

$$N_x = \int_{-h/2}^{h/2} \sigma_x\left(\frac{a-z}{a}\right)dz = \frac{E\,h}{(1-\nu^2)}\left\{\frac{\partial u}{\partial x} + \frac{\nu}{a}\left(\frac{\partial v}{\partial \varphi} - w\right) + \frac{h^2}{12a}\frac{\partial^2 w}{\partial x^2}\right\} \qquad (378)$$

The following calculation will show the treatment of logarithmic functions. The substitution of Equations 367 and 368 into Equation 376 and again into Equation 372 leads to the expression of force, N_φ

$$N_\varphi = \frac{E}{(1-\nu^2)}\int_{-h/2}^{h/2}\left[\left(\frac{1}{a}\frac{\partial v}{\partial \varphi} - \frac{z}{a(a-z)}\frac{\partial^2 w}{\partial \varphi^2} - \frac{w}{a-z}\right) + \nu\left(\frac{\partial u}{\partial x} - z\frac{\partial^2 w}{\partial x^2}\right)\right] dz \qquad (379)$$

The integration of this equation leads to

$$N_\varphi = \frac{E}{(1-\nu^2)}\left\{\frac{1}{a}\frac{\partial v}{\partial \varphi}z + w\,\ell n\,(a-z) + \nu\frac{\partial u}{\partial x} + \frac{1}{a}\frac{\partial^2 w}{\partial \varphi^2}\left[z + a\,\ell n(a-z)\right]\right\}_{-h/2}^{h/2} \qquad (380)$$

It is well known from the series expansion of the logarithmic function that

$$\ell n\left(\frac{1-x}{1+x}\right) = -2\left(x + \frac{x^3}{3} + \frac{x^5}{5} + \ldots.\right) \qquad (381)$$

In the present case, the following relation can be written

$$\ln \frac{\left(1 - \frac{h}{2a}\right)}{\left(1 + \frac{h}{2a}\right)} = -2\left[\frac{h}{2a} + \frac{h^3}{24a^3} + \ldots.\right] \tag{382}$$

where

$$0 < \frac{h}{2a} \ll 1$$

The rest of the terms were neglected as second-order quantities.

The application of Series 382 into Equation 380 leads to

$$N_\varphi = \frac{E\,h}{(1-\nu^2)}\left[\frac{1}{a}\left(\frac{\partial v}{\partial \varphi} - w\right) + \nu \frac{\partial u}{\partial x}\right] - \frac{E\,h^3}{12(1-\nu^2)\,a^3}\left(w + \frac{\partial^2 w}{\partial \varphi^2}\right) \tag{383}$$

The bending moments M_x and M_φ can be calculated easily also

$$M_x = -\frac{E\,h^3}{12(1-\nu^2)}\left\{\frac{\partial^2 w}{\partial x^2} + \frac{\nu}{a^2}\left(\frac{\partial v}{\partial \varphi} + \frac{\partial^2 w}{\partial \varphi^2}\right) + \frac{1}{a}\frac{\partial u}{\partial x}\right\} \tag{384}$$

$$M_\varphi = -\frac{E\,h^3}{12(1-\nu^2)}\left\{\frac{1}{a^2}\left(w + \frac{\partial^2 w}{\partial \varphi^2}\right) + \nu \frac{\partial^2 w}{\partial x^2}\right\} \tag{385}$$

The comparison of these equations with Reference 6, page 214 shows opposite signs in the terms of displacement, w. This difference can be found in the opposite sign convention of displacement w, as it was referenced in Subsection 4.5.1.

4.5.4 SIMPLIFIED EQUATIONS AND DONNELL'S DIFFERENTIAL EQUATIONS OF EQUILIBRIUM. In some cases the simplification of the general equations can be obtained; however, there is no golden rule for the general applications of the approximate equations. The basis of the following equations is to neglect terms which were generated from the curvature change (terms z/a). The equations of forces are, in their simplified forms

$$N_x = \frac{E\,h}{(1-\nu^2)}(\epsilon_x + \nu e_\varphi),\quad N_\varphi = \frac{E\,h}{(1-\nu^2)}(\epsilon_\varphi + \nu \epsilon_x),\quad N_{x\varphi} = N_{\varphi x} = G\,h\,\gamma_{x\varphi} \tag{386}$$

where

$$\epsilon_x = \frac{\partial u}{\partial x},\quad \epsilon_\varphi = \frac{1}{a}\left(\frac{\partial v}{\partial \varphi} - w\right),\quad \gamma_{x\varphi} = \frac{1}{a}\frac{\partial u}{\partial \varphi} + \frac{\partial v}{\partial x} \tag{387}$$

In Equation 386 the shear forces, $N_{x\varphi}$ and $N_{\varphi x}$, are equal, which assumes that the twisting moment, M_{φ}, is also zero in Equation 353. This approximation can sometimes lead to a contradiction. Equation 386, in this simplified case, represents the membrane forces. The bending and twisting moments, in the simplified case, are

$$M_x = -\frac{E h^3}{12(1-\nu^2)}\left[\varkappa_x + \nu \varkappa_{\varphi}\right]$$

$$M_{\varphi} = -\frac{E h^3}{12(1-\nu^2)}\left[\varkappa_{\varphi} + \nu \varkappa_x\right] \qquad (388)$$

$$M_{x\varphi} = M_{\varphi x} = \frac{E h^3}{12(1+\nu)} \varkappa_{x\varphi}$$

where

$$\varkappa_x = \frac{\partial^2 w}{\partial x^2}$$

$$\varkappa_{\varphi} = \frac{1}{a^2}\left(\frac{\partial v}{\partial \varphi} + \frac{\partial^2 w}{\partial \varphi^2}\right) \qquad (389)$$

$$\varkappa_{x\varphi} = \frac{1}{a}\left(\frac{\partial v}{\partial x} + \frac{\partial^2 w}{\partial x \partial \varphi}\right)$$

4.5.4.1 Donnell's Differential Equations of Equilibrium. A simplified form of shell equation may be derived based on Donnell's assumptions. The substitution of Equations 386 and 388 into Equations 357, 358 and 359 yields the three differential equations of equilibrium. Equation 391 was derived by neglecting the terms of bending theory or the terms containing h^2. Neglecting the third-order circumferential displacement terms, v, from Equation 392, a third equation was obtained in a final form.

$$\frac{\partial^2 u}{\partial x^2} + \frac{(1-\nu)}{2a^2}\frac{\partial^2 u}{\partial \varphi^2} + \frac{(1+\nu)}{2a}\frac{\partial^2 v}{\partial x \partial \varphi} - \frac{\nu}{a}\frac{\partial w}{\partial x} = -\frac{X(1-\nu^2)}{E h} \qquad (390)$$

$$\frac{(1+\nu)}{2}\frac{\partial^2 u}{\partial x \partial \varphi} + \frac{a(1-\nu)}{2}\frac{\partial^2 v}{\partial x^2} + \frac{1}{a}\frac{\partial^2 v}{\partial \varphi^2} - \frac{1}{a}\frac{\partial w}{\partial \varphi} = -\frac{Y(1-\nu^2)a}{E h} \qquad (391)$$

$$\nu \frac{\partial u}{\partial x} + \frac{1}{a}\frac{\partial v}{\partial \varphi} - \frac{w}{a} - \frac{h^2}{12}\left(a\frac{\partial^4 w}{\partial x^4} + \frac{2}{a}\frac{\partial^4 w}{\partial \varphi^2 \partial x^2} + \frac{\partial^4 w}{a^3 \partial \varphi^4}\right) = -Z\frac{a(1-\nu^2)}{E h} \qquad (392)$$

5/FREE VIBRATION OF CYLINDRICAL SHELLS WITH MEMBRANE-BENDING THEORY

The free vibration of cylindrical shells can be discussed on the basis of the theory of Section 4. The general theory of cylindrical shells enables us to investigate the effects of different edge conditions and the circumferential waves of the mode shapes. Three typical papers are reviewed. Each of them reported the solutions from different points of view:

a. The first paper (Reference 14) used Donnell's equations, and the frequency and mode shape equations were developed for relatively long cylinders. The applicable numbers of edge conditions are limited.

b. The second paper (Reference 15) utilized the general equations of cylindrical shells. The frequency and mode shape equations were developed, their solutions having been based on a numerical iteration scheme. Ten different edge conditions were discussed.

c. The third paper (Reference 16) discusses the energy method via Lagrange's equation of motion. The validity of the theory was also demonstrated by experiments.

5.1 A REVIEW OF YU'S PAPER: "FREE VIBRATIONS OF THIN CYLINDRICAL SHELLS HAVING FINITE LENGTH WITH FREELY SUPPORTED AND CLAMPED EDGES" (REFERENCE 14)

5.1.1 SUMMARY. The free vibrations of thin cylindrical shells are investigated on the basis of Donnell's approximate equations. A simplifying assumption was introduced for relatively long cylinders, and a simple solution was developed for the mode shapes. In this manner the frequency equation is also simplified. Three different edge conditions were discussed: 1) both edges simply supported, 2) one edge simply supported and the other clamped, and, finally, 3) both edges clamped. The frequencies are the highest for the clamped-clamped case, the lowest are for the simply supported case, and the frequencies of the clamped-simply supported case are between the two other cases. As a result of approximations, the characteristic equations for the three cases are found to be similar to the frequency equations for the lateral vibration of beams with similar end conditions, modified by the circumferential wave numbers. The applicable number of edge conditions are limited due to the approximations used in the development of the theory.

5.1.2 EXPLANATION OF THE THEORY. In the case of free vibration, the external forces can be expressed in terms of inertial forces

$$X = -\rho h \frac{\partial^2 u}{\partial t^2}, \qquad Y = -\rho h \frac{\partial^2 v}{\partial t^2}, \qquad Z = -\rho h \frac{\partial^2 w}{\partial t^2} \tag{393}$$

The substitution of Equation 393 into Equations 343, 345 and 347 leads to the first three equations of Yu's Equation 1. The fourth equation of Yu is the same as Equation 349 of this monograph, the fifth is the same as Equation 351, and the sixth is the same as Equation 354 of this monograph. Equation 3 of the paper is identical to Equations 390, 391 and 392 of the monograph, when Equation 393 is substituted into these equations. Equations 3, 4 and 5 of the paper are cited here

$$\frac{\partial^2 u}{\partial x^2} + \frac{(1-\nu)}{2a^2}\frac{\partial^2 u}{\partial \varphi^2} + \frac{(1+\nu)}{2a}\frac{\partial^2 v}{\partial x\,\partial \varphi} - \frac{\nu}{a}\frac{\partial w}{\partial x} = \frac{(1-\nu^2)}{E}\rho\frac{\partial^2 u}{\partial t^2} \qquad [3]$$

$$\frac{(1+\nu)}{2a}\frac{\partial^2 u}{\partial x\,\partial \varphi} + \frac{(1-\nu)}{2}\frac{\partial^2 v}{\partial x^2} + \frac{1}{a^2}\frac{\partial^2 v}{\partial \varphi^2} - \frac{1}{a^2}\frac{\partial w}{\partial \varphi} = \frac{(1-\nu^2)}{E}\rho\frac{\partial^2 v}{\partial t^2} \qquad [4]$$

$$\frac{\nu}{a}\frac{\partial u}{\partial x} + \frac{1}{a^2}\frac{\partial v}{\partial \varphi} - \frac{w}{a^2} - \frac{h^2}{12}\nabla^4 w = \frac{(1-\nu^2)}{E}\rho\frac{\partial^2 w}{\partial t^2} \qquad [5]$$

where

$$\nabla^4 = \nabla^2 \cdot \nabla^2 = \left(\frac{\partial^2}{\partial x^2} + \frac{\partial^2}{a^2\,\partial \varphi^2}\right)\left(\frac{\partial^2}{\partial x^2} + \frac{\partial^2}{a^2\,\partial \varphi^2}\right)$$

Applying $\frac{\partial^2}{\partial x^2}$, $\frac{\partial^2}{a^2\,\partial \varphi^2}$ and $\frac{\partial^2}{\partial t^2}$ to Equation 3, solving in each case for the term involving v, and substituting these expressions in the equation obtained by applying $\frac{\partial^2}{a\,\partial x\,\partial \varphi}$ to Equation 4, the following equation was obtained.

$$\nabla^4 u - \frac{\nu}{a}\frac{\partial^3 w}{\partial x^3} + \frac{1}{a^3}\frac{\partial^3 w}{\partial x\,\partial \varphi^2} = -\frac{2(1+\nu)}{E}\rho\frac{\partial^2}{\partial t^2}\left[\frac{(1-\nu^2)}{E}\rho\frac{\partial^2 u}{\partial t^2} - \frac{(3-\nu)}{2}\nabla^2 u + \frac{\nu}{a}\frac{\partial w}{\partial x}\right] \qquad [6]$$

Similarly, applying $\frac{\partial^2}{\partial x^2}$, $\frac{\partial^2}{a^2\,\partial \varphi^2}$ and $\frac{\partial^2}{\partial t^2}$ to Equation 4, solving in each case for the term involving u, and substituting these in Equation 3 (after applying $\frac{\partial^2}{a\,\partial x\,\partial \varphi}$ to it), one obtains

$$\nabla^4 v - \frac{(2+\nu)}{a^2}\frac{\partial^3 w}{\partial x^2\,\partial \varphi} - \frac{1}{a^4}\frac{\partial^3 w}{\partial \varphi^3} = -\frac{2(1+\nu)}{E}\rho\frac{\partial^2}{\partial t^2}\left[\frac{(1-\nu^2)}{E}\rho\frac{\partial^2 v}{\partial t^2} - \frac{(3-\nu)}{2}\nabla^2 v + \frac{1}{a^2}\frac{\partial w}{\partial \varphi}\right] \qquad [7]$$

It can be seen that v was eliminated from Equation 6 and u from Equation 7. A third equation can be derived, which contains only w as an independent variable. Applying $\frac{\nu}{a}\frac{\partial}{\partial x}$ to Equation 6 and $\frac{1}{a^2}\frac{\partial}{\partial \varphi}$ to Equation 7, and adding the results, the resulting equation contains terms w and $\left(\frac{\nu}{a}\frac{\partial u}{\partial x} + \frac{1}{a^2}\frac{\partial v}{\partial \varphi}\right)$. The resulting equation can be expressed in terms of w, since the expression $\left(\frac{\nu}{a}\frac{\partial u}{\partial x} + \frac{1}{a^2}\frac{\partial v}{\partial \varphi}\right)$ was obtained from Equation 5, as the function of w. The derivation yields finally

$$\frac{h^2}{12}\nabla^8 w + \frac{(1-\nu^2)}{a^2}\frac{\partial^4 w}{\partial x^4} = -\frac{2(1+\nu)}{E}\rho\frac{\partial^2}{\partial t^2}\left\{\left[\frac{(1-\nu^2)}{E}\rho\frac{\partial^2}{\partial t^2} - \frac{3-\nu}{2}\nabla^2\right]\right.$$

$$\left.\cdot\left[\frac{(1-\nu^2)}{E}\rho\frac{\partial^2 w}{\partial t^2} + \frac{w}{a^2} + \frac{h^2}{12}\nabla^4 w\right] + \frac{(1-\nu)}{2}\nabla^4 w + \frac{\nu^2}{a^2}\frac{\partial^2 w}{\partial x^2} + \frac{1}{a^4}\frac{\partial^2 w}{\partial \varphi^2}\right\} \quad [9]$$

The problem of free vibration was reduced now for the solutions of Equations 6, 7 and 9. It is assumed that the shell vibrates with normal modes and with an angular frequency, ω. The displacement components, u, v and w, are proportional to a simple harmonic function of ωt. The displacement functions must also be periodic in φ with period 2π; therefore, its components must be proportional to the sine or cosine of multiples of φ. Equations 6, 7, and 9 can be satisfied generally with the following functions.

$$\left.\begin{aligned} u &= \sum_{i=1}^{8} A_i e^{\lambda_i \frac{x}{\ell}} \cos m\varphi \sin \omega t \\ v &= \sum_{i=1}^{8} B_i e^{\lambda_i \frac{x}{\ell}} \sin m\varphi \sin \omega t \\ w &= \sum_{i=1}^{8} C_i e^{\lambda_i \frac{x}{\ell}} \cos m\varphi \sin \omega t \end{aligned}\right\} \quad [10]$$

in which ℓ is the length of the cylinder, m is an arbitrarily chosen positive integer equal to the number of circumferential waves, λ_i are the characteristic values of the eigenfunctions, and A_i, B_i and C_i are constant coefficients. Since Equation 9 is eighth-order and its auxiliary equations are of the eighth degree and have eight roots, each of the foregoing summations contains eight terms. This is the explanation of the summation of Equation 10. The substitution of Equation 10 into Equations 6, 7 and 9 leads to lengthy equations which can be solved by some numerical technique. For the sake of simplicity, our investigation is restricted to relatively long cylinders. In this case, the following assumption may be made

$$\frac{|\lambda_i^2| a^2}{m^2 \ell^2} \ll 1 \qquad [14]$$

The use of Inequality 14 reduces these lengthy equations to the following form

$$A_i = C_i \lambda_i M \frac{a}{\ell} \qquad (i = 1, 2, 3, 4) \qquad [15]$$

$$B_i = C_i N \qquad (i = 1, 2, 3, 4) \qquad [16]$$

$$(1 - \nu)(1 - \nu^2)\left(\frac{\lambda_i a}{\ell}\right)^4 = 2\Omega^3 - \Omega^2 [2 + (3 - \nu) m^2 + 2 k m^4]$$

$$+ \Omega [(1 - \nu) m^2 (m^2 + 1) + (3 - \nu) k m^6] - (1 - \nu) k m^8 \qquad [17]$$

where

$$k = \frac{h^2}{12 a^2}$$

$$\Omega = \frac{(1 - \nu^2)}{E} \rho a^2 \omega^2$$

$$M = \frac{2\nu\Omega + (1 - \nu) m^2}{2\Omega^2 - (3 - \nu) m^2 \Omega + (1 - \nu) m^4}$$

$$N = \frac{-2 m \Omega + (1 - \nu) m^3}{2\Omega^2 - (3 - \nu) m^2 \Omega + (1 - \nu) m^4}$$

Equation 17 is the frequency equation, and a specified boundary condition, λ_i, is determined; thereafter, the single unknown will be Ω, which contains the frequency. Since Equation 17 is fourth-order, the summation of Equation 10 has to also be reduced to four. Therefore, Equation 10 has four sets of values of A_i, B_i, and C_i. The root of λ_i can be obtained in the form

$$\lambda_1 = -\lambda_2 = K \qquad \text{and} \qquad \lambda_3 = -\lambda_4 = iK \qquad [18]$$

where K is a real number.

By the use of Equations 15 and 16, the displacement functions can be written

$$\left.\begin{aligned} u &= \frac{a}{\ell} M \sum_{i=1}^{4} C_i \lambda_i e^{\lambda_i \frac{x}{\ell}} \cos m\varphi \sin \omega t \\ v &= N \sum_{i=1}^{4} C_i e^{\lambda_i \frac{x}{\ell}} \sin m\varphi \sin \omega t \\ w &= \sum_{i=1}^{4} C_i e^{\lambda_i \frac{x}{\ell}} \cos m\varphi \sin \omega t \end{aligned}\right\} \qquad [10^*]$$

5.1.3 SHELLS WITH BOTH EDGES SIMPLY SUPPORTED. The boundary conditions for this case are

$$v = w = M_x = 0 \quad \text{at} \quad x = 0 \quad \text{and} \quad x = \ell$$

In the expression of bending moment, M_x, the term $\frac{1}{a^2}\frac{\partial v}{\partial \varphi}$ was neglected as a second-order quantity; therefore

$$M_x = -\frac{E h^3}{12(1-\nu^2)}\left(\frac{\partial^2 w}{\partial x^2} + \frac{\nu}{a^2}\frac{\partial^2 w}{\partial \varphi^2}\right)$$

The substitution of displacement functions 10* into the boundary conditions lead to

$$\left.\begin{aligned} w\big|_{x=0} = v\big|_{x=0} = 0 \qquad & \sum_{i=1}^{4} C_i = 0 \\ \text{and} \\ w\big|_{x=\ell} = v\big|_{x=\ell} = 0 \qquad & \sum_{i=1}^{4} C_i e^{\lambda_i} = 0 \\ M_x\big|_{x=0} = 0 \qquad & \sum_{i=1}^{4} C_i \lambda_i^2 = 0 \\ \text{and} \\ M_x\big|_{x=\ell} = 0 \qquad & \sum_{i=1}^{4} C_i \lambda_i^2 e^{\lambda_i} = 0 \end{aligned}\right\} \qquad [19]$$

Figure 64 shows the general arrangement

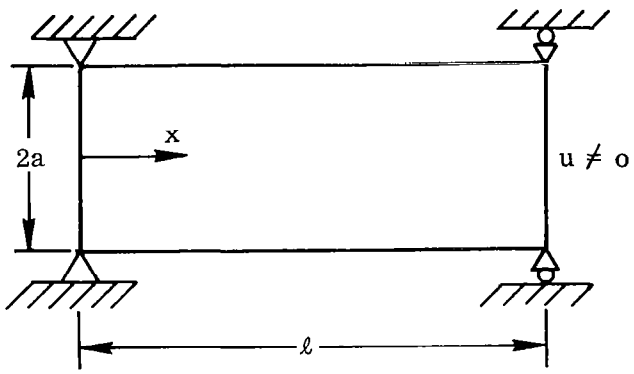

Figure 64. Illustration of Edge Conditions for Simply Supported Shell

The equations represent the boundary conditions and have two sets of unknown quantities, λ_i and C_i. To find λ_i, Equation10*was substituted into the boundary conditions; the non-trivial solution of the homogeneous equation system requires that the determinant of the system must be zero

$$\begin{vmatrix} 1 & 1 & 1 & 1 \\ e^{K} & e^{-K} & e^{iK} & e^{-iK} \\ K^2 & K^2 & -K^2 & -K^2 \\ K^2e^{K} & K^2e^{-K} & -K^2e^{iK} & K^2e^{-iK} \end{vmatrix} = 0$$

The solution of the determinant is

$$16\,iK^4 \sinh K \sin K = 0 \qquad [20]$$

Equation 20 is equivalent to

$$\sin K = 0 \qquad [20*]$$

The characteristic values of K are therefore given by

$$K = n\pi$$

where $n = 1, 2, 3 \ldots$.

The roots of λ_i are

$$\lambda_1 = n\pi \qquad \lambda_2 = -n\pi \qquad \lambda_3 = in\pi \qquad \lambda_4 = -in\pi$$

By substituting λ_i in Equation 17, the frequency equation becomes

$$2\Omega^3 - \Omega^2[2 + (3 - \nu)m^2 + 2km^4] + \Omega[(1 - \nu)m^2(m^2 + 1)$$

$$+ (3 - \nu)km^6] - (1 - \nu)km^8 - (1 - \nu)(1 - \nu^2)\left(\frac{n\pi a}{\ell}\right)^4 = 0 \qquad [21]$$

By use of a chosen value of n and m, the frequency can be obtained easily from the last equation.

Any three of the coefficients C_i may be put in terms of the fourth one by substituting the values λ_i just obtained into any three of Equation 19; the solution is

$$C_1 = C_2 = 0 \qquad \text{and} \qquad C_3 = -C_4$$

The displacement components can be written by the use of Equations 15, 16 and 10*

$$\left.\begin{aligned} u &= MC\frac{n\pi a}{\ell}\cos\frac{n\pi x}{\ell}\cos m\varphi \sin\omega t \\ v &= NC\sin\frac{n\pi x}{\ell}\sin m\varphi \sin\omega t \\ w &= C\sin\frac{n\pi x}{\ell}\cos m\varphi \sin\omega t \end{aligned}\right\} \qquad [22]$$

where C is an arbitrary constant.

5.1.4 SHELLS WITH BOTH EDGES CLAMPED. Figure 65 illustrates the general arrangement

The boundary conditions can be satisfied without difficulty

$$u = v = w = \frac{\partial w}{\partial x} = 0$$

at

$$x = 0 \qquad \text{and} \qquad x = \ell$$

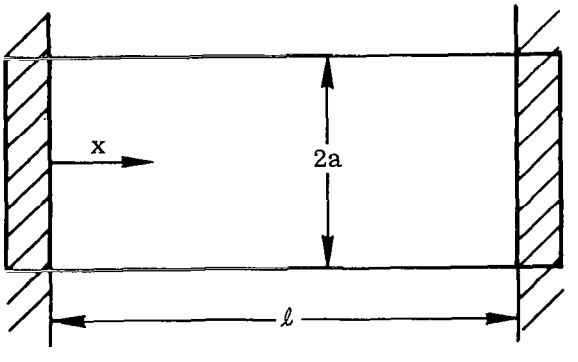

Figure 65. Illustration of Edge Condition for Clamped Shell

When displacement functions 10* are substituted into the boundary conditions, the following equations can be written

$$v\Big|_{x=0} = w\Big|_{x=0} = 0 \quad \sum_{i=1}^{4} C_i = 0 \quad \text{and} \quad v\Big|_{x=\ell} = w\Big|_{x=\ell} = 0 \quad \sum_{i=1}^{4} C_i e^{\lambda_i} = 0 \qquad [26]$$

$$\frac{\partial w}{\partial x}\Big|_{x=0} = u\Big|_{x=0} = 0 \quad \sum_{i=1}^{4} C_i \lambda_i = 0 \quad \text{and} \quad \frac{\partial w}{\partial x}\Big|_{x=\ell} = u\Big|_{x=\ell} = 0 \quad \sum_{i=1}^{4} C_i \lambda_i e^{\lambda_i} = 0$$

With the previous considerations, the determinant of the homogeneous equation system is

$$\begin{vmatrix} 1 & 1 & 1 & 1 \\ e^{K} & e^{-K} & e^{iK} & e^{-iK} \\ K & -K & iK & -iK \\ Ke^{K} & -Ke^{-K} & iKe^{iK} & -iKe^{-iK} \end{vmatrix} = 0$$

The solution of the determinant is

$$8iK^2(\cos K \cosh K - 1) = 0 \qquad [27]$$

or

$$(\cos K \cosh K - 1) = 0$$

Let K assume the form

$$K = n'\pi$$

The solution of Equation 27 yields the values of n'

$$n' = 1.500,\ 2.500,\ 3.500,\ \text{etc.}$$

The four roots of λ_i are

$$\lambda_1 = -\lambda_2 = n'\pi \quad \text{and} \quad \lambda_3 = -\lambda_4 = in'\pi$$

The substitution of the last equation into Equation 17 results in the frequency equation. The values of C_i can be derived as in the previous case; the displacement functions are

$$
\left.
\begin{aligned}
w &= 2C_1\Big[(\sinh n'\pi - \sin n'\pi) \\
&\quad - (\cosh n'\pi - \cos n'\pi)\Big]^{-1}\Big[(\sinh n'\pi - \sin n'\pi)\Big(\cosh\frac{n'\pi x}{\ell} \\
&\quad - \cos\frac{n'\pi x}{\ell}\Big) - (\cosh n'\pi - \cos n'\pi)\Big(\sinh\frac{n'\pi x}{\ell} - \sin\frac{n'\pi x}{\ell}\Big)\Big]\cos m\varphi \sin \omega t \\
u &= Ma\frac{\partial w}{\partial x} \\
v &= -\frac{Na}{m}\frac{\partial w}{\partial s}
\end{aligned}
\right\} \quad [29]
$$

5.1.5 SHELLS WITH ONE EDGE SIMPLY SUPPORTED AND THE OTHER EDGE CLAMPED. Figure 66 illustrates the boundary conditions.

The boundary conditions are

$$w = v = M_x = 0 \qquad \text{at } x = 0$$

$$u = v = w = \frac{\partial w}{\partial x} = 0 \qquad \text{at } x = \ell$$

which lead to

$$
\left.
\begin{aligned}
&\sum_i C_i = 0, \quad \sum_i C_i\lambda_i^2 = 0 \\
&\sum_i C_i e^{\lambda_i} = 0, \quad \sum_i C_i\lambda_i e^{\lambda_i = 0}
\end{aligned}
\right\} \quad (i = 1, 2, 3, 4)
$$

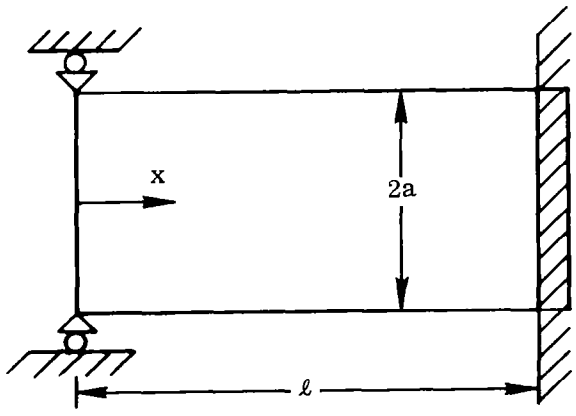

Figure 66. Illustration of Edge Conditions for Clamped Simply Supported Shell

Equating the determinant of the coefficients of C_i to zero yields

$$\tan K - \tanh K = 0 \qquad [30]$$

the roots of which are

$$K = n''\pi$$

with the consecutive values of n'' equal to

1.250, 2.250, 3.250, 4.250, ...

The four roots of λ_i are therefore

$$\lambda_1 = n''\pi, \quad \lambda_2 = -n''\pi, \quad \lambda_3 = in''\pi, \quad \lambda_4 = -in''\pi$$

To illustrate the theory, Professor Hoppmann's model and test results were used. The following constants were considered

$a = 1.9575$ in. $\quad h = 0.065$ in. $\quad E = 10 \times 10^7$ lb/in.^{2}

$\ell = 15.53$ in. $\quad \nu = 0.35$

Table 4 shows the test results (upper right numbers) and the results of theoretical calculation (lower left numbers). The "%" refers to the error between the theory and test results.

Table 4. Experimental and Theoretical Frequencies of Simply Supported Case

(Frequencies in Hz)

m \ n	1	2	3	4
2	742 12% 832	1880 27% 2395	— 5480	— 12,900
3	1330 10% 1460	1740 3.7% 1805	2470 15% 2850	— 4640
4	2480 5% 2610	2680 0% 2680	3040 -1.5% 2990	3710 -2.5% 3620
5	4060 1% 4120	4120 0.5% 4140	4340 -3.2% 4210	4780 -8.3% 4420

5.1.6 CONCLUSIONS. The paper reduced the free vibration of a thin cylindrical shell to the longitudinal direction for beam modes and to circumferential direction waves. The merit of the paper is its simplicity, the drawback of the theory is its limitations. The theory may be used for thin cylindrical shells with a length-to-radius ratio of $\ell/a \geq 4$.

5.2 A REVIEW OF FORSBERG'S PAPER: "INFLUENCE OF BOUNDARY CONDITIONS ON THE MODAL CHARACTERISTICS OF THIN CYLINDRICAL SHELLS" (REFERENCE 15)

5.2.1 SUMMARY. The theory has investigated all sixteen sets of homogeneous boundary conditions at each end of the shell. The equations of motion of the cylindrical shell were developed from Flügge's shell equations. The general solution of these equations was derived; however, the evaluation of the integration constants was obtained by numerical integration. With given sets of boundary conditions, length of cylinder, and an assumed circumferential modal pattern, a numerical iteration can be performed to find the frequency of vibration which will meet these conditions. The paper made an extensive parameter study and covered a great range of the variables. The paper also showed the peculiar frequency dip which was discovered previously by Arnold and Warburton. The frequency has been determined to six significant figures; such accuracy was necessary in order to obtain accurate values for the mode shapes. The numerical computation was done on an IBM 7094 computer.

5.2.2 EXPLANATION OF THE THEORY. Equation 1 of the paper can be derived from Equations 357 through 361; furthermore, Equation 393 is used to arrive at the equilibrium condition of the shell element. The sixth equation was derived from the moment equilibrium around the radius of the cylinder by Equation 353. All the equations have to be changed to Flügge's notation, Subsection 4.5.1, to agree with the paper. (The last statement is related to Equations 357 through 361.) The strain-displacement equations of the paper can be expressed from Equations 378 through 385, etc. Again the sign convention of Flügge has to be considered.

The differential equations of motion can be written, based on the previous substitutions

$$\left.\begin{aligned}
&u'' + \frac{1-\nu}{2}(1+k)\,u^{\cdot\cdot} + \frac{1+\nu}{2}\,v'^{\cdot} - k w''' + \frac{1-\nu}{2}k w'^{\cdot\cdot} + \nu w' - \gamma^2 \frac{\partial^2 u}{\partial t^2} = 0 \\
&\left(\frac{1+\nu}{2}\right)u'^{\cdot} + v^{\cdot\cdot} + \frac{1-\nu}{2}(1+3k)v'' - \frac{3-\nu}{2}k w''^{\cdot} + w^{\cdot} - \gamma^2 \frac{\partial^2 v}{\partial t^2} = 0 \\
&-k u''' + \frac{1-\nu}{2}k u'^{\cdot\cdot} + \nu u' - \frac{3-\nu}{2}k v''^{\cdot} + v^{\cdot} + w \\
&\quad + k\left[w^{IV} + 2w''^{\cdot\cdot} + w^{\cdot\cdot\cdot\cdot} + 2w^{\cdot\cdot} + w\right] + \gamma^2 \frac{\partial^2 w}{\partial t^2} = 0
\end{aligned}\right\} \quad [1]$$

where

$$()' = \frac{\partial ()}{\partial x}, \qquad ()^{\cdot} = \frac{\partial ()}{\partial \varphi}$$

$$\gamma^2 = \frac{\rho a^2 (1-\nu^2)}{E}, \qquad k = \frac{h^2}{12 a^2}$$

The general solution of Equation 1 can be written similarly, as was done in Reference 14, Equation 10. It can be proved that Equation 1 can also be reduced to an eighth-order equation of displacement, w. The general solution is

$$\left.\begin{aligned} u &= \sum_{s=1}^{8} \alpha_s A_s e^{\lambda_s x} \cos n\varphi \, e^{i\omega t} \\ v &= \sum_{s=1}^{8} \beta_s A_s e^{\lambda_s x} \sin n\varphi \, e^{i\omega t} \\ w &= \sum_{s=1}^{8} A_s e^{\lambda_s x} \cos n\varphi \, e^{i\omega t} \end{aligned}\right\} \qquad [2]$$

The substitution of Equation 2 into 1 yields an eighth-order algebraic equation for λ_s

$$\lambda_s^8 + g_{s6}\lambda_s^6 + g_{s4}\lambda_s^4 + g_{s2}\lambda_s^2 + g_{s0} = 0 \qquad [3]$$

where

$$g_{sk} = g_{sk}(h/a, \nu, n, \omega)$$

It can be shown that the solution of Equation 3 for vibration problems can always be expressed

$$\lambda = \pm a, \pm i\,b, \pm(c \pm i\,d)$$

where a, b, c, and d are real quantities. The displacement w can be expressed, based on Equation 1 and the last equation.

$$\begin{aligned} w = \Big[& C_1 e^{ax} + C_2 e^{-ax} + C_3 \cos bx + C_4 \sin bx \\ & + e^{cx}(C_5 \cos dx + C_6 \sin dx) \\ & + e^{-cx}(C_7 \cos dx + C_8 \sin dx) \Big] \cos n\varphi \, e^{i\omega t} \end{aligned} \qquad [4]$$

Similar expressions can be derived for displacements u and v. Equation 4 has been rewritten so that the complex constants, A_s, have been replaced by real constants, C_s. The equations of displacements, u and v, involve combinations of the constants, C_s,

the real and imaginary parts of α_s and β_s. Since α_s and β_s depend on λ_s, h/a, ν, n and ω, after the solution of Equation 3 is obtained, α_s and β_s can be evaluated.

5.2.3 BOUNDARY CONDITIONS. The author uses Kirckhoff's definition in formulating the boundary conditions. The normal shear force, S_x, may be expressed by the combinations of shear force, Q_x, and twisting moment, $M_{x\varphi}$; furthermore, the tangential shear force, T_x, may be expressed by the combinations of membrane shear force, $N_{x\varphi}$, and twisting moment, $M_{x\varphi}$. Figure 67 shows an element of the cross-section of a cylindrical shell with a twisting moment, $M_{x\varphi}$, on a length of ds. The twisting moment, $M_{x\varphi} \cdot ds$, on the element may be replaced by an equivalent group of three forces.

The two forces F_n on the left element are almost parallel to each other and must therefore have a moment equal to $M_{x\varphi}ds$; hence

$$F_n \cdot ds = M_{x\varphi}\, ds \tag{394}$$

Since they are slightly divergent, they have a horizontal resultant, $F_n d\varphi$, pointing to the left, which is compensated by the third force, $F_t = F_n d\varphi$. The three forces are statically equivalent to the distributed shearing stresses, which yield the twisting moment, $M_{x\varphi}$. The shear force, T_x, acting in the tangential direction can be calculated, based on Figure 67, as

$$T_x = N_{x\varphi} - \frac{F_t}{ds} = N_{x\varphi} - \frac{F_n\, d\varphi}{ds} = N_{x\varphi} - \frac{F_n\, a\, d\varphi}{a\, ds} \tag{395}$$

The following relations can be written, based on Equation 394

$$F_n\, a\, d\varphi = F_n\, ds = M_{x\varphi} ds$$

The substitution of the last equation into Equation 395 leads to

$$T_x = N_{x\varphi} - \frac{M_{x\varphi}}{a} \tag{396}$$

The normal shear force, S_x, can be expressed, again based on Figure 67, as

$$S_x = Q_x + \frac{\left(\frac{\partial F_n}{\partial \varphi}\, d\varphi\right)}{ds} = Q_x + \frac{\left(\frac{\partial F_n}{\partial \varphi}\, a\, d\varphi\right)}{a\, ds} = Q_x + \frac{\frac{\partial F_n}{\partial \varphi}\, ds}{a\, ds} \tag{397}$$

Equation 394 may be expressed as

$$\frac{\partial F_n}{\partial \varphi}\, ds = \frac{\partial M_{x\varphi}}{\partial \varphi} ds \tag{398}$$

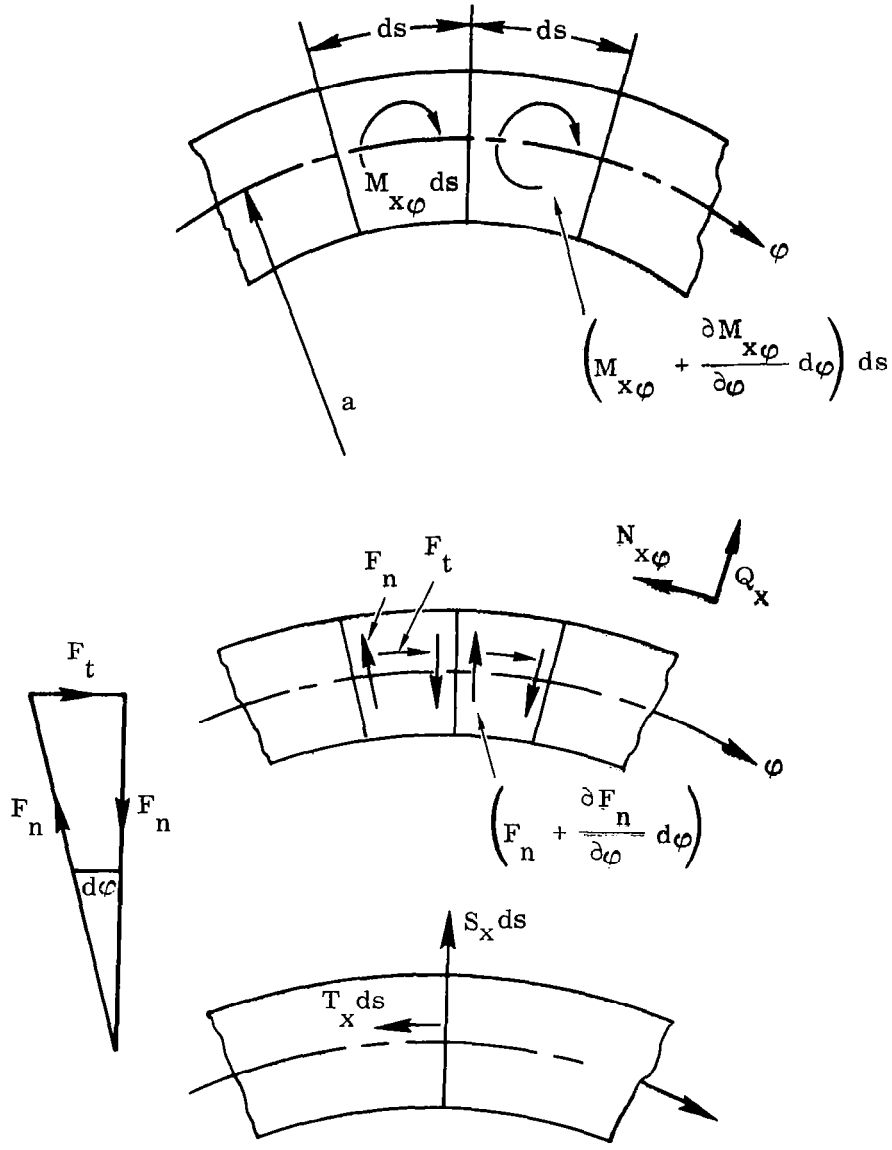

Figure 67. Shear Forces

The substitution of Equation 397 into Equation 398 yields

$$S_x = Q_x + \frac{1}{a} \frac{\partial M_{x\varphi}}{\partial \varphi} \tag{399}$$

Table 5, published by the author of Reference 15, shows 10 different edge conditions.

Table 5. List of Edge Conditions

Case No.	Description	Boundary Conditions x = 0	Boundary Conditions x = ℓ/a
1	Simple support without axial constraint (called "freely supported")	$w = 0$ $v = 0$ $M_x = 0$ $N_x = 0$	Same
2	Simple support without axial constraint at one end, with axial constraint at other	$w = 0$ $v = 0$ $M_x = 0$ $N_x = 0$	Same $u = 0$
3	Simple support with axial constraint	$w = 0$ $u = 0$ $v = 0$ $M_x = 0$	Same
4	Simple support, no tangential constraint (similar to Case 1, with $v \neq 0$)	$w = 0$ $M_x = 0$ $N_x = 0$ $T_x = 0$	Same
5	Simple support, axial constraint but no tangential constraint (similar to Case 3, with $v \neq 0$)	$w = 0$ $u = 0$ $M_x = 0$ $T_x = 0$	Same
6	Clamped end, without axial constraint	$w = 0$ $w' = 0$ $v = 0$ $N_x = 0$	Same
7	Clamped end, with axial constraint (called "fixed end")	$w = 0$ $w' = 0$ $u = 0$ $v = 0$	Same
8	Clamped end, no tangential constraint (similar to Case 6, but with $v \neq 0$)	$w = 0$ $w' = 0$ $N_x = 0$ $T_x = 0$	Same
9	Clamped end, with axial constraint but no tangential constraint (similar to Case 7, but with $v \neq 0$)	$w = 0$ $w' = 0$ $u = 0$ $T_x = 0$	Same
10	Simple support without axial constraint at one end, clamped with axial constraint at the other	$w = 0$ $v = 0$ $M_x = 0$ $N_x = 0$	Same $w' = 0$ $u = 0$

5.2.4 THE TECHNIQUE OF NUMERICAL COMPUTATION. The evaluation of numerical constants a, b, c and d can be made by iteration. The solution of this problem is determined by: 1) a given set of fixed a/h, ℓ/a and ν; 2) an assumed number of circumferential waves, numbers n; and 3) a specific set of boundary conditions for each end. The computation starts from some initial estimate for frequency, ω. An iteration can then be performed to satisfy simultaneously Equation 3 and the determinant D of the boundary conditions. An entire range of problems can be covered by varying the initial input to the determinant, D, which are the constants a/h, ℓ/a, ν, and n — or the boundary conditions. The solution can be obtained without any problem by this method; however, to obtain accurate values for the mode shapes, it is necessary to compute the frequencies to six significant figures. The numerical computation was performed on an IBM 7094 computer.

Figure 68 illustrates the coordinate system and sign convention applied in the theory, while Figure 69 shows the general character of the various mode shapes. The effect of the different edge conditions listed in Table 5 can be seen in Figures 70 through 73. All of these figures contain a nondimensional frequency; the expression for the frequency factor, ω_o, can be written

$$\omega_o = \frac{1}{a}\left[\frac{E}{\rho(1 - \nu^2)}\right]^{1/2} \qquad (400)$$

The "beam modes" of a cylindrical shell can be seen on Figures 71 and 72. Figure 73 illustrates a peculiar frequency dip, which was discovered earlier by Arnold and Warburton. The detailed explanation of this phenomenon will be covered in Reference 16.

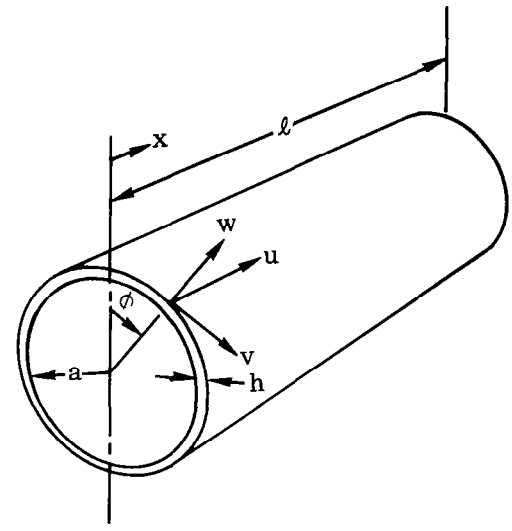

Figure 68. Coordinate System

5.2.5 CONCLUSIONS. As far as numerical results are concerned, this paper is the most accurate and general to date. The disadvantage of the theory is that any numerical computation has to be carried out by computer, which requires the ownership of the computer program.

5.3 A REVIEW OF ARNOLD AND WARBURTON'S PAPER: "FLEXURAL VIBRATIONS OF THE WALLS OF THIN CYLINDRICAL SHELLS HAVING FREELY SUPPORTED EDGES" (REFERENCE 16)

5.3.1 SUMMARY. This paper discussed the flexural vibration of a thin-walled cylindrical shell with simply supported edge conditions. Timoshenko's strain-displacement relations were introduced, and the kinetic and potential energy of the shell were derived. Since suitable functions were introduced for the displacement functions, the energy method led to Lagrange's equation of motion. It is worthwhile to mention that the

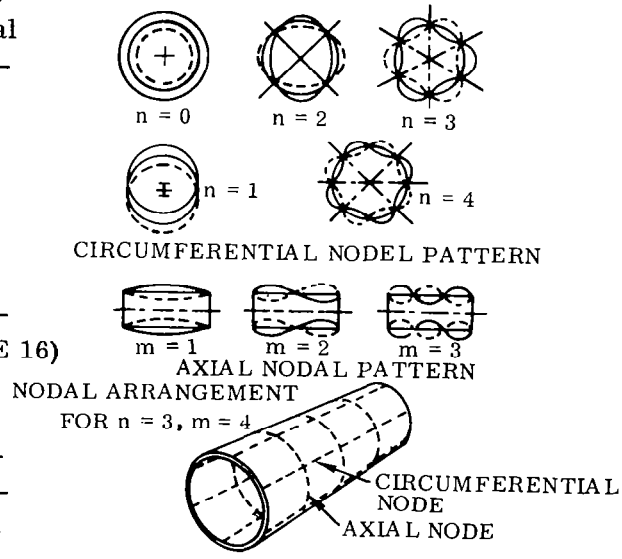

Figure 69. Character of Mode Shapes

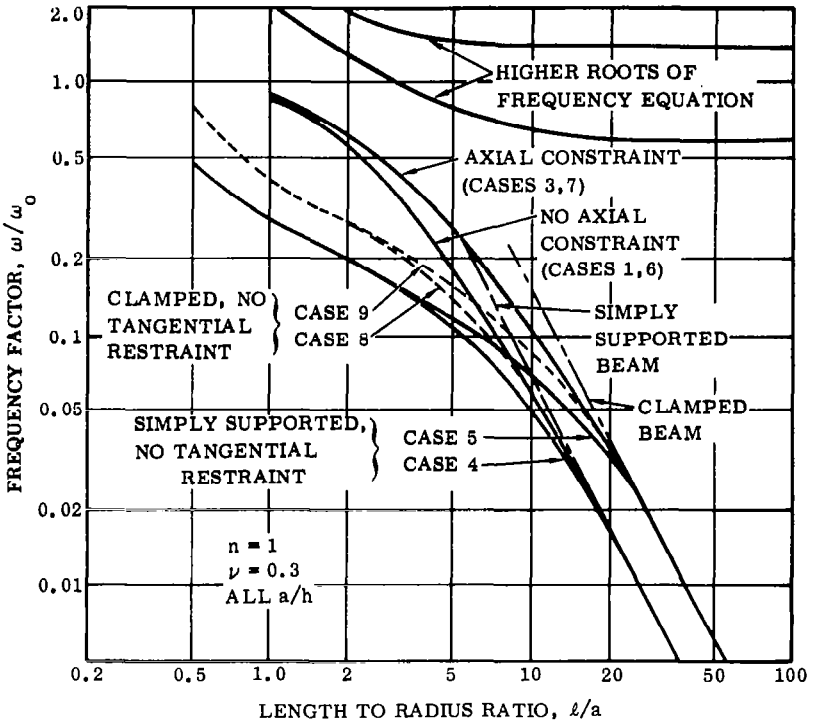

Figure 70. Frequency Distribution for n = 1

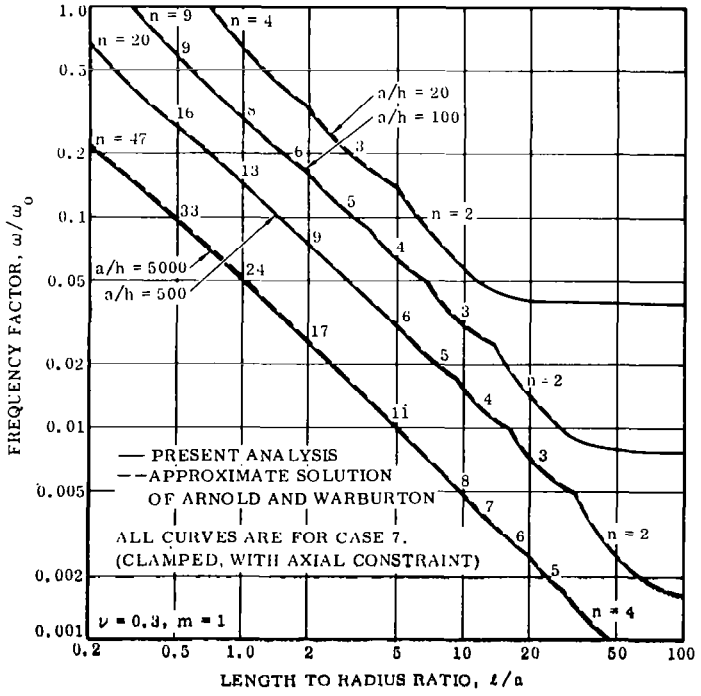

Figure 71. Frequency Envelope, Case 7 and Arnold and Warburton's Approximate Solution

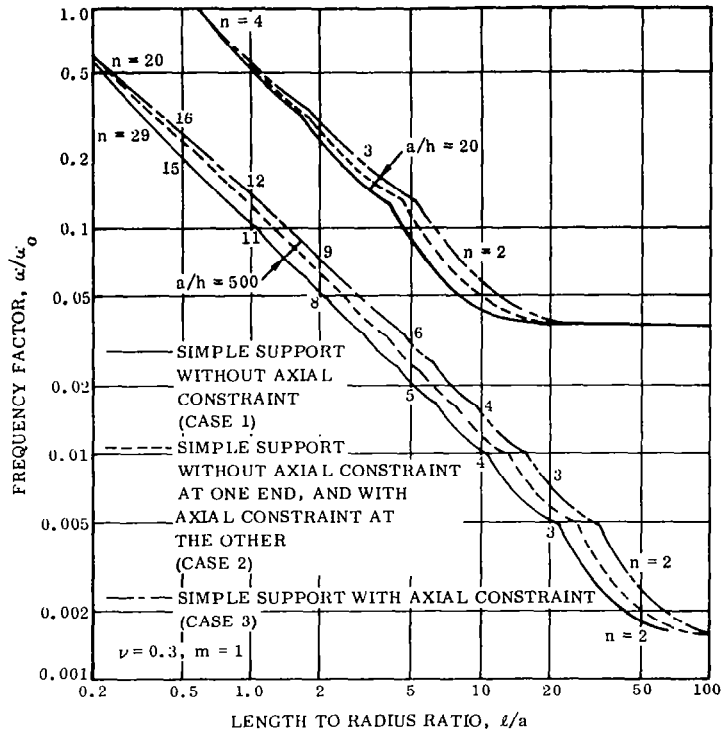

Figure 72. Frequency Envelope, Cases 1, 2, and 3

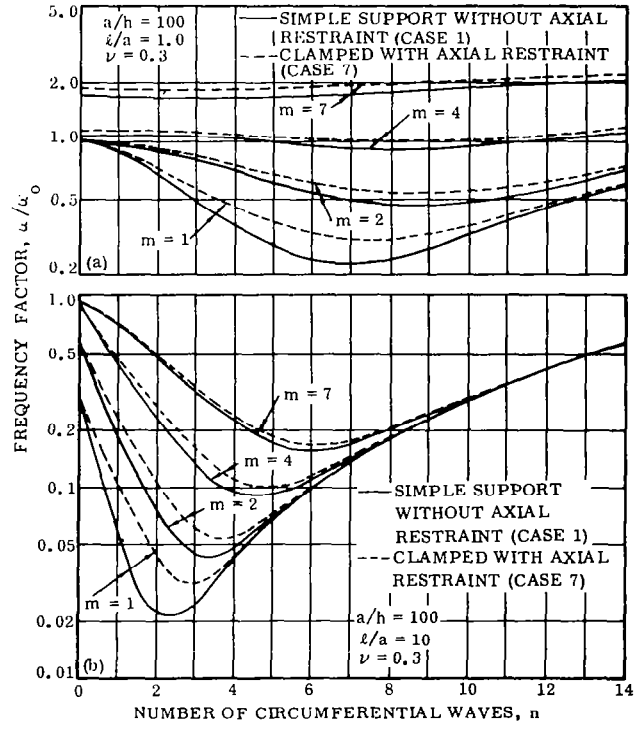

Figure 73. Frequency Distribution for $\ell/a = 1$ and $\ell/a = 10$

displacement functions used by the authors satisfy the differential equations of motion "exactly," as was proved by W. Flügge.

The Lagrange's equations result in a sixth-order frequency equation. Different numerical examples were discussed, and the theory was verified by test results. The authors discovered, first, a peculiar frequency dip; this phenomenon was explained fully by their theoretical and experimental investigations. Figure 74 shows the results. Figure 75 explains the frequency dip, based on the summation of bending and stretching energy.

5.3.2 EXPLANATION OF THE THEORY. A plane stress-strain relation is assumed. Therefore, the strain energy for a unit cubic element is, according to Figure 76,

$$S_o = \frac{1}{2}(\sigma_x \epsilon_x + \sigma_y \epsilon_y + \tau_{xy} \gamma_{xy}) \tag{401}$$

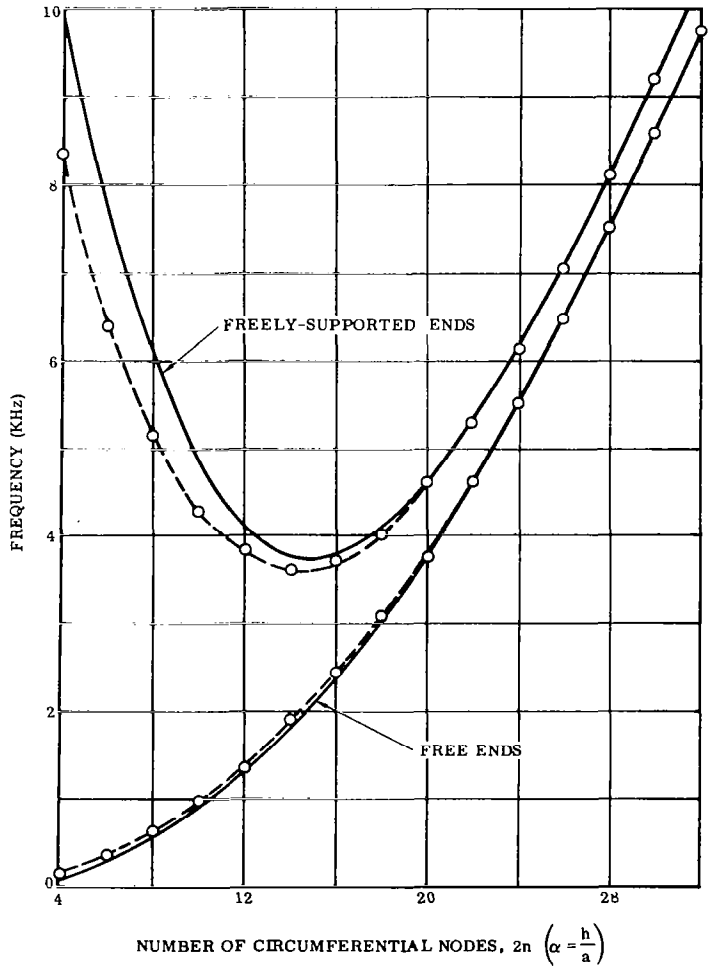

Figure 74. Experimental and Theoretical Frequency Curves (α = 0.01)

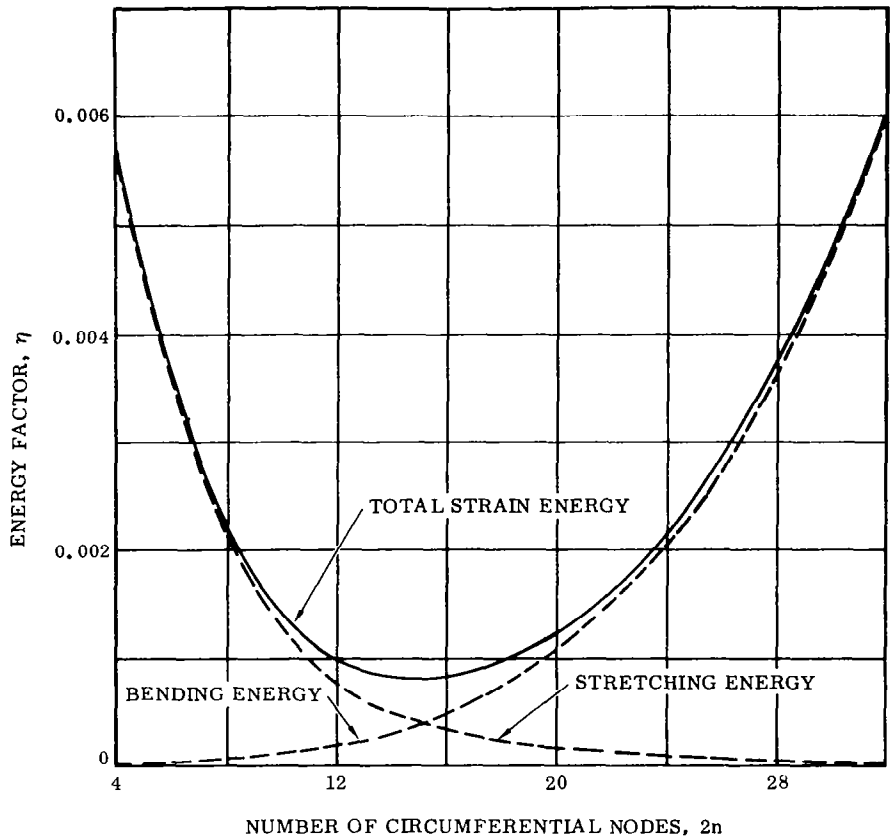

Figure 75. Strain Energy Due to Bending and Stretching ($\alpha = 0.01$; $h = 0.025$ in., $a = 2.51$ in.; $\ell = 2.065$ in.)

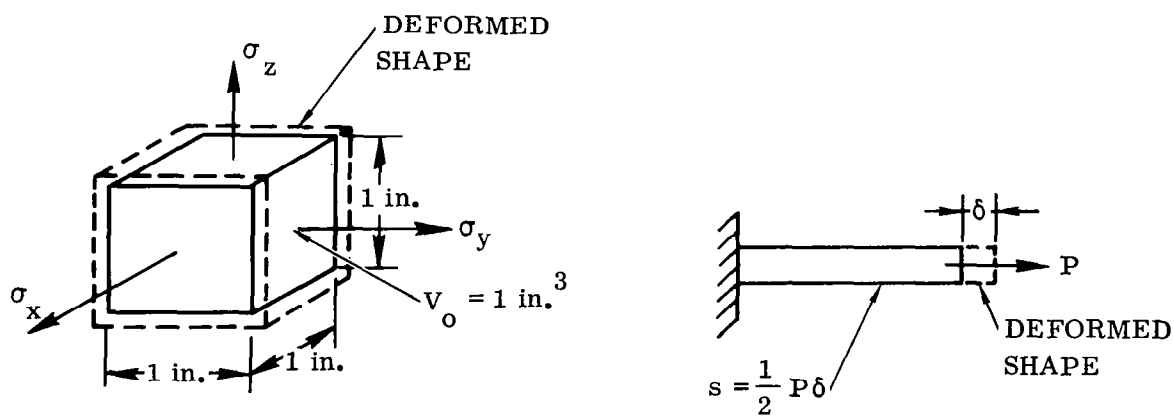

Figure 76. Deformations

The strain energy of a cylindrical shell can be expressed by the volume of the shell

$$S = \int_0^{2\pi} \int_0^{\ell} \int_{-h/2}^{h/2} S_o \, a \, d\varphi \, dx \, dz \tag{402}$$

Figure 77 illustrates the element of a cylindrical shell.

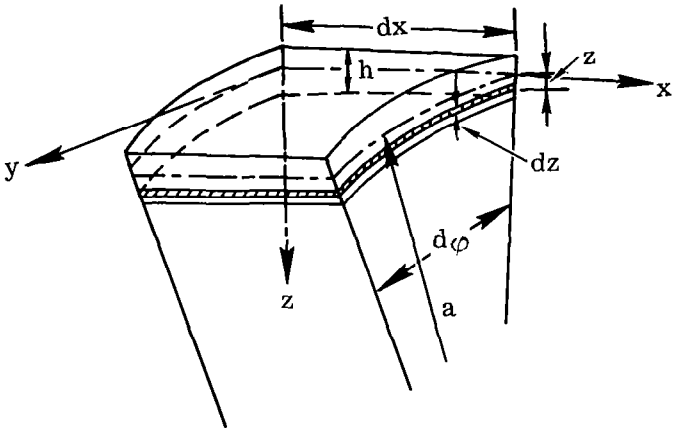

Figure 77. Cylindrical Shell Element

The stress can be expressed as a function of strain

$$\left.\begin{aligned} \sigma_x &= \frac{E}{(1-\nu^2)}(\epsilon_x + \nu\,\epsilon_\varphi) \\ \sigma_\varphi &= \frac{E}{(1-\nu^2)}(\epsilon_\varphi + \nu\,\epsilon_x) \\ \tau_{x\varphi} &= G\,\gamma_{x\varphi} \end{aligned}\right\} \tag{403}$$

where

$$G = \frac{E}{2(1+\nu)}$$

The substitution of Equation 403 into Equation 402 leads to

$$S = \frac{E}{2(1-\nu^2)} \int_0^{2\pi} \int_0^{\ell} \int_{-h/2}^{h/2} \left[\epsilon_x^2 + \epsilon_\varphi^2 + 2\nu\,\epsilon_x\,\epsilon_\varphi + \frac{(1-\nu)}{2}\gamma_{x\varphi}^2 \right] a \, d\varphi \, dx \, dz \quad [3]$$

Total strain can be expressed for any point of the shell thickness as the superposition of membrane and bending strain

$$\left.\begin{aligned} \epsilon_x &= \epsilon_{x,\,m} - z\,\varkappa_1 \\ \epsilon_\varphi &= \epsilon_{\varphi,\,m} - z\,\varkappa_2 \\ \gamma_{x\varphi} &= \gamma_{x,\varphi,m} - 2\,z\,\varkappa_{x\varphi} \end{aligned}\right\} \quad [4]$$

where subindex m = membrane.

In the next step Equation 4 has been expressed by Equations 387 and 389 of the strain-displacement functions. Equation 3 of the strain energy has now been expressed in terms of displacement functions. The displacement functions may be expressed in the case of simply supported edges

$$\left.\begin{aligned} u &= U \cos \frac{m\pi x}{\ell} \cos n\varphi \\ v &= V \sin \frac{m\pi x}{\ell} \sin n\varphi \\ w &= W \sin \frac{m\pi x}{\ell} \cos n\varphi \end{aligned}\right\} \qquad [6]$$

where n and m are respectively the circumferential and longitudinal wave length numbers and U, V and W are functions of time only.

Equation 6 is equivalent to Equation 22 of Section 5.1. These equations satisfy the differential equations of equilibrium as was proved by Flügge. Since Equation 3 was expressed in terms of displacements, the substitution of Equation 6 into this equation yields

$$\begin{aligned} S = \frac{\pi E h \ell}{4a(1-\nu^2)} \Bigg\{ & U^2\lambda^2 + (nV - W)^2 + 2\nu\lambda U(W - nV) + \left(\frac{1-\nu}{2}\right)(\lambda V - nU)^2 \\ & + \frac{h^2}{12a^2}\Big[\lambda^4 W^2 + (nV - n^2 W)^2 + 2\nu\lambda^2 W(n^2 W - nV) \\ & + 2(1-\nu)(\lambda V - \lambda n W)^2\Big]\Bigg\} \end{aligned} \qquad [7]$$

where

$$\lambda = \frac{m\pi a}{\ell}$$

The kinetic energy at any instant is given by

$$\left.\begin{aligned} T = \frac{\gamma}{2g}\int_0^{2\pi}\int_0^{\ell}\int_{-h/2}^{h/2}\left[\left(\frac{\partial u}{\partial t}\right)^2 + \left(\frac{\partial v}{\partial t}\right)^2 + \left(\frac{\partial w}{\partial t}\right)^2\right] a\, d\varphi\, dx\, dz \\ \text{where the specific weight, } \gamma = [\text{lb/in.}^3], \text{ or} \\ T = \frac{\gamma\pi h \ell a}{4g}[\dot{U}^2 + \dot{V}^2 + \dot{W}^2] \end{aligned}\right\} \qquad [8]$$

Since U, V and W are independent variables, to minimize the kinetic and potential energy, Lagrange's equation is applicable. The Lagrange equation is in general

$$\frac{\partial}{\partial t}\left(\frac{\partial E}{\partial \dot{q}_i}\right) - \frac{\partial E}{\partial q_i} = Q_i \tag{404}$$

where

q_i = generalized coordinates

E = total energy

Q_i = external forces

In the present case these quantities become

$$\left.\begin{array}{lll} q_1 = U & q_2 = V & q_3 = W \\ \dot{q}_1 = \dot{V} & \dot{q}_2 = \dot{V} & \dot{q}_3 = \dot{W} \\ E = T - S & \text{and} & Q_i = 0 \end{array}\right\} \tag{405}$$

The substitution of Equation 405 into Equation 404 leads to

$$\frac{\partial}{\partial t}\left(\frac{\partial T}{\partial \dot{U}}\right) - \frac{\partial T}{\partial U} = -\frac{\partial S}{\partial U} \qquad [9]$$

Two similar equations can be written in V and W.

The substitution of Equations 7 and 8 into Equation 9 leads to

$$\frac{\pi \gamma h \ell a}{2g}\ddot{U} - 0 = -\frac{\pi E h \ell}{2a(1-\nu^2)}\left[U\lambda^2 + \nu\lambda(W - nV) - n\frac{(1-\nu)}{2}(\lambda V - nU)\right] \qquad [10]$$

U, V and W are periodic with respect to time and may be written

$$U = A\cos\omega t \qquad V = B\cos\omega t \qquad W = C\cos\omega t \qquad [11]$$

where A, B and C are constants and ω is the angular natural frequency of the vibration. The substitution of Equation 11 into Equation 10 yields

$$\left[\lambda^2 - \frac{(1-\nu)}{2}n^2 - \Delta\right]A - \frac{(1+\nu)}{2}\lambda n B + \nu\lambda C = 0 \qquad [12]$$

where

$$\Delta = \frac{\gamma a^2 (1-\nu^2)\omega^2}{Eg} \tag{406}$$

Similarly, by substituting in the Lagrange equations for V and W

$$-\left(\frac{1+\nu}{2}\right)\lambda n A + \left\{\left(\frac{1-\nu}{2}\right)\lambda^2 + n^2 - \Delta + \beta[n^2 + 2(1-\nu)\lambda^2]\right\}B$$

$$- \left\{n + \beta[n^3 + (2-\nu)\lambda^2 n]\right\}C = 0 \quad [13]$$

and

$$\nu\lambda A - \left\{n + \beta[n^3 + (2-\nu)\lambda^2 n]\right\}B + [1 - \Delta + \beta(\lambda^2 + n^2)^2]C = 0 \quad [14]$$

where

$$\beta = h^2/12a^2$$

Eliminating A, B and C from Equations 12 to 14 leads to a cubic equation in Δ

$$\Delta^3 - K_2\Delta^2 + K_1\Delta - K_0 = 0 \quad [15]$$

where

$$\Delta = \frac{\dot{\gamma} a^2(1-\nu^2)\omega^2}{Eg}$$

and

ω = angular frequency

$$K_0 = \frac{1}{2}(1-\nu)^2(1+\nu)\lambda^4 + \frac{1}{2}(1-\nu) \times \beta[(\lambda^2+n^2)^4 - 2(4-\nu^2)\lambda^4 n^2$$

$$- 8\lambda^2 n^4 - 2n^6 + 4(1-\nu^2)\lambda^4 + 4\lambda^2 n^2 + n^4]$$

$$K_1 = \frac{1}{2}(1-\nu)(\lambda^2+n^2)^2 + \frac{1}{2}(3-\nu-2\nu^2)\lambda^2 + \frac{1}{2}(1-\nu)n^2$$

$$+ \beta\left[\frac{1}{2}(3-\nu)(\lambda^2+n^2)^3 + 2(1-\nu)\lambda^4 - (2-\nu^2)\lambda^2 n^2 - \frac{1}{2}(3+\nu)n^4 + 2(1-\nu)\lambda^2 + n^2\right]$$

and

$$K_2 = 1 + \frac{1}{2}(3-\nu)(\lambda^2+n^2) + \beta[(\lambda^2+n^2)^2 + 2(1-\nu)\lambda^2 + n^2]$$

It can be seen that Equation 15 is sixth-order in ω.

5.3.3 STRAIN ENERGY DUE TO BENDING AND STRETCHING OF A CYLINDRICAL SHELL. The substitution of Equation 11 into Equation 7 gives the maximum strain energy in terms of the component amplitudes.

$$S_{max} = \frac{\pi E h \ell}{4a(1-\nu^2)} \Big\{ A^2\lambda^2 + (C - nB)^2 + 2\nu\lambda A(C - nB)$$

$$+ \left(\frac{1-\nu}{2}\right)(\lambda B - nA)^2 + \beta[\lambda^4 C^2 + (n^2 C - nB)^2$$

$$+ 2\nu\lambda^2 C(n^2 C - nB) + 2(1-\nu)(\lambda B - \lambda n C)^2] \Big\} \qquad [16]$$

The first four terms give the strain energy due to stretching, and the remainder that due to bending.

By the elimination of the amplitude ratios between Equations 12, 13 and 14 and the use of expression A/C and B/C, an expression for stretching energy and one for bending energy are obtained.

The stretching energy can be stated as

$$S_s = \left[\frac{\pi E h \ell C^2}{4a(1-\nu^2)}\right]\left[\lambda^2\left(\frac{A}{C}\right)^2 + \left(1 - n\frac{B}{C}\right)^2\right.$$

$$\left. + 2\nu\lambda\left(\frac{A}{C}\right)\left(1 - n\frac{B}{C}\right) + \left(\frac{1-\nu}{2}\right)\left(\lambda\frac{B}{C} - n\frac{A}{C}\right)^2\right] \qquad [19]$$

The bending energy can be written

$$S_b = \beta\left[\frac{\pi E h \ell C^2}{4a(1-\nu^2)}\right]\left\{(\lambda^2 + n^2)^2 + [n^2 + 2(1-\nu)\lambda^2]\left(\frac{B}{C}\right)^2\right.$$

$$\left. - 2[(2-\nu)\lambda^2 n + n^3]\left(\frac{B}{C}\right)\right\} \qquad [20]$$

Equations 19 and 20 can be rewritten in the form

$$S_s = \eta_s\left[\frac{E\pi}{4(1-\nu^2)}\right]\ell C^2 \quad \text{and} \quad S_b = \eta_b\left[\frac{E\pi}{4(1-\nu^2)}\right]\ell C^2 \qquad [21]$$

where η_s and η_b are nondimensional energy factors for stretching and bending respectively.

Figure 78 shows the orientation of the coordinate system and the nodal pattern of the cylindrical shells.

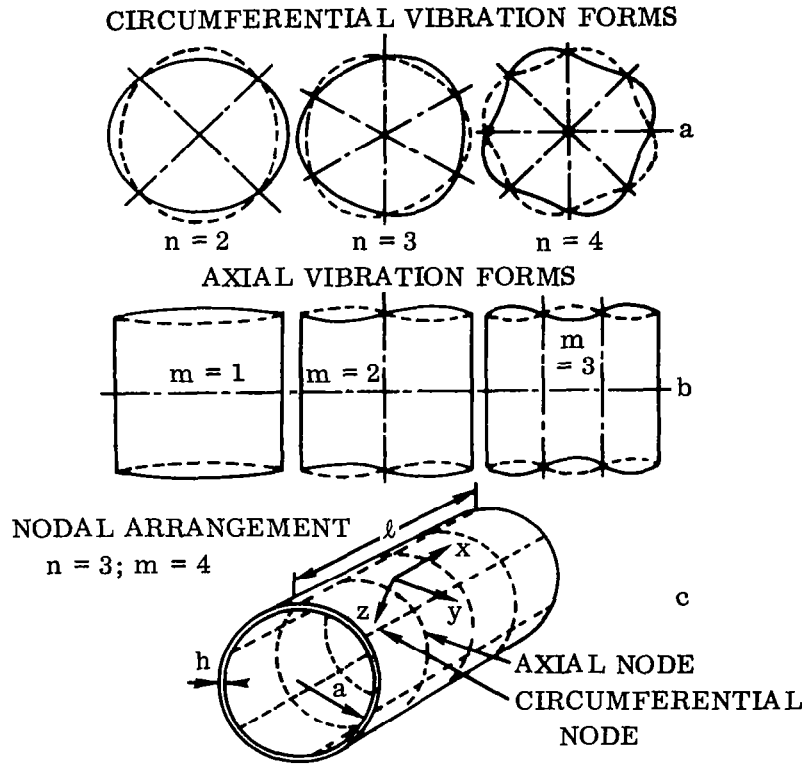

Figure 78. Orientation and Nodal Pattern of Cylindrical Shells

It can be seen that the minimum frequency coincides with the minimum strain energy and that the lowest frequency has not occurred at the lowest circumferential wave number. The effect of different thicknesses-over-mean-radius ratios, α, can be seen on Figure 79. The general arrangement of the vibration test can be seen on Figure 80.

5.3.4 CONCLUSIONS. The paper described the applied energy method of determining the vibrations of cylindrical shells; by a suitable choice of displacement functions, the problem of free vibration was reduced to Legendre's equations via a sixth-order frequency equation. The authors are the discoverers of the peculiar frequency dip, which was explained fully and also verified by their test results. In general, their theory shows good agreement with the test results. The theory cannot be expanded for arbitrary edge conditions, which is the limitation of this theory.

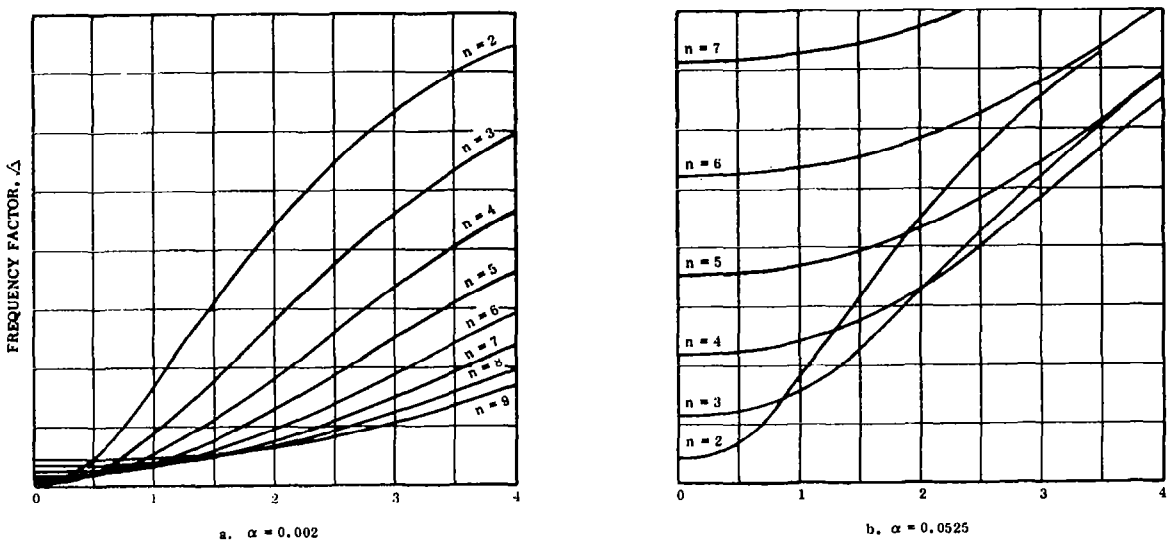

Figure 79. Effect of Thickness on Radius Ratio, $\lambda = \frac{m\pi a}{\ell}$

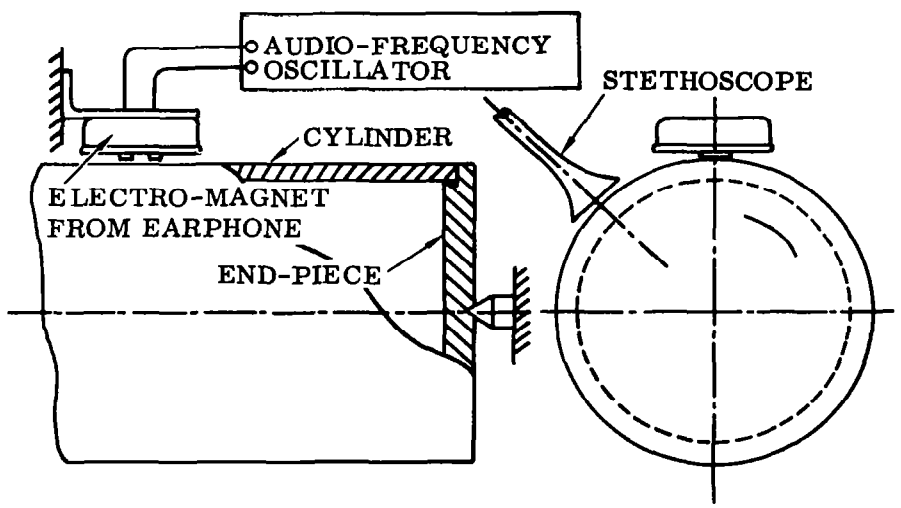

Figure 80. Experiment Arrangement

6/THEORY OF ORTHOTROPIC SHELLS

Our theoretical investigation was restricted to isotropic shells. However, many of the practical structures have rings and longitudinal stiffeners or are of honeycomb construction. Another type of shell structure can be built from plywood. It is obvious that the stretching and bending effects are different in different directions for these structures. Several theories were developed, and the present discussion will be restricted to two of them. One of them was developed by Flügge, which was based on theoretical considerations only; and the other theory, by Hoppmann, was based on test results. The equivalence of the two theories will be discussed.

6.1 THEORY OF W. FLÜGGE

A plate with uniform thickness but with different stiffness characteristics is considered first. Figure 81 shows the general arrangement and E_1 and E_2 represent the different moduli of elasticity.

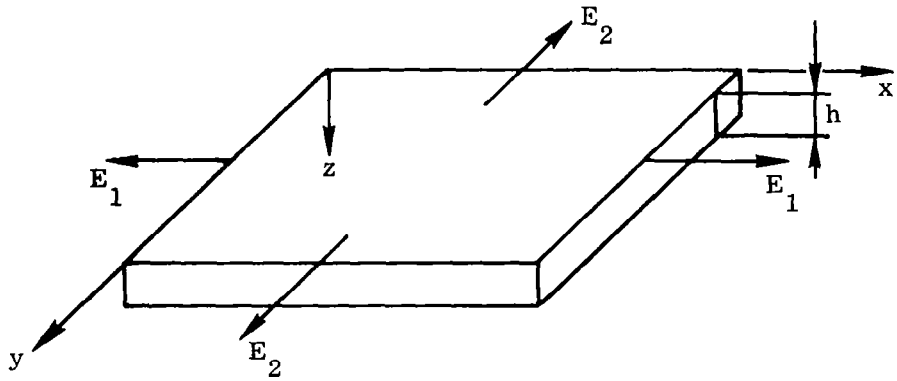

Figure 81. General Arrangement of Plate

In the isotropic case the forces can be expressed, based on Equation 386, as

$$N_x = \frac{E\,h}{(1-\nu^2)}(\epsilon_x + \nu\,\epsilon_\varphi) = \frac{E}{(1-\nu^2)}\,h\,\epsilon_x + \frac{\nu\,E}{(1-\nu^2)}\,h\,\epsilon_\varphi \tag{407}$$

The last equation may be expressed in the form

$$N_x = D_x\,\epsilon_x + D_\nu\,\epsilon_\varphi \tag{408}$$

A similar equation can be written for force N_φ

$$N_\varphi = D_\varphi\,\epsilon_\varphi + D_\nu\,\epsilon_x \tag{409}$$

The comparison of Equations 407 and 408 leads to the following relations

$$D_x = E_1 h \qquad D_\nu = E_\nu h \qquad \text{Furthermore} \quad D_\varphi = E_2 h \tag{410}$$

where

$$E_1 = E_2 = \frac{E}{(1 - \nu^2)} \qquad \text{and} \qquad E_\nu = \frac{\nu E}{(1 - \nu^2)} \tag{411}$$

Based on Equation 388 the bending moments may be expressed as

$$M_x = \frac{E h^3}{12(1 - \nu^2)} (\varkappa_x + \nu \varkappa_\varphi) = E_1 I \varkappa_x + E_\nu I \varkappa_\varphi \tag{412}$$

where

$$I = \frac{h^3}{12}$$

Equation 412 can be written, as in the previous case

$$M_x = K_x \varkappa_x + K_\nu \varkappa_\varphi \tag{413}$$

The comparison of Equations 412 and 413 leads again to

$$K_x = I E_1 \qquad \text{and} \qquad K_\nu = I E_\nu \tag{414}$$

In the present case, one has $E_1 = E_2$.

6.1.1 ORTHOTROPIC PLATE. The plate is usually called "orthotropic" when the material of the plate has three planes of symmetry with respect to its elastic properties. The plate has different moduli of elasticity in the different directions; in other words the strength of the plate has been varied in the different directions. In the orthotropic case, the former equations can be written considering the different moduli of elasticity E_1 and E_2. The forces in this case are

$$N_x = D_x \epsilon_x + D_\nu \epsilon_\varphi , \qquad N_\varphi = D_\varphi \epsilon_\varphi + D_\nu \epsilon_x \qquad \text{and} \qquad N_{x\varphi} = D_{x\varphi} \gamma_{x\varphi} \tag{415}$$

where

$$D_x = E_1 h , \qquad D_\varphi = E_2 h \qquad \text{and} \qquad D_\nu = E_\nu h$$

and

$$E_1 \neq E_2$$

The moment may be expressed as

$$M_x = K_x \varkappa_x + K_\nu \varkappa_\varphi, \quad M_\varphi = K_\varphi \varkappa_\varphi + K_\nu \varkappa_x \quad \text{and} \quad M_{x\varphi} = K_{x\varphi} \varkappa_{x\varphi} \tag{416}$$

where

$$K_x = IE_1, \quad K_\varphi = IE_2 \quad \text{and} \quad K_\nu = IE_\nu$$

and

$$E_1 \neq E_2$$

In the calculations of constants D_ν and K_ν, it is recommended that the average values be used. The calculations of the orthotropic coefficients will be discussed in three configurations.

6.1.2 PLYWOOD SHELL. Figure 82 illustrates a panel of a plywood shell. The first numbers of subindex E have been designated for the part of the plywood shell and the second numbers for the directions. The orthotropic constants were calculated, based on the previous considerations by Equation 417.

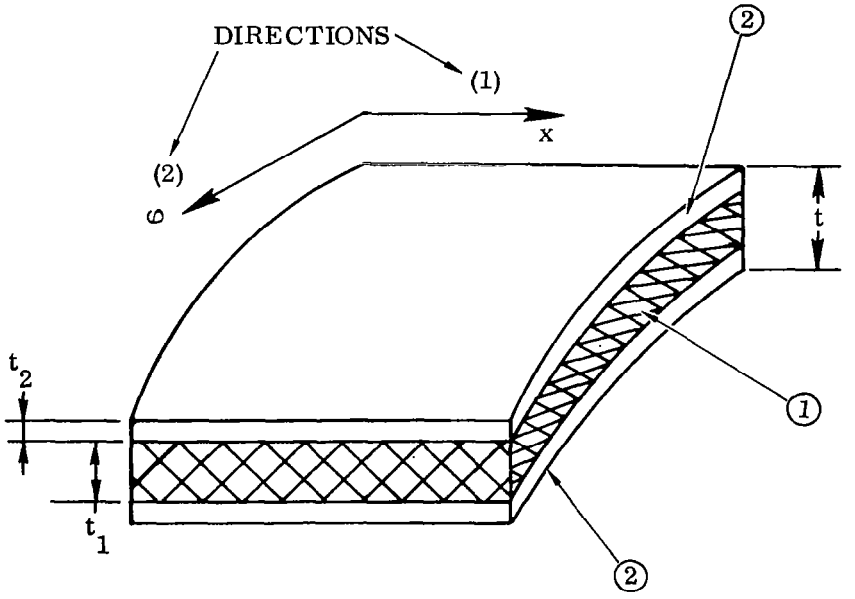

Figure 82. Plywood Shell

$$\left.\begin{aligned} D_x &= E_{11} t_1 + 2 E_{21} t_2 \qquad & D_\varphi &= E_{12} t_1 + 2 E_{22} t_2 \\ D_\nu &= E_\nu t & D_{x\varphi} &= G t \\ K_x &= \frac{1}{12}\left[E_{11} t_1^3 + E_{21}(t^3 - t_1^3)\right] \quad \text{etc.} \end{aligned}\right\} \tag{417}$$

6.1.3 CYLINDRICAL SHELLS WITH RINGS AND STRINGERS. Figure 83 shows a portion of the cylindrical shell with rings and Figure 84 illustrates the portion of the shell with longitudinal stringers. The orthotropic constant D_x associated with stretching of the middle surface may be calculated by adding the stretching effect of the stringer to the shell constant for a constant-thickness shell. The effect of the stringer can be expressed by an additional imaginary shell thickness, h_{av}. The calculation can be seen by Equation 418.

$$D_x = E_1 h + E h_{av} = \frac{E h}{(1 - \nu^2)} + E \frac{A_x}{b_2} \tag{418}$$

The orthotropic constant K_x associated with bending may be derived again by adding the bending effect of the stringer to the shell constant associated with constant thickness. Equations 412 and 414 expressed the basic concept; however, the moment of inertia of the stringer has to be divided by the spacing distance, b_2, since the moment of inertia of the shell with constant shell thickness was computed for a unit wide strip.

$$K_x = E_1 I + \frac{E(I_{stringer})}{b_2} = \frac{E h^3}{12(1 - \nu^2)} + \frac{E(I_x + A_x c_x^2)}{b_2} \tag{419}$$

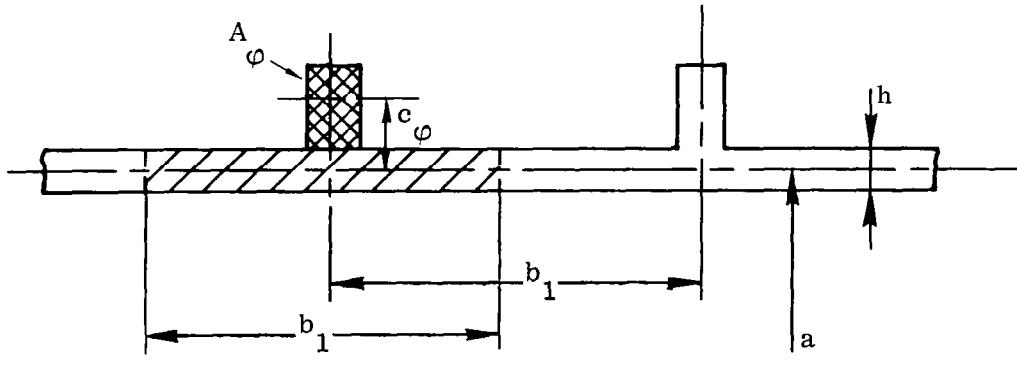

Figure 83. Cylindrical Shell with Rings

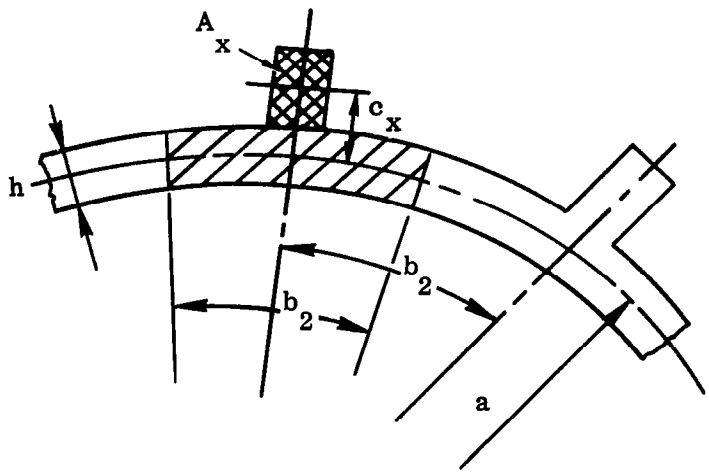

Figure 84. Shell with Longitudinal Stringers

The rest of the constants are given by Equation 420.

$$
\left.
\begin{aligned}
D_{\varphi} &= \frac{E h}{(1-\nu^2)} + E\frac{A_{\varphi}}{b_1}, \qquad D_{\nu} = \nu\frac{E h}{(1-\nu^2)} \\
D_{x\varphi} &= G h \\
K_{\varphi} &= \frac{E h^3}{12(1-\nu^2)} + \frac{E(I_{\varphi} + A_{\varphi} c_{\varphi}^2)}{b_1}, \qquad K_{\nu} = \frac{\nu E h^3}{12(1-\nu^2)} \\
K_{x\varphi} &= \frac{E h^3}{12(1+\nu)} + \frac{G I_x^*}{b_2} \\
K_{\varphi x} &= \frac{E h^3}{12(1+\nu)} + \frac{G I_{\varphi}^*}{b_1}
\end{aligned}
\right\} \qquad (420)
$$

where the moments of inertia, I_x^* and I_{φ}^*, represent the twisting of the stringers or the rings. The details of this theory can be found in Reference 6, page 293-307.

Flügge's orthotropic shell approximation and shell equations have the advantage of simplicity; and they are useful when there are no test results. It is obvious that this theory can be only approximate, since it does not take into account any stress concentrations and local deformations.

6.2 A REVIEW OF HOPPMANN'S PAPER: "ELASTIC COMPLIANCES OF ORTHOGONALLY STIFFENED PLATES" (REFERENCE 17)

6.2.1 SUMMARY. Hoppmann proposed an experimental evaluation of the orthotropic constants and described the test procedure. The essence of his theory can be summarized as follows.

The tests apply to a panel of a shell or a plate and define the elastic constants. This theory considers eight elastic constants. The elastic constants associated with stretching effects (membrane stress) can be expressed as C_{11}, C_{12} and C_{22}. The shear constant is expressed as C_{66}. These constants are associated with an equivalent shell or plate thickness of h_s.

The bending effects can be expressed by the following constants: S_{11}, S_{12} and S_{22}. The twisting effect is represented by the constant, S_{66}.

This second group of constants has another equivalent shell or plate thickness of h_b. Figure 85 shows a portion of a stiffened plate. Figure 86 illustrates the schematic diagram of bending and twisting. The schematic diagram of shear and tensile loadings are seen on Figure 87. The schematic of the foil-type displacement meter is shown in

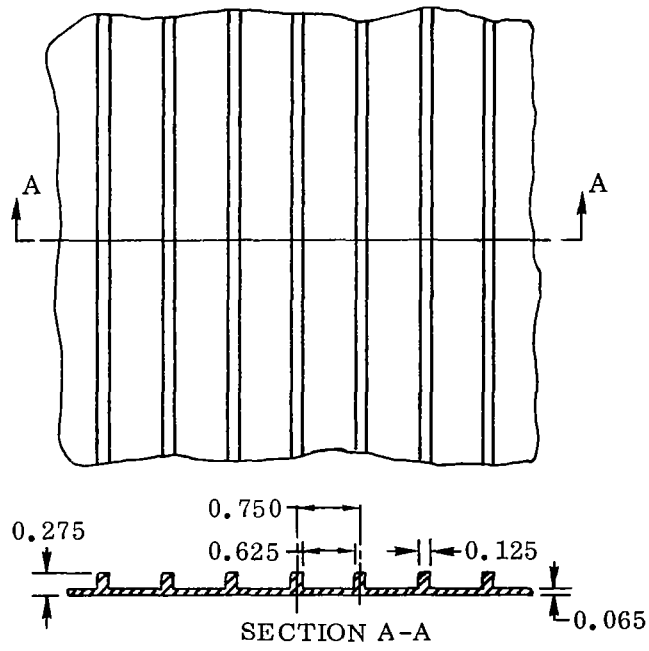

Figure 85. Details of Experimental Plates with Integral Stiffeners (Dimensions in Inches)

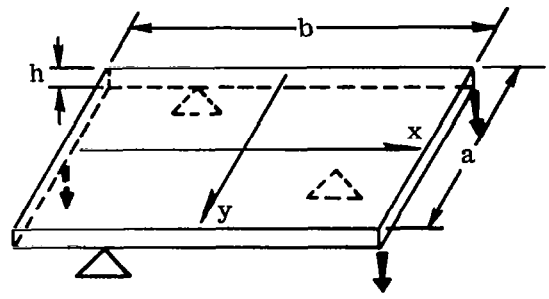

a. BENDING

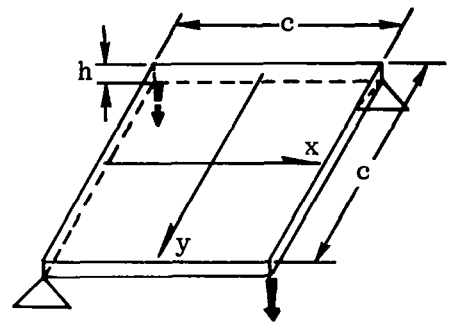

b. TWISTING

Figure 86. Diagrammatic Arrangement for Bending and Twisting Tests

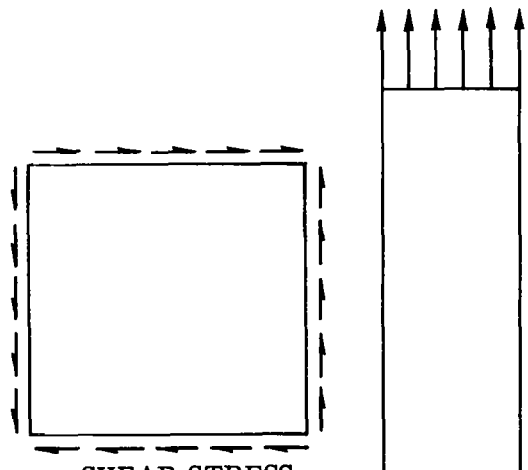

a. SHEAR STRESS

b. TENSILE STRESS (STRETCH)

Figure 87. Diagrammatic Arrangement Showing Shear and Tensile Loading

Figure 88. The paper presents photographs of the equipment for the bending and twisting tests; furthermore, the equipment for the tensile and shear tests is also shown. The results of the tests are tabulated in Tables 6 and 7.

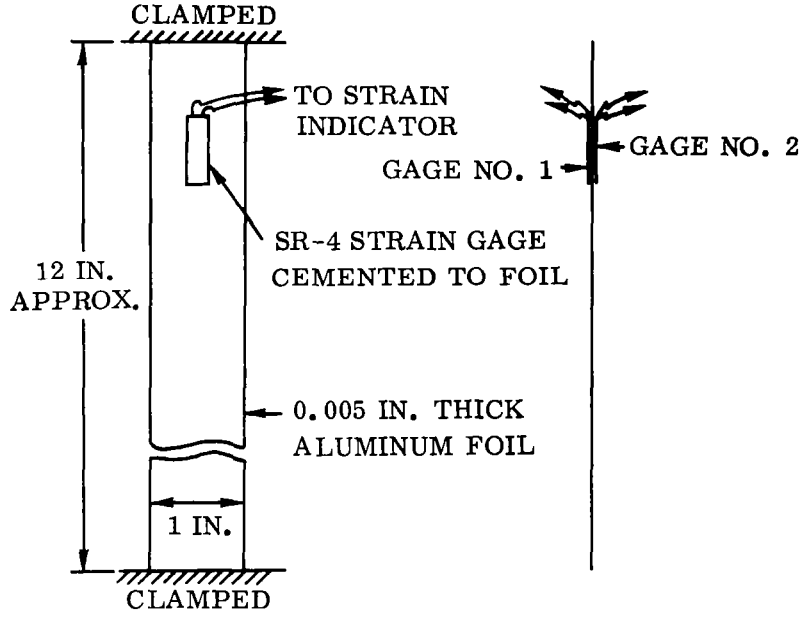

Figure 88. Schematic Diagram of Foil-Type Displacement Meter

Table 6. Orthotropic Elastic Constants (Bending and Twisting)

Plate	$\frac{S_{11}}{h_b^3} \times 10^6$	$\frac{S_{12}}{h_b^3} \times 10^6$	$\frac{S_{21}}{h_b^3} \times 10^6$	$\frac{S_{22}}{h_b^3} \times 10^6$	$\frac{S_{66}}{h_b^3} \times 10^6$
A	364	-127	-127	364	983
B	13.0	+1.4	-18.1	306	370
C	4.8	-1.7	-1.7	4.8	13

In the theory $S_{ij} = S_{ji}$, so in practical application an average of S_{12} and S_{21} is used.

Table 7. Orthotropic Elastic Constants (Stretching and Shearing in Plane of Middle Surface)

Plate	$\frac{C_{11}}{h_s} \times 10^6$	$\frac{C_{12}}{h_s} \times 10^6$	$\frac{C_{21}}{h_s} \times 10^6$	$\frac{C_{22}}{h_s} \times 10^6$	$\frac{C_{66}}{h_s} \times 10^6$
A	1.54	-0.54	-0.54	1.54	4.16
B	0.83	-0.29	-0.13	1.40	2.11
C	0.36	-0.12	-0.12	0.36	0.98

In the theory $C_{ij} = C_{ji}$, so in practical application an average of C_{12} and C_{21} is used.

6.2.2 EXPLANATION OF THE THEORY AND TEST RESULTS. The membrane stresses (stretching and shearing effects) can be written according to the paper

$$\epsilon_i'' = C_{ij}\sigma_j'' \tag{421}$$

where

$$(i, j = 1, 2)$$

$$\gamma'' = C_{66}\tau'' \tag{422}$$

The dummy index j means summation according to tensorial notation, and the double primes symbolize the membrane stresses and strains. Equation 421 can be written

$$\epsilon_i'' = C_{ij}\sigma_j'' = \sum_{i=1}^{2} C_{ij}\sigma_j \tag{423}$$

Equation 423 is, in terms of the components

$$\begin{aligned} \epsilon_1'' &= C_{11}\sigma_1'' + C_{12}\sigma_2'' \\ \epsilon_2'' &= C_{21}\sigma_1'' + C_{22}\sigma_2'' \end{aligned} \tag{424}$$

The stresses can be expressed from Equations 422 and 424

$$\left.\begin{aligned} \sigma_1'' &= \frac{1}{C^*}(C_{22}\epsilon_1'' - C_{12}\epsilon_2''), \qquad \sigma_2'' = \frac{1}{C^*}(C_{11}\epsilon_2'' - C_{21}\epsilon_1'') \\ \tau'' &= \frac{\gamma''}{C_{66}} \end{aligned}\right\} \tag{425}$$

where

$$C^* = \begin{vmatrix} C_{11} & C_{12} \\ C_{21} & C_{22} \end{vmatrix} \tag{426}$$

The bending stresses (bending and twisting effects) may be written

$$\epsilon_i' = S_{ij}\sigma_j' \tag{427}$$

where

$$(i, j = 1, 2)$$

$$\gamma' = S_{66}\tau' \tag{428}$$

The dummy index j means again the summation by tensorial notation, and the single primes symbolize the bending stresses and strains. Equation 427 can be expressed

$$\epsilon_i' = S_{ij}\sigma_j' = \sum_{i=1}^{2} S_{ij}\sigma_j' \tag{429}$$

The stresses were expressed in the terms of strains from Equation 429

$$\left.\begin{aligned} \sigma_1' &= \frac{1}{S^*}(S_{22}\epsilon_1' - S_{12}\epsilon_2') \\ \sigma_2' &= \frac{1}{S^*}(S_{11}\epsilon_2' - S_{21}\epsilon_1') \end{aligned}\right\} \tag{430}$$

where

$$S^* = \begin{vmatrix} S_{11} & S_{12} \\ S_{21} & S_{22} \end{vmatrix} \tag{431}$$

The shear stress is expressed, from Equation 428 as

$$\tau' = \frac{\gamma'}{S_{66}} \tag{432}$$

The membrane forces may be written by the introduction of an equivalent membrane thickness of the shell, h_s.

$$\left.\begin{aligned} N &= \sigma_i'' h_s \\ N_{ij} &= \tau'' h_s \end{aligned}\right\} \tag{433}$$

where (i, j = 1, 2).

The bending and twisting moments can be expressed similarly by the introduction of the equivalent bending shell thickness, h_b.

$$\left.\begin{aligned} M_i &= \sigma_i' \frac{h_b^3}{12} \\ M_{ij} &= \tau' \frac{h_b^3}{12} \end{aligned}\right\} \tag{434}$$

The isotropic constants are a special case of the orthotropic constants. The isotropic constants may be calculated by the comparison of Equations 433 and 386 and of Equations 388 and 434.

$$\left.\begin{aligned} C_{11} &= C_{22} = S_{11} = S_{22} = \frac{1}{E} \\ C^* &= S^* = \frac{(1 - \nu^2)}{E^2} \\ C_{12} &= C_{21} = S_{12} = S_{21} = -\frac{\nu}{E} \\ C_{66} &= 2 S_{66} = \frac{1}{G} = \frac{2(1 + \nu)}{E} \end{aligned}\right\} \tag{435}$$

and

$$h_s = h_b = h_m = h$$

Figure 89 illustrates the direction of the elastic constants relative to the plate stiffeners. The results of bending and twisting tests can be seen in Table 6. Table 7 demonstrates the results of the stretching and shearing tests. In these tables the plate A has a constant plate thickness, 0.065 inch, and plate C has a thickness of 0.275 inch. Plate B is the stiffened (orthotropic) plate; the elastic properties of plate B can be found between plate A and C.

6.2.3 CONCLUSIONS. The paper has demonstrated a practical method to measure the elastic compliances of a stiffened plate. The measurement can be extended for a panel of a shell, and the stiffeners of the shell panel can be in both perpendicular directions. This technique can also be useful to determine the elastic compliances of honeycomb structures.

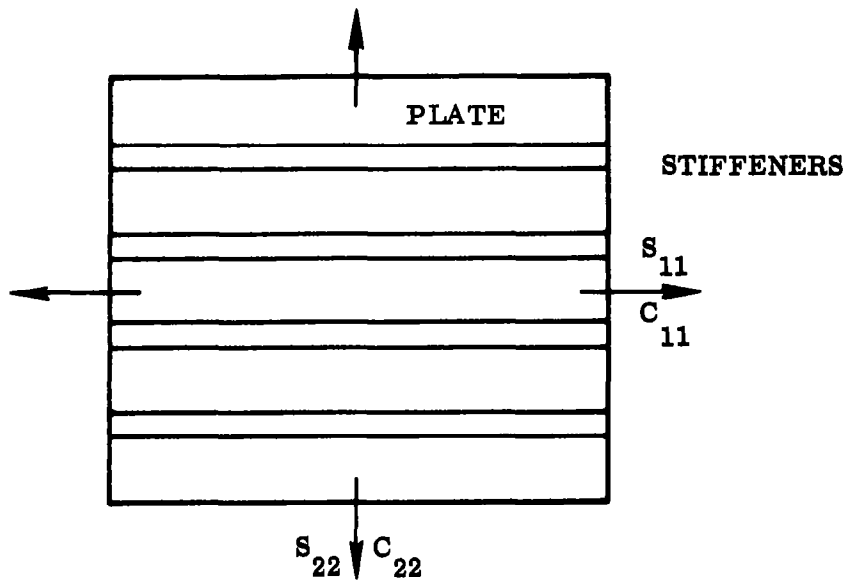

Figure 89. Direction of Constants

6.3 TRANSFORMATION OF HOPPMANN'S EXPERIMENTAL CONSTANTS TO FLÜGGE'S THEORETICAL CONSTANTS

The orthotropic elastic constants are necessary to solve for the frequency and mode shapes of a particular shell. The accurate method of obtaining these coefficients is by experiment. However, experimental results are not always available, and this is the reason for discussing Flügge's theoretical method. If a shell theory is formulated in terms of orthotropic constants using one of the methods, many times it is desirable to transfer the theory in terms of the other type of orthotropic constants.

Let us assume that the forces and moments were expressed by Flügge's method according to Equations 415, 416, 418, 419 and 420.

$$N_x = D_x \epsilon_x + D_\nu \epsilon_\varphi \tag{436}$$

$$\vdots$$

$$M_x = K_x \varkappa_x + K_\nu \varkappa_\varphi \tag{437}$$

$$\vdots$$

These forces and moments can be expressed, according to Hoppmann's theory, as

$$N_x = \int_{-h_s/2}^{h_s/2} \sigma_1'' \, dz = \frac{h_s}{C^*}(C_{22}\epsilon_x - C_{12}\epsilon_\varphi) \tag{438}$$

$$\vdots$$

$$M_x = \int_{-h_b/2}^{h_b/2} \sigma_1' \, z \, dz = -\int_{-h_b/2}^{h_b/2} \frac{1}{S^*}(S_{22}\varkappa_x - S_{12}\varkappa_\varphi) \, z^2 \, dz$$

Since the bending strains, ϵ_i', were expressed as the function of curvature, according to Equation 4 of Reference 16,

$$\epsilon_1' = -z\varkappa_1 \qquad \text{and} \qquad \epsilon_2' = -z\varkappa_2 \tag{439}$$

and

$$M_x = -\frac{h_b^3}{12\,S^*}(S_{22}\varkappa_x - S_{12}\varkappa_\varphi) \tag{440}$$

A comparison of Equations 436 and 438 leads to

$$D_x = \frac{h_s C_{22}}{C^*} \qquad D_\nu = -\frac{C_{12} h_s}{C^*} \qquad \text{and} \qquad D_\varphi = \frac{h_s C_{11}}{C^*} \tag{441}$$

A comparison of Equations 437 and 440 starts with the considerations of the opposite sign conventions by Flügge and Timoshenko.

$$K_x = \frac{h_b^3 S_{22}}{12\,S^*} \qquad K_\nu = -\frac{h_b^3 S_{12}}{12\,S^*} \qquad \text{and} \qquad K_\varphi = \frac{h_s^3 S_{11}}{12\,S^*} \tag{442}$$

Determinant 426 can be expressed by the use of Equation 441.

$$C^* = (C_{11}C_{22} - C_{12}^2) = \left(\frac{C^*}{h_s}\right)^2 [D_x D_\varphi - D_\nu^2] \tag{443}$$

Equation 443 can be expressed as

$$\frac{h_s}{C^*} = \frac{(D_x D_\varphi - D_\nu^2)}{h_s} \tag{444}$$

The substitution of Equation 444 into Equation 441 leads to

$$D_x = \frac{C_{22}(D_x D_\varphi - D_\nu^2)}{h_s} \tag{445}$$

Equation 445 is, in the final form,

$$\frac{10^6 C_{22}}{h_s} = \frac{10^6 D_x}{(D_x D_\varphi - D_\nu^2)}$$

$$\frac{10^6 S_{22}}{h_b^3} = \frac{10^6 K_x}{12(K_x K_\varphi - K_\nu^2)} \qquad \text{etc.} \tag{446}$$

For demonstration of the theory, Flügge's theoretical method will be used to compute the orthotropic constants. Table 8 shows the computed values and the test results of the orthotropic constants for a longitudinally stiffened cylindrical shell according to Reference 18.

Table 8. Computed and Experimental Orthotropic Constants

Configuration	Analytical	Experimental
$\frac{10^6 C_{22}}{h_s}$	1.47	1.40
$\frac{10^6 C_{66}}{h_s}$	4.14	2.11
$\frac{10^6 C_{11}}{h_s}$	1.00	0.83
$\frac{10^6 C_{12}}{h_s}$	-0.344	-0.21
$\frac{10^6 S_{22}}{h_b^3}$	322.0	306.0
$\frac{10^6 S_{11}}{h_b^3}$	10.27	13.0
$\frac{10^6 S_{12}}{h_b^3}$	-3.60	-8.30
$\frac{10^6 S_{66}}{h_b^3}$	490.0	370.0

The values in Table 9 were then used to calculate the model frequencies according to Hoppmann's equations for a longitudinal stiffened shell. (See Reference 18.) Table 6 shows the results with the different wave numbers for the analytical case using both the test coefficients and the analytical (Flügge) coefficients. Also shown are the frequencies obtained experimentally for the same shell. The modes for n = 2 and m = 2, 3, 4 and 5 could not be excited. This table shows that in some cases the error between the completely analytical and test cases can be as much as 41 percent; however, for the lower longitudinal wave numbers (m) the error is reasonable.

Table 9. Model Frequencies

	1	2	3	4	5	6
m	n	Test Constants Freq (Hz)	Calculated Constants Freq (Hz)	% Diff 2/3 - 1.00	Test Frequencies	% Error 5/3 - 1.00
1	2	750	694	8	700	1
	3	1150	1135	1	1270	12
	4	2100	2111	-0.5	2200	-4
	5	3340	3402	-2	3460	-1
2	2	2300	2020	14	—	—
	3	1700	1577	8	1830	16
	4	2350	2254	4	2600	10
	5	3510	3472	1	4080	18
3	2	4200	3716	13	—	—
	3	2870	2574	11	2640	2
	4	2970	2727	9	3360	23
	5	3900	3719	5	4120	11
4	2	6100	5466	11	—	—
	3	4360	3897	12	5490	41
	4	3960	3600	10	4100	14
	5	4620	4261	8.5	5130	20
5	2	7900	7186	10	—	—
	3	5900	5405	9	6100	13
	4	5100	4809	6	5200	8
	5	5600	5154	9	6100	18

6.4 A REVIEW OF HOPPMANN'S PAPER: "SOME CHARACTERISTICS OF THE FLEXURAL VIBRATIONS OF ORTHOGONALLY STIFFENED CYLINDRICAL SHELLS" (REFERENCE 18)

6.4.1 SUMMARY. The flexural vibrations of stiffened cylindrical shells were studied by theory and experiments. The theory utilized the experimental determination of the orthotropic constants developed previously by the author. (See Reference 17.) Three different configurations were studied theoretically and experimentally; one of these had equally spaced longitudinal stiffeners, the second had rings again equally spaced, and the third configuration was without any stiffeners (isotropic case). The theory is based on the orthotropic stress-strain relations developed previously in Reference 17. The strain energy expression of the shell was formulated in terms of experimentally determined orthotropic constants.

The effective shell thickness, h_s, associated with stretching and shearing of the middle surface and another shell thickness, h_b, associated with bending and twisting have been utilized in the development of the stress-displacement relations. The kinetic energy of the shell was expressed with the aid of the equivalent shell thickness, h_m. The theory has discussed the case of simply supported edges, and a suitable chosen displacement function reduced the energy expression to the Lagrange equation of motion. In other words, the energy expression was minimized by the use of the proper displacement functions and the application of the Lagrange equations of motion. The theory obtained a sixth-order frequency equation. The frequencies of the previously mentioned three different shell configurations were computed. All of the cylindrical shells were constructed with aluminum. Flexural vibrations were excited by an electromagnet, and the magnet was excited from an audio-oscillator which fed through a resonant-type RC circuit to increase the driving force. A specially designed pickup was used to determine the mode shapes, and the frequencies were also checked by means of a small crystal-type pickup. The results of the theoretical and experimental investigations of the frequencies were tabulated in the paper, and they are in fairly good agreement.

6.4.2 EXPLANATION OF THE THEORY, TEST APPARATUS AND THE TEST RESULTS. The elastic constants associated with bending and twisting can be expressed as

$$\left.\begin{aligned} \epsilon_i' &= S_{ij}\sigma_j' \\ \gamma' &= S_{66}\tau' \qquad \text{(i, j sum over 1, 2)} \end{aligned}\right\} \qquad [1]$$

The orthotropic stress-strain equations can be expressed by the elastic orthotropic constants, which are associated with stretching and shearing.

$$\left.\begin{aligned} \epsilon_i'' &= S_{ij}\sigma_j'' \\ \gamma'' &= C_{66}\tau'' \qquad \text{(i, j sum over 1, 2)} \end{aligned}\right\} \qquad [2]$$

Equations 1 and 2 were explained by Equations 421 through 434. The elastic constants S_{ij} and C_{ij}, determined from experiments, were fully discussed in Reference 17. The orthotropic elastic constants used in this paper are shown in Equation 3.

$$\left.\begin{aligned} &\frac{S_{11}}{h_b^3} \times 10^6 = 306 \qquad \frac{S_{12} \times 10^6}{h_b^3} = \frac{S_{21} \times 10^6}{h_b^3} = -8.3 \\ &\frac{S_{22}}{h_b^3} \times 10^6 = 13 \qquad \frac{S_{66}}{h_b^3} \times 10^6 = 370 \\ &\frac{C_{11}}{h_s} \times 10^6 = 1.4 \qquad \frac{C_{12} \times 10^6}{h_s} = \frac{C_{21} \times 10^6}{h_s} = -0.21 \\ &\frac{C_{22}}{h_s} \times 10^6 = 0.83 \qquad \frac{C_{66}}{h_s} \times 10^6 = 2.11 \end{aligned}\right\} \quad [3]$$

Units are inches and pounds.

The strain energy of a thin shell may be written

$$S = \frac{1}{2}\int_V (\sigma_1 \epsilon_1 + \sigma_2 \epsilon_2 + \tau\gamma)\, dV \quad [4]$$

where dV is an element of volume. σ and τ are stresses, while ϵ and γ are strains. Equation 4 is equivalent to Equations 402 and 403. The stresses may be expressed in the form

$$\left.\begin{aligned} \sigma_1 &= \sigma_1' + \sigma_1'' \\ \sigma_2 &= \sigma_2' + \sigma_2'' \\ \tau &= \tau' + \tau'' \end{aligned}\right\} \quad [5]$$

Equation 5 expresses the superposition of membrane and bending stresses. The explanation of Equation 5 can also be found in Equation 4 of Reference 16.

The strain energy in terms of orthotropic constants can be obtained by the substitution of Equations 1, 2, and 5 into Equation 4.

$$S = \frac{h_s}{2C^*}\int_A (-C_{22}\epsilon_1''^2 - C_{11}\epsilon_2''^2 + 2C_{12}\epsilon_1''\epsilon_2'')\, a\, d\phi\, dx$$

$$+\frac{h_b^3}{24\,S^*}\int_A (-S_{22}\varkappa_1^2 - S_{11}\varkappa_2^2 + 2S_{12}\varkappa_1\varkappa_2)\,a\,d\phi\,dx$$

$$+\frac{h_s}{2\,C_{66}}\int_A \gamma''^2\,a\,d\phi\,dx + \frac{h_b^3}{6\,S_{66}}\int_A \gamma'^2\,a\,d\phi\,dx \qquad [6]$$

where

a is the mean radius of the shell

ϕ is the angular location in a transverse section of the cylinder

x is the coordinate measured along the cylinder

In the expression of Equation 5, the terms associated with bending and twisting were integrated between $\pm(h_b/2)$ and the terms associated with stretching and shearing were integrated between $\pm(h_s/2)$.

The strain displacement relations can be expressed according to Equations 387 and 389.

$$\left.\begin{aligned} \epsilon_1'' &= \frac{\partial u}{\partial x} & \epsilon_2'' &= \frac{1}{a}\left(\frac{\partial v}{\partial \phi} - w\right) & \gamma'' &= \left(\frac{1}{a}\frac{\partial u}{\partial \phi} + \frac{\partial v}{\partial x}\right) \\ \varkappa_1 &= \frac{\partial^2 w}{\partial x^2} & \varkappa_2 &= \frac{1}{a^2}\left(\frac{\partial^2 w}{\partial \phi^2} + \frac{\partial v}{\partial \phi}\right) & \varkappa_{12} &= \frac{1}{a}\left(\frac{\partial^2 w}{\partial x\,\partial \phi} + \frac{\partial v}{\partial x}\right) \end{aligned}\right\} \qquad [7]$$

The substitution of Equation 7 into Equation 6 leads to a strain energy expression which consists of the displacements, elastic constants C_{ij} and S_{ij}, and the thicknesses, h_s and h_b. The fictitious thicknesses h_s and h_b are canceled from Equation 6 by the substitution of the numerical values of Expression 3 into Equation 6. Therefore, the strain energy is really independent of the thicknesses h_s and h_b.

The kinetic energy of the shell may be written in the following manner.

$$T = \frac{\rho}{2}\iiint\left[\left(\frac{\partial u}{\partial t}\right)^2 + \left(\frac{\partial v}{\partial t}\right)^2 + \left(\frac{\partial w}{\partial t}\right)^2\right] dV \qquad [9]$$

Equation 9 is equivalent to Equation 8 of Reference 16. If the integration is made through a mean thickness of the stiffened shell, then the volume integral is simply a surface integral to be integrated over the middle surface. The thickness of a stiffened shell may be designated to represent a mean thickness. The total mass can be written as $2\pi a\,\ell\rho h_m$. The radius of middle surface is a, the length of the shell is ℓ, and the mean density of the shell is ρ. After the above integration has been performed,

$$T = \frac{\rho h_m}{2} \int_A \left[\left(\frac{\partial u}{\partial t}\right)^2 + \left(\frac{\partial v}{\partial t}\right)^2 + \left(\frac{\partial w}{\partial t}\right)^2 \right] a \, d\phi \, dx \qquad [10]$$

It is obvious that ρh_m can be determined readily by dividing the total mass of the shell by $2\pi a \ell$. In the case of simply supported edges, the frequency equation can be derived with the aid of Lagrangian equations of motion. A further explanation can be found in Reference 16 of Equations 404, 405 and 4. For free vibrations they may be written

$$\frac{d}{dt}\left(\frac{\partial T}{\partial \dot{q}_i}\right) + \frac{\partial S}{\partial q_i} = 0 \qquad \text{where} \quad i = 1,2,3 \qquad [11]$$

Equation 11 can be also found in Reference 16 as Equation 9. The expressions for S and T have been derived and are given as Equations 6 and 10. The generalized coordinates, q_i, can be expressed according to Equation 405. The displacement functions can be expressed according to Equations 6 and 11 of Reference 16.

$$\left.\begin{aligned} u &= A \cos n\phi \cos\left(\frac{m\pi x}{\ell}\right) \cos \omega t \\ v &= B \sin n\phi \sin\left(\frac{m\pi x}{\ell}\right) \cos \omega t \\ w &= C \cos n\phi \sin\left(\frac{m\pi x}{\ell}\right) \cos \omega t \end{aligned}\right\} \qquad [12]$$

where m and n are integers.

The corresponding half longitudinal wave numbers are designated by numbers m, and the circumferential wave numbers are designated by numbers n. A, B, C are constants and ω is the angular frequency of vibration. The displacement functions satisfy the boundary conditions, since

$$w = v = 0 \qquad M_x = 0 \quad \text{at} \quad x = 0 \quad \text{and} \quad x = \ell \qquad [13]$$

Applying the Lagrangian equation to the expressions of the strain and kinetic energies, in exactly the same way as was explained by Equations 404, 406 and 9 through 11 of Reference 16, the Lagrangian Equations 11 becomes three homogeneous equations in the constants A, B and C.

$$\left.\begin{aligned} (\lambda_{11} - \Delta) A + \lambda_{12} B + \lambda_{13} C &= 0 \\ \lambda_{21} A + (\lambda_{22} - \Delta) B + \lambda_{23} C &= 0 \\ \lambda_{31} A + \lambda_{32} B + (\lambda_{33} - \Delta) C &= 0 \end{aligned}\right\} \qquad [14]$$

where

$$\Delta = \rho h_m \omega^2$$

and ρh_m is the mass per unit area of the middle surface of the shell. The λ_{ij}, given in terms of known quantities, are as follows.

$$\left.\begin{aligned}
\lambda_{11} &= (n^2 h_s/a^2 C_{66}) - C_{22}(\alpha^2 h_s/C^*) \\
\lambda_{22} &= (-h_s C_{11} n^2/a^2 C^*) - (h_b^3 S_{11} n^2/12 S^* a^4) \\
&\qquad + (h_s \alpha^2/C_{66}) + (h_b^3 \alpha^2/3 S_{66} a^2) \\
\lambda_{33} &= (-h_s C_{11}/C^* a^2) - (h_b^3 S_{22} \alpha^4/12 S^*) - (h_b^3 S_{11} n^4/12 S^* a^4) \\
&\qquad + (h_b^3 \alpha^2 n^2 S_{12}/6 S^* a^2) + (h_b^3/3)(n^2 \alpha^2/S_{66} a^2) \\
\lambda_{12} &= -[(\alpha C_{12} n h_s/a C^*) + (n \alpha h_s/a C_{66})] \\
\lambda_{13} &= (h_s \alpha C_{12}/a C^*) \\
\lambda_{23} &= (h_s C_{11} n/a^2 C^*) + (h_b^3 S_{11} n^3/12 S^* a^4) \\
&\qquad - (h_b^3 n \alpha^2 S_{12}/12 S^* a^2) - (h_b^3 n \alpha^2/3 S_{66} a^2)
\end{aligned}\right\} \quad [15]$$

where $\lambda_{ij} = \lambda_{ji}$ and $\alpha = (m\pi/\ell)$.

The non-trivial solution of determinant 14 yields

$$\Delta^3 - K_2' \Delta^2 + K_1' \Delta - K_0' = 0 \qquad [16]$$

where

$$K_2' = \lambda_{11} + \lambda_{22} + \lambda_{33}$$

$$K_1' = -\lambda_{12}^2 - \lambda_{13}^2 - \lambda_{23}^2 + \lambda_{11}\lambda_{22} + \lambda_{11}\lambda_{33} + \lambda_{22}\lambda_{33}$$

and

$$K_0' = \lambda_{11}\lambda_{22}\lambda_{33} - \lambda_{11}\lambda_{23}^2 - \lambda_{22}\lambda_{13}^2 - \lambda_{33}\lambda_{12}^2 + 2\lambda_{12}\lambda_{23}\lambda_{31}$$

It can be seen that Equation 16 is sixth-order in ω. The three roots of frequency Equation 16 represent longitudinal, shear, and flexural vibrations. The flexural vibrations will be investigated in the following paragraphs.

6.4.2.1 Vibration Experiments and Results. All of the shells were constructed with aluminum. The vibration experiments were performed on three types of shells as shown in Figure 90. Figure 91 presents a general idea of the dimensions of the models. The paper gives a detailed description of the test apparatus. Flexural vibrations were excited by an electromagnet, for which it was necessary to cement a small piece of iron to the surface of the shell. The magnet is mounted on a horizontal track and its position is adjustable. The magnet is excited from an audio-oscillator which feeds through a resonant-type RC circuit to increase the driving force. To associate the frequency with the appropriate mode shape, a capacitive pickup was constructed and used. The electrical output from the pickup is fed through a preamplifier and into the screen of an oscilloscope. The frequencies were also checked by a small crystal-type pickup. The calculated frequencies of the flexural vibrations, along with the experimentally determined frequencies, are shown in Tables 10 and 11.

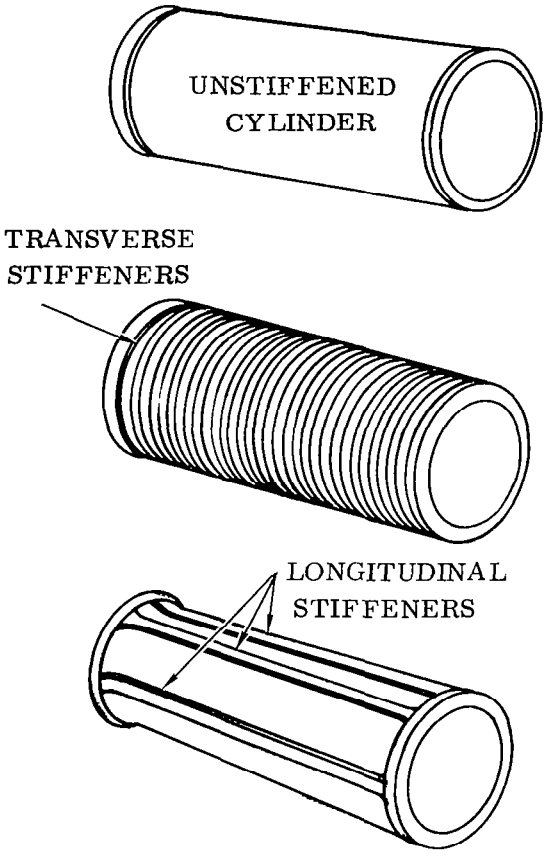

Figure 90. Experimental Cylindrical Shells

Table 12 shows the computed frequencies of the isotropic case along with the experimental results. The frequencies of the isotropic case can be obtained by substitution of Equation 435 (isotropic constants) into Equations 15 and 16 of the reference paper. For all three tables the upper figure in each

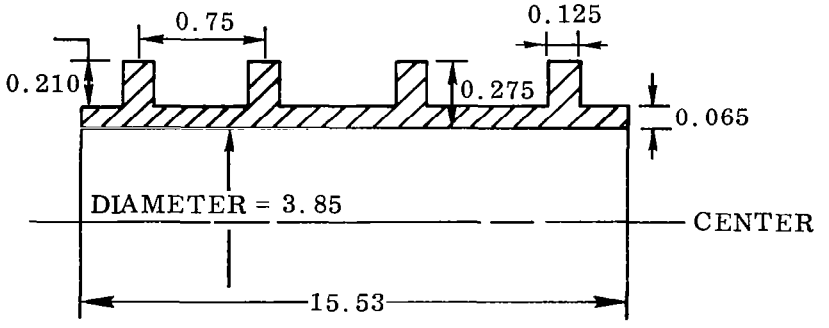

Figure 91. Dimensions of the Experimental Model

Table 10. Frequency of Flexural Vibration of Cylinder With Parallel Ring Stiffeners (Hz)

n \ m	1	2	3	4	5
2	1530 1530	2100 2040	3330 3200	4860 4440	6480 6200
3	4230 4080	4320 4090	4500 4520	5040 5000	5760 5700
4	8100	8100	8190 7520	8280 7800	 7920
5	13, 050	13, 100	13, 140	13, 230 11, 400	

Note: Upper figure in each box is calculated frequency. (Also Tables 8,9)
Lower figure in each box is experimental frequency. (Also Tables 8,9)

Table 11. Frequency of Flexural Vibration of Cylinder With Parallel Longitudinal Stiffeners (Hz)

n \ m	1	2	3	4	5
2	750 700	2300	4200	6100	7900
3	1150 1270	1700 1830	2870 2640	4360 5490	5900 6100
4	2100 2200	2350 2600	2970 3360	3960 4100	5100 5200
5	3340 3460	3510 4080	3900 4120	4620 5130	5600 6100

Table 12. Frequency of Flexural Vibration of Cylindrical Shell of Constant Thickness Without Stiffeners (Hz)

n \ m	1	2	3	4
2	743 742	2120 1880	4020	5780
3	1300 1330	1720 1740	2650 2470	3970
4	2430 2480	2570 2680	2950 3040	3590 3710
5	3900 4060	4000 4120	4200 4340	4550 4780

box is the calculated frequency, and the lower figure in each box is the experimental frequency. The maximum discrepancies are approximately 10 percent for the unstiffened shell, 20 percent for the shell with longitudinal stiffeners, and 18 percent for the shell with circular stiffeners. Furthermore, except for very few cases, the discrepancies are less than 5 percent.

Reference 16 discussed an interesting phenomenon — that in a certain range the more complex modal patterns were associated with lower frequencies of vibration. This phenomenon has recently been called the Arnold-Warburton effect and was also discovered in the orthotropic case by Hoppmann.

Specifically, it may be noted that in Table 7 for m/n given by 5/2, the frequency is 6200 Hz, whereas for m/n given by 5/3 the frequency is only 5700 Hz. This effect is also verified by the corresponding calculated frequencies as 6480 Hz versus 5760 Hz. Similar effects can also be noted in Table 8. It is also interesting to discuss the excitability of modes of vibration. For the shell without stiffeners the experimentally determined frequencies can be excited for all sets of values m/n. Those few frequencies missing from Table 9 are omitted simply because they were not tried. In Table 7, however, frequencies could not be excited for increasing n; while, as shown in Table 8, the frequencies could not be excited for increasing m. This phenomenon may be explained by a possible bias in the excitability of the modes of vibration for such stiffened shells.

6.4.3 CONCLUSIONS. The paper presents an interesting comparison between theory and test results. Professor Hoppmann was able to show the Arnold-Warburton effect in the orthotropic case and a bias of the excitability of the modes of vibration for such shells.

The disadvantage of the theory can be seen in the applicability of other types of edge conditions.

6.5 A REVIEW OF PENZES' PAPER: "THE EFFECT OF BOUNDARY CONDITIONS ON FLEXURAL VIBRATIONS OF THIN ORTHOGONALLY STIFFENED CYLINDRICAL SHELLS" (REFERENCE 19)

6.5.1 SUMMARY. The paper presents a theoretical study of the flexural vibration of orthogonally stiffened thin cylindrical shells with the following edge conditions:

a. Both edges clamped.

b. One edge clamped and the other simply supported.

c. Both edges simply supported.

W. H. Hoppmann II published a paper in 1958 entitled "Some Characteristics of the Flexural Vibrations of Orthogonally Stiffened Cylindrical Shells" (Reference 18). His

paper treated the problem of simply supported edge conditions. The present work generalizes this problem for the edge conditions mentioned above.

Hoppmann's orthotropic-shell theory was used to derive the orthotropic stress-strain law in the author's paper (References 17 and 18). However, the derivation of the frequency equations is different. Hoppmann's approach was to use an energy method (i.e., Lagrangian equations of motion) to derive the frequency equations. The author derived the equations of motion of the orthotropic cylindrical shell by the equilibrium conditions of the shell element. These three differential equations reduced in the isotropic case to the Donnell type of differential equations.

The three differential equations were rearranged in a manner similar to that for the isotropic case (Reference 14), and the combinations of these equations uncoupled the equations. The longitudinal displacement, u, and the tangential displacement, v, were expressed in terms of the normal displacement, w, by two differential equations. A third differential equation was also derived in terms of normal displacement, w.

The general solution was obtained which satisfies these differential equations and contains the undetermined characteristic value, λ_i. The substitution of the general solution in the differential equations leads to three homogeneous equations which are eighth-order in the characteristic value of λ_i. After some simplifications the equations were reduced to a fourth-order system in λ_i. This set of equations, coupled with the boundary conditions, is sufficient to determine the characteristic frequencies and mode shapes of the system.

A comparison of Hoppmann's theory and test results with the theory presented here, for the case of both edges simply supported, shows approximately the same degree of error. Test results for other edge conditions are nonexistent.

The edge conditions have a significant effect on the modal characteristics of a cylinder with strong longitudinal stiffeners, but the effect is relatively small for cylinders with transverse stiffeners.

The computations showed that the cylinder with longitudinal stiffeners in a clamped-simply supported edge condition, compared with both edges simply supported, showed a frequency increase of 37 percent for the lowest mode and that the percentage difference gradually decreased for the higher modes. A comparison of the clamped-clamped edge condition and the both-edges-simply-supported condition showed a frequency increase of 89 percent for the lowest mode and that the percentage difference again gradually decreased with the higher modes.

The peculiar dip in the frequency spectrum, which was discovered by Arnold and Warburton for isotropic shells, is also shown to exist with different edge conditions for stiffened shells (Reference 16).

6.5.2 EXPLANATIONS OF THE THEORY AND TEST RESULTS. Hoppmann's orthotropic stress-strain laws were utilized in the derivations, and his nomenclature and notation were also used (Reference 18). The differential equations of motion were formulated for the shell element on the basis of Donnell's assumptions. The detailed derivation of Equations 1, 2 and 3 of this paper can be performed based on Equations 421 through 434 and Equations 387 and 389 of this monograph. The rearrangement and combination of these equations led to uncoupling them, as done in the isotropic case (Reference 14, Equations 6, 7 and 9).

$$L_4(u) + \frac{c_{12}}{a}\frac{\partial^3 w}{\partial x^3} + \frac{c_{11}}{a^3}\frac{\partial^3 w}{\partial x\,\partial\varphi^2} = \frac{A}{C^*}\frac{\partial^2}{\partial t^2}\left[L_t(u) - \frac{c_{12}\,c_{66}}{a}\frac{\partial w}{\partial x}\right] \qquad [1]$$

$$L_4(v) - \frac{(c_{66}+c_{12})}{a^2}\frac{\partial^3 w}{\partial x^2\partial\varphi} - \frac{c_{11}}{a^4}\frac{\partial^3 w}{\partial\varphi^3} = \frac{A}{C^*}\frac{\partial^2}{\partial t^2}\left[L_t(v) - \frac{c_{11}\,c_{66}}{a^2}\frac{\partial w}{\partial\varphi}\right] \qquad [2]$$

$$B\,L_8(w) + \frac{C^*}{a^2}\frac{\partial^4 w}{\partial x^4} = -\frac{A}{C^*}\frac{\partial^2}{\partial t^2}\left\{A\,c_{66}\frac{\partial^2}{\partial t^2}L_{t,B}(w) + C^*\,L_4(w) - L_2[L_{t,B}(w)] + \frac{c_{12}^2\,c_{66}}{a^2}\frac{\partial^2 w}{\partial x^2} + \frac{c_{11}^2\,c_{66}}{a^4}\frac{\partial^2 w}{\partial\varphi^2}\right\} \qquad [3]$$

The following constants and differential operators were introduced in the previous equations.

$$A = \frac{(\rho h_m)}{h_s}C^* \qquad B = \frac{h_b^3\,C^*}{12\,h_s} \qquad [4]$$

$$L_2(\,) = (C^* + c_{22}\,c_{66})\frac{\partial^2(\,)}{\partial x^2} + \frac{(C^* + c_{11}\,c_{66})}{a^2}\frac{\partial^2(\,)}{\partial\varphi^2}$$

and

$$L_t(\,) = L_2(\,) - A\,c_{66}\frac{\partial^2(\,)}{\partial t^2}$$

$$L_4(\,) = c_{22}\frac{\partial^4(\,)}{\partial x^4} + \frac{(c_{66} + 2\,c_{12})}{a^2}\frac{\partial^4(\,)}{\partial x^2\,\partial\varphi^2} + \frac{c_{11}}{a^4}\frac{\partial^4(\,)}{\partial\varphi^4} \qquad [5]$$

$$L_{4,B}(\,) = \left[\frac{s_{22}}{S^*}\frac{\partial^4(\,)}{\partial x^4} + \frac{2}{a^2}\left(\frac{1}{s_{66}} - \frac{s_{12}}{S^*}\right)\frac{\partial^4(\,)}{\partial x^2\,\partial\varphi^2} + \frac{s_{11}}{a^4 S^*}\frac{\partial^4(\,)}{\partial\varphi^4}\right]$$

$$L_8( ) = L_4 [L_{4,B}( )]$$

and

$$L_{t,B} = A \frac{\partial^2 ( )}{\partial t^2} + B L_{4,B}( ) + \frac{c_{11}}{a^2}$$

The general solution of Equations 1, 2 and 3 may be expressed in the same form that Yi - Yuan Yu formulated in the isotropic case (Reference 14, Equation 10).

$$\left.\begin{aligned} u &= \sum_i A_i e^{\lambda_i x/\ell} \cos m\varphi \sin \omega t \\ v &= \sum_i B_i e^{\lambda_i x/\ell} \sin m\varphi \sin \omega t \\ w &= \sum_i C_i e^{\lambda_i x/\ell} \cos m\varphi \sin \omega t \end{aligned}\right\} \quad (i = 1, 2 \ldots . 8) \qquad [6]$$

where

ℓ is the length of the cylinder

m is an arbitrarily chosen positive integer equal to the number of circumferential waves

λ_i are the characteristic values of the eigenfunctions

and

A_i, B_i and C_i are constant coefficients

The substitution of Equation 6 into Equations 1, 2 and 3 leads to lengthy expressions which can be solved by numerical techniques (Reference 15). In the following discussion the general solution is restricted to relatively long cylinders with a fairly small number of longitudinal waves and a relatively large number of circumferential waves. In these cases the following assumptions may be made

$$(\ldots) \frac{|\lambda_i^2| a^2}{m^2 \ell^2} \ll 1 \qquad [7]$$

The expression in parentheses represents some combination of the orthotropic constants. The use of the absolute value for λ_i indicates that it may be imaginary. Inequality 7 is the generalized expression of the isotropic case, which was discussed in Reference 14, Equation 14. The introduction of Inequality 7 into Equations 1 and 2 simplifies these equations significantly.

$$A_i = \left(\frac{a}{\ell}\right) D \lambda_i C_i \qquad \text{and} \qquad B_i = F C_i \qquad [8]$$

where

$$\left.\begin{aligned} D &= \frac{1}{N}\left(\frac{c_{11} m^2}{a^4} - \frac{A}{C^*}\frac{c_{12} c_{66}}{a^2}\omega^2\right) \\ F &= \frac{c_{11} m}{N a^2}\left(\frac{m^2}{a^2} - \frac{A}{C^*} c_{66}\omega^2\right) \\ N &= A^2 \frac{c_{66}}{C^*}\omega^2 - \frac{A(C^* + c_{11} c_{66})}{a^2 C^*} m^2 \omega^2 + \frac{c_{11}}{a^4} m^4 \end{aligned}\right\} \qquad [9]$$

and

Inequality 7 introduced into Equation 3 leads to a simplified frequency equation.

$$\frac{C^{*2}}{a^2}\left(\frac{\lambda_i}{\ell}\right)^4 = A^3 c_{66}\omega^6 - A^2\left(T m^2 + \frac{c_{66} c_{11}}{a^2} + H c_{66} m^4\right)\omega^4$$

$$+ A\left[\frac{c_{11} C^* m^4}{a^4} + \left(\frac{c_{11}}{a^2} + H m^4\right) T m^2 - \frac{c_{11}^2 c_{66}}{a^4} m^2\right]\omega^2 - \frac{H c_{11} C^*}{a^4} m^8 \qquad [10]$$

where

$$H = \frac{h_b^3 C^* s_{11}}{12 h_s a^4 S^*} \qquad \text{and} \qquad T = \frac{(C^* + c_{11} c_{66})}{a^2} \qquad [11]$$

The characteristic value of λ_i and the coefficients C_i can now be evaluated from the boundary conditions as was done in the isotropic case (Reference 14). The displacement components now contain only four constants due to the simplifications introduced by Inequality 7; since Equation 10 is now of the fourth degree, there will be only four roots of λ_i and four sets of values for A_i, B_i and C_i. The displacement components are

$$u = a D \frac{\partial w}{\partial x}, \qquad v = -\frac{F}{m}\frac{\partial w}{\partial \varphi} \qquad [12]$$

$$w = \sum_{i=1}^{4} C_i e^{\lambda_i x/\ell} \cos m\varphi \sin \omega t \qquad [13]$$

The roots of λ_i are expressed as

$$\lambda_1 = -\lambda_2 = R \qquad \lambda_3 = -\lambda_4 = iR \qquad [14]$$

where R is a real number.

In the expression for bending moment 15, the term $\frac{1}{a^2}\frac{\partial v}{\partial \varphi}$ was omitted to satisfy the boundary conditions with the available constants.

$$M_x = -\frac{h_b^3}{12\,S^*}\left(s_{22}\frac{\partial^2 w}{\partial x^2} - \frac{s_{12}}{a^2}\frac{\partial^2 w}{\partial \varphi^2}\right) \qquad [15]$$

It is assumed that the simply supported shell can move freely in the longitudinal direction and remains circular at the supports. The boundary conditions for this case are

$$v = w = M_x = 0 \qquad [16]$$

at

$$x = 0 \text{ or } \ell \text{ or both}$$

The clamped edge condition may be written in the form

$$u = v = w = \frac{\partial w}{\partial x} = 0 \qquad [17]$$

at

$$x = 0 \text{ or } \ell \text{ or both}$$

The following three boundary conditions were considered: clamped-clamped, clamped-simply supported, and both edges simply supported. The characteristic values of R may be expressed from the boundary conditions as

$$R = n\pi \qquad [18]$$

where the different values of n can be seen in Table 10.

If the displacement functions are substituted into any of the previously described boundary conditions, the derivations lead to a homogeneous equation system in C_i. The value of n can be evaluated, taking the determinant of the homogeneous equation system equal to zero. The displacement functions were derived from any three equations of the boundary conditions. This leads to the same derivations as Equations 19 through 30 of Reference 14. The displacement functions are exact in the case of both edges simply supported, and the solutions are only approximate in the cases of clamped-simply supported and both edges clamped (Reference 22). The frequencies of the longitudinally stiffened cylinder of Reference 18 were calculated and the effect of different edge conditions was investigated according to Table 13. The bottom number in each box corresponds to the case of both edges simply supported, the middle number to the clamped-simply supported case, and the upper number to the case of both edges clamped. Due to the approximations involved in the theory, some of the frequencies

Table 13. Frequencies (in Hz) for the Longitudinally Stiffened Cylinder of Reference 18 With Different Edge Conditions

m \ n	1.506 1.25 1.00	2.50 2.25 2.00	3.50 3.25 3.00	4.50 4.25 4.00	5.50 5.25 5.00
2	1579 1149 836	4233 3412 2698	9171 7557 6267	— — —	— — —
3	1422 1328 1276	2298 1197 1750	4019 3514 3059	6552 5838 5178	— — —
4	2284 2265 2255	2509 2422 2358	3135 2932 2762	4264 3934 3636	5891 5439 5016
5	3560 3555 3552	3623 3598 3580	3821 3754 3699	4251 4117 4002	4984 4770 4577

were not computed in Table 13; however, these frequencies are also missing from Professor Hoppmann's test results, Reference 18, Table 11.

6.5.3 CONCLUSIONS. The significant effects of different edge conditions on longitudinally stiffened cylinders have been exhibited. The present theory is recommended for cases in which the length-to-radius ratio is greater than or equal to 4, because of the approximations applied in the development of simplified frequency equations.

7/VARIATIONAL METHODS IN THE THEORY OF THIN ELASTIC SHELLS

So far, our investigations have been restricted to simple geometries, where the solutions of the governing partial differential equations lead to a closed-form solution of the problem in terms of some known functions. The presently developed theories can be extended to any geometry; however, the mathematical treatment of the problems becomes more difficult and only approximate solutions can be developed. Since the variational methods have to be applied for partial differential equations, or for other cases of ordinary differential equations with variable coefficients, some of the important principles of the variational methods related to these problems will be discussed. One of the direct methods is developed by Ritz, another formulated by Galerkin. The purpose of the following discussion is to explain the restrictions of these methods.

7.1 VARIATIONAL PROBLEMS CONNECTED WITH DIFFERENTIAL EQUATIONS

Let us consider first the following ordinary differential equation.

$$\frac{d}{dx}\left[p(x)\frac{dy}{dx}\right] - q(x)\,y - f(x) = 0 \tag{447}$$

where the coefficients p and q are the functions of the independent variable x, and where f is also considered as a function of x only. The solution of differential equation 447 can be expressed by

$$y = y(x) \tag{448}$$

Let us show the equivalence of solution 448 with the solution of the minimum of the following integral expression.

$$I = \int_{x_0}^{x_1}\left[p(x)\left(\frac{dy}{dx}\right)^2 + q(x)\,y^2 + 2\,f(x)\,y\right]dx \tag{449}$$

where

$$x_0 \leq x \leq x_1 \tag{450}$$

Let us find the solution y of integral 449, when the expression of the integral is minimum and the curve y(x) passes through the given points (x_0, y_0) and (x_1, y_1). Assume that y(x) is a function giving the integral I a minimum value. Let $\eta(x)$ by any continuous function that is also continuous with its derivatives, vanishing at the ends $\eta(x_0) = \eta(x_1) = 0$. It is assumed that the function $y(x) + \alpha\eta(x)$ satisfies the same

boundary conditions at the ends as $y(x)$, and that α is sufficiently small. The proper value of α leads as close as one pleases to the function $y(x)$. Since $y(x)$ is designated as the solution of the minimum integral I, for $\alpha \neq 0$ (but small), it can be written

$$I(y + \alpha\eta) \geq I(y) \tag{451}$$

Our interest is in the minimum value of the integral I as a function of α with the specified value $\alpha = 0$. Therefore one has

$$\left.\frac{d\, I(y + \alpha\eta)}{d\alpha}\right|_{\alpha=0} = 0 \tag{452}$$

This equation may be expressed in terms of Equation 449 as follows.

$$\frac{d}{d\alpha}\int_{x_0}^{x_1}\left[p(y' + \alpha\eta')^2 + q(y + \alpha\eta)^2 + 2f(y + \alpha\eta)\right]dx\Bigg|_{\alpha=0} = 0 \tag{453}$$

where

$$= \frac{d}{dx} \tag{454}$$

Perform the differentiation and substitute the value $\alpha = 0$ into Equation 453, and one has

$$\frac{d}{d\alpha} I(y + \alpha\eta)_{\alpha=0} = 2\int_{x_0}^{x_1} (py'\eta' + qy\eta + f\eta)\, dx \tag{455}$$

This integral can be written by the customary symbolical notation.

$$\delta I = \left.\frac{d}{d\alpha} I(y + \alpha\eta)\right|_{\alpha=0} = 0 \tag{456}$$

Let us express the first term of Equation 455 in a different form. For this purpose integrate these terms by parts.

$$\int_{x_0}^{x_1} py'\eta'\, dx = (py'\eta)\Big|_{x=x_0}^{x=x_1} - \int_{x_0}^{x_1} \frac{d}{dx}(py')\eta(x)\, dx \tag{457}$$

According to our basic definition the function $\eta(x)$ is zero at the points x_0 and x_1 or

$$\eta(x_0) = \eta(x_1) = 0 \tag{458}$$

Therefore

$$(py'\eta)\Big|_{x=x_0}^{x=x_1} = 0 \tag{459}$$

Equation 457 can be expressed by the substitution of Equation 459 as

$$\int_{x_0}^{x_1} py'\eta'\,dx = -\int_{x_0}^{x_1} \frac{d}{dx}(py')\eta(x)\,dx \tag{460}$$

The substitution of Equation 460 into Equations 455 and 456 yields

$$\delta I = -2\int_{x_0}^{x_1} \left\{\frac{d}{dx}[p(x)\,y'] - qy - f\right\}\eta(x)\,dx = 0 \tag{461}$$

The last integral expression must be equal to zero, whatever the function $\eta(x)$ satisfying the conditions indicated above. This condition is possible only if the function $y(x)$ satisfies the differential equation:

$$\frac{d}{dx}(py') - qy - f = 0 \tag{462}$$

Figure 92 illustrates the previous theory.

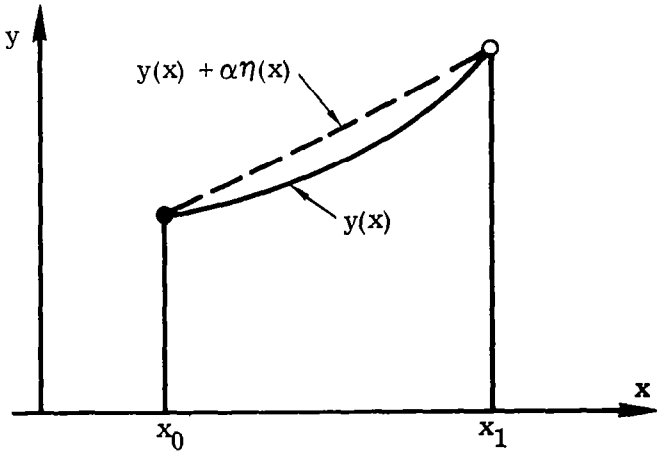

Figure 92. Concept of Variational Integral

It can be proved according to Reference 21, page 243, that the integral 449 is an absolute extremum requiring the following conditions.

$$p(x) > 0 \qquad q(x) \geq 0 \tag{463}$$

for

$$x_0 \leq x \leq x_1$$

The satisfaction of Condition 463 leads to the uniqueness and exactness of the solution $y(x)$. (For further information see Reference 21, page 244.)

It is also useful to note that any linear differential equation of the second order is the Euler equation

for some integral type (Equation 449). For this reason it is sufficient to show that such an equation can always be reduced to the form of Equation 462. To show this, consider the equation

$$py'' + ry' - qy = f \tag{464}$$

Multiply Equation 464 by $e^{\int \frac{r-p'}{p} dx}$ and it can be calculated easily that

$$pe^{\int \frac{r-p'}{p} dx} y'' + re^{\int \frac{r-p'}{p} dx} = \frac{d}{dx}\left[pe^{\int \frac{r-p'}{p} dx} y'\right] \tag{465}$$

The form of Equation 465, after the multiplication, is

$$\frac{d}{dx}\left(pe^{\int \frac{r-p'}{p} dx} y'\right) - qe^{\int \frac{r-p'}{p} dx} y = fe^{\int \frac{r-p'}{p} dx} \tag{466}$$

This last equation may be written in the form of Equation 462.

$$\frac{d}{dx}(p^*y') - q^*y = f^* \tag{467}$$

where

$$\left.\begin{aligned} p^*(x) &= p(x) \cdot e^{\int \frac{r-p'}{p} dx} \\ q^*(x) &= q(x) \cdot e^{\int \frac{r-p'}{p} dx} \\ f^*(x) &= f(x) \cdot e^{\int \frac{r-p'}{p} dx} \end{aligned}\right\} \tag{468}$$

It is therefore proved that Equation 467 is in the form of Equation 462.

7.2 RITZ'S METHOD

One of the approximate techniques to solve differential equations is the Ritz method. Application of the method will be shown by the solution of the previously discussed self-adjoint differential equation.

$$L(y) = \frac{d}{dx}(py') - qy - f = 0 \tag{469}$$

under the conditions that

$$y(x_0) = y_0 \qquad \text{and} \qquad y(x_1) = y_1 \tag{470}$$

It is also assumed that the previously stated condition is valid, as follows.

$$p(x) > 0 \qquad q(x) \geq 0 \qquad \text{for} \qquad x_0 \leq x \leq x_1 \tag{463}$$

The solution of the differential equation 469 is the same as the solution of the minimum integral, as it was already proved previously. (For further information see Equations 449 through 462.)

$$I(y) = \int_{x_0}^{x_1} \left[(p y'^2 + q y^2 + 2fy)\right] dx \tag{449}$$

For mathematical convenience, let us assume that the end conditions are homogeneous.

$$y(0) = y(\ell) = 0 \tag{471}$$

If this is not the case, it can be contrived by introducing for y in Equation 469 a new unknown z defined by

$$y = z + \frac{x}{\ell} y_1 + \frac{(\ell - x)}{\ell} y_0 \tag{472}$$

It is now assumed that the approximate solution may be expressed in a form

$$y_n = \sum_{k=1}^{N} a_k \varphi_k(x) \tag{473}$$

where the functions of $\varphi_k(x)$ satisfy the prescribed boundary conditions and the value N expresses the number of terms in the series. The substitution of Equation 473 into Equation 449 leads to

$$I(y_n) = \int_0^{\ell} (p y_n'^2 + q y_n^2 + 2f y_n) dx = \int_0^{\ell} \left[p(\Sigma a_k \varphi_k')^2 + q(\Sigma a_k \varphi_k)^2 + 2f \Sigma a_k \varphi_k\right] dx = \sum_{k,s=1}^{N} A_{k,s} a_k a_s + 2 \sum_{k=1}^{N} B_k a_k \tag{474}$$

where

$$A_{k,s} = A_{s,k} = \int_0^{\ell} (p \varphi_k' \varphi_s' + q \varphi_k \varphi_s) dx \qquad \text{and} \qquad B_k = \int_0^{\ell} f \varphi_k \, dx \ldots . \tag{475}$$

Differentiate expression 474 with respect to a_s, and one has, in two forms,

$$\frac{1}{2}\frac{\partial I(y_n)}{\partial a_s} = \int_0^{\ell} (p y_n' \varphi_s' + q y_n \varphi_s + f\varphi_s)\, dx = 0 \tag{476}$$

where

$$s = 1,2 \ldots N$$

or

$$\sum_{k=1}^{N} (A_{k,s}\, a_k + B_s) = 0 \tag{477}$$

where

$$s = 1,2 \ldots N$$

In the case of free vibration problems the function $f \equiv 0$ and therefore $B_s \equiv 0$. In this case the Ritz method yields to the following equation.

$$\sum_{k=1}^{N} A_{k,s}\, a_k = 0 \tag{478}$$

where

$$s,k = 1,2 \ldots N$$

Equation 478 represents a homogeneous equation system, and the nontrivial solution of this system requires that the determinant of the system be zero.

$$\det|A_{k,s}| = 0 \tag{479}$$

The unknown frequencies can be calculated from determinant 479.

The application of Ritz's method is restricted to the condition 463, which cannot be satisfied in some problems.

7.3 GALERKIN'S METHOD

Another approximate technique has been developed by B. G. Galerkin. His method has some advantages over Ritz's method for certain problems. Let the previously mentioned differential Equation 469 serve as an example. Let us integrate the first term of Equation 476 by parts, using the fact that φ_k and y_n are equal to zero at the ends.

$$\int_0^{\ell} p y_n' \varphi_s'\, dx = \left[p y_n' \varphi_s\right]_0^{\ell} - \int_0^{\ell} \frac{d}{dx}(p y_n')\varphi_s\, dx = -\int_0^{\ell} \frac{d}{dx}(p y_n')\varphi_s\, dx \tag{480}$$

since

$$\left[py_n'\varphi_s\right]_0^{\ell} = 0$$

The replacement of the first term in Equation 476 by expression 480 and utilizing the brief notation of Equation 469, equation system 477 is expressed in a simple form.

$$\int_0^{\ell}\left[\frac{d}{dx}(py_n') - qy_n - f\right]\varphi_s\,dx = \int_0^{\ell} L(y_n)\varphi_s\,dx = 0 \tag{481}$$

where

$$s = 1,2 \ldots N$$

Galerkin's method can be formulated by Equation 481. The transformation of equation system 477 into Equation 481 given above shows that in application to the given problem the methods of Ritz and Galerkin lead to one and the same approximate solution, although the method of Galerkin makes possible the simpler and more direct setting-up of the respective system. However, the fundamental advantage of the method of Galerkin is that in applying it, one does not use the connection between the given boundary problem and the variational problem. It can therefore be employed in the case of any equation of second order. It does not require the preliminary reduction of the equation to self-adjoint form, nor necessarily the satisfaction of Condition 463, either.

The previous ideas can be extended to two variables. Let us investigate the solution of the following equation.

$$L(u) = 0 \tag{482}$$

where L is some differential operator in two variables, the solution of which satisfies homogeneous boundary conditions. Let us assume that the approximate solution can be expressed in the following form.

$$\bar{u}(x,y) = \sum_{i=1}^{N} C_i\varphi_i(x,y) \tag{483}$$

where $\varphi_i(x,y)$ is a certain system of functions, chosen beforehand, satisfying the same boundary conditions and where C_i are undetermined coefficients. The functions $\varphi_i(x,y)$ are considered to be linearly independent and to represent the first N functions of some system of functions that is complete in the given region. In order that $\bar{u}(x,y)$ be an exact solution of the given equation, it is required that $L(\bar{u})$ be identically equal to zero; this is equivalent to the requirement of the orthogonality of Expression $L(\bar{u})$ to all the functions of the system φ_i ($i = 1, \ldots N \ldots$). However, having only N constants $C_1, C_2, \ldots, C_N$ satisfies only N conditions of orthogonality. Stating the problem in terms of mathematics,

$$\iint_A L[\bar{u}(x,y)]\varphi_i(x,y)\,dx\,dy = \iint_A L\left[\sum_{j=1}^{N} C_j\varphi_i(x,y)\right]\varphi_i(x,y)\,dx\,dy \tag{484}$$

where

$$i,j = 1,2, \ldots, N$$

which serves to determine the coefficients C_i.

It can be stated that Galerkin's technique has no connection in general with variational problems. This is therefore a perfect universally applicable method.

7.4 GALERKIN'S METHOD APPLIED FOR EIGENVALUE PROBLEMS

Let us assume the following differential equation.

$$L(y) = \frac{d}{dx}[p(x)\,y'] - qy + \lambda y = 0 \tag{485}$$

with the following boundary conditions

$$y(0) = y(\ell) = 0 \tag{486}$$

It is also assumed that the expression λ is the function of the unknown angular frequencies.

$$\lambda = \lambda(\omega_n) \tag{487}$$

Let us assume that the solution can be expressed as

$$y_n = \sum_{k=1}^{N} a_k\varphi_k(x) \tag{488}$$

where φ_i is a complete system of functions that satisfy conditions 486. It is assumed that instead of identical satisfaction of Equation 485 only the orthogonality of the left side will be satisfied for functions $\varphi_1, \ldots, \varphi_N$. This assumption leads to the following equation.

$$\int_0^{\ell} L(y_n)\varphi_j\,dx = \int_0^{\ell}\left\{\frac{d}{dx}[p(x)\,y_n'] - q(x)\,y_n + \lambda y_n\right\}\varphi_j\,dx = 0 \tag{489}$$

where

$$j = 1,2, \ldots, N$$

The substitution of Equation 488 into Equation 489 yields

$$\sum_{i=1}^{N}(\alpha_{i,j} + \lambda\gamma_{i,j})\,a_i = 0 \tag{490}$$

where

$$i,j = 1, 2, \ldots, N$$

and

$$\left.\begin{aligned}\alpha_{i,j} &= \int_0^{\ell}\left\{\frac{d}{dx}[p(x)\varphi_i'] - q(x)\varphi_i\right\}\varphi_j\,dx \\ \gamma_{i,j} &= \int_0^{\ell}\varphi_i\varphi_j\,dx\end{aligned}\right\} \tag{491}$$

Equation system 490 can also be written in another form.

$$\sum_{i=1}^{N}A_{i,j}\,a_i = 0 \tag{492}$$

where

$$A_{i,j} = (\alpha_{i,j} + \lambda\gamma_{i,j}) \tag{493}$$

The system of Equation 492 is a homogeneous system of N equations in N unknowns. It has a nontrivial solution only when the determinant of this system equals zero.

$$D = \begin{vmatrix}(\alpha_{1,1} + \lambda\gamma_{1,1}) & \cdots & (\alpha_{n,1} + \lambda\gamma_{n,2}) \\ \vdots & & \\ (\alpha_{1,n} + \lambda\gamma_{1,n}) & \cdots & (\alpha_{n,n} + \lambda\gamma_{n,n})\end{vmatrix} = 0 \tag{494}$$

The unknown frequencies can be evaluated from determinant 494 as $\lambda_1, \lambda_2 \ldots \lambda_N$. For each $\lambda = \lambda_m$ systems of equations, Equation 492 will have a nonzero solution $a_i^{(m)}$, which will give us the function that corresponds to

$$y_m(x) = \sum_{i=1}^{N}a_i\varphi_i(x)$$

It is understood that these functions are determinate only to an arbitrary constant or accurate to a factor.

The unknown coefficients a_i can be now calculated from equation system 492.

$$\left.\begin{aligned} A_{1,1}a_1 + A_{2,1}a_2 + \ldots + A_{n,1}a_n &= 0 \\ A_{1,2}a_1 + A_{2,2}a_2 + \ldots + A_{n,2}a_n &= 0 \\ &\vdots \\ A_{1,n}a_1 + A_{2,n}a_2 + \ldots + A_{n,n}a_n &= 0 \end{aligned}\right\} \qquad (495)$$

where expressions $A_{1,n}, \ldots, A_{n,n}$ were calculated by a specified frequency $\lambda_m = \lambda(\omega_m)$.

7.5 A REVIEW OF PENZES' AND BURGIN'S PAPER: "FREE VIBRATIONS OF THIN ISOTROPIC OBLATE-SPHEROIDAL SHELLS" (REFERENCE 20)

7.5.1 SUMMARY. The theory of free vibration of thin isotropic, elastic shells has been developed by Love. He found that the characteristic mode shapes for spherical shells are described by associated Legendre functions.

Hoppmann discussed both free and forced vibrations of a thin elastic, orthotropic spherical shell, which is the general case of Love's spherical-shell problem. Baker conducted experimental studies on a spherical shell and showed the physical existence of the two sets of frequencies that were first theoretically predicted by Lamb (Reference 13).

There exists extensive literature on free vibrations of spherical shells, but only a few papers deal with the free vibrations of ellipsoidal shells, and numerical results are lacking.

The problem of the free vibration of a thin isotropic, oblate spheroidal shell has been solved by Galerkin's method. Membrane theory and harmonic axisymmetric motion have been assumed in order to derive the differential equations of motion. This derivation leads to two ordinary differential equations with variable coefficients that can be reduced to one ordinary second-order differential equation with variable coefficients. The resulting eigenvalue problem is solved by Galerkin's method. It is shown that Galerkin's solution for the oblate spheroid yields the exact solution for the sphere as the eccentricity of the oblate spheroid goes to zero. It is also shown that two sets of frequencies exist for the oblate spheroidal shell. After the frequencies are determined, the tangential displacements are obtained as solutions of a homogeneous system of equations.

The normal displacements were calculated based on the known tangential displacements from the second equilibrium equation.

7.5.2 EXPLANATION OF THE THEORY AND THE NUMERICAL RESULTS. Let us assume that the deformation in a vibrating oblate, spheroidal shell is momentless; that is, that membrane-type stresses are of major concern. Let us also assume axi-symmetric vibrations. If we then introduce inertia forces at the surface of the shell, the equations of motion may be written as follows (see Figure 93, Equations 105 and 110).

$$(\partial/\partial\phi)(r_0 N_\phi) - N_\theta r_1 \cos\phi = \rho r_0 r_1 h \frac{\partial^2 v}{\partial t^2} \qquad [1]$$

$$r_0 N_\phi + r_1 \sin\phi N_\theta = \rho r_0 r_1 h(\partial^2 w/\partial t^2) \qquad [2]$$

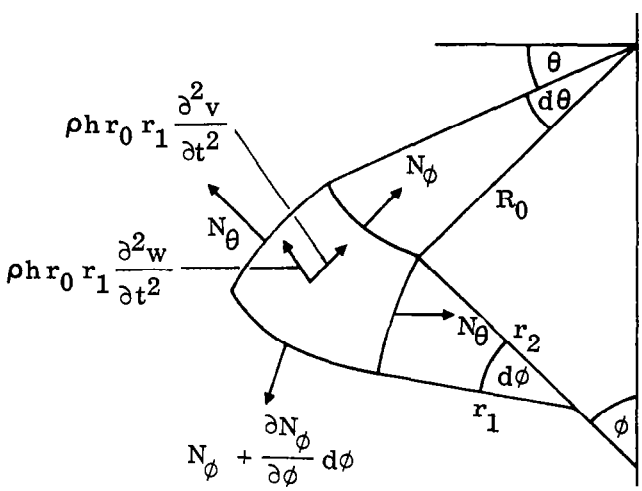

Figure 93. Element of Shell

where ρ is the specific mass density, v is the tangential displacement (tangent to meridian), positive toward north pole, w is the normal displacement, positive toward center, h is the shell thickness,

$$r_0 = r_2 \sin\phi$$

$$r_1 = \frac{(1-e^2)\,a}{(1-e^2\cos^2\phi)^{3/2}} \qquad [3]$$

$$r_2 = \frac{a}{(1-e^2\cos^2\phi)^{1/2}}$$

e is the eccentricity of an oblate spheroid, a is the major axis of an oblate spheroid, and N_ϕ, N_θ equal forces per unit length of the shell.

The detailed calculation of Equation 3 can be seen by Equations 74, 79 and 80.

The forces expressed in terms of strain are from Equations 85 and 89.

$$N_\phi = [E h/(1-\nu^2)](\epsilon_\phi + \nu\epsilon_\theta) \qquad [4]$$

$$N_\theta = [E h/(1-\nu^2)](\epsilon_\theta + \nu\epsilon_\phi) \qquad [5]$$

where E is the modulus of elasticity and ν is Poisson's ratio. The strains in terms of displacements may be written from Equations 140 and 142

$$\epsilon_\phi = (1/r_1)[(\partial v/\partial\phi) - w] \qquad \epsilon_\theta = (1/r_2)(v\cot\phi - w) \qquad [6]$$

Substituting Equations 3 and 6 into Equations 4 and 5 for N_ϕ, N_θ and then substututing the values of N_ϕ, N_θ into Equations 1 and 2, the equations of motion are obtained in terms of displacements as follows.

$$(1 - x^2)^2(1 - e^2x^2)^3(\partial^2 v/\partial x^2) - 2x(1 - x^2)(1 - e^2x^2)^2$$
$$\times [1 + (1 - 2x^2)e^2](\partial v/\partial x) - (1 - e^2x^2)\{\nu + (1 - \nu)x^2$$
$$- [(1 + \nu)x^2 - \nu x^4]e^2(1 - e^2)\}v + (1 - x^2)^{3/2}(1 - e^2x^2)^2$$
$$\times [(1 + \nu) - (\nu + x^2)e^2](\partial w/\partial x) - x(1 - x^2)^{1/2}(1 - e^2x^2)$$
$$\times [4(1 - x^2) - (2x^2 - 3x^4 + 1)e^2]e^2 w$$
$$= A(1 - e^2)^2(1 - x^2)(\partial^2 v/\partial t^2) \qquad [7]$$

and

$$-(1 - x^2)(1 - e^2x^2)^2[\nu(1 - e^2) + (1 - e^2x^2)](\partial v/\partial x)$$
$$+ x(1 - e^2x^2)[\nu(1 - e^2x^2) + (1 - e^2)](1 - e^2)v$$
$$- (1 - x^2)^{1/2}(1 - e^2x^2)[2\nu(1 - e^2)(1 - e^2x^2) + (1 - e^2x^2)^2$$
$$+ (1 - e^2)^2]w = A(1 - e^2)^2(1 - x^2)^{1/2}(\partial^2 w/\partial t^2) \qquad [8]$$

where

$$x = \cos\phi \qquad [9]$$

and

$$A = \rho[(1 - \nu^2)a^2/E] = (1 + \nu)B \qquad [10]$$

In solving the equations of motion (Equations 7 and 8) for a complete shell, it should be noted that there are no physical boundary conditions. The conditions to be imposed are that the displacements should be single-valued and bounded at every point of the oblate spheroid including the north and south poles.

Let us assume separation of variables, and let

$$v(x, t) = v_n(x)\,T_n(t) \qquad w(x, t) = w_n(x)\,T_n(t) \qquad [11]$$

Assuming harmonic motion,

$$d^2 T_n/dt^2 = -p_n^2 T_n \qquad [12]$$

where p_n is the angular frequency of the shell.

Substituting Equations 11 and 12 into Equations 7 and 8, the two partial differential equations were reduced to two ordinary differential equations with variable coefficients.

Equation 8 may be expressed in the following form

$$w_n = \left[-\alpha(x)\frac{dv_n}{dx} + \beta(x)\, v_n\right]/\gamma(x) \qquad [13]$$

where

$$\alpha(x) = (1 - x^2)(1 - e^2x^2)^2[\nu(1 - e^2) + (1 - e^2x^2)] \qquad [14]$$

$$\beta(x) = x(1 - e^2x^2)(1 - e^2)[\nu(1 - e^2x^2) + (1 - e^2)] \qquad [15]$$

$$\gamma(x) = (1 - x^2)^{1/2}\Big\{(1 - e^2x^2)[2\nu(1 - e^2)(1 - e^2x^2) + (1 - e^2x^2)^2 + (1 - e^2)^2] - A(1 - e^2)^2 p_n^2\Big\} \qquad [16]$$

The substituion of w_n into Equation 7 yields an ordinary differential equation for v_n as follows.

$$E_1(x)(d^2v_n/dx^2) - E_2(x)(dv_n/dx) + E_3(x)\, v_n = 0 \qquad [17]$$

where

$$E_1 = (1 - x^2)^2(1 - e^2x^2)^3\gamma^2 - (1 - x^2)^{3/2}(1 - e^2x^2)^2[(1 + \nu) - (\nu + x^2)e^2]\alpha\gamma \qquad [18]$$

$$E_2 = 2x(1 - x^2)(1 - e^2x^2)^2[1 + (1 - 2x^2)e^2]\gamma^2 - (1 - x^2)^{3/2}(1 - e^2x^2)^2[(1 + \nu) - (\nu + x^2)e^2] \times [\gamma(\beta - \alpha') + \alpha\gamma'] - x(1 - x^2)^{1/2}(1 - e^2x^2] \times [4(1 - x^2) - (2x^2 - 3x^4 + 1)e^2]e^2\alpha\gamma \qquad [19]$$

and

$$E_3 = A(1 - e^2)^2 p_n^2(1 - x^2)\gamma^2 + (1 - x^2)^{3/2}(1 - e^2x^2)^2 \times [(1 + \nu) - (\nu + x^2)e^2](\beta'\gamma - \beta\gamma') - (1 - e^2)(1 - e^2x^2) \times \Big\{\nu + (1 - \nu)x^2 - [(1 + \nu)x^2 - \nu x^4]e^2\Big\} - x(1 - x^2)^{1/2}(1 - e^2x^2)[4(1 - x^2) - (2x^2 - 3x^4 + 1)e^2]e^2\beta\gamma \qquad [20]$$

where

$$' = (d/dx) \qquad [21]$$

The free vibration of the thin oblate spheroidal shell is reduced by Equation 17 to a second-order differential equation with variable coefficients. Owing to the complexity of the problem, a closed-form analytical solution does not seem to exist. Galerkin's method was applied to solve Equation 17 as one of the most feasible methods to employ for this problem.

The detailed explanation of Galerkin's method can be seen in Section 7.3 and 7.4.

Galerkin's Method. Equation 17 may be expressed by a linear differential operator and the undetermined tangential displacement v_n as follows.

$$L(v_n) = 0 \qquad [22]$$

The linear differential operator can be written in the form

$$L(\,) = E_1(d^2/dx^2)(\,) - E_2(d/dx)(\,) + E_3(\,) \qquad [23]$$

The theory of Section 7.3 and 7.4 was applied for the present problem. The solution was developed based on Equations 482 through 489. The solution of Equation 22 may be expressed in the form

$$\bar{v}_n(x) = \sum_{i=1}^{N} a_i \varphi_i(x) \qquad [24]$$

where the a_i are undetermined coefficients and where $\varphi_i(x)$ is a certain system of functions satisfying the boundary conditions and being the first N functions of a system that is complete within the range $-1 \leqq x \leqq 1$. The condition that $L(\bar{v})$ be identically equal to zero is equivalent to the requirement that the expression $L(\bar{v})$ be orthogonal to all the functions of the system $\varphi_i(x)$, $i = 1, \ldots, N$. We chose as the system $\varphi_i(x)$ the associated Legendre functions of order 1, $[P_i^1(x)]$, since these functions represent the exact analytical solution for the sphere.

The substitution of Equation 24 into 22 yields to the orthogonality condition of the following N linear equations for the undetermined coefficients a_i.

$$\sum_{i=1}^{N} \left\{ \int_{-1}^{+1} L[P_i^1(x)] \cdot P_i^1(x)\,dx \right\} a_i = 0 \qquad [25]$$

where $j = 1, 2, \ldots, N$. Equation 25 can be written in another form.

$$\sum_{i=1}^{N} A_{ij} a_i = 0 \qquad [26]$$

where $j = 1, 2, \ldots, N$, and

$$A_{ij} = \int_{-1}^{+1} L[P_i^1(x)] P_j^1(x)\, dx \qquad [27]$$

The condition for the existence of a nontrivial solution of the system of homogeneous equations (Equation 26) represents the frequency equation for the problem, which can be written in a determinant form.

$$\det(A_{ij}) = 0 \qquad [28]$$

Properties of $\det A_{ij}$

a. Sphere. For the case of thin spherical shell $e = 0$, the differential operator L is reduced to

$$L(\,) = (1 - x^2)(d^2/dx^2)(\,) - 2x(d/dx)(\,) + [\lambda_n - (1/1 - x^2)](\,) \qquad [29]$$

where

$$\lambda_n = [(2 - Bp_n^2)(Ap_n^2 + 1 - \nu)/(1 - \nu - Bp_n^2)] \qquad [30]$$

The determinant can then be written

$$\det[A_{ij}] = \begin{vmatrix} (\lambda_n - 2) & 0 & 0 & \cdots \\ 0 & (\lambda_n - 6) & 0 & \cdots \\ 0 & 0 & (\lambda_n - 12) & \cdots \\ \vdots & \vdots & & \end{vmatrix} = 0 \qquad [31]$$

Equation 31 yields the exact closed-form solution for the thin spherical shell.

b. Oblate Spheroidal Shell. It can be easily shown that, in the expression of A_{ij} according to Equation 27,

$$A_{ij} = \int_{-1}^{1} L[P_i^1(x)] P_j^1(x)\, dx \qquad [32]$$

the integrand is an odd function wherever i+j is odd; and in that case,

$$A_{ij} = 0 \qquad [33]$$

The determinant of the system of homogeneous equations (Equation 26) can be expressed in the following form.

$$\det[A_{ij}(p_n)] = \begin{vmatrix} A_{11}(p_n) & 0 & A_{31}(p_n) & 0 & \cdots \\ 0 & A_{22}(p_n) & 0 & A_{42}(p_n) & \cdots \\ A_{13}(p_n) & 0 & A_{33}(p_n) & 0 & \cdots \\ 0 & A_{24}(p_n) & 0 & A_{44}(p_n) & \cdots \\ \vdots & \vdots & \vdots & \vdots & \end{vmatrix} = 0 \qquad [34]$$

Mode Shapes of Oblate Spheroidal Shell. The tangential mode shape v_n can be obtained from Equation 24 and 26. The even modes can be separated from the odd modes by observing Equation 34. The eigenfrequencies p_n, satisfying Equation 34, were found digitally on an IBM-7094 computer.

For any particular solution p_n, the undetermined coefficients a_i can be determined up to a multiplicative factor. By arbitrarily setting $a_n = 1$, the a_i i=1, 2, ..., (n-1), (n+1), ..., N are uniquely determined.

Numerical Example. For numerical illustration of the theory, a thin oblate-spheroidal shell having the following properties is considered: major axis a = 60 in., minor axis b = 43.5 in., eccentricity e = 0.68874, Poisson's ratio $\nu = 0.28$, modulus of elasticity $E = 2.8 \times 10^7$ lb/in.^{2}, and specific density $\rho = 7.34 \times 10^{-4}$ lb·sec^2/in.^{4}. For comparison, a spherical shell is also considered with radius a = 60 in.

Angular Frequencies. The frequencies of the oblate spheroidal shell are calculated from Equations 27 and 34. The frequencies of the spherical shell are calculated from Equations 30 and 31. Table 14 shows the results where the numbers in the appropriate columns represent the frequencies of the oblate-spherical shell and the spherical shell.

Table 14. Angular Frequencies

	Unbounded Set p_n' (rad/sec)		Bounded Set p_n'' (rad/sec)	
n	Sphere	Oblate Spheroid	Sphere	Oblate Spheroid
1	6,644.6	7,869.1	0	—
2	9,185.1	10,774.0	2403.4	2049.7
3	12,290.8	14,269.9	—	—

Table 15. Convergence of Frequencies of Second Mode

N	Unbounded Set p_2' (rad/sec)	$v_2(x) = \sum_{i=1}^{N} a_i P_i^1(x)$ Δ
2	14,120	
		2350
4	11,770	
		700
6	11,070	
		230
8	10,840	
		60
10	10,780	
		6
12	10,774	
14	—	

Table 15 shows the convergence of the frequencies with increasing numbers of terms of the second mode. Figure 94 shows the frequencies as a function of the eccentricity for the second mode of the unbounded set.

Mode Shapes. The mode shapes were calculated from Equations 24 and 25. The coefficients a_i are tabulated in Table 16 for the unbounded set. Figure 95 shows the tangential and normal mode shapes of the unbounded set for mode numbers n = 1,2,3.

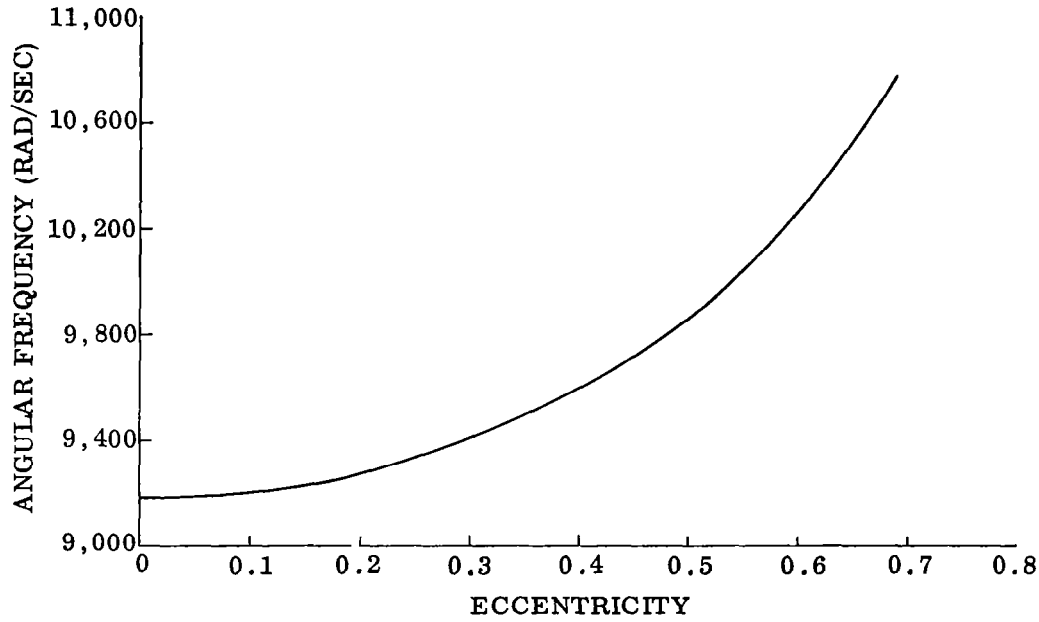

Figure 94. Second Mode, Unbounded Set. 8 Terms Approximation

Table 16. a_i of Unbounded Set $v_n = \sum_{i=1}^{N} a_i P_i^1(x)$

n \ i	1	2	3	4	5	6	7	8	9	10	11	12	13	14	15
1	1.00	0	1.1494 $\times 10^{-1}$	0	9.7168 $\times 10^{-3}$	0	−1.3053 $\times 10^{-3}$	0	−1.5699 $\times 10^{-3}$	0	−9.0184 $\times 10^{-4}$	0	−5.1082 $\times 10^{-4}$	0	−7.4458 $\times 10^{-5}$
2	0	1.00	0	2.2436 $\times 10^{-1}$	0	3.7382 $\times 10^{-3}$	0	4.5001 $\times 10^{-3}$	0	−4.7106 $\times 10^{-4}$	0	−5.1497 $\times 10^{-4}$	0	...	...
3	−8.8844 $\times 10^{-1}$	0	1.00	0	3.2821 $\times 10^{-1}$	0	7.9366 $\times 10^{-3}$	0	1.1622 $\times 10^{-3}$	0	2.3651 $\times 10^{-3}$	0	1.35186 $\times 10^{-4}$	0	...

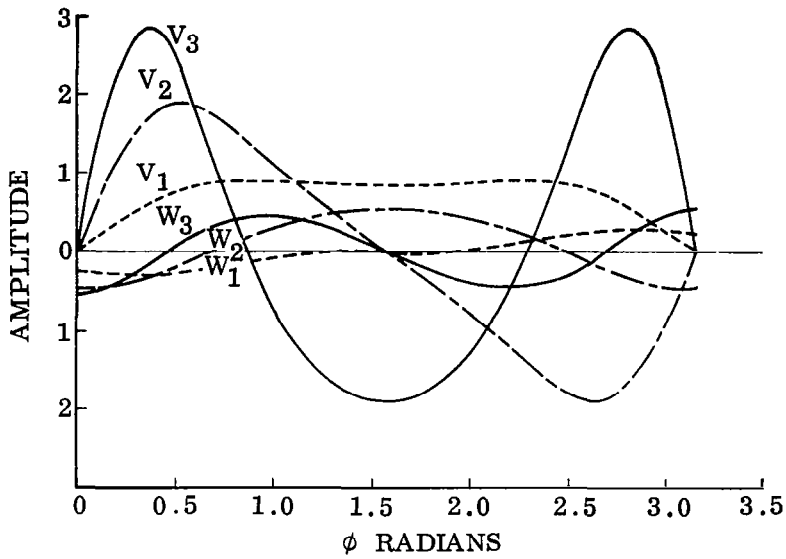

Figure 95. Mode Shapes of Unbounded Set. ---: V_1, W_1. ---: V_2, W_2. —: V_3, W_3

7.5.3 CONCLUSIONS. For the free vibration of thin isotropic, oblate spheroid shells Galerkin's method was employed, which involves a series that converges rapidly for small eccentricities; the convergence is also satisfactory for larger eccentricities. The existence of two sets of frequencies (bounded and unbounded) for a complete shell has also been shown.

8/A LIST OF AVAILABLE COMPUTER PROGRAMS

The following list includes the available computer programs, which are related to several of the references discussed previously.

1. Reference 14, Digital Program to Calculate Orthotropic Cylindrical Shell Frequencies, Convair Memorandum CD-67-033-SPS, 30 March 1967.

2. Reference 15, Natural Frequencies of Modal Characteristics of Thin Vibrating Circular Cylinders, Program No. 3603, Convair Memorandum CCD-Prop-022.

3. Reference 20, Oblate Spheroidal Shell, Frequencies, Program No. 3737A, and Oblate Spheroidal Shell Mode Shapes, Program No. 3737B.

9/REFERENCES

1. Lord Rayleigh, Theory of Sound, 2nd Edition, Dover, New York, 1945.

2. H. Lamb, "On the Vibrations of a Spherical Shell," Proc. London Math. Soc. 14, pp. 50-56, London, 1883.

3. A. E. H. Love, A Treatise on the Mathematical Theory of Elasticity, 4th Edition, pp. 512-552, Dover, New York, 1944.

4. S. Timoshenko and S. Woinowsky-Krieger, The Theory of Plates and Shells, 2nd Edition, McGraw-Hill Book Co, 1959.

5. S. Timoshenko, Theory of Elastic Stability, McGraw Hill Book Co., 1961.

6. W. Flügge, Stresses in Shells, 2nd printing, Springer-Verlag, 1962.

7. A. L. Goldenveizer, Theory of Elastic Thin Shells, Pergamon Press, 1961.

8. E. T. Whittaker and G. N. Watson, A Course of Modern Analysis, 3rd Edition, Cambridge at the University Press, 1920.

9. Bateman Manuscript Project (California Institute of Technology), Higher Transcendental Functions, McGraw-Hill Book Co. Inc., Volume 2, 1953-55.

10. T. M. MacRobert, Spherical Harmonics, Dover Publications Inc., 1948.

11. A. E. H. Love, "The Small Free Vibrations and Deformations of a Thin Elastic Shell," Phil. Trans. Roy. Soc. 179, pp. 495-537, 1888.

12. H. Lamb,"On the Vibrations of a Spherical Shell," London Math. Soc. Proc. 14, pp. 51-56, 1883.

13. W. E. Baker, "Axisymmetric Modes of Vibrations of Thin Spherical Shell," J. Acoust. Soc. Am. 33, pp. 1749-1758, 1961.

14. Yu, Yi-Yuan,"Free Vibrations of Thin Cylindrical Shells Having Finite Length With Freely Supported and Clamped Edges,"J. Appl. Mech. 22, pp. 547-552, 1955.

15. K. Forsberg,"Influence of Boundary Conditions on the Modal Characteristics of Thin Cylindrical Shells,"AIAAI. 2, pp. 2150-2157, 1964.

16. Arnold and Warburton, "Flexural Vibrations of the Walls of Thin Cylindrical Shells Having Freely Supported Ends," Proc. Roy. Soc. (London) A197, p. 238, 1949.

17. W. H. Hoppmann, II, "Elastic Compliances of Orthogonally Stiffened Plates," Proc. Soc. Exptl. Stress Anal. 14, No. 1, pp. 137-144, 1956.

18. W. H. Hoppmann, II, "Some Characteristics of the Flexural Vibrations of Orthogonally Stiffened Cylindrical Shells," J. Acoust. Soc. Am. Vol. 30, No. 1, pp. 77-82, January 1958.

19. L. E. Penzes, "The Effect of Boundary Conditions on Flexural Vibrations of Thin Orthogonally Stiffened Cylindrical Shells," J. Acoust. Soc. Am., No. 13807, 12.7, October 1967.

20. L. E. Penzes and G. Burgin, "Free Vibrations of Thin Isotropic Oblate-Spheroidal Shells," J. Acoust. Soc. Am., Vol. 39, No. 1, pp. 8-13, January 1966.

21. L. V. Kantorovich and V. I. Krylov, Approximate Methods of Higher Analysis, Interscience Publishers Inc., New York, 1958.

22. Discussion of Reference 14 by G. B. Warburton, J. Appl. Mech. 23, pp. 484-487, 1956.

"The aeronautical and space activities of the United States shall be conducted so as to contribute . . . to the expansion of human knowledge of phenomena in the atmosphere and space. The Administration shall provide for the widest practicable and appropriate dissemination of information concerning its activities and the results thereof."

—NATIONAL AERONAUTICS AND SPACE ACT OF 1958

NASA SCIENTIFIC AND TECHNICAL PUBLICATIONS

TECHNICAL REPORTS: Scientific and technical information considered important, complete, and a lasting contribution to existing knowledge.

TECHNICAL NOTES: Information less broad in scope but nevertheless of importance as a contribution to existing knowledge.

TECHNICAL MEMORANDUMS: Information receiving limited distribution because of preliminary data, security classification, or other reasons.

CONTRACTOR REPORTS: Scientific and technical information generated under a NASA contract or grant and considered an important contribution to existing knowledge.

TECHNICAL TRANSLATIONS: Information published in a foreign language considered to merit NASA distribution in English.

SPECIAL PUBLICATIONS: Information derived from or of value to NASA activities. Publications include conference proceedings, monographs, data compilations, handbooks, sourcebooks, and special bibliographies.

TECHNOLOGY UTILIZATION PUBLICATIONS: Information on technology used by NASA that may be of particular interest in commercial and other non-aerospace applications. Publications include Tech Briefs, Technology Utilization Reports and Notes, and Technology Surveys.

Details on the availability of these publications may be obtained from:

SCIENTIFIC AND TECHNICAL INFORMATION DIVISION

NATIONAL AERONAUTICS AND SPACE ADMINISTRATION

Washington, D.C. 20546